Eva Morava
Matthias Baumgartner
Marc Patterson
Shamima Rahman
Johannes Zschocke
Verena Peters *Editors*

JIMD Reports

Volume 35

SSIEM

Springer

JIMD Reports
Volume 35

Eva Morava
Editor-in-Chief

Matthias Baumgartner · Marc Patterson · Shamima Rahman · Johannes Zschocke
Editors

Verena Peters
Managing Editor

JIMD Reports
Volume 35

Springer

SSIEM

ISSN 2192-8304 ISSN 2192-8312 (electronic)
JIMD Reports
ISBN 978-3-662-55832-4 ISBN 978-3-662-55833-1 (eBook)
DOI 10.1007/978-3-662-55833-1

This Springer imprint is published by Springer Nature
The registered company is Springer-Verlag GmbH Germany
The registered company address is: Heidelberger Platz 3, 14197 Berlin, Germany

Contents

JIMD Reports
DOI 10.1007/8904_2016_16

CASE REPORT

Cerebrotendinous Xanthomatosis Presenting with Infantile Spasms and Intellectual Disability

Austin Larson • James D. Weisfeld-Adams • Tim A. Benke • Penelope E. Bonnen

Received: 10 August 2016 / Revised: 15 September 2016 / Accepted: 20 September 2016 / Published online: 18 November 2016

Abstract Cerebrotendinous xanthomatosis (CTX) is an inborn error of metabolism leading to progressive multisystem disease. Symptoms often begin in the first decade of life with chronic diarrhea, cataracts, developmental delay, intellectual disability, and cerebellar or pyramidal dysfunction. Later manifestations include tendon xanthomas, polyneuropathy, and abnormal neuroimaging. Pathogenic biallelic variants in *CYP27A1* leading to compromised function of sterol 27-hydroxylase result in accumulation of detectable toxic intermediates of bile acid synthesis rendering both genetic and biochemical testing effective diagnostic tools. Effective treatment with chenodeoxycholic acid is available, making early diagnosis critical for patient care. Here we report a new patient with CTX and describe the early signs of disease in this patient. Initial symptoms included infantile spasms, which have not previously been reported in CTX. Developmental delay, mild intellectual disability with measured cognitive decline in childhood, was also observed. These clinical signs do not traditionally compel testing for CTX, and we highlight the need to consider this rare but treatable disorder among the differential diagnosis of children with similar clinical presentation. Increased awareness of early signs of CTX is important for improving time to diagnosis for this patient population.

Communicated by: Nancy Braverman, M.D.,M.Sc.

A. Larson · J.D. Weisfeld-Adams
Department of Pediatrics, Section of Genetics, University of Colorado School of Medicine, Aurora, CO, USA

A. Larson (✉)
Children's Hospital Colorado, Mail Stop 153, 13123 E 16th Ave, Aurora, CO 80045, USA
e-mail: Austin.Larson@UCDenver.edu

T.A. Benke
Departments of Pediatrics, Pharmacology, Neurology and Otolaryngology, University of Colorado School of Medicine, Aurora, CO, USA

P.E. Bonnen (✉)
Department of Molecular and Human Genetics, Baylor College of Medicine, One Baylor Plaza, Houston, TX 77030, USA
e-mail: pbonnen@bcm.edu

Introduction

Cerebrotendinous xanthomatosis (CTX, OMIM 213700) is an autosomal recessive disorder of bile acid synthesis that manifests as a progressive, multi-system disease. Biallelic pathogenic variants in the gene *CYP27A1* cause deficiency of the enzyme produced by *CYP27A1*, sterol 27-hydroxylase, resulting in the accumulation of cholesterol, cholestanol, and other intermediates in tissues and the pathology that characterizes CTX (Panzenboeck et al. 2007). Elevated cholestanol in serum and elevated urine bile alcohols are characteristic diagnostic findings in patients with CTX. The clinical features of CTX vary widely, even within families. Bilateral cataracts are one of the most common features of CTX and are usually noted in the second decade of life, though the age of onset is variable (Cruysberg et al. 1995; Mignarri et al. 2014; Degos et al. 2016). Other common pediatric manifestations of CTX include intellectual disability or developmental delay (60% of patients, mean age of 6 years at diagnosis) and epilepsy (33% of patients, mean age of diagnosis 10 years) (Mignarri et al. 2014). Chronic diarrhea may begin in infancy and continue into adulthood (Verrips et al. 2000). Rarely, cholestatic liver disease of infantile onset has been reported (Clayton et al. 2002). Cerebellar and pyramidal signs also appear in

childhood with polyneuropathy typically developing in the third or fourth decade of life. The most common abnormality on magnetic resonance imaging (MRI) of the brain in CTX is T2 hyperintensity of the dentate nuclei of the cerebellum (Barkhof et al. 2000). The tendon xanthomas for which CTX is named do not typically appear until much later in the course of the disease if at all (Mignarri et al. 2014).

The largest reported case series of CTX patients consisted of 55 patients (Mignarri et al. 2014). The mean age at diagnosis was 35 years with mean age of onset of symptoms at 9 years, implying that delays to diagnosis are significant and that opportunities for early treatment initiation have historically been missed. The incidence of CTX is not known, but recent estimates range from 1:134,970 to 1:461,358 in Europeans and even higher in Asians (~1:70,000), also supporting the notion that some cases may go undiagnosed (Appadurai et al. 2015). Noninvasive testing of cholesterol metabolites and bile acid intermediates facilitates diagnosis of CTX. In addition, 7α-hydroxy-4-cholesten-3-one (7α4C) is helpful in diagnosis and monitoring of treatment for CTX. Serum levels of 7α4C are more significantly elevated in individuals with CTX than other metabolites, and 7α4C levels exhibit dramatic responses to treatment (Mignarri et al. 2016). 7α4C crosses the blood-brain barrier more efficiently than cholestanol and may be a significant contributing factor to pathogenesis in the central nervous system (Panzenboeck et al. 2007).

Treatment is available for CTX that is effective at remediating symptoms and, if started in childhood, can prevent clinical manifestation of the disease (Berginer et al. 2015). Thus, the identification of individuals with CTX at a young age significantly benefits patients and families. Given the importance of early diagnosis and initiation of treatment, we report here a case of CTX presenting with infantile spasms, highlighting the need to consider this rare but treatable disorder among the differential diagnosis of children presenting with seizures, even in the first year of life.

Materials and Methods

Molecular Genetic Testing

CYP27A1 sequencing was performed by Baylor Miraca Genetics Laboratory (Houston, TX) using next-generation sequencing methods and confirmed using Sanger sequencing. The detected pathogenic variant was submitted to the Leiden Open Variation Database by the authors.

Biochemical Testing

Cholestanol testing was performed by the Kennedy Krieger Institute (Baltimore, MD). Serum bile acid metabolite levels were performed by Baylor Miraca Genetics Laboratory (Houston, TX). Urine bile alcohol testing was performed by Cincinnati Children's Hospital (Cincinnati, OH).

Imaging

MRI of the brain was performed using standard clinical protocols and images were reviewed by a pediatric neuroradiologist.

Cognitive testing

Cognitive testing was performed on a clinical basis by a licensed neuropsychologist.

EEG

EEG with video was performed using standard clinical protocols and was reviewed by board-certified epileptologists.

Results

The patient, a Caucasian female, was the first live birth to a 30-year-old mother who had one prior pregnancy. Regular prenatal care was obtained, and there were no concerns for exposures during the pregnancy. The patient was born at term via normal spontaneous vaginal delivery and did not require neonatal resuscitation, though nasal fracture was noted on initial exam. Early growth and development were appropriate, and the patient initially presented at 4 months with clusters of tonic extensor spasms. Brain MRI at that time was normal. Routine electroencephalogram (EEG) showed hypsarrhythmia (>300 μV) with multifocal discharges and electrodecrements without clinical accompaniment. She was treated with adrenocorticotropic hormone (ACTH, 20 units injected daily for 4 weeks) followed by zonisamide for a diagnosis of infantile spasms. Repeat EEG at 7 months of age was normal. She also had infantile torticollis and resultant positional plagiocephaly. She did not have additional clinical seizures after ACTH administration, and zonisamide treatment was discontinued after 1 year of therapy. Prolonged overnight EEG at 6 years demonstrated slowing of the occipital dominant rhythm, and multifocal epileptiform discharges of low voltage and frequency but no seizures were captured.

The patient required treatment for constipation and had nocturnal enuresis until age 6 years. Developmental concerns prior to the initiation of schooling consisted of mildly abnormal speech articulation, clumsiness with occasional falls, and difficulty with fine motor tasks such as handwriting and buttoning clothing. Upon enrollment in kindergarten, the patient was unable to complete grade-level work. Repeat MRI of the brain was again unremarkable. At age 8 years, the Wechsler Intelligence Test for Children IV (WISC-IV) was administered with a full scale intelligence quotient (FSIQ) of 75. There were specific concerns for poor executive function out of proportion to other deficits. Neuropsychological testing was repeated at age 12 years, and FSIQ on the WISC-IV was found to be 63, which is a one standard deviation decrease from the previous testing. Verbal skills were strong but memory and reasoning were weak.

The patient failed a routine vision screen at age 12 and was referred to an ophthalmologist. She was diagnosed with cataracts and underwent bilateral lens extraction with intraocular artificial lens implantation. Given her history of developmental regression and bilateral cataracts, serum cholestanol level was obtained and found to be 20.39 μg/mL (normal <3.71 μg/mL). Urine bile alcohols showed elevated polyhydroxylated bile alcohol glucuronides. Molecular genetic testing showed an apparently homozygous variant in *CYP27A1* (NM_000784): c.1016C>T (p.Thr339Met), an allele which has previously been reported in other patients with a clinical and biochemical diagnosis of CTX (Reshef et al. 1994; Gupta et al. 2007). MRI of the brain showed faint T2 hyperintensities of the cerebellar dentate nuclei bilaterally. On physical examination at age 12, the patient had hyperactive deep tendon reflexes, increased muscle tone of the lower extremities with mild contractures at the knees and ankles, mild ataxia, no evidence of sensory neuropathy, and no evidence of tendon xanthomas. Serum aspartate aminotransferase (AST) was mildly elevated at the time of diagnosis, 38 units/L (normal <31 units/L).

The patient was started on CDCA 500 mg daily and after 1 month, cholestanol level decreased to 10.34 μg/mL (Table 1). Serum bile acid profile performed at that time showed 7α4C level of 2.51 μmol/L (normal <0.05 μmol/L). CDCA was increased to 750 mg daily and studies were repeated after 6 months at that dose. Cholestanol level decreased to 3.31 μg/mL. 7α4C level decreased to 0.47 μmol/L. The patient has tolerated CDCA therapy well without gastrointestinal discomfort. AST remained mildly elevated with CDCA treatment at 32 units/L. There was mild elevation of alanine aminotransferase (ALT) from 21 to 44 units/L (normal <31 units/L) with CDCA treatment. Aminotransferase levels have been monitored due to the known risk of hepatotoxicity with CDCA treatment (Huidekoper et al. 2016).

Table 1 Plasma biochemical markers show response to CDCA treatment

	Cholestanol (μg/mL)	7αC4 (μmol/L)
Normal	<3.71	<0.05
Pretreatment	20.4	–
CDCA, 500 mg	10.3	2.5
CDCA, 750 mg	3.3	0.5

The patient has one healthy sibling and one sibling with autism. Her mother has well-controlled adult-onset epilepsy. These three unaffected family members have normal serum cholestanol concentration. The mother and father were both found to be heterozygous for the *CYP27A1* pathogenic variant, confirming that the patient has two pathogenic alleles *in trans*. The patient's father has cataracts due to adult-onset glaucoma.

Discussion

We report a new case of CTX with infantile spasm, developmental delay, intellectual disability, and pediatric cognitive decline. CTX is a multisystem degenerative disease that is usually diagnosed after a protracted delay from initial symptomatic onset due to nonspecific early symptoms, variable clinical presentation, and a course that typically progresses over decades. Given that effective treatment is available and can prevent disease progression, diagnosis is critically important for patients and greater awareness of the disease and earliest manifestations beneficial. Cataracts are the most commonly occurring pediatric sign, with an average age of onset in the second decade of life. Importantly there are also earlier clinical symptoms that present in the first decade of life with significant frequency. Two-thirds of patients have intellectual disability or developmental delay, and one-third of patients with CTX are diagnosed with epilepsy, including a small number of patients with epilepsy very early in life (Pedroso et al. 2012; Kauffman et al. 2012, Mignarri et al. 2014). Chronic diarrhea can be one of the earliest clinical signs of CTX that appears in less than half of cases (Mignarri et al. 2014).

The number of known genetic etiologies of infantile spasms has increased dramatically in recent years with the advent of chromosomal microarray, large sequencing panels, and whole exome sequencing (Michaud et al. 2014; Paciorkowski et al. 2011). To date, *CYP27A1* has not been reported in published cohorts of patients with

infantile spasms who have undergone broad molecular genetic testing. This implies that, while important to include in the differential for this patient population, CTX is unlikely to be a common diagnosis in this setting. The patient reported in this paper had normal chromosomal microarray, but did not have whole exome sequencing after diagnosis of CTX to evaluate for additional genetic etiologies of infantile spasms. We cannot exclude the possibility that there is a second unrelated etiology of infantile spasms for this patient since there are no available tests with 100% sensitivity to detect all possible causes of seizures and developmental delay, not even whole exome sequencing. However, since the time of her initial seizures, she has had progressive features of CTX including development of cataracts, dentate nucleus MRI abnormalities, ataxia, and lower extremity spasticity. Importantly, there have not been any additional findings that are inconsistent with CTX, leading to our conclusion that CTX is the most likely etiology of her infantile spasms.

Therapy consists of decreasing synthesis of toxic bile acid intermediates to provide negative feedback on the pathway. Multiple studies have reported clinical efficacy of CDCA in CTX including lengthy longitudinal studies after initiation of therapy. Importance of early initiation of therapy was emphasized by a recent report of 18 patients with up to 23 years on CDCA therapy in which there was a correlation between early age at initiation of CDCA therapy and improved neurological outcomes (Yahalom et al. 2013). There are fewer reports of outcomes during childhood with CDCA treatment of those that become symptomatic at an early age. In a report of five patients treated with CDCA, two of three patients that had developmental delay in childhood showed improvement of 10 points or more on intelligence quotient testing after 2 years of treatment (Van Heijst et al. 1998). Four members of one family were treated with CDCA, and the two children that were asymptomatic at the time of initiating treatment remained so 14 years later (Berginer et al. 2009).

This case emphasizes the importance for neurologists, ophthalmologists, gastroenterologists, and geneticists to maintain a high index of suspicion for CTX in the setting of consistent clinical features. In light of the availability of CDCA as a specific and effective treatment, clinicians should consider testing for CTX with biochemical assays or sequencing of *CYP27A1* when evaluating children for apparently idiopathic epilepsy, even with onset in the first year of life and especially if additional features of CTX are present.

Acknowledgments The authors wish to thank the family for their participation in this study. PEB is supported by National Institute of Neurological Disorders and Stroke of the National Institutes of Health under award number R01NS083726.

Synopsis

CTX can present with infantile spasm, developmental delay, and cognitive decline in childhood.

Conflicts of Interest

AL, JDW-A, and TAB declare no conflicts of interest. PEB is a paid consultant to Retrophin, Inc.

Author Contributions

AL, JDW-A, and TAB: patient clinical evaluation, conception and design, and analysis and interpretation of data. AL and PEB: conception and design, drafting the article, and revising it critically for important intellectual content.

Compliance with Ethics Guidelines

All testing for this patient was performed as standard clinical care and thus was not considered human subject research.

References

Appadurai V, DeBarber A, Chiang P-W et al (2015) Apparent underdiagnosis of cerebrotendinous xanthomatosis revealed by analysis of ~60,000 human exomes. Mol Genet Metab 116: 298–304

Barkhof F, Verrips A, Wesseling P et al (2000) Cerebrotendinous xanthomatosis: the spectrum of imaging findings and the correlation with neuropathologic findings. Radiology 217:869–876. pubs.rsna.org

Berginer VM, Gross B, Morad K et al (2009) Chronic diarrhea and juvenile cataracts: think cerebrotendinous xanthomatosis and treat. Pediatrics 123:143–147

Berginer VM, Salen G, Patel SB (2015) Cerebrotendinous xanthomatosis. In: Rosenberg RN, Pascual JM (eds) Rosenberg's molecular and genetic basis of neurological and psychiatric disease. Academic Press, Elsevier, London, pp. 589–598

Clayton PT, Verrips A, Sistermans E et al (2002) Mutations in the sterol 27-hydoxylase gene (CYP27A) cause hepatitis of infancy as well as cerebrotendinous xanthomatosis. J Inherit Metab Dis 25:501–513

Cruysberg JR, Wevers RA, van Engelen BG et al (1995) Ocular and systemic manifestations of cerebrotendinous xanthomatosis. Am J Ophthalmol 120:597–604

Degos B, Nadjar Y, Amador M et al (2016) Natural history of cerebrotendinous xanthomatosis: a paediatric disease diagnosed in adulthood. Orphanet J Rare Dis 11:41

Gupta RP, Patrick K, Bell NH (2007) Mutational analysis of CYP27A1: assessment of 27-hydroxylation of cholesterol and 25-hydroxylation of vitamin D. Metabolism 56:1248–1255

Huidekoper HH, Vaz FM, Verrips A, Bosch AM (2016) Hepatotoxicity due to chenodeoxycholic acid supplementation in an infant with cerebrotendinous xanthomatosis: implications for treatment. Eur J Pediatr 175:143–146

Kauffman MA, Gonzalez-Morón D, Consalvo D, Kochen S (2012) Cerebrotendinous xanthomatosis revealed in drug-resistant epilepsy diagnostic workup. Am J Med Sci 343:332–333

Michaud JL, Lachance M, Hamdan FF et al (2014) The genetic landscape of infantile spasms. Hum Mol Genet 23:4846–4858

Mignarri A, Gallus GN, Dotti MT, Federico A (2014) A suspicion index for early diagnosis and treatment of cerebrotendinous xanthomatosis. J Inherit Metab Dis 37:421–429

Mignarri A, Magni A, Del Puppo M et al (2016) Evaluation of cholesterol metabolism in cerebrotendinous xanthomatosis. J Inherit Metab Dis 39(1):75–83. doi:10.1007/s10545-015-9873-1, Epub 2015 Jul 8

Paciorkowski AR, Thio LL, Rosenfeld JA et al (2011) Copy number variants and infantile spasms: evidence for abnormalities in ventral forebrain development and pathways of synaptic function. Eur J Hum Genet 19:1238–1245

Panzenboeck U, Andersson U, Hansson M et al (2007) On the mechanism of cerebral accumulation of cholestanol in patients with cerebrotendinous xanthomatosis. J Lipid Res 48: 1167–1174

Pedroso JL, Pinto WB, Souza PV et al (2012) Early-onset epilepsy as the main neurological manifestation of cerebrotendinous xanthomatosis. Epilepsy Behav 24:380–381

Reshef A, Meiner V, Berginer VM, Leitersdorf E (1994) Molecular genetics of cerebrotendinous xanthomatosis in Jews of north African origin. J Lipid Res 35:478–483

Van Heijst A, Verrips A, Wevers RA et al (1998) Treatment and follow-up of children with cerebrotendinous xanthomatosis. Eur J Pediatr 157:313–316

Verrips A, Hoefsloot LH, Steenbergen GC et al (2000) Clinical and molecular genetic characteristics of patients with cerebrotendinous xanthomatosis. Brain 123(Pt 5):908–919

Yahalom G, Tsabari R, Molshatzki N, et al (2013) Neurological outcome in cerebrotendinous xanthomatosis treated with chenodeoxycholic acid: early versus late diagnosis. Clin Neuropharmacol 36:78–83. journals.lww.com

JIMD Reports
DOI 10.1007/8904_2016_17

RESEARCH REPORT

Hyperammonemia as a Presenting Feature in Two Siblings with *FBXL4* Variants

Sarah U. Morton* · Edward G. Neilan* · Roy W.A. Peake · Jiahai Shi · Klaus Schmitz-Abe · Meghan Towne · Kyriacos Markianos · Sanjay P. Prabhu · Pankaj B. Agrawal

Received: 19 April 2016 / Revised: 3 October 2016 / Accepted: 5 October 2016 / Published online: 18 November 2016

Abstract Early-onset mitochondrial encephalomyopathy is a rare disorder that presents in the neonatal period with lactic acidosis, hypotonia, and developmental delay. Sequence variants in the nuclear-encoded gene *FBXL4* have been previously demonstrated to be a cause of early-onset mitochondrial encephalomyopathy in several unrelated families. We have identified a pair of siblings with mutations in *FBXL4* who each presented in the neonatal period with hyperammonemia, low plasma levels of aspartate, low urine levels of tricarboxylic acid cycle intermediates suggesting a defect in anaplerosis, and cerebellar hypoplasia in addition to lactic acidosis and other classic signs of mitochondrial encephalomyopathy. After initial clinical stabilization, both subjects continued to have episodic exacerbations characterized by lactic acidosis and hyperammonemia. Previously reported cases of *FBXL4* mutations are reviewed and compared with these affected siblings. These two new cases add to the spectrum of disease caused by mutations in *FBLX4* and suggest possible benefit from anaplerotic therapies.

Communicated by: John Christodoulou, MB BS PhD FRACP FRCPA

Authors Sarah U. Morton and Edward G. Neilan equally contributed to the manuscript.

Electronic supplementary material: The online version of this chapter (doi:10.1007/8904_2016_17) contains supplementary material, which is available to authorized users.

S.U. Morton · K. Markianos · P.B. Agrawal
Division of Newborn Medicine, Boston Children's Hospital and Harvard Medical School, 300 Longwood Ave, Hunnewell 4, Boston, MA 02115, USA

S.U. Morton · M. Towne · K. Markianos · P.B. Agrawal
Gene Discovery Core, The Manton Center for Orphan Disease Research, Boston Children's Hospital and Harvard Medical School, Boston, MA, USA

E.G. Neilan · K. Schmitz-Abe · M. Towne · P.B. Agrawal (✉)
Division of Genetics and Genomics, Boston Children's Hospital and Harvard Medical School, Boston, MA, USA
e-mail: pagrawal@enders.tch.harvard.edu

R.W.A. Peake
Department of Laboratory Medicine, Boston Children's Hospital and Harvard Medical School, Boston, MA, USA

J. Shi
Department of Biomedical Sciences, City University of Hong Kong, Pok Fu Lam, Hong Kong

S.P. Prabhu
Department of Radiology, Boston Children's Hospital and Harvard Medical School, Boston, MA, USA

Introduction

Mitochondria are maternally derived and function to produce adenosine triphosphate (ATP) via oxidative phosphorylation. Abnormalities in mitochondrial function can lead to a variety of diseases including mitochondrial encephalomyopathy. Early-onset forms of encephalomyopathy present in the neonatal period and are characterized by lactic acidosis, hypotonia, developmental delay, and progressive neurologic disease.

Genetic variants linked to mitochondrial disease can be found in either the nuclear or mitochondrial DNA. Some mitochondrial diseases are characterized by mitochondrial DNA (mtDNA) depletion, with affected cells having less total mtDNA per cell. Diseases with mtDNA depletion are often caused by defects in a single gene such as *POLG*, a nuclear-encoded DNA polymerase essential for mitochondrial DNA replication (Tang et al. 2011; El-Hattab and Scaglia 2013).

More recently, mutations in the nuclear gene *FBXL4* were demonstrated to be a cause of mitochondrial encephalomyopathy in several patients who had defective oxidative phosphorylation (Bonnen et al. 2013; Gai et al. 2013). FBXL family member proteins, characterized by leucine-rich repeats containing of F-box motifs, interact with SKP1-CUL1-F-box protein (SCF) E3 ubiquitin ligases (Van Rechem et al. 2011). *FBXL4* was first identified as a component of the SCF ubiquitin ligase complex via yeast two-hybrid screen (Winston et al. 1999). The SCF complex is active in phosphorylation-dependent ubiquitination. The FBXL4 protein has an N-terminal mitochondrial localization signal and localizes within the intermembrane space of mitochondria (Gai et al. 2013).

A recent review summarized the phenotypic spectrum present in 28 cases with *FBXL4* mutations (Huemer et al. 2015). A total of 23 sequence variants in *FBXL4*, with 14 missense, 7 loss-of-function, and 2 splice site mutations among patients with early-onset mitochondrial encephalomyopathy, were identified. Two additional sequence variants have since been reported (van Rij et al. 2016; Barøy et al. 2016). Patients with nonsense mutations had more severe phenotypes than those with missense changes (Bonnen et al. 2013; Gai et al. 2013). Fibroblasts and myocytes from affected individuals demonstrated decreased mitochondrial DNA (mtDNA) content, loss of the mitochondrial membrane potential, and decreased respiratory chain enzyme activity (Antoun et al. 2015). It is hypothesized that the defect in oxidative phosphorylation is due to the depletion of mtDNA. Expression of wild-type FBXL4 protein in skin fibroblasts from affected patients rescued the defects in mtDNA content and oxidative phosphorylation activity (Antoun et al. 2015).

Here we describe two siblings who both presented in the neonatal period with lactic acidosis, hypotonia, and cerebral atrophy. Unique to these cases, we observed severe depletion of tricarboxylic acid cycle (TCA) intermediates and of the anaplerotic amino acid aspartate. Because aspartate is required to provide nitrogen to form argininosuccinate in the urea cycle, its depletion may be contributing to the severe hyperammonemia observed in these cases. Both biochemically and clinically, the presentation of these siblings with *FBXL4* missense variants closely mimicked the findings associated with pyruvate carboxylase deficiency. However, after pyruvate carboxylase deficiency was ruled out by gene sequencing, a muscle biopsy for mitochondrial studies was performed in the older child (sibling 1, S1), which revealed depletion of mtDNA relative to nuclear DNA, consistent with the prior findings of mtDNA depletion in other patients affected by FBXL4 gene mutations.

Case Reports

Sibling 1

Sibling 1 (S1), a male infant, was born at 38 2/7 weeks' gestation by cesarean section for fetal heart rate decelerations and intrauterine growth restriction (IUGR). At birth he appeared healthy and he was transferred to the newborn nursery. By 18 h of life he displayed temperature instability, deep breathing, and hypoglycemia as low as 1.4 mmol/L (reference interval: 2.2–5.6). Clinical characteristics are summarized in Supplemental Table 1. A venous blood gas at 18 h of life identified pH 7.09, pCO_2 16 mmHg, and pO_2 92 mmHg. Additional testing revealed a plasma ammonia level of 174 μmol/L (reference interval: 16–47) and plasma lactate level of 27 mmol/L (reference interval: 0.5–2.2). The hyperammonemia was treated with continuous infusions of sodium benzoate and sodium phenyl acetate, while the acidosis was corrected with sodium bicarbonate. Peak plasma ammonia was >362 μmol/L. He also had abnormal coagulation with an international normalized ratio of 2.63 (reference interval: 0.87–1.13), prothrombin time 24.9 s (reference interval: 9.4–11.8), partial thromboplastin time 104.4 s (reference interval: 24–32), and fibrinogen 114 mg/dL (reference interval: 200–400). Specific coagulation factors were not interrogated. Liver function otherwise appeared unaffected as evidenced by normal plasma alanine transaminase activity 14 unit/L (reference interval: 3–54), albumin 3.0 g/dL (reference interval: 2.5–4.0), and total bilirubin 4.0 g/dL (reference interval: 4.2–6.6).

Because S1 manifested neonatal hypoglycemia with severe and persistent hyperammonemia and metabolic acidosis, characterized by both ketosis and lactic acidosis, his initial metabolic differential diagnosis included the possibilities of pyruvate carboxylase deficiency or an organic acidemia, similarly capable of secondary inhibition of the urea cycle, such as propionic acidemia or methylmalonic acidemia. On his first day at our institution, an emergency urine organic acid profile demonstrated a remarkable, nearly complete absence of TCA cycle intermediates (Fig. 1a). For comparison, a typical urine organic acid profile is shown in Supplemental Fig. 1. Concurrent analysis of plasma amino acids demonstrated elevations of alanine at 1,280 μmol/L (reference interval: 120–499), citrulline at 98 μmol/L (reference interval: 2–50), proline at 916 μmol/L (reference interval: 66–300), and lysine at 593 μmol/L (reference interval: 54–271), whereas the glutamine level was within the reference interval at 716 μmol/L (reference interval: 322–1,084). The amino acid profile also showed a low-normal aspartate level at 3 μmol/L (reference interval: 3–17). These findings were

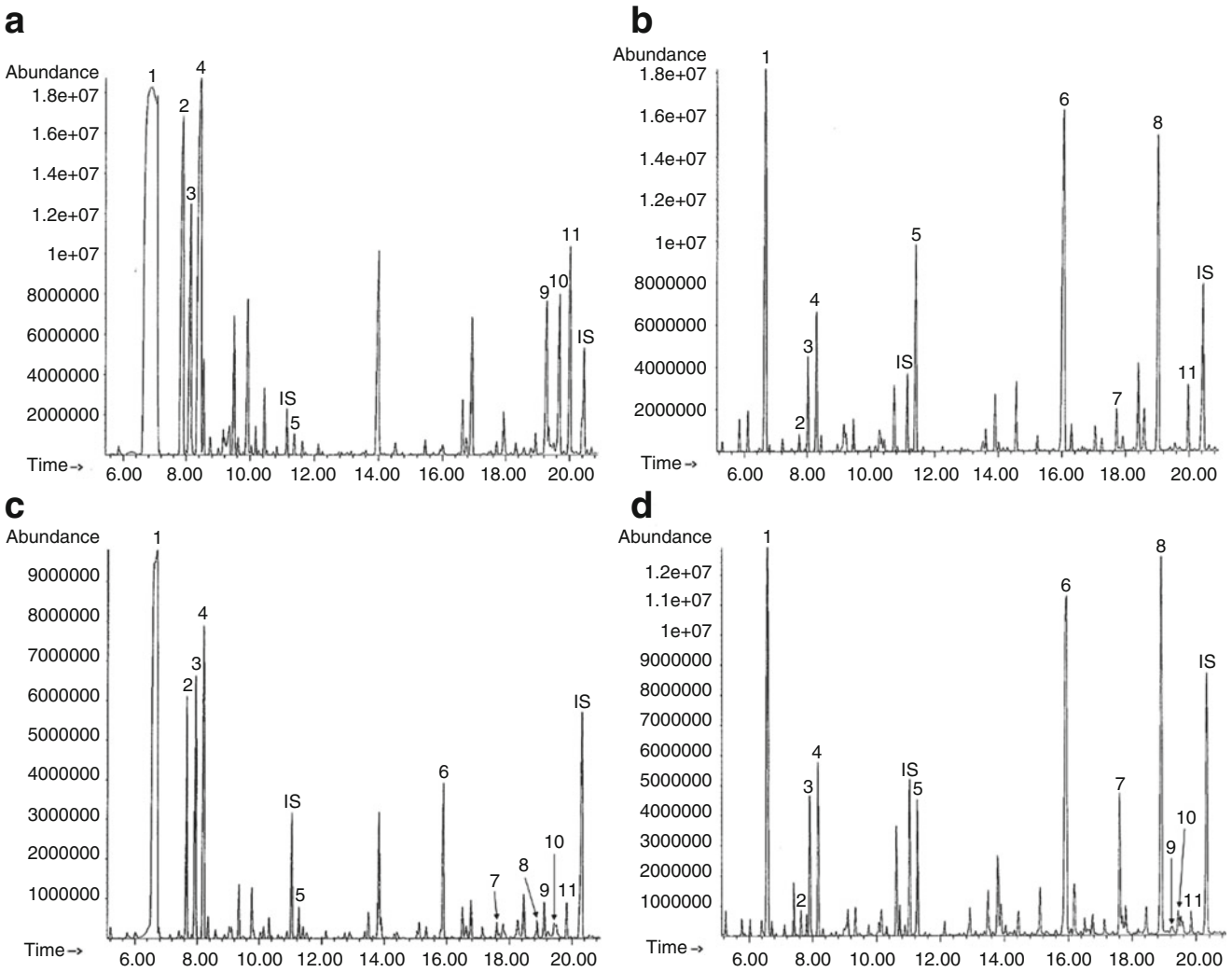

Fig. 1 Representative gas chromatography-mass spectrometry (GC-MS) organic acid chromatograms from urine specimens. (**a**) Urine sample collected from S1 on presentation prior to administering treatment. The tricarboxylic acid cycle intermediates 2-ketoglutarate, aconitate, and citrate were undetectable in the urine on presentation. (**b**) Urine sample collected from S1 after treatment with aspartate and citrate. (**c**) Urine sample collected from S2 on presentation prior to administering treatment. (**d**) Urine sample collected from S2 after treatment with aspartate and citrate. *Horizontal axis* reflects retention time, and *vertical axis* reflects total ion abundance. The following peak numbers correspond to compounds detected in both chromatograms: (*1*) lactate, (*2*) 2-hydroxybutyrate, (*3*) pyruvate, (*4*) 3-hydroxybutyrate, (*5*) fumarate, (*6*) 2-ketoglutarate, (*7*) aconitate, (*8*) citrate, (*9*) unsaturated sebacate, (*10*) sebacate, (*11*) 4-hydroxyphenyllactate. Internal standards (IS): 2-ketocaproate (approximately 11.0 min) and pentadecanoate (approximately 20.3 min)

obtained at the same time as the severely elevated plasma lactate level of 27 mmol/L and were consistent with an initial working diagnosis of pyruvate carboxylate (PC) deficiency. Supplementation with citrate, aspartate, biotin, carnitine, and thiamine was commenced in the NICU, and the patient's biochemical abnormalities stabilized considerably. With this treatment, the depletion of TCA cycle intermediates in the urine was quickly corrected (Fig. 1b). Plasma lactate levels normalized and the hyperammonemia resolved. The use of citrate and aspartate supplementation to promote anaplerosis was based on case reports of its effectiveness in PC deficiency (Mochel et al. 2005). Given the dismal prognosis of neonatal PC deficiency, triheptanoin was also later administered as an anaplerotic substrate for the TCA cycle. However, this was discontinued, since its use appeared to be associated with vomiting.

Genetic sequencing of the pyruvate carboxylase (*PC*) gene, as well as 101 nuclear genes associated with mitochondrial disease, was normal. Enzymatic activity assays using patient fibroblasts demonstrated normal activities of PC, pyruvate dehydrogenase, and phosphoenolpyruvate carboxykinase.

Brain MRI on day of life six demonstrated diffuse T2 hyperintensity of the supratentorial deep and subcortical white matter within the frontal, parietal, occipital, and temporal lobes (Fig. 2a). The cerebellum and brainstem

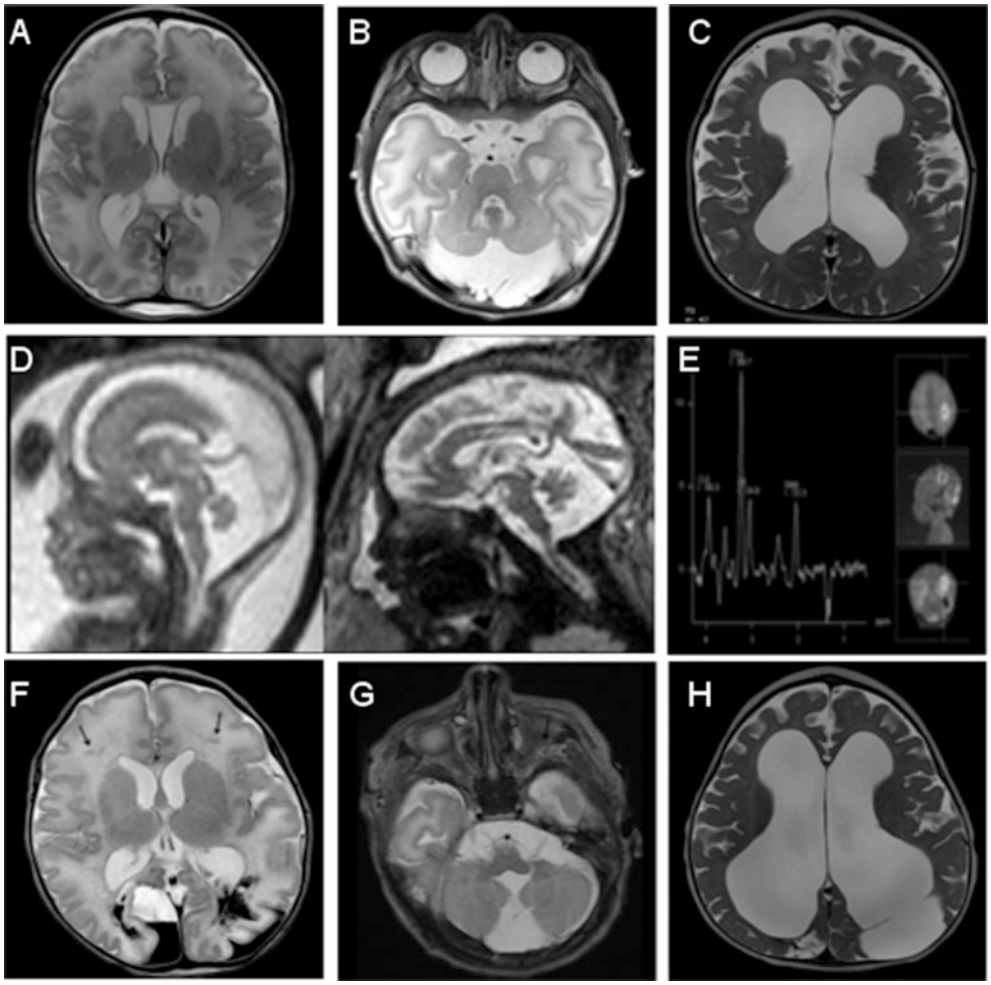

Fig. 2 Brain abnormalities in affected siblings on magnetic resonance imaging (MRI). (**a**) Axial T2-weighted images of S1 at 6 days of life image show diffuse white matter hyperintensity in the periventricular and subcortical white matter. (**b**) Axial T2-weighted image of S1 at 6 days of age shows enlarged retrocerebellar cerebrospinal fluid (CSF) space and a hypoplastic cerebellar hemisphere. (**c**) Axial T2-weighted image of S1 at 28 months of age shows marked cerebral atrophy. (**d**) Fetal MRI scans of S2 at 21 +5 (*left*) and 34+5 weeks' gestation (*right*) show enlarged retrocerebellar CSF spaces. (**e**) Single voxel magnetic resonance spectroscopy of S2 at 5 days old performed at TE 144 ms from the parietal white matter shows an inverted doublet of lactate at 1.33 ppm. (**f**) Axial T2-weighted image of S2 at 5 days of life shows large areas of extensive intraparenchymal and intraventricular hemorrhage in the bilateral parietal and occipital lobes. Smaller areas of hemorrhage are seen along the expected course of the medullary veins in the frontal white matter (*arrows*). (**g**) Axial T2-weighted image of S2 at 5 days of age shows prominence of the retrocerebellar cystic space with a hypoplastic inferior vermis and small, slightly dysmorphic cerebellar hemispheres. (**h**) Axial T2-weighted image of S2 at 25 months of age shows marked atrophy with ex-vacuo dilatation of the ventricular system and sulcal spaces in the frontal and temporal regions. In addition, sequelae of the prior hemorrhage are seen as porencephalic changes and encephalomalacia in the bilateral (left more than right), parietal, and occipital lobes. Periventricular white matter continues to show abnormal T2 hyperintensity

were hypoplastic (Fig. 2b). Electroencephalogram (EEG) at 2 weeks of life was abnormal due to excessive multifocal sharp waves, delta brushes, and excessive discontinuity in sleep consistent with nonspecific encephalopathy. No epileptic activity was noted.

S1 also had symptomatic persistent pulmonary hypertension (PPHN) requiring inhaled nitric oxide in the first week of life until it resolved. He had cardiomyopathy and progressive dilation of the pulmonary artery with *z*-score of 5–6, as well as a mildly dilated ascending aorta, without evidence of cerebrovascular dilation on MRI. His hypotonia was persistent, and he had oromotor dysfunction with aspiration of thin liquids. Following NICU discharge, he continued to be treated with biotin, L-aspartic acid, citric acid-potassium citrate and sodium bicarbonate. As an outpatient, his plasma ammonia was usually normal, except during intermittent illnesses. However, his lactic acid levels were chronically elevated (usually between 5 and 10 mmol/

L), and his plasma aspartate levels were often at the lower limit of normal despite ongoing enteral aspartate supplementation.

Muscle biopsy at 8 months was notable only for mild excess variation in fiber size diameter affecting type 1 fibers more than type 2 fibers. There were occasional nuclei with prominent regenerative nucleoli on electron microscopy, but findings were otherwise normal. Trichrome staining revealed normal connective tissue and myofibrillar structures; in addition, there were no ragged red fibers. PAS stain revealed a normal content and appearance of glycogen, which digested appropriately with dispase. Oil Red O stain revealed a normal content of lipid. NADH, ATPase, COX, and SDH histochemical stain revealed the normal findings. Mitochondria were normal in number, distribution, and morphology on electron microscopy. Biochemical testing for electronic transport chain complex I–IV activity in skeletal muscle biopsy demonstrated low activity of all complexes, though citrate synthase activity was also low so the corrected enzyme activity was within normal limits.

S1 also had global developmental delay as he began to sit at approximately 1 year of age and independently bear weight on his legs at 2 years. Serial MRI, with the last at 24 months of life, documented progressive cerebral atrophy and cavitation of the basal ganglia without diffusion abnormality (Fig. 2c). The patient had cerebral visual impairment with optic disc atrophy, nystagmus, and mild to moderate bilateral sensorineural hearing loss.

After an initial period of metabolic stability at home, he presented again at 23 months of age with a second episode of hyperammonemia. Subsequently, he continued to have repeated admissions to the ICU for hyperammonemia, some requiring dialysis. He passed away at 40 months while receiving palliative care at home.

Sibling 2

Sibling 2 (S2), a female infant, was born at 38 6/7 weeks' gestation via vaginal delivery. Given the family history, she had baseline studies taken soon after birth that demonstrated elevated plasma lactic acid level of 13.3 mmol/L (reference interval: 0.5–2.2) and hyperammonemia (plasma ammonia, 134 μmol/L; reference interval: 16–47). Supplementation with citric acid and aspartate was initiated immediately. Extensive metabolic evaluation demonstrated decreased plasma aspartate of 3 μmol/L (reference interval: 3–17) with increased levels of proline at 350 μmol/L (reference interval: 66–300), lysine at 286 μmol/L (reference interval: 54–271), and alanine at 796 μmol/L (reference interval: 120–499), consistent with the pyruvate-carboxylase-deficiency-like syndrome of her brother. Urine organic acids demonstrated significant depletion of TCA cycle intermediates such as citrate (Fig. 1c). After initiation of citric acid at 0.12 mmol/kg/hr and aspartate supplementation of 250 mg every 3 h, hyperammonemia resolved. The urine organic acid profile after supplementation demonstrated the presence of a proportionally abundant citrate peak consistent with exogenous citrate administration (Fig. 1d). No muscle biopsy was conducted given the similarity of her disease phenotype to that of her brother.

Prenatal imaging had raised concerns for enlarged retrocerebellar space and small cerebellum (Fig. 2d). Brain MRI in the first week of life demonstrated extensive hemorrhages within the parenchyma, ventricles, and enlarged extra-axial spaces (Fig. 2f). The vermis and cerebellar hemispheres were hypoplastic (Fig. 2g). Single voxel MR spectroscopy from a voxel placed in the left parietal white matter demonstrated a prominent inverted doublet indicating elevated brain lactate (Fig. 2e).

During her NICU admission, she demonstrated poor oral feeding ability, and even with gastrostomy tube feedings, she had significant daily emesis. She received continuing supplementation with biotin, aspartic acid, and citric acid-potassium citrate. She was discharged home at 3 weeks of age at a weight of 2.66 kg and receiving via gastrostomy tube biotin 20 mg per day, citric acid-sodium citrate 1.5 mEq every 3 h, and L-aspartic acid 250 mg every 3 h. She remained reasonably stable on similar therapy for most of the next 2 years. Like her brother, she had chronic lactic acidosis (usually 5–10 mmol/L), intermittent hyperammonemia, and plasma aspartate levels that remained often close to the lower limit of normal despite her enteral supplements.

Her visual acuity was 20/190 at 12 months and nystagmus was noted. Brain MRI at 24 months demonstrated persistent white matter T2 hyperintensity, progressive predominant frontotemporal atrophy and porencephaly, and encephalomalacia in the parietal and occipital lobes at the sites of prior hemorrhage (Fig. 2h). She had a significant developmental delay and by 23 months of life was unable to sit unsupported.

Between 9 and 23 months of age, S2 had four admissions to the ICU for acidosis with varying degrees of hyperammonemia, from mild to severe. In the most acute episode, at 23 months of age, without a clear inciting illness, she presented with altered mental status, plasma lactic acid 13.4 mmol/L (reference interval: 0.5–2.2), and severe hyperammonemia of 443 μmol/L (reference interval: 12–38), which required emergency hemodialysis for treatment. At 24 months of age, she was hospitalized again with recurrent vomiting, persistent lactic acidosis, and mild hyperammonemia. Lumbar puncture during this final hospitalization revealed a CSF lactic acid level of 10 mmol/L, notably almost twice the level previously obtained in plasma (6 mmol/L). To treat her persistent lactic

acidosis, she required continuous infusion with up to 70 mEq/kg/day of sodium bicarbonate. After this 5-week hospitalization, S2 was transitioned to palliative care at home and passed away at 26 months.

Materials and Methods

Patient Enrollment

The proband (S1), both parents, the affected sibling (S2), and an unaffected sibling were enrolled in an IRB-approved study at Boston Children's Hospital (BCH) (Fig. 3a).

Urine Organic Acid Analysis

Urine organic acids were extracted into ethyl acetate and diethyl ether and converted to trimethylsilyl derivatives prior to analysis by gas-chromatography mass spectrometry using a GC 6890 N/ MS 5975 system with a DB-1 column (Agilent, Santa Clara, CA).

Muscle mtDNA Assay

Total genomic DNA extracted from frozen muscle tissue from S1 was assayed quantitatively for mtDNA and the 18S ribosomal RNA gene using qRT-PCR (MNG Laboratories, Atlanta, Georgia). The ratio of the number of PCR cycles to reach threshold was calculated, with larger values indicating lower numbers of mtDNA.

DNA Preparation, Exome Sequencing, and Data Analysis

Total genomic DNA was extracted from peripheral blood lymphocytes using QIAmp DNA Mini Kit (Qiagen). DNA from the proband, affected sibling, unaffected sibling, and both biological parents was sent for whole exome sequencing (WES) to Axeq Technologies. Samples were prepared as an Illumina sequencing library and enriched for exomic sequences using the Illumina Exome Enrichment protocol. The captured libraries were sequenced using Illumina HiSeq 2000 Sequencers. The reads were mapped to the human genome assembly UCSC hg19 using Burrows-Wheeler Alignment (BWA version 0.5.8). Single nucleotide polymorphisms (SNPs) and small insertions/deletions were called with SAMtools (version 0.1.7). The resulting VCF files were analyzed using a custom-built, rule-based "Variant Explorer" pipeline capable of integrating SNP chip, linkage, sequencing, and functional database information. In this case only the sequencing and database components were used. We selected likely pathogenic variants to include nonsynonymous, splice site, and indel variants with an allele frequency <0.001 in the NHLBI exome variant server database (EVS) (http://evs.gs.washington.edu/EVS/) or

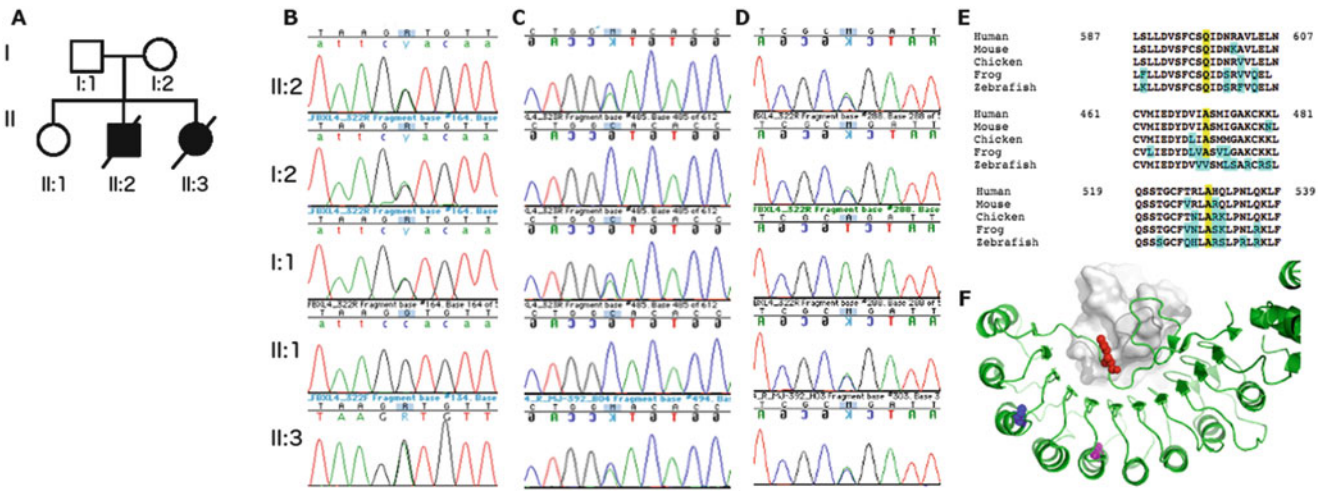

Fig. 3 Sequence analysis reveals compound heterozygosity in affected siblings but not unaffected family members. (**a**) Pedigree of the families carrying FBXL4 variants. The probands were II:2 (S1) and II:3 (S3). (**b**) Sequence analysis for nucleotide 1411. Maternally inherited c.1411G>A variant was presented in S1 (II:2) and S2 (II:3) but not the unaffected sibling (II:1). (**c**) Sequence analysis for nucleotide 1586. Paternally inherited c.1586C>A variant was presented in S1 (II:2) and S2 (II:3) but neither the mother (I:2) nor the unaffected sibling (II:1). (**d**) Sequence analysis for nucleotide 1790. Maternally inherited c.1790 A>C variant was presented in S1 (II:2), unaffected sibling (II:1), and S2 (II:3) but not the father (I:1). (**e**) Amino acid sequence alignment at the location of identified variants. Residues highlighted in *yellow* are the conserved amino acids affected by the genetic variant, and those highlighted in *blue* are nonconserved amino acids. (**f**) Predicted protein structure of FBXL4 with sites of identified variants highlighted. Shown in *sphere*, p. Gln597 is colored in *red*, p. Ala471 in *purple* and p. Ala529 in *blue*. The hypothetical position of a potential binding partner of FBXL4 leucine-rich repeat (LRR) domain is shown in *gray*

<0.01 in 1000 Genomes Project, phase 3, (http://www.1000genomes.org). The variants were also evaluated for frequency by ExAC database (http://www.exac.broadinstitute.org). The pathogenicity of the variants was evaluated in silico using polyphen-2, SIFT, and MutationTaster programs.

Results

Whole Exome Sequencing

Whole exome sequencing was performed on genomic DNA from the proband and both parents. The mean read depth was 100–115×, and >10× coverage of the target region was 98.1–98.7%. Nine hundred nine variants were non-synonymous, splice site, and indel variants of which 323 satisfied the frequency filtration criteria described above. Of those variants, 34 were de novo dominant or recessive (homozygous or compound heterozygous). Genes carrying those variants were further evaluated for human disease or animal models overlapping with the phenotype. Only one gene, *FBXL4,* was identified to be significant based on the human phenotype already associated with *FBXL4* variants and the protein's mitochondrial function.

Both S1 and S2 were found to have three variants in *FBXL4* (Fig. 3b–d). Two variants in the leucine-rich repeat domains were inherited from the mother: Chr6:99322230 (hg19):NM_012160:exon9: c.1790 A>C:p. Gln597Pro and Chr6:99323582 (hg19):NM_012160:exon8: c.1411G>A:p. Ala471Thr. The paternal variant present in both affected siblings was Chr6:99323407 (hg19):NM_012160:exon8: c.1586C>A:p. Ala529Glu.

The unaffected sibling carried both the maternal variants but not the paternal variant. In the ExAC database, the variant p. Gln597Pro is present in heterozygous state in two controls (allele frequency of 0.000016), while the other two variants (p. Ala471Thr and p. Ala529Glu) are absent. Both p. Ala471Thr and p. A529E variants have not been previously seen in patients with *FBXL4*-related disease. All the three variants were predicted to be pathogenic by MutationTaster, while the polyphen-2 and SIFT software programs deemed the Gln597Pro and Ala529Glu variants pathogenic and Ala471Thr benign. All three amino acid residues are very well conserved among the vertebrates (Fig. 3e).

FBXL4 belongs to the F-box protein family, containing an approximately 40-amino acid motif, the F-box in the N-terminus. The C-terminus of FBXL4 contains at least nine tandem leucine-rich repeats (LRR), which is similar to the LRR domain of S-phase kinase-associated protein 2 (SCF Skp2) with more than 40% similarity, suggesting the overall structure of FBXL4 LRR domain is similar to that of Skp2 LRR domain. Based on the structure of Skp2 LRR domain (PDB code: 2ASS), we built a structural model of FBXL4 LRR domain with the highlights of three altered residues using PyMOL (The PyMOL Molecular Graphics System) (Fig. 3f). In the model, a Skp2 LRR binding partner, cyclin-dependent kinases regulatory subunit 1 (CKS1), is shown in gray to suggest the hypothetical position of binding partners of FBXL4 LRR domain. Colored in red, Gln597 is located at the loop near the potential binding partner. A mutation at residue 597 likely affects the binding of FBXL4 to its binding partners. Residues Ala471 in purple and Ala529 in blue are at the back of the LRR domain. Mutations at these two residues might change the structural stability or orientation of the leucine-rich repeats, which can subsequently disrupt the function of FBXL4.

Mitochondrial DNA Depletion Assay

Clinical diagnostic testing of the frozen muscle tissue for mtDNA depletion (MNG Laboratories, Atlanta, GA) revealed a statistically significant depletion of mtDNA relative to nuclear DNA, with a prolonged quantitative PCR mtDNA/18S DNA amplification time ratio of 0.8 (mean 0.68; 95th percentile 0.75), a test in which the higher ratio indicates decreased mtDNA copy number.

Discussion

Previous studies have identified 25 mutations in *FBXL4* that were associated with mitochondrial diseases (Bonnen et al. 2013; Gai et al. 2013; Huemer et al. 2015; van Rij et al. 2016; Barøy et al. 2016). Common clinical phenotypes include hypotonia, cerebral atrophy, developmental delay, and episodic lactic acidemia with or without hyperammonemia. Here we report a case of two siblings who shared three genetic variants in *FBXL4* and presented with hyperammonemia, depletion of TCA intermediates in urine, low plasma aspartate levels, poor feeding, and frequent vomiting in addition to the shared characteristics mentioned above. We hypothesize that the depletion of TCA cycle intermediates contributed our patients' frequently low aspartate levels, which then led to secondary urea cycle dysfunction and resulted in hyperammonemia. Given the known role of FBXL4 in protein ubiquitination, it is also possible that FBXL4 participates directly in ubiquitination of proteins related to the urea cycle.

One of the *FBXL4* variants (p. Gln597Pro) found in this sibling pair has been previously identified in a 9-year-old girl from a previous case series (Gai et al. 2013). Interestingly, she presented with relatively mild disease and was alive at 8 years of age. She also carried a deleterious frame-shift mutation in *FBXL4*, so the

Gln597Pro mutation is likely to have some residual function given her relatively long survival. Though there are relatively few cases reported from which to draw genotype-phenotype correlations, it seems that the presence of three *FBXL4* variants in our patients increased their disease severity.

Patients with *FBXL4* mutations have been found to have additional clinical features not commonly associated with mitochondrial encephalomyopathy such as IUGR and microcephaly. In the recent review of mitochondrial encephalomyopathy due to *FBXL4* mutation, the mean age at presentation was 115 days, and 11 of 18 patients had survived to a median follow-up time of 46 months (Huemer et al. 2015). The phenotypes of the siblings described here represent a more extreme presentation of the *FBXL4* disease spectrum as evidenced by the early presentation, short lifespan, and presence of other significant metabolic derangement in the form of severe hyperammonemia.

The early treatment of our second patient's neonatal hyperammonemia with supplemental citrate and aspartate appears to have been effective, such that she did not require treatment with sodium phenyl acetate and sodium benzoate during the neonatal period, as was needed by her older sibling. Its successful use here suggests possible consideration of the same treatment for other patients with FBXL4 deficiency. Elevations of TCA cycle intermediates are generally observed in patients with mitochondrial disease, so the deficiency in TCA cycle intermediates in these patients may suggest a more direct role for FBXL4 function in the TCA cycle. This may be why our patients responded well to supplementation of TCA cycle intermediates.

Other genes have been associated with syndromes of early-onset mitochondrial encephalopathy with hyperammonemia. Recently, a family with multiple members presenting with lethargy, lactic acidosis, and hyperammonemia were found to have a deficiency of carbonic anhydrase VA (van Karnebeek et al. 2014). The hyperammonemia resolved with supplementation of carglumic acid, indicating that there were effects on both oxidative phosphorylation and urea cycle metabolism as in the cases presented here. However, the mechanism of hyperammonemia in that case is presumed to be due to decreased intracellular bicarbonate inhibiting urea cycle initiation. In these siblings with genetic variants in *FBXL4*, ongoing supplementation with citric acid and aspartate leads to temporary resolution of lactic acid and hyperammonemia. We hypothesize that this contributed to resolving both abnormalities because aspartate is required to provide nitrogen to form argininosuccinate in the urea cycle and therefore its depletion may be contributing to the hyperammonemia. Identification of additional patients with deleterious *FBXL4* variants will help associate specific mutations with the range of disease phenotypes.

Conclusion

In summary, we describe two siblings with three missense variants in *FBXL4* presenting with lactic acidosis and hyperammonemia. This case report expands the phenotype of FBXL4-associated mitochondrial encephalomyopathy to include early, severe hyperammonemia in the setting of TCA cycle disruption. This finding points to an expanded role for FBXL4 beyond oxidative phosphorylation. Further studies into the role of FBLX4 in TCA and urea cycle chemistry could help to guide directed therapy for patients with *FBXL4* mutations, given the improvement noted with supplementation of citric acid and aspartate.

Acknowledgments The authors will like to thank the family for their support and enrollment. This work was made possible by grants from the following institutions: PBA was supported by 1R01AR068429-01 from the National Institute of Arthritis and Musculoskeletal and Skeletal Diseases (NIAMS) of National Institute of Health (NIH) and U19HD077671 from NICHD/NHGRI/NIH. SUM was supported by T32 HD7466-19 awarded to the Newborn Medicine Division at BCH. The Manton Center for Orphan Disease Research Gene Discovery Core, Boston Children's Hospital, also supported the work. Sanger sequencing was performed by the Molecular Genetics Core Facility of the IDDRC at Boston Children's Hospital, supported by National Institutes of Health grant P30 HD18655.

Synopsis

FBXL4 variants are associated with mitochondrial encephalopathy, and this report expands upon the known phenotype by describing a sibling pair with early-onset mitochondrial encephalopathy complicated by hyperammonemia associated with low-normal aspartate levels.

Compliance with Ethics Guidelines

Sarah Morton, Edward Neilan, Roy Peake, Jiahai Shi, Klaus Schmitz-Abe, Meghan Towne, Kyriacos Markianos, Sanjay Prabhu, and Pankaj Agrawal declare that they have no conflict of interest.

All procedures followed were in accordance with the ethical standards of the responsible committee on human experimentation (institutional and national) and with the Helsinki Declaration of 1975, as revised in 2000. Informed consent was obtained from the parents of the children included in the study.

Author Contributions: Drs. Morton, Neilan, and Agrawal had full access to all of the data in the study and took responsibility for the integrity of the data and the accuracy of the data analysis. Study concept and design: Morton, Neilan, Agrawal. Acquisition of Data: Morton, Neilan, Towne,

Agrawal. Analysis and interpretation of data: Morton, Neilan, Peake, Shi, Schmitz-Abe, Markianos, Agrawal. Drafting of the manuscript: Morton, Neilan, Agrawal. Critical revision of the manuscript for important intellectual content: All authors. Statistical analysis: Schmitz-Abe, Markianos. Obtained funding: Agrawal. Administrative, technical, or material support: Towne, Agrawal. Study supervision: Morton, Neilan, Agrawal.

References

Antoun G, McBride S, Vanstone JR et al (2015) Detailed biochemical and bioenergetic characterization of FBXL4-related encephalomyopathic mitochondrial DNA depletion. JIMD Rep. doi:10.1007/8904_2015_491

Barøy T, Pedurupillay CRJ, Bliksrud YT et al (2016) A novel mutation in FBXL4 in a Norwegian child with encephalomyopathic mitochondrial DNA depletion syndrome 13. Eur J Med Genet 59:342–346. doi:10.1016/j.ejmg.2016.05.005

Bonnen PE, Yarham JW, Besse A et al (2013) Mutations in FBXL4 cause mitochondrial encephalopathy and a disorder of mitochondrial DNA maintenance. Am J Hum Genet 93:471–481. doi:10.1016/j.ajhg.2013.07.017

Ebrahimi-Fakhari D, Seitz A, Kölker S, Hoffmann GF (2015) Recurrent stroke-like episodes in FBXL4-associated early-onset mitochondrial encephalomyopathy. Pediatr Neurol 53:549–550. doi:10.1016/j.pediatrneurol.2015.08.018

El-Hattab AW, Scaglia F (2013) Mitochondrial DNA depletion syndromes: review and updates of genetic basis, manifestations, and therapeutic options. Neurotherapeutics 10:186–198. doi:10.1007/s13311-013-0177-6

Gai X, Ghezzi D, Johnson MA et al (2013) Mutations in FBXL4, encoding a mitochondrial protein, cause early-onset mitochondrial encephalomyopathy. Am J Hum Genet 93:482–495. doi:10.1016/j.ajhg.2013.07.016

Huemer M, Karall D, Schossig A, Abdenur JE (2015) Clinical, morphological, biochemical, imaging and outcome parameters in 21 individuals with mitochondrial maintenance defect related to FBXL4 mutations. J Inherit Metab Dis 38(5):905–914. doi:10.1007/s10545-015-9836-6

Mochel F, DeLonlay P, Touati G et al (2005) Pyruvate carboxylase deficiency: clinical and biochemical response to anaplerotic diet therapy. Mol Genet Metab 84:305–312. doi:10.1016/j.ymgme.2004.09.007

Tang S, Wang J, Lee N-C et al (2011) Mitochondrial DNA polymerase gamma mutations: an ever expanding molecular and clinical spectrum. J Med Genet 48:669–681. doi:10.1136/jmedgenet-2011-100222

van Karnebeek CD, Sly WS, Ross CJ et al (2014) Mitochondrial carbonic anhydrase VA deficiency resulting from CA5A alterations presents with hyperammonemia in early childhood. Am J Hum Genet 94:453–461. doi:10.1016/j.ajhg.2014.01.006

Van Rechem C, Black JC, Abbas T et al (2011) The SKP1-Cul1-F-box and leucine-rich repeat protein 4 (SCF-FbxL4) ubiquitin ligase regulates lysine demethylase 4 A (KDM4A)/Jumonji domain-containing 2 A (JMJD2A) protein. J Biol Chem 286:30462–30470. doi:10.1074/jbc.M111.273508

van Rij MC, Jansen FAR, Hellebrekers DMEI et al (2016) Polyhydramnios and cerebellar atrophy: a prenatal presentation of mitochondrial encephalomyopathy caused by mutations in the FBXL4 gene. Clin Case Rep 4:425–428. doi:10.1002/ccr3.511

Winston JT, Koepp DM, Zhu C et al (1999) A family of mammalian F-box proteins. Curr Biol 9:1180–1182. doi:10.1016/S0960-9822(00)80021-4

JIMD Reports
DOI 10.1007/8904_2016_18

RESEARCH REPORT

Intracranial Hypertension in Cystinosis Is a Challenge: Experience in a Children's Hospital

Nieves Martín-Begué · Silvia Alarcón · Charlotte Wolley-Dod · Luis Enrique Lara · Álvaro Madrid · Paola Cano · Mireia del Toro · Gema Ariceta

Received: 25 July 2016 / Revised: 5 October 2016 / Accepted: 10 October 2016 / Published online: 18 November 2016

Abstract *Background*: Cystinosis is a rare systemic lysosomal disease affecting mainly the kidney and eye. Ocular involvement in cystinosis is universal being the presence of cystine crystals in the cornea a diagnostic criterion and one of the earliest manifestations of the disease. Neuro-ophthalmologic manifestations are considered a rare and late complication in these patients. The aim of this article is to report the unexpectedly high incidence of intracranial hypertension in children with cystinosis at our centre.

Methods: This study included eight children (0–16 years of age) with cystinosis seen at the paediatric ophthalmology department, Hospital Universitari Vall d'Hebron (Barcelona, Spain), a tertiary hospital, over the last 5 years.

Results: Three girls and five boys, mean age: 9.6 years (range: 5–14 years), were studied. During follow-up, 4 out of 8 developed papilledema and confirmed high cerebrospinal fluid (CSF) pressure. The only symptomatic child presented an Arnold–Chiari anomaly with enlarged ventricles, whereas the other three, all asymptomatic, were diagnosed by scheduled fundoscopy and had normal neuroimaging studies. All four patients had at least one known risk factor for developing intracranial hypertension: initiation of growth hormone therapy, tapering of corticosteroids, acute renal failure and Arnold–Chiari malformation. Two of them required a ventriculoperitoneal shunt.

Conclusions: Our results show that intracranial hypertension can occur more frequently than expected in patients with cystinosis. Furthermore, visual prognosis depends on early diagnosis and prompt treatment. A multidisciplinary approach is necessary, and we recommend fundoscopic examinations in all paediatric patients with cystinosis whether or not they present symptoms.

Abbreviations

CKD	Chronic kidney disease
CSF	Cerebrospinal fluid
GFR	Glomerular filtration rate
ICP	Increased intracranial pressure
IH	Intracranial hypertension
LP	Lumbar puncture
MRI	Magnetic resonance imaging
MRV	Magnetic resonance venography
PTCS	Pseudotumor cerebri syndrome
rhGH	Recombinant human growth hormone
VA	Visual acuity

Introduction

Cystinosis (OMIM #219800) is a rare systemic lysosomal disease that mainly affects the kidney and eye. It is an autosomal recessive disease caused by mutations of the

Communicated by: Carla E. Hollak, M.D.

My co-authors have all contributed to this manuscript: planning, conducting and reporting of the work described in the article, and approval of this submission.

N. Martín-Begué (✉) · S. Alarcón · C. Wolley-Dod
Department of Paediatric Ophthalmology, Hospital Vall d'Hebron, Barcelona, Spain
e-mail: nmartin@vhebron.net

L.E. Lara · Á. Madrid · P. Cano · M. del Toro · G. Ariceta
Department of Paediatric Nephrology, Hospital Vall d'Hebron, Barcelona, Spain

P. Cano
Department of Paediatric Neurosurgery, Hospital Vall d'Hebron, Barcelona, Spain

M. del Toro
Department of Paediatric Neurology, Hospital Vall d'Hebron, Barcelona, Spain

CTNS gene (Touchman et al. 2000), with an estimated incidence of 1 in 100,000 live births. Most patients present with severe Fanconi syndrome from infancy and progressive renal impairment. Neurocognitive involvement is generally mild but very frequent, even in children. The primary cognitive deficits in these patients occur in the areas of visual-spatial ability, visual-motor coordination and short-term visual memory (Viltz and Trauner 2013). Prognosis depends on early diagnosis, and the prompt initiation of cysteamine treatment (Gahl and Nesterova 2010).

Ocular involvement is universal in cystinotic patients. The presence of cystine crystals in the cornea is a diagnostic criterion and one of the earliest manifestations. Crystals are also deposited in other ocular structures such as the conjunctiva, iris, choroid and retina (Richler et al. 1991; Dureau et al. 2003; Tsilou et al. 2007). Neuro-ophthalmologic manifestations are considered a rare and late complication in these patients (Nesterova and Gahl 2008).

Increased intracranial pressure (ICP) in children is often secondary to traumatic brain injury, hydrocephalus, brain tumours or intracranial infections. However, pseudotumor cerebri syndrome (PTCS) is uncommon in childhood, with an estimated incidence of 0.1–1 per 100,000. PTCS is a condition defined by elevated ICP in the absence of clinical, laboratory or radiologic evidence of infection, vascular abnormality, intracranial space-occupying lesion or hydrocephalus (Rangwala and Liu 2007; Friedman et al. 2013). PTCS has been reported in few patients with cystinosis; however, its real incidence remains unknown (Dogulu et al. 2004; Rogers and McGregor 2010).

The aim of this study was to report the unexpectedly high incidence of intracranial hypertension (IH) in children with cystinosis followed at our centre. We would like to discuss why patients with cystinosis have a higher incidence of IH and why IH is more severe than in the normal paediatric population.

Methods

The study included eight children with cystinosis followed at the paediatric ophthalmology department of a tertiary hospital, over the last 5 years. Cystinosis was confirmed in all cases with a white blood cell cystine content >1 nmol 1/2 cystine/mg protein and a positive genetic diagnosis. There were three girls and five boys with a mean age of 9.6 years (range: 5–14 years). During their regular ophthalmologic follow-up, 4 out of 8 developed papilledema (Table 1). Brain magnetic resonance imaging (MRI) with magnetic resonance venography (MRV) was performed in all cases with papilledema and, unless contraindicated, cerebrospinal fluid (CSF) pressure was measured by lumbar puncture (LP).

We had previously examined our patients annually; however, in January 2015 our protocol was changed to at least one visit every 3 months in five patients because they were enrolled in a clinical trial conducted locally to study the efficacy and safety of a new topical cysteamine formulation in viscous solution.

Results

Case 1: A 9-year-old girl was diagnosed with cystinosis at the age of 7 months. She had Fanconi syndrome and mild reduction in the glomerular filtration rate (GFR). Her chronic treatment included oral and topical cysteamine, vitamin D3, potassium and phosphate salt supplements, thiazides, carnitine, omeprazole, losartan and recombinant human growth hormone (rhGH) (0.34 mg/kg/week). She had been treated with rhGH for 3 years. Ophthalmologic examination 10 months previously had been unremarkable except for the presence of corneal crystals. She had complained of headache and loss of vision during the previous weeks as well as non-specific back pain. Ophthalmologic assessment showed visual acuity (VA) of 20/60 in her right eye and hand movements in her left eye, with a left relative afferent pupillary defect. Colour vision was severely impaired. Fundus examination revealed severe bilateral disc oedema (Fig. 1). MRI and MRV revealed an Arnold–Chiari anomaly and enlarged ventricles. Venous sinus thrombosis was ruled out. Owing to the Arnold–-Chiari anomaly, an LP was not done and neurosurgeons performed a continuous recording of CSF pressure. ICP was 30 cm of water (the normal value in children is ≤25 cm of water) (Friedman et al. 2013). Blood pressure and extensive coagulation studies were strictly normal. She was diagnosed with "fulminant" intracranial hypertension. Owing to the severity of the papilledema and significant visual loss, the patient underwent ventriculoperitoneal shunting within 1 week of diagnosis. Treatment with rhGH had been stopped at presentation. Unfortunately, VA and visual fields were severely affected. Fundus examination revealed optic disc atrophy and right macular atrophy.

Case 2: A 10-year-old boy was diagnosed with cystinosis at the age of 12 months, with a successful kidney transplant 12 months previously. His medications prior to admission included oral and topical cysteamine, tacrolimus, mycophenolic acid, methylprednisolone (on a tapering dose), enalapril, omeprazole and rhGH (0.36 mg/kg/week). Regular treatment with rhGH had been stopped immediately after transplantation but was resumed 2 weeks before our visit. Ophthalmologic examination 7 months before had

Table 1 Characteristics of patients with cystinosis and intracranial hypertension

Patients	Age (years)	Gender/age at diagnosis (months)	Genetic diagnosis	Cystine levels nmol ½ cys/mg prot	Serum Cr (mg/dL)	Renal status	BP (mmHg)	Risk factors IH
1	11	F/7	Homozygous/ 57Kbdel	1.75	0.86	CKD 2	116/63	Arnold–Chiari rhGH
2	10	M/12	Heterozygous/ 57Kbdel /297-312del16pb	2.7	1.6	K Tx (12 months before)	102/68	rhGH Corticosteroids (tapering) Acute renal failure
3	7	M/6	Homozygous/ 646dupA	4.09	0.66	K Tx (11 months before)	99/69	Corticosteroids (tapering)
4	6	M/20	Heterozygous 57Kbdel – c.682-1G>T	1.46	0.81	CKD 2	97/55	rhGH

BP blood pressure, *CKD* chronic kidney disease, *Cr* creatinine, *cys* cysteine, *F* female, *IH* intracranial hypertension, *K Tx* kidney transplant, *M* male, *prot* protein, *rhGH* recombinant human growth hormone

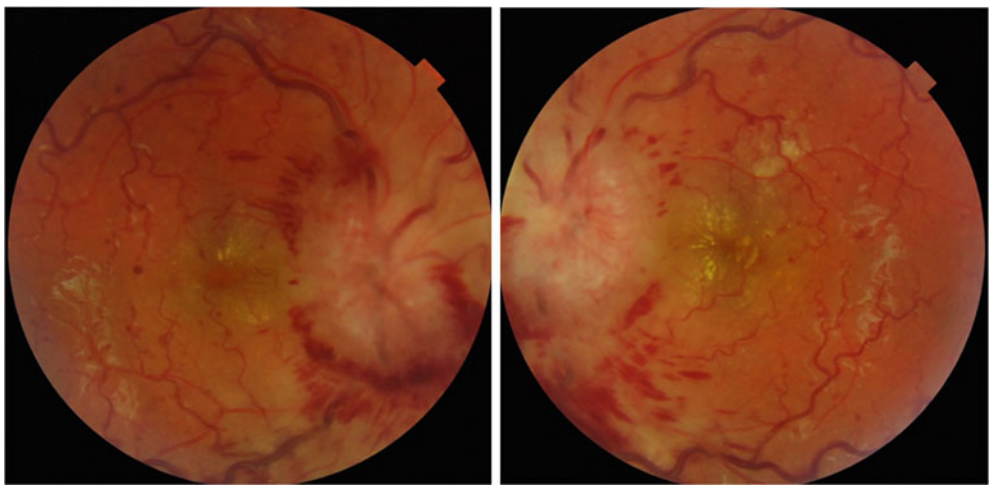

Fig. 1 Severe bilateral disc oedema with dilated veins, many exudates and multiple peripapillary and peripheral retinal haemorrhages in both eyes of Case 1 (right eye on the left and left eye on the right)

been unremarkable except for corneal crystals. The patient was evaluated by the ophthalmology department in order to be enrolled in our clinical trial. He often complained of epigastric pain, nausea and reflux and occasional headache that were attributed to the cystinosis itself or treatment-related side effects. Although ophthalmologic assessment showed normal VA, the optic discs were swollen. MRI and MRV revealed great distension of the perioptic subarachnoid space (Fig. 2). LP yielded an opening pressure of 36 cm of water with normal CSF composition. Routine laboratory tests revealed acute graft dysfunction attributed to acute rejection and treatment with rhGH was stopped. The patient received three IV pulses of methylprednisolone and oral acetazolamide. However, the acetazolamide caused severe metabolic acidosis and had to be stopped. Corticosteroids were not sufficiently effective to control IH and the patient required ventriculoperitoneal shunting. Fortunately, his renal function improved. His VA is currently normal; however, the visual field shows an enlarged blind spot and fundus examination reveals mild optic disc atrophy.

Case 3: A 7-year-old boy was diagnosed with cystinosis at 6 months of age. He had had a successful kidney transplant 11 months before the visit. His medication included oral and topical cysteamine, tacrolimus, mycophenolic acid,

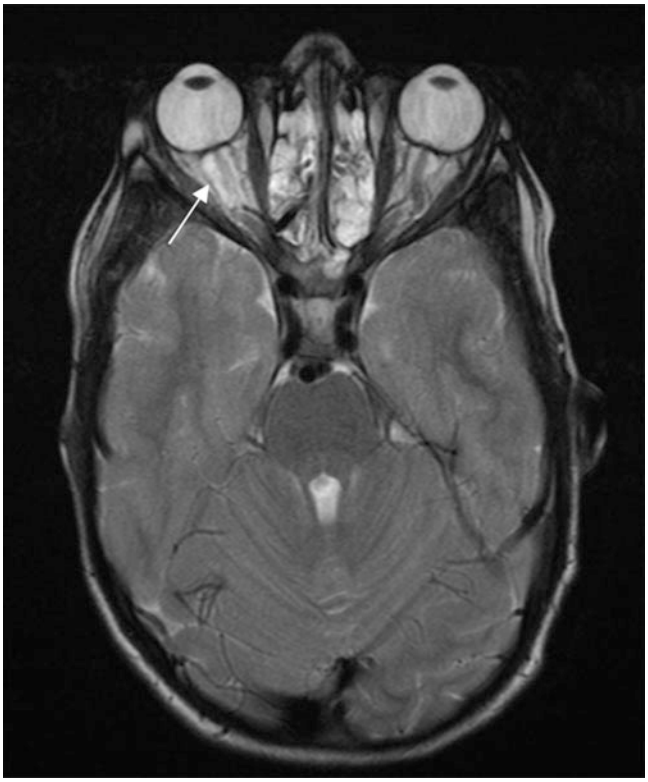

Fig. 2 MRI T2-weighted axial image showing distension of the perioptic subarachnoid space (*arrow*) and flattening of the posterior aspect of the globe in Case 2

methylprednisolone (on a tapering dose), losartan and labetalol. Ocular examination 2 months previously had been normal, except for corneal crystals. He was seen at a scheduled visit for our clinical trial with no visual or systemic complaints. His VA was normal but fundus examination showed bilateral optic disc swelling. MRI and MRV were unremarkable and LP revealed an opening pressure of 37 cm of water with normal CSF composition. Treatment was initiated with oral acetazolamide (8 mg/kg/day) b.i.d. and corticosteroids (0.5 mg/kg/day). Low doses of acetazolamide were administered as the patient developed severe metabolic acidosis requiring large doses of oral sodium bicarbonate. A follow-up visit 1 month later revealed normal optic discs. VA and visual field were also normal.

Case 4: A 6-year-old boy was diagnosed with cystinosis at the age of 20 months. His medication prior to admission included oral and topical cysteamine, vitamin D3, candesartan and rhGH (0.3 mg/kg/week) that had been started 4 weeks earlier. Ocular examination 1 month previously had been normal, except for corneal crystals. Papilledema was detected during a routine eye examination at a scheduled visit in our clinical trial. MRI and MRV were unremarkable except for mild distension of the perioptic subarachnoid space and a partially empty sella. LP revealed an opening pressure of 25 cm of water with normal CFS composition. rhGH was stopped and treatment was initiated with oral acetazolamide (2.5 mg/kg/day) b.i.d. A follow-up visit 1 month later revealed normal optic discs and his VA was also normal. Visual fields were not performed because of his young age.

Discussion

Intracranial hypertension is considered a rare and late complication in patients with cystinosis. However, two reports suggested a higher incidence of PTCS in patients with cystinosis than in the general population: Dogulu et al. (2004) found an estimated frequency of 5% of PTCS in their study of approximately 150 patients and Rogers and McGregor (2010) reported three patients out of six with PTCS. In our series, 4 out of 8 children developed intracranial hypertension, three had PTCS and the fourth a pathologic MRI.

Cystinosis is a multisystemic disease and patients are treated with several different drugs. Many potential risk factors are associated with the development of secondary PTCS: renal failure, vitamin D deficiency, treatment with rhGH, thyroxine and calcineurin inhibitors, and tapering of

steroids. Also, cystinosis per se may play a primary role in the development of IH as the deposit of cystine in meninges and arachnoid villi may reduce CSF absorption (Viltz and Trauner 2013; Parnes et al. 2008; Ross et al. 1982). Furthermore, Rao et al. (2015) reported that children with cystinosis have a 12-fold higher prevalence of Chiari I malformations than the general paediatric population. Poor metabolic disease control may also contribute to IH, as observed in two of our patients (Cases 2 and 3) who maintained elevated cystine levels despite maximum cysteamine doses. A relationship between the preservation of renal glomerular function and compliance with cysteamine treatment has also been reported (Nesterova et al. 2015), and we thought it could also have a relationship with IH.

Furthermore, treatment with cysteamine may also contribute to IH development since it is described as a potential adverse effect on the prescription drug labelling (PROCYSBI® (cysteamine bitartrate) delayed-release capsules. Label information). However, in our opinion, it is difficult to establish a cause-and-effect relationship between cysteamine treatment and IH as many other risk factors coincide at the same time in these patients.

It is important to note the association of rhGH therapy and PTCS (Rogers et al. 1999). Reeves and Doyle (2002) reported the prevalence in the GH-treated population to be approximately 100 times higher than in the general paediatric population. Temporary discontinuation of rhGH is required, with a later prescription at a lower dose which usually prevents the reappearance of IH. Children with chronic kidney disease (CKD) treated with rhGH are more likely to develop PTCS than those with other primary diseases (Reeves and Doyle 2002; Koller et al. 1997; Blethen et al. 1996). It is postulated that the antidiuretic effect of rhGH could be the cause of IH and that effect could be more evident in patients with a decreased GFR (Souza and Collett-Solberg 2011). Alternatively, or in addition, GH may cross the blood–brain barrier and raise local levels of insulin-like growth factor I which, in turn, increases CSF production from the choroid plexus (Darendeliler 2009). In children with cystinosis, this mechanism could trigger other concurrent risk factors such as reduced posterior cranial space and CSF flow obstruction caused by cystine crystals.

Our patients were receiving rhGH doses between 0.3 and 0.36 mg/kg/week, the standard doses in children with CKD, owing to growth hormone resistance. Therefore, IH in cystinosis could be due not only to rhGH treatment but also to the higher doses used. This could explain why patients 2 and 4 developed IH within the first 4 weeks of rhGH treatment. However, patient 1 developed that complication after 3 years of rhGH treatment, and the causal relationship between rhGH and IH is thus difficult to establish in this case and could be related to Arnold–Chiari malformation. Malozowski et al. (1995) reported that higher doses and increased frequency of administration since the introduction of rhGH in 1985 may be contributing to the development of IH in some patients. However, Reeves and Doyle (2002) found no relationship between the rhGH dose and IH development.

Severe growth retardation is a clinical hallmark in children with cystinosis. In the literature, rhGH treatment in those patients has been reported to be safe and effective (Wühl et al. 2001; Besouw et al. 2012); thus, the possible adverse effects of rhGH observable in a few patients should be weighed against the known treatment benefits before initiating therapy, and rigorous controls should be programmed.

Furthermore, patients with cystinosis have many risk factors and their renal disease may complicate the use of conventional IH treatment. Since acetazolamide in our patients caused significant metabolic acidosis owing to persistent or residual Fanconi syndrome, we recommend low doses. Half of our patients needed a ventriculoperitoneal shunt. Case 1 presented “fulminant” IH with acute presentation of profound vision loss and severe papilledema becoming legally blind despite prompt treatment. Overall, our results show that IH in patients with cystinosis is more aggressive than in paediatric patients with IH. Nevertheless, in Cases 3 and 4, prompt diagnosis led to the resolution of papilledema without visual damage with systemic treatment alone.

Another important issue we wish to emphasize is that some of the clinical manifestations in these patients may be attributable to their renal disease or their medications rather than to IH, which can delay the diagnosis. Nausea and vomiting could be non-specific symptoms of cystinosis secondary to the deposition of crystals in the digestive system. Side effects of oral cysteamine include nausea, vomiting and headache, with the latter also being a main complaint in IH. It is important to remember that, among young children with IH, headache is less common than in adults and they are more often asymptomatic.

An important limitation of our study was the small case series, and it cannot be assumed that all patients with cystinosis have the same risk.

Conclusion

Ophthalmologists are used to being concerned about cystine crystals in the cornea and retina; however, we must become more aware of the possibility of optic nerve disease.

Our results show that IH can occur more frequently than expected in patients with cystinosis. A multidisciplinary approach is necessary since these patients present many risk

factors and their renal disease may also complicate the use of conventional IH treatment. The prescription of rhGH in cystinosis is almost universal, but we recommend starting at the lowest effective dose, with gradual increases up to the therapeutic dose.

Visual prognosis depends on early diagnosis and prompt treatment which cannot rely on clinical symptoms alone. We recommend regular and standardized fundoscopic examinations especially in children with risk factors, such as initiation of rhGH, tapering of corticosteroids and treatment with calcineurin inhibitors after kidney transplantation.

Take-Home Message

Intracranial hypertension is an unexpected complication in patients with cystinosis and regular fundoscopic examinations are recommended to rule out papilledema.

Compliance with Ethics Guidelines

Conflict of Interest

Nieves Martín-Begué, Silvia Alarcón, Charlotte Wolley-Dod, Luis Enrique Lara, Álvaro Madrid, Paola Cano, Mireia del Toro and Gema Ariceta declare that we have no conflict of interest.

Informed Consent

All procedures followed were in accordance with the ethical standards of the responsible committee on human experimentation (institutional and national) and with the Helsinki Declaration of 1975, as revised in 2000 (5). Informed consent was obtained from all patients for being included in this study. Additional informed consent was obtained from all patients (or from their parents) for which identifying information is included in this article.

References

Besouw MT, Van Dyck M, Francois I et al (2012) Detailed studies of growth hormone secretion in cystinosis patients. Pediatr Nephrol 27:2123–2127

Blethen SL, Allen DB, Graves D et al (1996) Safety of recombinant deoxyribonucleic acid-derived growth hormone: the national cooperative growth study experience. J Clin Endocrinol Metal 81: 1704–1710

Darendeliler F (2009) Safety of growth hormone treatment. J Clin Res Pediatr Endocrinol 1:36–43

Dogulu CF, Tsilou E, Rubin B et al (2004) Idiopathic intracranial hypertension in cystinosis. J Pediatr 145:673–678

Dureau P, Broyer M, Dufier J (2003) Evolution of ocular manifestations in nephropathic cystinosis: a long-term study of a population treated with cysteamine. J Pediatr Ophthalmol Strabismus 40:142–146

Friedman DI, Liu GT, Digre KB (2013) Revised diagnostic criteria for the pseudotumor cerebri syndrome in adults and children. Neurology 81:1159–1165

Gahl WA, Nesterova G (2010) Cystinosis: the post-transplant era. Eur Nephrol 4:55–61

Koller EA, Stadel BV, Malozowski SN (1997) Papilledema in 15 renally compromised patients treated with growth hormone. Pediatr Nephrol 11:451–454

Malozowski S, Tanner SA, Wysowski DK et al (1995) Benign intracranial hypertension in children with growth hormone deficiency treated with growth hormone. J Pediatr 126:996–999

Nesterova G, Gahl W (2008) Nephropathic cystinosis: late complications of a multisystemic disease. Pediatr Nephrol 23:863–878

Nesterova G, Williams C, Bernardini I et al (2015) Cystinosis: renal glomerular and renal tubular function in relation to compliance with cysteine-depleting therapy. Pediatr Nephrol 30: 945–951

Parnes A, Wassner SJ, Weinstein JM (2008) A case of intracranial hypertension and papilledema associated with nephropathic cystinosis and ocular involvement. Binocul Vis Strabismus Q 23: 37–40

PROCYSBI® (cysteamine bitartrate) delayed-release capsules. Label information. Summary of product characteristics. http://www.ema.europa.eu/docs/en_GB/document_library/EPAR_Product_Information/human/002465/WC500151313.pdf. Accessed 22 Jan 2016

Rangwala LM, Liu GT (2007) Pediatric idiopathic intracranial hypertension. Surv Ophthalmol 52:597–617

Rao KI, Hesselink J, Trauner DA (2015) Chiari I malformation in nephropathic cystinosis. J Pediatr 167:1126–1129

Reeves GD, Doyle DA (2002) Growth hormone treatment and pseudotumor cerebri: coincidence or close relationship? J Pediatr Endocrinol Metab 15:723–730

Richler M, Milot J, Quigley M et al (1991) Ocular manifestations of nephropathic cystinosis: the French-Canadian experience in a genetically homogeneous population. Arch Ophthalmol 109: 359–362

Rogers AH, Rogers GL, Bremer DL et al (1999) Pseudotumor cerebri in children receiving recombinant human growth hormone. Ophthalmology 106:1186–1190

Rogers DL, McGregor ML (2010) Increased intracranial pressure in patients with cystinosis. J Pediatr Ophthalmol Strabismus 47: e1–e3

Ross DL, Strife CF, Towbin R et al (1982) Nonabsorptive hydrocephalus associated with nephropathic cystinosis. Neurology 32: 1330–1334

Souza FM, Collet-Solberg PF (2011) Adverse effects of growth hormone replacement therapy in children. Arq Bras Endocrinol Metab 55: 559–565

Touchman JW, Anikster Y, Diatrich NL et al (2000) The genomic region encompassing the nephropathic cystinosis gene (CTNS): complete sequencing of a 200-Kb segment and discovery of a novel gene within the common cystinosis-causing deletion. Genome Res 10:165–173

Tsilou E, Zhou M, Gahl W et al (2007) Ophthalmic manifestations and histopathology of infantile nephropathic cystinosis: report of a case and review of the literature. Surv Ophthalmol 52:97–105

Viltz L, Trauner DA (2013) Effect of age at treatment on cognitive performance in patients with cystinosis. J Pediatr 163:489–492

Wühl E, Haffner D, Offner G et al (2001) European Study Group on Growth hormone treatment in children with nephropathic cystinosis: Long-term treatment with growth hormone in short children with nephropathic cystinosis. J Pediatr 138:880–887

JIMD Reports
DOI 10.1007/8904_2016_19

CASE REPORT

Severe Respiratory Acidosis in Status Epilepticus as a Possible Etiology of Sudden Death in Lesch–Nyhan Disease: A Case Report and Review of the Literature

Alison Christy • William Nyhan • Jenny Wilson

Received: 08 August 2016 / Revised: 18 October 2016 / Accepted: 21 October 2016 / Published online: 18 November 2016

Abstract *Introduction*: Lesch–Nyhan disease (LND) is an X-linked disorder of purine metabolism, associated with self-mutilation, dystonia, and chorea. Seizures are uncommon in LND. Patients with LND are at risk for sudden and unexpected death. The etiology of this is unknown, but appears to occur from a respiratory process. We propose that respiratory failure secondary to subclinical seizure may lead to sudden death in these patients.

Case: We report a case of an 11-year-old boy with LND who had two episodes of nocturnal gasping. The second event was immediately followed by a 10 min generalized seizure. Upon arrival at the hospital, an arterial blood gas test revealed a severe respiratory acidosis. Following aggressive treatment of his seizures, this patient did well, and was discharged home on oxcarbazepine with rectal diazepam. No further seizures have been noted in 1 year of follow-up.

Conclusions: In this case report and review, we hypothesize that sudden death from respiratory failure in Lesch–Nyhan disease may in some cases be due to seizure-induced respiratory failure, akin to sudden unexpected death in epilepsy (SUDEP). We suggest screening for paroxysmal respiratory events; consideration of electroencephalography for patients with LND presenting in respiratory distress or failure; and consideration of more aggressive treatment of seizures in these patients.

Brief Summary:

We present an 11-year-old boy with Lesch–Nyhan disease (LND) who developed respiratory failure and severe respiratory acidosis from his first known seizure, which evolved to subclinical status epilepticus. We propose that patients with LND have a predisposition to respiratory failure and sudden death, which in some cases may be provoked by seizure (sudden unexpected death in epilepsy, or SUDEP).

Communicated by: William Ross Wilcox, MD, PhD

Competing interests: None declared

A. Christy (✉) · J. Wilson
Department of Pediatric Neurology, Oregon Health and Science University, Mail Code CDRC-P, 707 SW Gaines Street, Portland, OR 97239, USA
e-mail: christy@ohsu.edu

W. Nyhan
Department of Pediatrics, University of California, 9500 Gilman Drive #0830, La Jolla, San Diego, CA 92093, USA

Introduction

Lesch–Nyhan disease (LND) is an X-linked recessive disorder resulting from a deficiency in hypoxanthine–guanine phosphoribosyl transferase (HPRT). This disorder of purine metabolism leads to overproduction of hypoxanthine and uric acid. Patients develop nephrolithiasis, gouty arthritis, and neurological manifestations including dystonia, choreoathetosis, ballismus, and a behavioral disease that includes disinhibited behavior and severe, stereotyped self-injury. Epilepsy may occur in LND, with estimates ranging from 2–3% (Jinnah et al. 2006; Jinnah et al. 2010); however, other studies have found a risk of seizure up to 30%, although this may be due to misinterpretation of abnormal movements as seizure (de Gemmis et al. 2010; Markowski-Leeman and Jinnah 2013). Seizures in LND usually begin in childhood, and are typically classified as generalized tonic-clonic (Jinnah et al. 2006).

Historically, many patients with LND died early of aspiration pneumonia, renal failure or urosepsis, though some patients with LND have been noted to die suddenly.

Table 1 Case studies of sudden death in Lesch Nyhan syndrome

Case	Author	Heralding events	Known seizures	Circumstances of death	Age of death (years)	Autopsy	Cause of death
1	Hoefnagel et al. (1965)	None	N	After an attack of acute abdominal pain	13	N	Unknown
2	Hoefnagel et al. (1965)	Two prior generalized seizures	Y	Died after generalized seizure and vomiting	8	N	Unknown
3	Basserman et al. (1979)	None	N	Sudden death in sleep after a few days with fevers to 38 °C and poor intake	7	Y	Cardiac dilation: assumed to be caused by cardiac failure as a result of viral infection
4	Watts et al. (1982)	Recurrent episodes of flaccid tetraparesis	N	Sudden death in sleep, found "twisted," with emesis	18	Y	Brain and spinal cord with non-specific signs of anoxia
5	Mizuno (1986)	Intermittent abdominal pain	N	Died suddenly while writing a letter	19	N	Unknown
6	Mizuno (1986)	None	N	Sudden death in sleep	7	Y	No cause identified
7	Neychev and Jinnah (2006)	Four episodes of respiratory arrest with coma after emesis	N	Sudden death in sleep	15	N	Unknown
8	Neychev and Jinnah (2006)	One episode of unexplained respiratory arrest	N	Sudden death	45	N	Unknown
9	Neychev and Jinnah (2006)	None	N	Sudden death	41	Y	No cause identified
10	Neychev and Jinnah (2006)	One episode of unexplained apnea and arrest	N	Sudden death	34	Y	No cause identified
11	Neychev and Jinnah (2006)	None	N	Respiratory arrest and coma; remained comatose until death	21	N	Unknown

N none, *Y* yes

Case studies of sudden death in LND (Table 1) have posited a variety of putative respiratory mechanisms, including aspiration, laryngospasm, and central apnea (Neychev and Jinnah 2006). Though the frequency of this phenomenon is uncertain, one report of ten patients with LND, followed for 3–19 years, reported two sudden deaths (Mizuno 1986). Sleep-related respiratory abnormalities, including sleep apnea, are not common in this disease, although a decrease in slow wave and REM sleep with abnormal sleep-associated body movements has been described (Saito et al. 1998). The underlying etiology of sudden death in LND is unknown.

We present an 11-year-old boy with LND who presented in subclinical status epilepticus with severe respiratory failure as a "near-miss" of sudden death in LND. We hypothesize that patients with LND may be at increased risk of respiratory failure, which in some cases may be provoked by seizure.

Case Presentation

In the early morning on the day of presentation, the 11-year-old boy's parents heard "hiccupping" or gasping from his room. He was found pale and unresponsive and was given a rescue breath. When emergency personnel arrived, he was alert with normal oxygen saturations. He was brought to the emergency department where aspiration was suspected but chest X-ray was negative. He was discharged home.

Later that morning, he had another episode of gasping, followed by a convulsive seizure. The seizure stopped after 10 min without intervention, but afterwards the patient was unresponsive and apneic. He was taken back to the emergency department, where providers saw no respiratory effort, and decided to intubate. He seized again and was loaded with 15 mg PE (phenytoin equivalent)/kg fosphenytoin. Venous blood gas revealed significant respiratory

acidosis (pH 6.9, pCO_2 >110 mmHg, HCO_3 27 mmol/L), with a lactate of 3.3 mmol/L. He had a white blood cell count of 32 Kcu/mm, normal electrolytes and liver function, and a mild elevation in creatinine (0.74 mg/dl). Due to concern for meningitis in the setting of new-onset seizures, he was started on antibiotics. His cerebrospinal fluid was unremarkable, and antibiotics were stopped when cultures returned negative.

After transfer to the pediatric intensive care unit, he was placed on continuous electroencephalographic (EEG) monitoring which revealed subclinical status epilepticus with alternating unilateral frontotemporal seizures (Fig. 1). The interictal background showed moderate generalized slowing. His seizures were treated with benzodiazepines, fosphenytoin (5 mg PE/kg/day), and valproate (5 mg/kg every 6 h). Seizures decreased in frequency and stopped approximately 18 h after admission. EEG monitoring was continued for another two days, with no recurrence of electrographic seizures.

Magnetic resonance imaging (MRI) of his brain, done with and without contrast, was notable for T2 diffusion-restriction and increased T2 fluid attenuation inversion recovery (FLAIR) signal in the bilateral hippocampi (Fig. 2). No other acute abnormalities or underlying structural abnormalities were identified on his MRI of the brain. An MRI C-spine was included given his respiratory failure and hyperreflexia on exam, and a reported association of LND with atlantoaxial instability (Shewell and Thompson 1996), but this was normal. His urine purines showed a hypoxanthine level of 403.3 mmol/mol creatinine (normal range 0–38.6).

After extubation he remained in the hospital for two days, with no further respiratory concerns or clinical seizures. He returned to his baseline level of function prior to discharge. He was discharged on oxcarbazepine and has had no further seizures on this medication for the last year.

During a sleep study performed 10 months after discharge, the patient had normal oxygen saturation during sleep with no obstructive apneas, central apneas, or hypopneas recorded. Sleep efficiency was reduced (69%; normal 75–85%). There was an increase in deep or N3 sleep (51%; normal 15–25%).

Past Medical History

The patient was initially diagnosed with cerebral palsy, but by age 3, he developed self-mutilatory behaviors, including finger-biting and lip-biting. He was diagnosed with LND initially by HPRT assay. Genetic testing revealed a large deletion in the HPRT1 gene, involving exons 7 through 9. He was maintained on allopurinol. He had a normal routine EEG at 22 months of age which was performed for staring spells which were ultimately not felt to be seizure.

His family history is significant for a paternal familial facial myokymia that was reportedly studied at Shriner's Children's Hospital. His mother had seizures in childhood and was briefly on medication.

Discussion

We report the case of an 11-year-old boy with LND who presented with what appeared to be a primary respiratory event, which was ultimately found to be seizure-related. There are elements of this case that are atypical for LND. He has an unusual family history of maternal childhood seizures and paternal myokymia. Our patient's sleep study showed increased time spent in deep sleep, in contrast to previously described adult patients with LND who had diminished deep sleep (Saito et al. 1998), but did not show any central or obstructive apnea that could theoretically trigger a seizure. Convulsive seizures are uncommon in LND; however, the respiratory arrest and apnea that has been described preceding sudden death in LND (Table 1) sounds consistent with the semiology of this patient's subclinical seizures.

This raises the possibility that sudden death in LND could be a seizure-related phenomenon, akin to sudden death in epilepsy (SUDEP). SUDEP is a rare but known complication of epilepsy defined as a sudden, unexpected, witnessed or unwitnessed, non-traumatic, and non-drowning death that occurs in benign circumstances in an individual with epilepsy, with or without evidence for a seizure, and excludes documented status epilepticus, in which post-mortem examination does not reveal a cause of death (Nashef et al. 2012). SUDEP typically presents in patients with poorly controlled generalized convulsions, though seizures are hypothesized to contribute to sudden death in other situations such as sudden infant death syndrome (SIDS) or sudden unexplained death in childhood (SUDC) (Hesdorffer et al. 2015). Subclinical seizures can create profound post-ictal hypoxia and could theoretically lead to death (Maglajlija et al. 2012), particularly in a metabolically abnormal brain. Metabolic abnormalities can affect cardiorespiratory function, autonomic nervous responses, or neurotransmitter release, all posited to increase the risk of SUDEP (Devinsky et al. 2016).

Individuals with LND are at risk for sudden death, and our case suggests that seizure-related respiratory failure may be a possible mechanism. One prior case has been reported associated with known epilepsy (Hoefnagel et al.), though other cases had features which may have been suggestive of seizure (Watts et al.), and some were associated with prior unexplained episodes of respiratory

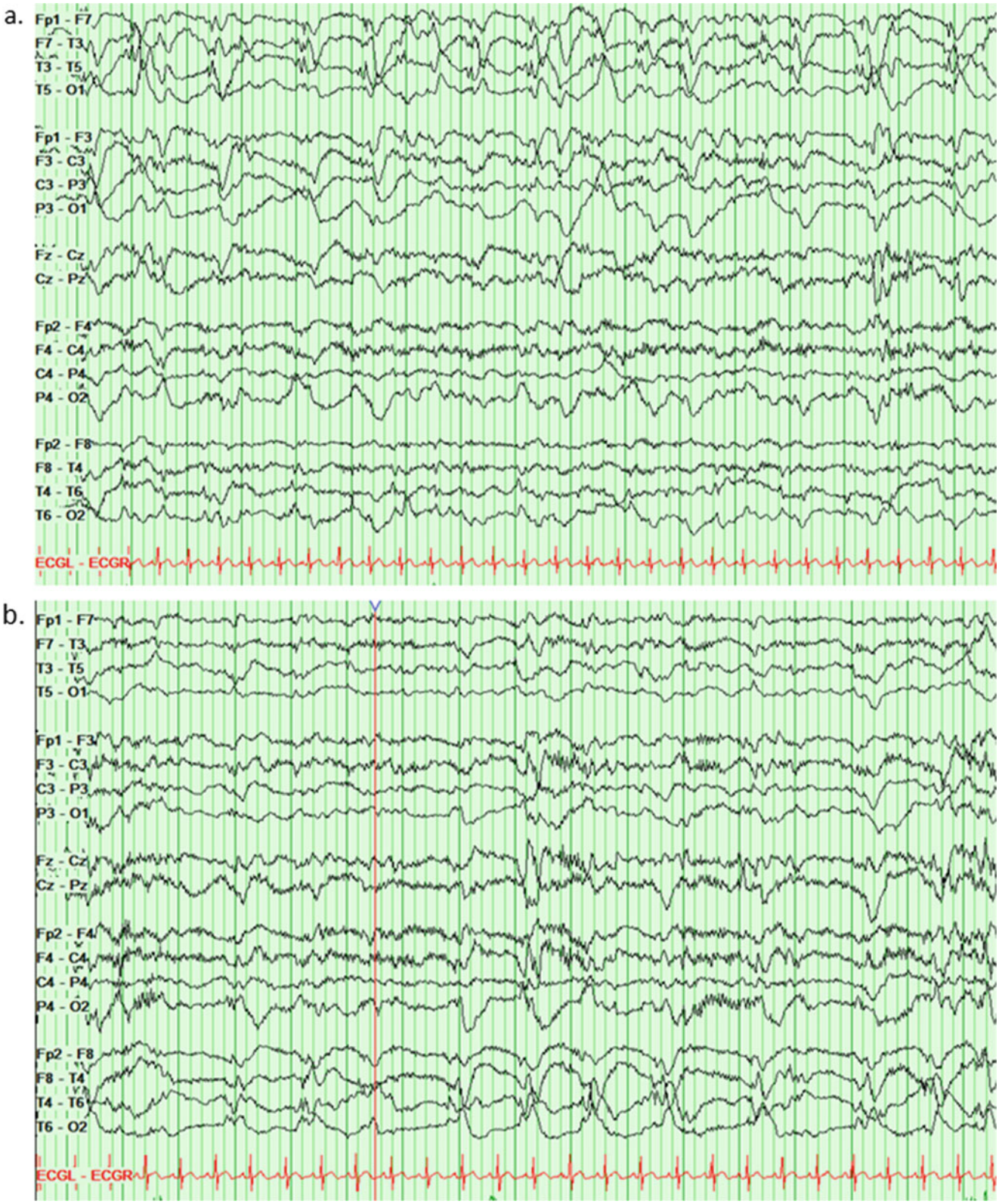

Fig. 1 Electrocephalogram demonstrating status epilepticus in a patient with Lesch–Nyhan disease with alternating unilateral frontotemporal electrographic seizures (**a**, left-sided seizure; **b**, right-sided). Background showed moderate generalized slowing, consistent with encephalopathy

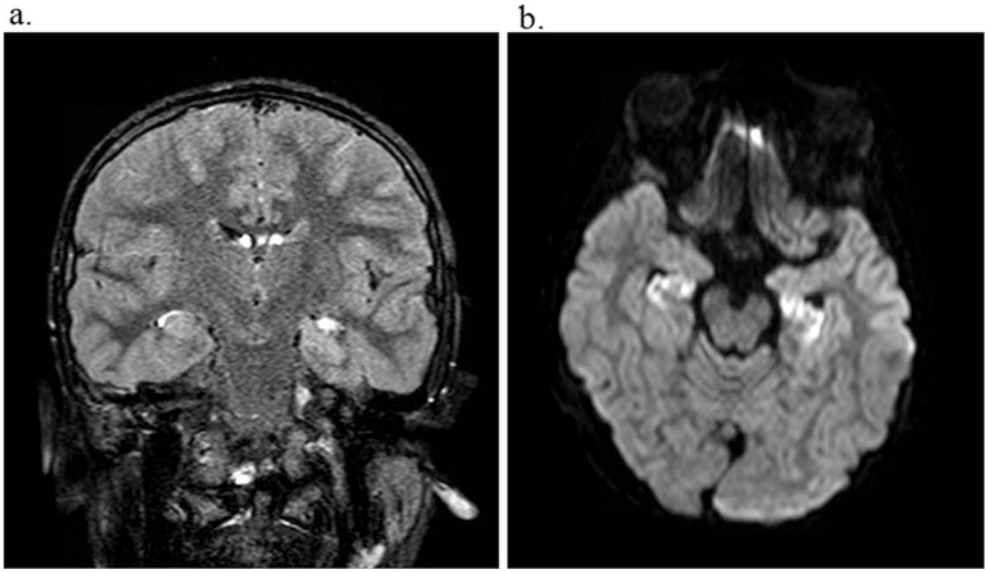

Fig. 2 MRI from the date of presentation showing increased T2 FLAIR signal (**a**) and T2 diffusion restriction (**b**) in the bilateral hippocampi, most likely secondary to seizure

arrest, as in our case (Neychev and Jinnah 2006) (Table 1). In our patient, heralding episodes of respiratory symptoms were felt likely to be an ictal or post-ictal phenomenon. Our case raises the possibility that individuals with LND may present with seizures with atypical semiology, and that respiratory failure in the setting of seizure may be one etiology of sudden death in LND. We suggest routinely asking LND patients about apnea and other respiratory symptoms, with consideration of an EEG for patients with these symptoms. In LND patients with clinical events suggestive of seizure, or a history of paroxysmal respiratory events and an abnormal EEG, a possible increased risk of sudden death should play a role in the discussion of initiating anti-epileptic medication. While earlier treatment (e.g., after suspected seizure or abnormal EEG) could be considered, medications could impact respiratory function of individuals with LND and may be risky in these patients. These decisions should be made carefully on a case-by-case basis. Further research is needed to understand the mechanism of sudden death in LND.

Conclusion

The severity of the acidosis in this patient presenting in subclinical status epilepticus after a first recognized seizure suggests that the sudden death from respiratory failure seen in LND could result from an unrecognized or first seizure. We suggest screening LND patients for paroxysmal respiratory symptoms, and considering seizure as a possible etiology.

Contributions of Individual Authors

Alison Christy prepared the article. Jenny Wilson and William Nyhan provided guidance and editing.

Guarantor for the Article

Alison Christy.

Compliance with Ethics Guidelines

Competing Interests

Alison Christy, William Nyhan and Jenny Wilson declare they have no competing interests.

Funding

No funding was received for this study.

Ethics

No ethics board approval was required for this study.

References

Basserman R, Gutensohn W, Jahn H, Springmann JS (1979) Pathological and immunological observations in a case of Lesch-Nyhan syndrome. Eur J Pediatr 132:93–98

Devinsky O, Hesdorffer DC, Thurman DJ, Lhatoo S, Richerson G (2016) Sudden unexpected death in epilepsy: epidemiology, mechanisms, and prevention. Lancet Neurology 15 (10):1075–1088

de Gemmis P, Anesi L, Lorenzetto E et al (2010) Analysis of the HPRT1 gene in 35 Italian Lesch-Nyhan families: 45 patients and 77 potential female carriers. Mutat Res 692(1–2):1–5

Hesdorffer DC, Crandall LA, Friedman D, Devinsky O (2015) Sudden unexplained death in childhood: a comparison of cases with and without a febrile seizure history. Epilepsia 56:1294–1300

Hoefnagel D, Andrew D, Mireault NG, Berndt WO (1965) Hereditary choreoathetosis, self-mutilation and hyperuricemia in young males. NEJM 273(3):130–135

Jinnah HA, Visser JE, Harris JC et al (2006) Delineation of the motor disorder of Lesch-Nyhan disease. Brain 129 (5):1201–1217

Jinnah HA, Ceballos-Picot I, Torres RJ et al (2010) Attenuated variants of Lesch-Nyhan disease. Brain 133(3):671–689

Maglajlija V, Walker MC, Kovac S (2012) Severe ictal hypoxemia following focal, subclinical temporal electrographic scalp seizure activity. Epilepsy Behav 24(1):143–145

Markowski-Leeman BA, Jinnah HA (2013) Lesch-Nyhan disease and epilepsy. In: Pearl P (ed) Inherited metabolic epilepsies. Demos Medical Publishing, New York, pp 227–246

Massey CA, Sowers LP, Dlouhy BJ, Richerson GB (2014) Mechanisms of sudden unexpected death in epilepsy: the pathway to prevention. Nat Rev Neurol 10(5):271–282

Mizuno T (1986) Long-term follow-up of ten patients with Lesch-Nyhan syndrome. Neuropediatrics 17:158–161

Nashef L, So EL, Ryvlin P, Tomson T (2012) Unifying the definitions of sudden unexpected death in epilepsy. Epilepsia 53(2):227–233

Neychev VK, Jinnah HA (2006) Sudden death in Lesch-Nyhan disease. DevMed and Child Neurol 48(11):923–926

Saito Y, Hanaoka S, Fukumizu M et al (1998) Polysomnographic studies of Lesch-Nyhan syndrome. Brain Dev 20(8):579–585

Shewell PC, Thompson AG (1996) Atlantoaxial instability in Lesch-Nyhan syndrome. Spine 21(6):757–762

Watts RWE, Spellacy E, Gibbs DA, Allsop J, McKeran RO, Slavin GE (1982) Clinical, post-mortem, biochemical and therapeutic observations on the Lesch-Nyhan syndrome with particular reference to the neurological manifestations. QJM 201:43–78

JIMD Reports
DOI 10.1007/8904_2016_20

RESEARCH REPORT

Vitamin B_{12} Administration by Subcutaneous Catheter Device in a Cobalamin A (cblA) Patient

E. Maines • G. Morandi • G. Gugelmo • F. Ion-Popa • N. Campostrini • A. Pasini • M. Vincenzi • F. Teofoli • M. Camilot • A. Bordugo

Received: 12 September 2016 / Revised: 18 October 2016 / Accepted: 25 October 2016 / Published online: 18 November 2016

Abstract Cobalamin A deficiency (cblA) is an inherited disorder of intracellular cobalamin metabolism, caused by impaired 5′-deoxy-adenosylcobalamin (AdoCbl) synthesis. Hydroxocobalamin (OHCbl) is the cornerstone of cblA treatment because vitamin B12 may completely restore AdoCbl deficiency. Parenteral administration, intravenous, subcutaneous or intramuscular, is generally required to achieve effect. Daily injections represent a problem for the parents and the caregivers, and this may lead to poor compliance and scarce adherence to the long-term treatment.

Our report describes the case of a patient with cblA deficiency, diagnosed by newborn screening, positively treated with daily OHCbl administration by a subcutaneous injection port (i-port advanceTM). After the insertion of the device, we checked methylmalonic acid (MMA) levels weekly for the first month and then monthly. MMA level remained always in the normal range.

To date, placement of a subcutaneous catheter to minimize the pain related to parenteral vitamin B12 punctures has been described only in a patient with deficiency of the enzyme methylmalonyl-CoA mutase (MUT). No other experiences are described in the literature.

Our case shows that OHCbl administration using a subcutaneous catheter is safe and effective even in patients with cblA deficiency. The use of subcutaneous devices may reduce difficulties in providing parenteral daily injections which is the main reason discouraging physicians and families to use such an invasive treatment. Moreover, our experience may be translated to other inherited metabolic disorders, such as cobalamin C (cblC) disease, which may require daily parenteral drug administration.

Methylmalonic acidurias are a heterogeneous group of inborn errors of metabolism biochemically characterized by the accumulation of methylmalonic acid (MMA) in body fluids and tissues. Isolated methylmalonic aciduria may be caused by a complete or partial deficiency of the enzyme methylmalonyl-CoA mutase (MUT) or by a defect in the synthesis of its cofactor 5′-deoxy-adenosylcobalamin (AdoCbl), derived from vitamin B_{12}. Three inherited disorders of intracellular cobalamin metabolism are caused by impaired AdoCbl synthesis: cblA (OMIM 251100), cblB (OMIM 251110), and cblD-variant 2 (OMIM 277410) (Baumgartner et al. 2014; Merinero et al. 2008).

Most patients with isolated MMAuria present in the newborn period or infancy with acute deterioration of their general clinical condition, metabolic acidosis and hyperammonemia, evolving to coma and death, if patients are not treated. Initial acute management includes stopping protein intake and starting intravenous (IV) glucose. Combined treatment including parenteral L-carnitine, hydroxocobalamin (OHCbl), sodium benzoate, L-arginine, and N-carbamylglutamate should be given until a provisional diagnosis has been made (Baumgartner et al. 2014). OHCbl is the cornerstone of cblA treatment because vitamin B_{12} may completely restore AdoCbl deficiency and OHCbl, if available, is preferred over cyanocobalamin. Parenteral administration, IV, subcutaneous (SQ) or intramuscular (IM), is generally required to achieve effect. To date, the efficacy of oral OHCbl in MMA patients is still debated and yet not proved.

Communicated by: Manuel Schiff

E. Maines (✉) · G. Morandi · G. Gugelmo · F. Ion-Popa · N. Campostrini · A. Pasini · M. Vincenzi · F. Teofoli · M. Camilot · A. Bordugo
Inherited Metabolic Diseases Unit, Department of Pediatrics, Regional Centre for Newborn Screening, Diagnosis and Treatment of Inherited Metabolic Diseases and Congenital Endocrine Diseases, Azienda Ospedaliera Universitaria Integrata, Verona, Italy
e-mail: evelina.maines@gmail.com

Responsiveness to vitamin B_{12} should be carefully checked in all patients with MMA, because it may significantly influence the prognosis and may also suggest which complementation group the patient belongs to.

Long-term prognosis of MMAurias strongly correlates with vitamin B_{12} responsiveness, which is typically found in all cblA patients, and less commonly in cblB and MUT patients (Baumgartner et al. 2014).

Patients with cblA are usually treated in the long term with OHCbl 1–2 mg IM or SQ 1–7 times a week, but cobalamin dosage has to be adjusted to MMA excretion and clinical status in cobalamin-responsive patients. Long-term treatment includes also oral L-carnitine supplementation, and protein restriction (Grünewald et al. 2014).

Parenteral daily injections represent a problem for the parents and the caregivers, and this may lead to poor compliance and scarce adherence to the long-term treatment.

We report the case of a newborn presented at the second day of life with recurrent vomiting, lethargy, and poor general condition associated with a biochemical picture of metabolic acidosis (pH 7.24, pCO_2 16 mmHg, HCO_3 6.9 mmol/L, AG 33 mmol/L) and hyperammonemia (271 μmol/L). Newborn screening (NBS) results were available at 50 h of life and highlighted increased propionylcarnitine (C3 11.63 μmol/L, n.r. 0.60–3.30 μmol/L) and its ratios to free carnitine (C3/C0 0.78, n.r. 0.05–0.27) and to acetylcarnitine (C3/C2 0.4, n.r. 0.03–0.17). Heptadecanoylcarnitine (C17 0.3 μmol/L, n.r. 0.02–0.08 μmol/L) was also high. Second tier tests showed increased MMA (>200 μmol/L, n.r. <5 μmol/L) and methylcitric acid (6 μmol/L, n.r. <1 μmol/L), but normal homocysteine (Hcy).

Diagnosis of isolated MMA was confirmed by high MMA excretion in the urine (5,500 mmol/mol of creatinine) and normal plasma total Hcy level (7.6 μmol/L, n.r. ≤10 μmol/L).

While the confirmatory tests were carried out, we started detoxification therapy with sodium benzoate, carbamylglutamate, L-arginine, L-carnitine, and OHCbl, associated with a protein-free diet. We used IM OHCbl at the dosage of 1 mg/day. We observed in 48 h a dramatic reduction of blood and urine MMA levels. Plasma MMA levels decreased from 453.8 to 5.5 μmol/L. Also MMA values on dried blood spot (DBS) dramatically reduced in 3 days, changing from 429.5 to 6.55 μmol/L.

Vitamin B_{12}-responsive phenotype was confirmed by complementation analysis on fibroblasts, suggesting a defect of AdoCbl synthesis, in particular cblA deficiency. MMAA gene analysis identified two heterozygous mutations in MMAA gene (Allele 1: c.445_448del; Allele 2: c.733+1G>A).

The patient was treated with 1 mg of OHCbl (1 mg/mL solution) IM a day associated with L-carnitine and a protein content of 1.8 g/Kg/day, which represents safe protein level for age.

To simplify parents' administration of OHCbl and to reduce the patient discomfort of multiple injections, we utilized a subcutaneous injection port (i-port advance™). The dosage of OHCbl (1 mg/mL solution) remained the same and the drug continued to be administered once daily. The subcutaneous catheter was exchanged by the parents every 5 days.

After the insertion of the device, we checked MMA levels on DBS weekly for the first 2 weeks and then monthly.

MMA levels remained always in the normal range. The mean DBS MMA level was of 2.43 μmol/L (range 0.75–6.55 μmol/L) and 1.97 μmol/L (range 0.4–6.15 μmol/L) before and after the application route was changed, respectively.

The patient is now 5 months old, he is growing well, and his neurological development is normal. No acute episode of metabolic derangement occurred.

At present, the subcutaneous injection port is still well tolerated. Parents have been educated to use independently the device and to adopt precautions to prevent infections of the site of injection. Parents report no problem with the use of the device and are happy to reduce the pain of injections.

The experience on parenteral OHCbl treatment for inborn errors of metabolism derives mostly from cobalamin C (cblC) patients (Carrillo-Carrasco et al. 2011). In these patients parenteral OHCbl (IV, SQ, or IM) is the only form of cobalamin proven to be beneficial (Carrillo-Carrasco et al. 2011). Many centers manage infants by providing 1 mg of parenteral OHCbl daily, but in the long term the frequency of administration is usually decreased to minimize daily injections and the dose is frequently not increased to account for their weight gain. Although these practices are based on limited evidence, they may be responsible of providing progressively sub-therapeutic cobalamin serum levels, a possible risk factor for progression of complications in patients with cblC disease (Carrillo-Carrasco et al. 2011).

Placement of a subcutaneous catheter to minimize the pain related to parenteral punctures has been described only in a patient with MMA due to MUT (Freehauf et al. 2011). No other experiences are described in the literature. Nevertheless, there are some conditions, such as cblC, where using a subcutaneous catheter may be very useful in the long-term treatment.

Our case shows that OHCbl administration using a subcutaneous catheter is safe and effective even in patients with cblA deficiency. The use of subcutaneous devices may reduce difficulties in providing parenteral daily injections

which is the main reason discouraging physicians and families to use such an invasive treatment. Hopefully this practice will improve adherence and compliance in the long term.

Moreover, our experience may be translated to other inherited metabolic disorders which require daily parenteral drug administration.

Acknowledgments The authors are grateful to Prof. Dr. med. Matthias Baumgartner and Prof. Dr. med. Johannes Häberle of University Children's Hospital Zürich, Division for Metabolic Diseases, for complementation analysis on fibroblasts culture and molecular analysis of MMAA gene.

Compliance with Ethics Guidelines

Conflict of Interest

Evelina Maines declares that she has no conflict of interest.

Grazia Morandi declares that she has no conflict of interest.

Giorgia Gugelmo declares that she has no conflict of interest.

Florina Ion-Popa declares that she has no conflict of interest.

Natascia Campostrini declares that she has no conflict of interest.

Andrea Pasini declares that he has no conflict of interest.

Monica Vincenzi declares that she has no conflict of interest.

Francesca Teofoli declares that she has no conflict of interest.

Marta Camilot declares that she has no conflict of interest.

Andrea Bordugo declares that he has no conflict of interest.

All procedures followed were in accordance with the Helsinki Declaration of 1975.

Details of the Contributions of Individual Authors

Dr. Maines E and Dr. Morandi G conceived the study and wrote the draft. Dr. Ion-Popa F, Campostrini N, Pasini A, Vincenzi M, Teofoli F, and Camilot M performed biochemical analysis and ensured the accuracy of the data. Dr. Gugelmo G performed dietetic evaluation of the patient. Dr. Bordugo A revised the manuscript critically for important intellectual content.

References

Baumgartner MR et al (2014) Proposed guidelines for the diagnosis and management of methylmalonic and propionic acidemia. Orphanet J Rare Dis 9:130

Carrillo-Carrasco N et al (2011) Combined methylmalonic acidemia and homocystinuria, cblC type. Clinical presentations, diagnosis and management. Inherit Metab Dis 35:91–102

Freehauf CL et al (2011) Use and benefit of a subcutaneous indwelling catheter for cobalamin administration in B12 responsive methylmalonic acidemia. Mol Genetic Metab 102:282

Grünewald S et al (2014) Emergency diagnostic procedures and emergency treatment. In: Blau N, Duran M, Gibson KM, Dionisi-Vici C (eds) Physician's guide to the diagnosis, treatment, and follow-up of inherited metabolic diseases. Springer, Berlin/Heidelberg, p 217

Merinero B et al (2008) Methylmalonic acidemia: examination of genotype and biochemical data in 31 patients belonging to mut, cblA or cblB complementation group. J Inherit Metab Dis 31:55–66

JIMD Reports
DOI 10.1007/8904_2016_21

CASE REPORT

Expansion of the Phenotypic Spectrum of Propionic Acidemia with Isolated Elevated Propionylcarnitine

Gerarda Cappuccio · Paldeep S. Atwal · Taraka R. Donti · Kiki Ugarte · Nadia Merchant · William J. Craigen · V. Reid Sutton · Sarah H. Elsea

Received: 06 August 2016 / Revised: 26 October 2016 / Accepted: 02 November 2016 / Published online: 30 November 2016

Abstract We report three patients with elevations of propionylcarnitine (C3), one without elevations of 2-methylcitrate and 3-hydroxypropionate in urine organic acid analysis, and the other two showing only mild elevations, all of whom were subsequently confirmed to have propionic acidemia by molecular analysis of *PCCA* and *PCCB* genes. To date, they have had a mild clinical course. These cases illustrate the importance of considering high C3 as the only biochemical abnormality in a diagnosis of propionic acidemia. Since mild C3 elevations may be overlooked and considered non-diagnostic in isolation, we advise considering a diagnosis of propionic acidemia even in the absence of significant elevations 2-methylcitrate or 3-hydroxypropionate in urine organic acid analysis.

Communicated by: Georg Hoffmann

Authors Gerarda Cappuccio and Paldeep S. Atwal contributing equally to the work.

G. Cappuccio
Department of Translational Medicine, Sector of Pediatrics, University of Naples Federico II, Naples, Italy

G. Cappuccio · P.S. Atwal · T.R. Donti · K. Ugarte · N. Merchant · W.J. Craigen · V.R. Sutton · S.H. Elsea (✉)
Department of Molecular and Human Genetics, Baylor College of Medicine, One Baylor Plaza, Houston, TX 77030, USA
e-mail: elsea@bcm.edu

G. Cappuccio · P.S. Atwal · T.R. Donti · V.R. Sutton
Baylor Genetics Laboratories, One Baylor Plaza, Houston, TX 77030, USA

P.S. Atwal
Department of Clinical Genomics, Center for Individualized Medicine, Mayo Clinic, Jacksonville, FL 32224, USA

Abbreviations

2-MCA	2-Methylcitrate
3-OHP	3-Hydroxypropionate
C3	Propionylcarnitine

Introduction

Inborn errors of metabolism (IEMs) can have a severe impact on human health through the buildup of toxic metabolites resulting in serious, often fatal, diseases. Newborn screening (NBS) is used for early diagnosis of IEMs to avoid potentially catastrophic physical and neurological effects.

Propionic acidemia (PA) is an IEM affecting 1 in 50,000 to 1 in 100,000 individuals (Wikoff et al. 2007) resulting from a defect in the enzyme propionyl-CoA carboxylase (PCC). This enzyme is involved in metabolism of the branched chain amino acids, valine and isoleucine, and other propiogenic substrates. The clinical spectrum of PA is wide and ranges from an acute neonatal-onset to milder late-onset forms, and the clinical course is dominated by the risk of relapses of life threatening episodes of metabolic decompensation, with potential risk of death or further neurological damage. Patients with a mild form of PA on carnitine therapy have been described with severe and fatal hypertrophic cardiomyopathy in the absence of episodes of metabolic decompensation (Mardach et al. 2005). The underlying biochemical cause of the variability of neurological sequelae is not known.

The diagnosis of PA is based on the presence of elevated propionylcarnitine (C3) and possibly increased glycine and alanine in plasma and elevations in 2-methylcitrate (2-MCA) and 3-hydroxypropionate (3-OHP) with absence of

methylmalonic acid (MMA) in urine organic acid analysis, as well as other metabolites derived from propionyl-CoA catabolism (Al-Dirbashi et al. 2014). Since C3 is not sensitive or specific, the diagnostic sensitivity is improved using acylcarnitine ratios (increased ratio of C3 to C2) (Turgeon et al. 2010).

Early diagnosis of PA is the key to effective management. Diagnosis of PA through NBS may lead to improved health outcomes with a lower mortality rate for affected children and lower stress for their parents (Grünert et al. 2012; Lücke et al. 2004; Waisbren et al. 2003). With the implementation of NBS for PA, a more favorable outcome has been observed when treatment is promptly started. The mainstay of the long-term treatment is a low-protein, high-energy diet and carnitine supplementation. Treatment with N-carbamylglutamate has been proved to reduce ammonia and glutamine in propionic acidemia patients (Mew et al. 2010). Liver transplantation has also been employed in PA and has been demonstrated to end hyperammonemic episodes (Silva et al. 2014).

Here, we describe three children with extremely mild PA whose diagnosis was initially based on isolated elevations of C3. By reporting these unusually mildly affected individuals, that lack metabolic abnormalities typically considered necessary for a diagnosis of PA, we expand the phenotypic spectrum of PA and raise the index of suspicion the clinician must have to capture the full spectrum of individuals affected with PA.

Case Reports

Patient 1

Patient 1 was a full-term healthy female who initially presented for abnormal second NBS with borderline C3 and elevated C3/C2. Confirmatory testing in the course of standard newborn screening follow-up, including plasma amino acid analysis, urine organic acid analysis, and plasma acylcarnitine analysis was performed. Initial plasma acylcarnitine analysis showed elevated C3 at 23,930 nmol/L (normal range 0–870 nmol/L). Qualitative urine organic acid analysis showed only moderate elevations in methylcitric acid and 3-hydroxypropionate, and plasma amino acids showed moderately increased glycine of 490 mmol/L (normal range 104–344 mmols/L). She was found to have hyperammonemia (183 μmol/L, normal range 47–80 μmol/L) and elevated lactate (3.7 mmol/L (normal range 0.2–2.0 mmol/L). She was admitted for management with IV dextrose fluids, IV sodium benzoate, and IV levocarnitine. Since her initial admission, she had no further episodes of hyperammonemia. At her 4-year follow-up, she was noted to have reached all her developmental milestones at appropriate ages, and her growth was normal. She is currently managed with a protein-restricted diet, sodium benzoate, and levocarnitine. Apart from repeated isolated elevations in C3 on plasma acylcarnitine analysis and mild elevations of glycine, she shows no biochemical evidence of propionic acidemia with no detectable analytes suggestive of PA in repeated qualitative urine organic acid analyses. Sanger sequencing identified compound heterozygous pathogenic mutations in the *PCCA* gene in trans-configuration: c.223G>C (p. A75P) and c.923dupT (p. L308FfsX35) that have been previously identified and characterized (Campeau et al. 1999; Pérez et al. 2003; Yang et al. 2004). No mutations were identified in *PCCB*.

Patient 2

Patient 2 was a full-term male with no perinatal complications who had a normal initial but whose second NBS identified borderline elevated C3 and elevated C3/C2 at around 3 weeks of life (Table 1). He had been feeding with no issues at home, and there were no developmental concerns at the time of diagnosis. Confirmatory testing included urine organic acid analysis, plasma acylcarnitine analysis, and plasma amino acid analysis. The initial acylcarnitine analysis showed significant isolated elevation of C3 11,028 nmols/L, normal range: 0–870 nmols/L, while urine organic acids and plasma amino acids were unremarkable. He was started on a protein-restricted diet and levocarnitine. Molecular testing confirmed the diagnosis of PA by finding two heterozygous bi-allelic variants, c.562G>A (p. G188R) and c.1127G>A (p. R376H), in *PCCB* gene. The first mutation was previously reported (Pérez et al. 2003), while the second variant is a novel mutation predicted to be pathogenic (Table 2). At 20 months of age, there were no growth concerns, and he was developmentally normal (walking and two words sentences). He had two urine acylglycine analyses performed during routine follow-up, and on a single analysis, propionylglycine was very mildly elevated at 2.7 mmols/mol creatinine (normal range 0–2 mmols/mol creatinine), the other analysis was normal. No other metabolic abnormalities were detected on urine organic acid analysis performed three times (2-methylcitrate was not detected), and he has not suffered an acute metabolic decompensation to date.

Patient 3

Patient 3 was a full-term female who initially presented with an abnormal second NBS that showed elevated C3/C2 ratios but normal C3 levels. At 3 weeks of life, follow-up testing of urine organic acids revealed the presence of 2-methylcitrate and unremarkable plasma amino acids. The

Table 1 Biochemical and molecular findings from three patients with propionic acidemia

Current age	Patient 1 4 years old	Patient 2 20 months	Patient 3 3 years old
Newborn screens (NBS) nmol/L			
NBS 1[a] (nmol/L)	C3 = 5,900 C3/C2 = 0.54	C3 = 6,340 C3/C2 = 0.38	C3 = 3,000 C3/C2 = 0.18
NBS 2[a] (nmol/L)	C3 = 4,380 C3/C2: 0.99	C3 = 4,110 C3/C2 = 0.68	C3 = 3,890 C3/C2 0.48
Initial C3 Normal range: 0–870 nmol/L	40,240	11,028	2,440
Average C3 at follow-up (excludes initial C3)	32,085 nmol/L	13,943 nmol/L	4,263 nmol/L
Most recent C3	23,930 nmol/L	19,602 nmol/L	3,185 mol/L
Urine 3-hydroxypropionic acid (3-OHP), qualitative	Modest elevation	Normal	Normal
Urine 2-methylcitrate (2-MCA), qualitative	Modest elevation	Normal	Modest elevation
Urine propionylglycine, targeted Normal range: 0–2	N/A	2.7	N/A
PCCA/PCCB sequence analysis	*PCCA*[b]: c.923dupT (p. L308FfsX35) c.223G>C(p. A75P)	*PCCB*[c]: c.562G>A (p. G188R) c.1127G>A (p. R376H)	*PCCA*[b]: c.1284+1G>A c.1999C>T (p. P667S)

N/A not performed

[a] Newborns (1–6 days old) C3 ≥ 6,360 nmol/L (borderline), C3 ≥ 8,260 nmol/L (elevated) and C3/C2≥0.35 (elevated); newborns (7 or greater days old), C3 ≥ 4,040 nmol/L (borderline), C3 ≥ 5,490 nmol/L (elevated), C3/C2≥0.2 (elevated)

[b] *PCCA*: NM_000282

[c] *PCCB*: NM_000532

Table 2 Molecular profile and bioinformatic prediction of *PCCA* and *PCCB* novel variants

Gene	Amino acid changes	ExAC frequency	Homozygotes in ExAC	SIFT pred	Polyphen2 HDIV score	Polyphen2 HDIV pred	Mutation taster score	Radial SVM pred	CADD phred
PCCB	PCCB:NM_000532: exon11:c. G1127A: p. Arg376His	0.00003295	0	Deleterious	1.0	Damaging	1.000	D	32
PCCA	PCCA:NM_000282: exon22:c. C1999T: p. Pro667Ser	0	0	Deleterious	0.999	Damaging	1.000	D	20.3

acylcarnitine profile at this time revealed C3 of 4,930 nmols/L (normal range 0–1,120 nmol/L), and a normal plasma ammonia level. Her diagnosis was confirmed with molecular testing of *PCCA* which showed heterozygous bi-allelic variants: a known pathogenic variant, c.1284+1G>A (Campeau et al. 2001), and a novel likely pathogenic missense variant, c.1999C>T (p. Pro667Ser) (Table 2). She is managed on a protein restricted diet and levocarnitine. Currently at age three, she does not have any growth or developmental concerns, and she has reached all developmental milestones at the appropriate ages. She has no history of metabolic decompensation leading to hospitalizations, emergency room visits, or any minor or major illnesses.

Discussion

In patients with PA, propionyl-CoA accumulates in the body, eventually causing downstream elevations in several compounds, including C3, 2-MCA, 3-OHP, and glycine. PA is included in the NBS core panel, to rule out a subset of C3-related metabolic disorders resulting from propionate accumulation (PA, methylmalonic aciduria (MMA), certain

cobalamin (Cbl) disorders). C3 is not specific for PA and a second-tier strategies analyzing methylmalonic acid, 3-hydroxypropionic acid, and 2-methylcitric acid from the initial DBS have been developed (la Marca et al. 2007; Lindner et al. 2008; Matern et al. 2007). Many laboratories use ratios of C3 to other acylcarnitine species (C2, C0, C16) or to methionine to improve specificity and sensitivity of C3 test (Wikoff et al. 2007).

In virtually all reported cases of PA including atypical and mild ones, the diagnosis is supported by concurrent abnormal acylcarnitine profile and urine organic acids that identify the disease-specific 2-MCA and 3-OHP (Al-Dirbashi et al. 2014; Weisfeld-Adams et al. 2010; Pérez-Cerdá et al. 2000). In this report, two individuals with compound heterozygous mutations in *PCCA/PCCB* present with significant C3 elevations in the absence of or only modest elevation in 2-MCA or 3-OHP, escaping the classic biochemical hallmarks for the PA diagnosis. Moreover, patient 1 showed a typical, albeit mild, biochemical profile of PA but without significant clinical symptoms.

All the mutations identified in the patients reported have been previously described with the exception of two novel mutations: one in *PCCB* c.1127G>A (p. Arg376His) and one in *PCCA* c.1999C>T (p. Pro667Ser). Both novel mutations are predicted pathogenic and are rare: the mutation in *PCCB* c.1127G>A showed a low frequency in ExAC (0.00003295) without homozygous patients while the mutation in *PCCA* c.1999C>T is not reported in ExAC (Table 2). Mutations in *PCCB* (c.1127G>A and c.1126C>T) in the same codon of the novel variant of patient 2 (c.1127G>T), and in *PCCA* (c.1999C>T and c.2002G>A) adjacent to the novel variant of patient 3 (c.1997 T>A), have been reported pathogenic in PA patients (Desviat et al. 2006; Kraus et al. 2012).

Most patients with PA showed nonatal onset, but later onset in adolescence or adulthood has been described (Lee et al. 2009). Recent studies indicated heart defects and renal failure as late-onset PA phenotypes (Lee et al. 2009; Pena et al. 2012; Vernon et al. 2013), suggesting disease progression still takes place in the mildest cases of PA. Close follow-up remains crucial to the well-being of these "mild" PA patients.

Our cases show a stable clinical course with a more favorable natural history (without metabolic decompensations), normal growth and a favorable neurocognitive development. We posit the lack of clinical manifestations could be due to the absence of significant elevations of potentially neurotoxic metabolites such as 2-MCA and 3-OHP. A potential pathophysiological correlation between high levels of 2-MCA and 3-OHP and neurological issues, for a secondary impairment of mitochondrial energy production, has already been described (Pérez-Cerdá et al. 1998; Schreiber et al. 2012).

Treatment in PA is accomplished mainly through dietary restriction, particularly of the protein substrates, and carnitine supplementation. The available treatments do not allow significant reduction of circulating 3-OHP, 2-MCA, glycine, and C3 (Pena and Burton 2012). All patients described here are on carnitine supplementation and a modified diet. The chronic treatment for these patients is necessary since the uncertainty about the long-term prognosis of PA, even in apparent milder cases such as theirs.

Acknowledgments We thank Dr. Q. Sun for critical discussion.

Take-Home Message

The absence of 2-methylcitrate and 3-hydroxypropionate might be misleading in the diagnostic process for patients with propionic acidemia.

Authors' Contribution

GC and PSA were involved in conception and design of the study. TRD, KU, and NM analyzed and interpreted the data. QS, VRS, and WJC reviewed and revised critically the manuscript for important intellectual content. SHE supervised the work, coordinated the preparation of the work for publication, and is the corresponding author. All authors have approved the submission of the manuscript.

Competing Interest Statement

The authors declare no competing interests.

Ethics Statement

All procedures followed were in accordance with the ethical standards of the U.S. Department of Health and Human Services and were approved by the Baylor College of Medicine Institutional Review Board in accordance with Helsinki Declaration of 1975 as revised in 2000. This study was approved with a waiver of informed consent.

References

Al-Dirbashi OY, McIntosh N, McRoberts C, Fisher L, Rashed MS, Makhseed N, Geraghty MT, Santa T, Chakraborty P (2014) Analysis of methylcitrate in dried blood spots by liquid chromatography-tandem mass spectrometry. JIMD Rep 16:65

Campeau E, Desviat LR, Leclerc D, Wu X, Pérez B, Ugarte M, Gravel RA (2001) Structure of the PCCA gene and distribution of mutations causing propionic acidemia. Mol Genet Metab 74:238–247

Campeau E, Dupuis L, León-Del-Rio A, Gravel R (1999) Coding sequence mutations in the alpha subunit of propionyl-CoA Carboxylase in patients with propionic acidemia. Mol Genet Metab 67:11–22

Desviat LR, Clavero S, Perez-Cerdá C, Navarrete R, Ugarte M, Perez B (2006) New splicing mutations in propionic acidemia. J Hum Genet 51:992–997

Grünert SC, Müllerleile S, De Silva L, Barth M, Walter M, Walter K, Meissner T, Lindner M, Ensenauer R, Santer R (2012) Propionic acidemia: neonatal versus selective metabolic screening. J Inherit Metab Dis 35:41–49

Kraus JP, Spector E, Venezia S, Estes P, Chiang P-W, Creadon-Swindell G, Müllerleile S, De Silva L, Barth M, Walter M (2012) Mutation analysis in 54 propionic acidemia patients. J Inherit Metab Dis 35:51–63

la Marca G, Malvagia S, Pasquini E, Innocenti M, Donati MA, Zammarchi E (2007) Rapid 2nd-tier test for measurement of 3-OH-propionic and methylmalonic acids on dried blood spots: reducing the false-positive rate for propionylcarnitine during expanded newborn screening by liquid chromatography-tandem mass spectrometry. Clin Chem 53:1364–1369

Lee TM, Addonizio LJ, Barshop BA, Chung WK (2009) Unusual presentation of propionic acidaemia as isolated cardiomyopathy. J Inherit Metab Dis 32:97–101

Lindner M, Ho S, Kölker S, Abdoh G, Hoffmann GF, Burgard P (2008) Newborn screening for methylmalonic acidurias – optimization by statistical parameter combination. J Inherit Metab Dis 31:379–385

Lücke T, Pérez-Cerdá C, Baumgartner M, Fowler B, Sander S, Sasse M, Scholl S, Ugarte M, Das AM (2004) Propionic acidemia: unusual course with late onset and fatal outcome. Metab 53:809–810

Mardach R, Verity MA, Cederbaum SD (2005) Clinical, pathological, and biochemical studies in a patient with propionic acidemia and fatal cardiomyopathy. Mol Genet Metab 85:286–290

Matern D, Tortorelli S, Oglesbee D, Gavrilov D, Rinaldo P (2007) Reduction of the false-positive rate in newborn screening by implementation of MS/MS-based second-tier tests: the Mayo Clinic experience (2004–2007). J Inherit Metab Dis 30:585–592

Mew NA, McCarter R, Daikhin Y, Nissim I, Yudkoff M, Tuchman M (2010) N-carbamylglutamate augments ureagenesis and reduces ammonia and glutamine in propionic acidemia. Pediatr 126: e208–e214

Pena L, Burton BK (2012) Survey of health status and complications among propionic acidemia patients. Am J Med Genet A 158A:1641–1646

Pena L, Franks J, Chapman KA, Gropman A, Mew NA, Chakrapani A, Island E, MacLeod E, Matern D, Smith B (2012) Natural history of propionic acidemia. Mol Genet Metab 105:5–9

Pérez B, Desviat LR, Rodríguez-Pombo P, Clavero S, Navarrete R, Perez-Cerdá C, Ugarte M (2003) Propionic acidemia: identification of twenty-four novel mutations in Europe and North America. Mol Genet Metab 78:59–67

Pérez-Cerdá C, Merinero B, Martí M, Cabrera JC, Peña L, García MJ, Gangoiti J, Sanz P, Rodríguez-Pombo P, Hoenicka J, Richard E, Muro S, Ugarte M (1998) An unusual late-onset case of propionic acidaemia: biochemical investigations, neuroradiological findings and mutation analysis. Eur J Pediatr 157:50–52

Pérez-Cerdá C, Merinero B, Rodríguez-Pombo P, Pérez B, Desviat LR, Muro S, Richard E, García MJ, Gangoiti J, Ruiz Sala P, Sanz P, Briones P, Ribes A, Martínez-Pardo M, Campistol J, Pérez M, Lama R, Murga ML, Lema-Garrett T, Verdú A, Ugarte M (2000) Potential relationship between genotype and clinical outcome in propionic acidaemia patients. Eur J Hum Genet 8:187–194

Schreiber J, Chapman KA, Summar ML, Ah Mew N, Sutton VR, MacLeod E, Stagni K, Ueda K, Franks J, Island E, Matern D, Peña L, Smith B, Urv T, Venditti C, Chakarapani A, Gropman AL (2012) Neurologic considerations in propionic acidemia. Mol Genet Metab 105:10–15

Silva HM, Nassogne MC, Smets F, Stéphenne X, Scheers I, Veyckemans F, Pirotte T, Bourdeaux C, de Magnée C, Reding R, Sokal E (2014) Liver transplantation for propionic acidemia. J Pediatr Gastroenterol Nutr (Epub ahead of print)

Turgeon CT, Magera MJ, Cuthbert CD, Loken PR, Gavrilov DK, Tortorelli S, Raymond KM, Oglesbee D, Rinaldo P, Matern D (2010) Determination of total homocysteine, methylmalonic acid, and 2-methylcitric acid in dried blood spots by tandem mass spectrometry. Clin Chem 56:1686–1695

Vernon HJ, Bagnasco S, Hamosh A, Sperati CJ (2013) Chronic kidney disease in an adult with propionic acidemia. JIMD Rep 12:5–10

Waisbren SE, Albers S, Amato S, Ampola M, Brewster TG, Demmer L, Eaton RB, Greenstein R, Korson M, Larson C (2003) Effect of expanded newborn screening for biochemical genetic disorders on child outcomes and parental stress. JAMA 290:2564–2572

Weisfeld-Adams JD, Morrissey MA, Kirmse BM, Salveson BR, Wasserstein MP, McGuire PJ, Sunny S, Cohen-Pfeffer JL, Yu C, Caggana M, Diaz GA (2010) Newborn screening and early biochemical follow-up in combined methylmalonic aciduria and homocystinuria, cblC type, and utility of methionine as a secondary screening analyte. Mol Genet Metab 99:116–123

Wikoff WR, Gangoiti JA, Barshop BA, Siuzdak G (2007) Metabolomics identifies perturbations in human disorders of propionate metabolism. Clin Chem 53:2169–2176

Yang X, Sakamoto O, Matsubara Y, Kure S, Suzuki Y, Aoki Y, Yamaguchi S, Takahashi Y, Nishikubo T, Kawaguchi C, Yoshioka A, Kimura T, Hayasaka K, Kohno Y, Iinuma K, Ohura T (2004) Mutation spectrum of the PCCA and PCCB genes in Japanese patients with propionic acidemia. Mol Genet Metab 81:335–342

JIMD Reports
DOI 10.1007/8904_2016_23

CASE REPORT

Previously Unreported Biallelic Mutation in *DNAJC19:* Are Sensorineural Hearing Loss and Basal Ganglia Lesions Additional Features of Dilated Cardiomyopathy and Ataxia (DCMA) Syndrome?

Sema Kalkan Ucar · Johannes A. Mayr · René G. Feichtinger · Ebru Canda · Mahmut Çoker · Saskia B. Wortmann

Received: 12 August 2016 / Revised: 09 November 2016 / Accepted: 11 November 2016 / Published online: 08 December 2016

Abstract *Background:* Dilated cardiomyopathy (DCM), non-progressive cerebellar ataxia (A), testicular dysgenesis, growth failure, and 3-methylglutaconic aciduria are the hallmarks of DNAJC19 defect (or DCMA syndrome) due to biallelic mutations in *DNAJC19*. To date DCMA syndrome has been reported in 19 patients from Canada and in two Finnish siblings. The underlying pathomechanism is unknown; however, DNAJC19 is presumed to be involved in mitochondrial membrane related processes (e.g., protein import and cardiolipin remodeling). Here, we report an additional patient with progressive cerebellar atrophy and white matter changes.

Patient and Methods: A Turkish boy presented at age 2 months with dilated cardiomyopathy (initially worsening then stabilizing in the second year of life), growth failure, bilateral cryptorchidism, and facial dysmorphism. Mental and motor developmental were, respectively, moderately and severely delayed. Profound intentional tremor and dyskinesia, spasticity (particularly at the lower extremities), and dystonia were observed. Sensorineural hearing loss was also diagnosed. MRI showed bilateral basal ganglia signal alterations. Plasma lactate levels were increased, as was urinary excretion of 3-methylglutaconic acid. He deceased aged 3 years.

Results: Sanger Sequencing of *DNAJC19* confirmed the clinical diagnosis of DNAJC19 defect by revealing the previously unreported homozygous stop mutation c.63delC (p.Tyr21*). Investigation of enzymes of mitochondrial energy metabolism revealed decreased activity of cytochrome *c* oxidase in muscle tissue.

Discussion: Sensorineural hearing loss and bilateral basal ganglia lesions are common symptoms of mitochondrial disorders. This is the first report of an association with DNAJC19 defect.

Introduction

Dilated cardiomyopathy with ataxia (DCMA syndrome, MIM #610198, *DNAJC19*) is one of the inborn errors of metabolism with 3-methylglutaconic aciduria (3-MGA-uria) as a discriminating feature (Wortmann et al. 2013). It was first described in the Canadian Dariusleut Hutterite population in 18 patients (Davey et al. 2006). The major clinical features of DCMA include a severe, early onset dilated cardiomyopathy (DCM), in some cases accompanied by long QT syndrome, and an ataxia (A) due to non-progressive cerebellar atrophy. Prenatal or postnatal growth failure is universally seen, as is significant motor delay, and

Communicated by: Garry Brown

Mahmut Çoker and Saskia B. Wortmann contributing equally to this manuscript.

Electronic supplementary material: The online version of this chapter (doi:10.1007/8904_2016_23) contains supplementary material, which is available to authorized users.

S.K. Ucar (✉) · E. Canda · M. Çoker
Division of Metabolic Disease, Ege University Medical Faculty, Department of Pediatrics, Izmir, 35100, Turkey
e-mail: sema.kalkan.ucar@ege.edu.tr

J.A. Mayr · R.G. Feichtinger · S.B. Wortmann
Department of Pediatrics Salzburger Landeskliniken and Paracelsus Medical University Salzburg, Salzburg, Austria

a cerebellar syndrome with ataxia. Male genital anomalies are also frequently reported and range from isolated cryptorchidism to severe perineal hypospadias. Additional features include optic atrophy, a mild increase in hepatic enzymes with microvesicular hepatic steatosis, a normochromic microcytic anaemia, and mild to borderline non-progressive mental retardation.

The precise function of DNAJ19 in human mitochondria is unknown. An effect on mitochondrial protein import or cardiolipin remodeling via prohibitin proteins has been suggested (Davey et al. 2006; Richter-Dennerlein et al. 2014). This is in line with other inborn errors of metabolism with 3-methylglutaconic aciduria (3-MGA-uria) (e.g., TAZ defect or Barth syndrome, SERAC1 defect or MEGDEL syndrome) affecting phospholipid remodeling (Wortmann et al. 2013) and can show more or less mitochondrial dysfunction in muscle (Wortmann et al. 2012; Thiels et al. 2016).

Till date only three further patients have been described (Ojala et al. 2012; Al Teneiji et al. 2016). Interestingly, white matter alterations and progressive (in contrast to non-progressive) bilateral basal ganglia lesions have been reported as additional features in one of these patients (Al Teneiji et al. 2016). Here we report the case of a Turkish boy and expand the mutational and biochemical abnormalities and the clinical spectrum.

Methods

Measurements of the Respiratory Chain Enzymes in Muscle

Skeletal muscle tissue samples were homogenized in extraction buffer (20 mmol/l Tris-HCl, pH 7.6, 250 mmol/l sucrose, 40 mmol/l KCl, 2 mmol/l EGTA) and subsequently centrifuged at 600 g to generate the post-nuclear supernatant (600 g homogenate), which was used for measurement of OXPHOS enzyme activities and Western blot analysis. Citrate synthase (CS) and OXPHOS enzyme activities were determined as published elsewhere (Berger et al. 2003, Feichtinger et al. 2014, Mayr et al. 2004, Meierhofer et al. 2004). Briefly, rotenone-sensitive complex I activity was measured spectrophotometrically as NADH/decylubiquinone oxidoreductase. The enzyme activities of citrate synthase, complex IV (ferro-cytochrome c/oxygen oxidoreductase), and the oligomycin-sensitive ATPase activity of the F_1F_0 ATP synthase (complex V) were measured in buffer conditions as previously described (Rustin et al. 1994). Succinate dehydrogenase activity (SDH; complex II) was determined as described (Rustin et al. 1994) with slight modifications (Feichtinger et al. 2014). Buffer conditions and the procedure for determination of complex III activity were as reported previously (Feichtinger et al. 2014). All spectrophotometric measurements were performed at 37°C.

Immunoblotting

For western blot analysis, a total of 10 µg protein of 600 g homogenate (generated as described above) or fibroblast mitochondria was separated on 10% acrylamide/bisacrylamide gels and transferred to nitrocellulose membranes using the Biorad Trans-Blot Turbo Blotting System. Washing and blocking procedures were performed as previously described (Feichtinger et al. 2014).

The following primary antibody dilutions, incubation times, and temperatures were used: monoclonal mouse anti-NDUFS4 (1:1,000; 1 h, room temperature; Abcam; ab55540), monoclonal mouse anti-VDAC1 (Porin) (1:1,000; 1 h, room temperature, Abcam, ab17734), and polyclonal rabbit anti-MT-CO2 (COX2) (1:1,000; overnight, 4°C; Abcam, ab79393). After washing, the membranes were incubated with primary antibodies as follows: NDUFS4, VDAC1, and MT-CO2. Since NDUFS4 and MT-CO2 have the same molecular weight, the western blot was incubated two times for 15 min in stripping buffer (25 mmol/l glycine, 2% SDS, pH 2) after VDAC1. The clean blot was blocked again and incubated with MT-CO2.

NDUFS4 and VDAC1 were labeled with polymer-HRP-antimouse (1:100; 1 h, room temperature, EnVision kit, Dako), MT-CO2 with labeled polymer-HRP-anti-rabbit (1:100; 1 h, room temperature, EnVision kit, Dako). Detection was carried out with Lumi-Light PLUSPOD substrate (Roche).

Genetic Investigations

A karyogram and Sanger Sequencing of *DNAJC19* (NM_145261.3, primers available upon request) were performed using standard methods. Parental DNA and DNA from siblings were unavailable.

Case Report and Results

Clinical and Neurological Presentation, Cerebral MRI Findings

The boy was the sixth child of Turkish parents who are first degree cousins (Fig. 1). Two older brothers and two older sisters died before the age of 13 months; however, no details were available. He was born with a low birth weight (−2.5 SD) at 38 weeks of gestation. Placental abruption was reported, no more details were available.

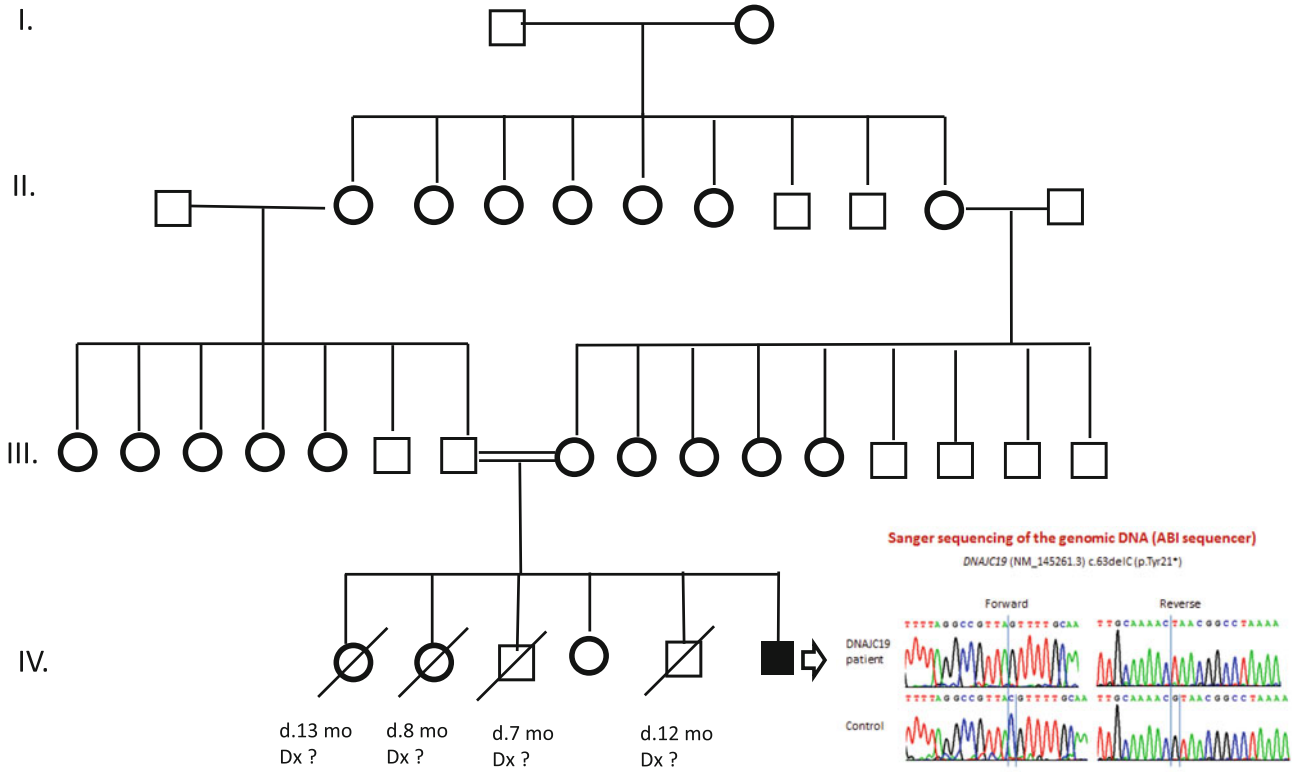

Fig. 1 The pedigree of the family and results from index patient's Sanger Sequencing of the genomic DNA

At age 2 months a systolic murmur was detected, subsequent echocardiography revealed a spherical configuration of the left ventricle (end diastolic diameter 2.7 cm (ref. range: 1.8–2.3 cm)) and a diminished ejection fraction (45%, (ref. range: 56–78%)). Treatment with digoxin, furosemide, and an ACE inhibitor was initiated. Two months later an increase in the trabeculation of the left ventricle was detected. The ejection fraction initially improved to 57% (4 months) and 68% (12 months), but later worsened to 50% (1.5 years) and then stabilized around age 2 years. The left ventricular end diastolic diameter at follow-up was 3.3 (ref. range: 2.4–3.1 cm) cm and 3.2 cm (ref. range: 2.5–3.2 cm), respectively. ECG did not reveal conduction defects.

Motor development was severely delayed (supported seating at 10 months, rolling over at 20 months) and he has not learned to walk. At age 2 years he made eye contact for a short time and recognized his mother and spoke only one word. He reacted to and laughed at bright colored objects (toys, mobile phones, etc.). Seizures were not reported. The cerebral MRI (at 2.5 years) showed reduced cerebellar volume and increased basal ganglia signal on the T2-weighted images (particularly putamen and globus pallidus), with correspondingly reduced signal on the T1-weighted images. In the same level diffusion-weighted imaging was characterized by diffusion restriction (Fig. 2).

Currently he is aged 2 years and 5 months, anthropometrics are within normal limits. The minor facial features are shown in Fig. 2. He has a 2/6 systolic murmur with punctum maximum at 3rd - 4th intercostal space. Bilateral cryptorchidism and a short penis length (2.3 cm (−2 SD)) were noted. The patient can only follow the gaze for a short time and babbles. He has no head control, shows mild muscular atrophy, spasticity (particularly of the lower extremities), profound intentional tremor, dystonia, and dyskinesia, and has no fine motor skills (e.g., no grasping). He has severe hyperkinetic involuntary movements such as jerky explosive "rolling over."

Auditory evoked potential (AEP) performed at 2.5 years revealed a bilateral sensorineural hearing loss (Fig. 2). The parents did not agree to treatment until this time. The pelvic ultrasound scan failed to detect the presence of testicles in the channel and in the pelvis.

The patient deceased during the reviewing process of this manuscript due to aspiration aged 3 years.

Clinical Chemical, Metabolic, and Endocrine Findings

The patient had a microcytic, hypochromic anemia (hemoglobin 11.4 g/l (ref. range: 12–15), erythrocyte count 5.34 × 10E12/l (ref. range: 3.78–5.4), mean red cell volume 64.5 fl (ref. range: 77–95), mean red cell hemoglobin 21.4 pg (ref. range: 23–31.2), and red cell distribution

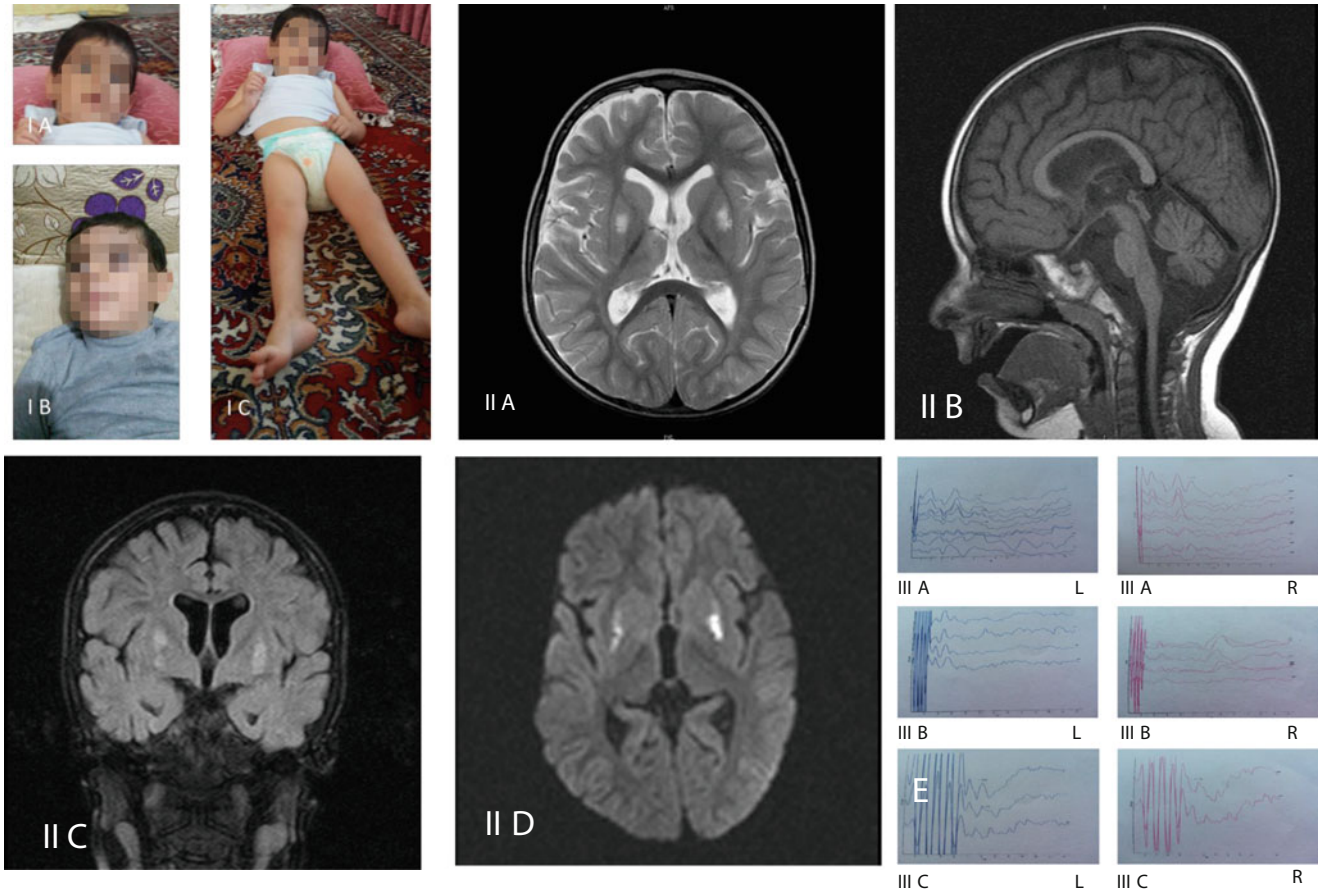

Fig. 2 Main physical, imaginary, and auditory findings of our patient at the age of 2.5 years. (**I**) Picture of the patient: (*IA*) Thick diffuse eyebrows, short palpebral fissures with upper eyelid retraction and prominent forehead, (*IB*) Large, low set protruding ears, thin and parrot-like nose, long curly eyelashes, and hypertrichosis, (*IC*) Spasticity of the lower limbs. (**II**) Magnetic resonance imaging of the brain: (*IIA*) Axial T2-weighted image shows bilateral hyperintense aspect of basal ganglia (putamen and globus pallidus), (*IIB*) Sagittal T1-weighted image shows a globally reduced cerebellar volume. The axial dark flue image demonstrates a prominence of cerebellar folias, (*IIC*) The flair coronal image demonstrates bilateral basal ganglia hyperintensities, (*IID*) Diffusion-weighted image (DWI b1000) shows an impaired diffusion in the bilateral basal ganglia. White matter alterations were not seen. (**III**) Auditory evoked potential (AEP) results: The cut-off of hearing loss was defined according to the mean hearing loss at frequencies of 250, 500, and 2,000 Hz as follows (normal hearing $\leq$ 20 dB hearing loss): (*A*) Threshold detected by click acoustic warning was 65 dB for left ear and 90 dB for right ear, (*B*) At frequencies of 500 Hz the threshold for both ears was 90 dB, (*C*) There was no response at the frequency of 2,000 Hz in both ears. *Abbreviations*: *L* left ear, *R* right ear

width 21% (ref. range: 11.6–14.6%)). He received no iron therapy. The plasma alanine aminotransferase (141 U/L (ref. range: 5–45 U/L)), aspartate aminotransferase (149 U/L (ref. range: 15–55 U/L)), and gamma-glutamyl transferase (324 U/L (ref. range <55 U/L)) were elevated. Ammonia was slightly elevated 73 µmol/L (ref. range: 21–50). Total and conjugated bilirubin were within the normal range. Serum total cholesterol level was low 2.87 mmol/l (ref. range: 3.36–5.09 mmol/l). Albumin and CK were normal. The plasma lactate (4.07 mmol/l (ref. range < 2.1 mmol/l)) and lactate–pyruvate ratio 97.39 (redox state, ref. range <20) were high. Urinary organic acid analyses revealed elevated excretion of 3-methylglutaconic acid (120–130 mmol/l creatinine, ref. range <15), 3-methylglutarate (95 mmol/mol creatinine, ref. range <5), ethylmalonic acid (116–120 mmol/mol creatinine, ref. range <14.6), and succinate (162 mmol/mol creatinine, ref. range <5). FSH was elevated 9.34 mIU/ml (ref. range 0.26–3.0) before puberty, LH as well as free and total testosterone was within the normal range.

Measurements of the Respiratory Chain Enzymes in Muscle

The investigation of enzymes of mitochondrial energy metabolism in muscle showed activities at the lower range of normal in relation to the protein content of most enzymes, however, cytochrome *c* oxidase was significantly decreased (53% of the lower limit of the reference range 79 mUnits/mg protein, reference range 148–392). In relation to the mitochondrial marker enzyme citrate synthase a similar decrease of cytochrome *c* oxidase to 0.48 mUnits/

mUnits citrate synthase (reference range 0.83–2.4) was also observed (more details in the supplementary material).

Genetic Investigations

The chromosome analysis on the karyogram was 46, XY. Sanger Sequencing of *DNAJC19* (NM_145261.3) revealed a previously unreported variant c.63delC (p.Tyr21*) in homozygous state (Fig. 1). This frameshift mutation is predicted to initiate a premature stop codon. This finally leads to the production of a severely truncated protein, if any. This mutation is neither present in the ExAC (http://exac.broadinstitute.org) nor KAVIAR (http://db.systemsbiology.net/kaviar) databases.

Discussion

It is often challenging and time-consuming to obtain a specific diagnosis in pediatric patients with multi-organ disease without using exome sequencing. In the patient reported here the combination of early onset dilated non-compaction cardiomyopathy with global developmental delays led to metabolic screening. The finding of 3-MGA-uria reduced the list of (known) differential diagnoses to: DNAJC19 defect (or DCMA syndrome), AGK defect (or Sengers syndrome, frequent additional finding cataracts), and TAZ defect (or Barth syndrome, frequent additional finding neutropenia). The latter two were considered less likely given the movement disorder and cryptorchidism of the patient reported here.

DNAJC19 defect was first described in a Canadian Hutterite population (Davey et al. 2006, Sparkes et al. 2007). In 2012 Ojala et al. reported a second affected family (Ojala et al. 2012) and recently another patient (Al Teneiji et al. 2016) was described. Table 1 gives an overview of all patients reported to date.

Sensorineural hearing loss, dysmorphic facial feature, and basal ganglia alteration were the three differences between our patient and those previously described.

Based on the similarity of DNAJC19 and yeast Tim14 protein it was suggested that DCMA phenotype might be the result of defective import and assembly of mitochondrial proteins through the TIM23 translocase pathway (Davey et al. 2006). Abnormal gathering of TIM23 transporter is the underlying pathomechanism of another (mitochondrial) disorder, Mohr–Tranebjaerg syndrome (biallelic mutations in *TIMM8A*) (Rothbauer et al. 2001). Sensorineural deafness, visual loss, intellectual disability, and movement disorders are the main components of this progressive neurodegenerative disorder (Tranebjaerg et al. 1995). Deafness is also found in another inborn error of metabolism with 3-MGA-uria as a discriminating feature (SERAC1 defect (Wortmann et al. 2012)) and is frequently seen in mitochondrial disorders (Ammar et al. 2016) which could indicate that it is a part of the clinical spectrum of DNAJC19 defect. Alternatively, isolated hearing loss is a frequent finding and could also be due to a second (genetic) disorder.

The dysmorphic features described in our patient are probably consistent with the heterogeneous clinical presentations of children with mitochondrial disorders (Nissenkonr et al. 1999).

Reduced cerebellar volume, described as non-progressive in the original Hutterite family (Davey et al. 2006) and as progressive cerebellar atrophy (Al Teneiji et al. 2016), was also present (Fig. 2). Additionally, our patient showed bilateral basal ganglia alterations, another well-known and common feature of mitochondrial disorders (Baertling et al. 2016). No white matter involvement was seen. The latter may have been a transient finding, as it was seen only in one MRI taken at the age of 4 years in one patient (Al Teneiji et al. 2016).

Gathering more patient data also allows more insight into the underlying pathomechanism. We report clearly reduced cytochrome *c* oxidase (complex IV) activity in muscle tissue and fibroblast cell cultures. In previously reported patients with DNAJC19 defect alterations in the respiratory chain activity have been reported. Ojala et al. (2012) described diminished complex I, II, and IV activity in skeletal muscle (not in cardiac muscle) and Al Teneiji et al. (2016) reported reduced activity of both NADH-Q1-reductase (complex I) and NADH-cytochrome *c* reductase in muscle and succinate cytochrome *c* reductase (complex II) in fibroblasts in one patient. In general, mitochondrial dysfunction not affecting a specific enzyme (complex) is in line with the findings in other disorders of the biosynthesis and remodeling of phospholipids (TAZ defect, SERAC1 defect) (Thiels et al. 2016).

Finally, our presentation of another patient suggests that DNAJC19 defect may not be as rare as previously thought but presumably still under diagnosed.

In conclusion, we report the fourth family with DNAJC19 defect (or DCMA syndrome), with details of the mutational spectrum and describing sensorineural hearing loss, dysmorphic features, and basal ganglia alterations on MRI for the first time in this disorder. This report further supports a thorough clinical investigation in the presence of a strong biomarker which can lead to a swift diagnosis without performing exome sequencing.

Synopsis

Sensorineural hearing loss and bilateral basal ganglia lesions may be additional features of dilated cardiomyopathy and ataxia syndrome.

Table 1 Clinical features of the present patient and the previously described patients

	Davey et al. (2006) ($N = 18$)	Ojala et al. (2012) ($N = 2$)	Al Teneiji et al. (2016) ($N = 1$)	This report ($N = 1$)
Ancestry	Canadian Hutterite	Finnish	Not reported	Turkish
Gender	11 male, 7 female (11/7)	Male	Female	Male
Current age	$N = 11$ alive (median age 18 m, range 4–96 m), 7 deceased (median age 13 y, range 10–22 y)	One alive 17 m, one deceased 13 m	Alive 13 y	Deceased 3 y
c.DNA change	Homozygous c.130-1G>C	Homozygous c.300delA, (p.Ala101Profs*10)	Homozygous c.280+1_280+5delGTAAG	Homozygous c.63delC, (p.Tyr21*)
Mutation type	Splice site	Frame shift	Splice site deletion	Stop
Consanguinity	$F_r = 0.0445$[a]	No	Yes	Yes
IUGR	8/18 (44%)	No	Not reported	Yes
Growth failure	18/18 (100%)	Yes	Yes	Yes
Dysmorphic features	Not reported	No	Not reported	Yes, low set ears, thick eyebrows, parrot nose, fish-mouth
Cardiac findings	DCM (12/18 (67%))	DCM with non-compaction	DCM of left ventricle with non-compaction	DCM
Mental Retardation	10/18 (55%)	Not reported	Yes	Yes
Cerebral imaging	Not reported	P1: normal MRI (3 y), P2: normal ultrasound (age was not reported), marginally reduced neuronal density of the dentate nucleus (autopsy)	Normal MRI (2 y); cerebellar atrophy and white matter changes (4 y), progressive cerebellar atrophy no white matter changes (10 y)	MRI: reduced cerebellar volume; basal ganglia alterations (2.5 y)
Seizures	2/18 (11%)	No	No	No
Hypotonia	Not reported	Yes	Yes	Yes
Deafness	Not reported	No	No	Yes
Optic atrophy	4/18 (22%)	No	Not reported	No
Oculomotor apraxia	2/18 (11%)[b]	No	No	No
Cryptorchidism	12/18 (66%)	P1: Not reported P2: right sided cryptorchism, chorda penis	Not reported	Testicular dysgenesis
Microcytic, hypochromic anemia	12/18 (66%)	Yes	Not reported	Yes
Liver dysfunction	8/18 (44%)	1/2	Yes	Yes
3-Methylglutaconic acid	"Five to ten-fold increase" (data not shown)	P1: 130 mmol/l creatinine (NR<15 mmol/l creatinine) P2: no excretion (at 10 m)	Initially moderately elevated (value was not reported), later undetectable	120 mmol/mol creatinine (NR<20 mmol/mol creatinine)

Abbreviations: *P* patient, *IUGR* intrauterine growth failure, *DCM* dilated cardiomyopathy, *m* months, *y* years, *NR* normal range

[a] This value of random inbreeding shows that high inbreeding in the Hutterite population is not the result of any preference for consanguineous marriage, but instead is a reflection of the small and isolated nature of the population, resulting in a situation where most available mates are related (Relethford 2012)

[b] Benson et al. 2016 followed up two patients from the Davey et al. (2006) series and reported oculomotor apraxia as a feature

Compliance with Ethics Guidelines

Conflict of Interest

Sema Kalkan Ucar, Johannes A. Mayr, René G. Feichtinger, Ebru Canda, Mahmut Çoker, and Saskia B. Wortmann declare that they have no conflict of interest.

Informed Consent

The parents consented for case report.

Author Contributions

Sema Kalkan Ucar diagnosed the patient, drafted the manuscript, reviewed the literature, and approved final version of the manuscript.

Johannes A. Mayr performed the laboratory investigations, drafted laboratory information details, and approved final version of the manuscript.

René G. Feichtinger performed the laboratory investigations, drafted laboratory information details, and approved final version of the manuscript.

Ebru Canda participated in the clinical follow-up of the patient and approved final version of the manuscript.

Mahmut Çoker is a senior clinician and provided supervision in data analysis and completing the manuscript.

Saskia B. Wortmann is a senior clinician and provided supervision in data analysis and completing the manuscript.

References

Al Teneiji A, Siriwardena K, George K, Mital S, Mercimek-Mahmutoglu S (2016) Progressive cerebellar atrophy and a novel homozygous pathogenic DNAJC19 variant as a cause of dilated cardiomyopathy ataxia syndrome. Pediatr Neurol 62(15):58–61

Ammar M, Tabebi M, Sfaihi L et al (2016) Mutational screening in patients with profound sensorineural hearing loss and neurodevelopmental delay: description of a novel m.3861A > C mitochondrial mutation in the MT-ND1 gene. Biochem Biophys Res Commun 474(4):702–708

Baertling F, Klee D, Haack TB et al (2016) The many faces of paediatric mitochondrial disease on neuroimaging. Childs Nerv Syst. PMID: 27449766

Benson MD, Ferreira P, MacDonald IM (2016) Oculomotor apraxia and dilated cardiomyopathy with ataxia syndrome: a case report. Ophthalmic Genet 7:1–3

Berger A, Mayr JA, Meierhofer D et al (2003) Severe depletion of mitochondrial DNA in spinal muscular atrophy. Acta Neuropathol 105(3):245–251

Davey KM, Parboosingh JS, McLeod DR et al (2006) Mutation of DNAJC19, a human homologue of yeast inner mitochondrial membrane co-chaperones, causes DCMA syndrome, a novel autosomal recessive Barth syndrome-like condition. J Med Genet 43(5):385–393

Feichtinger RG, Weis S, Mayr JA et al (2014) Alterations of oxidative phosphorylation complexes in astrocytomas. Glia 62(4):514–525

Mayr JA, Paul J, Pecina P et al (2004) Reduced respiratory control with ADP and changed pattern of respiratory chain enzymes as a result of selective deficiency of the mitochondrial ATP synthase. Pediatr Res 55(6):988–994

Meierhofer D, Mayr JA, Foetschl U et al (2004) Decrease of mitochondrial DNA content and energy metabolism in renal cell carcinoma. Carcinogenesis 25(6):1005–1010

Nissenkonr A, Zeharia A, Lev D et al (1999) Multiple presentation of mitochondrial disorders. Arch Dis Child 81:209–214

Ojala T, Polinati P, Manninen T et al (2012) New mutation of mitochondrial DNAJC19 causing dilated and noncompaction cardiomyopathy, anemia, ataxia, and male genital anomalies. Pediatr Res 72(4):432–437

Relethford JH (2012) Inbreeding. In: Relethford JH (ed) Human population genetics, 1st edn. Wiley-Blackwell, pp 49–76

Richter-Dennerlein R, Korwitz A, Haag M et al (2014) DNAJC19, a mitochondrial cochaperone associated with cardiomyopathy, forms a complex with prohibitins to regulate cardiolipin remodeling. Cell Metab 20(1):158–171

Rothbauer U, Hofmann S, Muhlenbein N et al (2001) Role of the deafness dystonia peptide 1 (DDP1) in import of human Tim23 into the inner membrane of mitochondria. J Biol Chem 276:37327–37334

Rustin P, Chretien D, Bourgeron T et al (1994) Biochemical and molecular investigations in respiratory chain deficiencies. Clin Chim Acta 228(1):35–51

Sparkes R, Patton D, Bernier F (2007) Cardiac features of a novel autosomal recessive dilated cardiomyopathic syndrome due to defective importation of mitochondrial protein. Cardiol Young 17(2):215–217

Thiels C, Fleger M, Huemer M et al (2016) Atypical clinical presentations of TAZ mutations: an underdiagnosed cause of growth retardation? JIMD Rep. PMID:26724946

Tranebjaerg L, Schwartz C, Eriksen H et al (1995) A new X- linked recessive deafnesssyndrome with blindness, dystonia, fracture, and mental deficiency is linked to Xq22. J Med Genet 32:257–263

Wortmann SB, Vaz FM, Gardeitchik T et al (2012) Mutations in the phospholipid remodeling gene SERAC1 impair mitochondrial function and intracellular cholesterol trafficking and cause dystonia and deafness. Nat Genet 44(7):797–802

Wortmann SB, Duran M, Anikster Y et al (2013) Inborn errors of metabolism with 3-methylglutaconic aciduria as discriminative feature: proper classification and nomenclature. J Inherit Metab Dis 36(6):923–928

JIMD Reports
DOI 10.1007/8904_2016_24

CASE REPORT

Lysosomal Storage Disorders in Nonimmune Hydrops Fetalis (NIHF): An Indian Experience

Jayesh Sheth • Mehul Mistri • Krati Shah • Mayank Chaudhary • Koumudi Godbole • Frenny Sheth

Received: 09 September 2016 / Revised: 22 October 2016 / Accepted: 14 November 2016 / Published online: 08 December 2016

Abstract Lysosomal storage disorders (LSD) are rare inherited neurovisceral inborn errors of metabolism which may present as nonimmune hydrops fetalis (NIHF) during pregnancy. Although causes of NIHF are highly diverse, LSDs are one of the underlying causes of NIHF. The aim of this study was to elucidate most frequent causes of LSDs presenting as NIHF in Indian population. Several fetal tissues were investigated for enzymatic diagnosis of LSDs using modified fluorometric assays in the current prospective study carried out at our national tertiary center from 2006 through 2016. Other general causes of NIHF were ruled out. Twenty-one percent (7/33) of cases were confirmed to have LSDs. Two patients were diagnosed with Hurler syndrome; two had Sly syndrome and one each of Niemann-Pick disease type A/B, Gaucher's disease, and mucolipidosis. Four of eleven cases (36%) with recurrent NIHF were found to have LSDs. In spite of extreme rarity of LSDs, they should be considered as a potential cause of NIHF, especially with recurrent NIHF. Specific investigations of LSD leading to definitive diagnosis may aid the clinician in providing accurate genetic counseling and prenatal diagnosis to the patients and help in subsequent pregnancies to the families. Furthermore, early intervention and management with enzyme replacement therapy may be planned for the lysosomal storage disorders where available.

Communicated by: Markus Ries, MD, PhD, MHSc, FCP

J. Sheth (✉) · M. Mistri · K. Shah · F. Sheth
FRIGE's Institute of Human Genetics, FRIGE House, Jodhpur Gam Road, Satellite, Ahmedabad 380 015, India
e-mail: jshethad1@gmail.com; mistrimehul@yahoo.co.in; drkratishah@gmail.com; fshethad1@googlemail.com

M. Chaudhary
Department of Fetal Medicine, May Flower Hospital, Ahmedabad 380 009 Gujarat, India
e-mail: dr11mayank@rediffmail.com

K. Godbole
Department of Genetics, Deenanath Mangeshkar Hospital, Pune, India
e-mail: koumudig@gmail.com

Introduction

Nonimmune hydrops fetalis is defined as the accumulation of excess pathological fluid in fetal soft tissues and serous cavities detected by ultrasonography where isoimmunization has been excluded (Machin 1989). During intrauterine life, it presents with subcutaneous edema and effusion in two or more serous cavities such as pericardial, pleural, and ascites and is associated with polyhydramnios or placental thickening (>4 cm in second trimester and >6 cm in the third trimester) (Society for Maternal-Fetal Medicine (SMFM) et al. 2015). The varied pathophysiologic mechanisms involved in NIHF are intrauterine anemia and heart failure, hypoproteinemia, and various structural anomalies that interfere with fetoplacental circulation (Machin 1989). NIHF is commonly seen with a reported incidence of around 3 per 10,000 births with much higher incidence during first and second trimester in about 85% of all fetal hydrops cases (Ismail et al. 2001). The etiology of NIHF is complex and remains unknown in 15–25% of patients even after extensive investigations (Bellini et al. 2009). Among diverse etiologies of NIHF, the most common are cardiovascular followed by chromosomal, hematologic, infection, thoracic, lymphatic dysplasia, twin-to-twin transfusion, urinary tract malformations, and an inborn error of metabolism (IEM) (Bellini et al. 2009). Inborn errors of metabolism are the heterogeneous group of autosomal recessive rare inherited disorders, with lysosomal storage disorders (LSD) as the most common subtype. To enumerate, there are 14 different LSDs: Hurler

syndrome (MPS-I; OMIM #607014), Morquio-A (MPS-IVA; OMIM #253000), Sly syndrome (MPS-VII; OMIM #253220), galactosialidosis (OMIM #256540), sialidosis (OMIM #256550), GM1 gangliosidosis (OMIM #230500), Gaucher type 2 (OMIM #230900), Niemann-Pick disease types A and C (NPD-A and NPC; OMIM #257200, #257220), Farber granulomatosis (OMIM #228000), Wolman disease (OMIM #278000), mucolipidosis II (I-cell disease; OMIM #252500), sialic acid storage disease (ISSD; OMIM #269920), and multiple sulfatase deficiency (OMIM #272200) which have been shown to be associated with NIHF and congenital ascites (Burin et al. 2004). The present study was planned to identify the commonest LSD in the Indian population and report any new cause of LSD among the growing list of various storage disorders during pregnancy. There lies an importance of enzymatic studies in the chorionic villous sample or amniotic cultured cells, once the most common conditions associated with nonimmune fetal hydrops have been ruled out.

Materials and Methods

The present prospective study was planned in 33 cases of NIHF during 2006–2016. All the procedures were followed in accordance with the ethical standards of the committee on human experimentation (institutional and national) and with the Helsinki Declaration of 1975, as revised in 2000 (5). Informed consent was obtained from all patients for inclusion in the study.

They were referred from different parts of the country for further investigation of hydrops. Only those cases with normal chromosome study from the placental or fetal tissue or cord blood, an absence of TORCH infection, negative Coombs test, an absence of any other infection as ruled out by normal complete blood count (CBC), and absence of any liver disease in the mother during pregnancy were included in the study. Demographic details of all patients recruited for the study are listed in Table 1. Among all, 21 cases were investigated during the prenatal period; 6 cases were investigated from placental and/or fetal tissue obtained as a product of conception (POC) and the other 6 cases from cord blood obtained from the neonate.

Prenatal sampling was done depending upon the stage of pregnancy, fetal position, and maternal health. Chorionic villous sampling (CVS) and/or amniocentesis were carried out between 10–13 and 15–18 weeks of gestation, respectively, as per the standard procedure. In the case of high-risk pregnancy, planned pregnancy termination was carried out and fetal tissue was collected. The CVS/AF (amniotic fluid) samples and/or POC material were collected in a sterile collection medium (10–15 mg fetal tissue). CVS/POC cells were checked for maternal contamination followed by washing with phosphate-buffered saline. The cells were inoculated in the growth medium and were processed under 5% CO_2 similar to AF as per standard protocol. The cells were harvested after obtaining confluence and protein activity was determined. The final concentration of protein was adjusted to 2–10 mg/ml for lysosomal enzyme study. In the case of hydropic newborn, cord blood samples were collected and enzyme activity was carried out using the synthetic 4-methylumbelliferone-fluorogenic substrate as described earlier (Sheth et al. 2004). The enzyme activity was expressed as nmol/h/mg of protein.

All lysosomal enzymes except for NPC, Farber, and Wolman disease that are known to be associated with NIHF were investigated as shown in Table 2. These include α-iduronidase (EC3.2.1.76) for MPS-I, β-galactosamine-6-sulfatase (EC3.1.6.10) for MPS-IVA, β-D-glucuronidase (EC 3.2.1.31) for MPS-VII, sphingomyelinase (EC 3.1.4.12) for NPD-A/B, β-D-galactosidase (EC 3.2.1.23) for GM1 gangliosidosis, β-glucosidase (EC 3.2.1.21) for Gaucher disease, and total and free *N*-acetylneuraminic acid for ISSD.

Results

A study of lysosomal enzyme was carried out in 33 NIHF cases. This included 21 (63.3%) pregnancies investigated from cultured CVS or AF cells as prenatal cases, 6 (18.1%) cases with miscarriages that were investigated from cultured POC cells, and an equal number of cord blood cases ($n = 6$; 18.1%) were studied in newborn. Among these, seven cases (21.1%) of NIHF were found to be associated with different LSDs like mucopolysaccharide disorders (MPS-1 and MPS-VII) two in each, sphingolipid disorder (NPD-A/B and Gaucher's disease) one in each, and one with receptor defect (I-cell) as shown in Table 3. The study includes 11 cases with recurrence of NIHF in more than one pregnancy while remaining 22 cases presented as NIHF for the first time that includes three pregnancies with consanguineous marriages.

Two cases of MPS-I and one case each of I-cell and NPD-A/B were diagnosed prenatally from cultured amniotic fluid cells. A case of Gaucher's disease and two cases of MPS-VII were diagnosed from cultured CVS cells and POC, respectively. Those with confirmed LSDs with an etiology of NIHF were referred for prenatal diagnosis during subsequent pregnancy whereas POC cases were referred to know the cause of NIHF after finding the normal chromosomal study and ruling out other causes. None of the consanguineous families were detected to have LSDs associated with NIHF. Four out of 11 (36%) cases with a history of recurrent NIHF had LSD as its etiology. The reference range of aforementioned lysosomal enzymes was established in various tissues as shown in Table 4.

Table 1 Demographic details of patients recruited for investigation of NIHF

Sr. No.	Tissue	Gestational age (weeks)	Patient age (years)	Consanguinity	USG findings	Previous history of NIHF	Enzyme study
1	AF	18	30	No	Hydrops	No	Normal
2	AF	20		No	IUD	Yes	Normal
3	CV	11	23	No	IUD	No	Normal
4	POC	18	26	Yes	Fetal ascites	Yes	Normal
5	CV	13	25	No	Fetal ascites	No	*Gaucher*
6	CV	12	29	No	Hydrops and IUD	No	Normal
7	POC	22		No	Hydrops	Yes	Normal
8	POC	12	29	No	IUGR and hydrops	No	Normal
9	AF	16	23	No	IUD due to hydrops	No	Normal
10	AF	28	25	No	Polyhydramnios	Yes	Normal
11	Cord blood	25	35	No	Polyhydramnios	No	Normal
12	Cord blood	28	25	No	Hydrops	No	Normal
13	AF	16	26	No	Fetal edema	No	*NPD-A/B*
14	AF	14	30	No	Hydrops	Yes	Normal
15	Cord blood	28	28	No	Hydrops	No	Normal
16	AF	16	32	No	Hydrops	Yes	Normal
17	Cord blood	28	27	No	Hepatomegaly, cardiomegaly, pulmonary hypoplasia, ascites	No	Normal
18	AF	16	21	No	NIL	Yes	Normal
19	AF	20	26	No	Cystic hygroma and hydrops	Yes	*MPS-I*
20	Cord blood	19		No	Hydrops	Yes	Normal
21	Cord blood	28	31	Yes	Ascites	No	Normal
22	AF	18	30	No	Hydrops	Yes	*I-cell*
23	AF	28	29	No	Fetal edema	No	Normal
24	AF	20	30	No	Hydrops	No	Normal
25	AF	19	24	No	Hydrops	No	*MPS-I*
26	POC	18	32	No	Hydrops	No	Normal
27	AF	20	20	No	Polyhydramnios	No	Normal
28	POC	20	27	No	Hydrops with ascites	No	*MPS-VII*
29	AF	19	27	No	Hydrops	No	Normal
30	POC	18	28	No	Hydrops	Yes	*MPS-VII*
31	AF	19	28	No	Hydrops	No	Normal
32	CV	13	26	No	Hydrops	No	Normal
33	AF	20	22	Yes	Hydrops	No	Normal

Discussion

Nonimmune hydrops fetalis is a serious and life-threatening sign pointing towards a varied etiology. Though the overall incidence of NIHF is very low, it accounts for nearly 3% mortality in the perinatal period (Swain et al. 1999). This incidence may be higher, however, because intrauterine fetal death and in utero spontaneous resolution are likely to mask the true incidence. With the availability of advanced diagnostic facilities, the etiology can be determined in 60–85% of cases (Bellini et al. 2009). In our study 33 cases of NIHF, storage disorders were diagnosed in seven patients (21%). In a recent systematic review, LSD occurrence was seen in 5.2% of NIHF cases and 17.4% if all idiopathic cases were taken into consideration (Gimovsky et al. 2015). The higher percentage of 21% (7/33) in the present study shows the significance of LSDs as the underlying cause of NIHF. The current study has the largest yield compared to studies systematically reviewed by Whybra et al. (2012) and recently reported by Vianey-Saban et al. (2016). This could be attributed to the ascertainment bias as being a national referral center dedicated to LSDs and a referral may have been sent after a comprehensive workup. The recurrence of NIHF may have given a clue to the genetic

Table 2 Investigation of lysosomal enzymes

Sr. No.	Enzyme	Substrate	Disorder
1	α-Iduronidase	4-mu-α-L-iduronide	Hurler (MPS-I)
2	β-Galactosamine-6-sulfatase	4-mu-β-Galactose-6-sulfate	Morquio (MPS-IVA)
3	β-D-Glucuronidase	4-mu-β-D-glucuronide	Sly (MPS-VII)
4	Sphingomyelinase	4-mu-A-D-mannopyranoside	NPD-A/B
5	β-D-Galactosidase	4-mu-β-D-galactopyranoside	GM1 gangliosidosis
6	β-Glucosidase	4-mu-β-D-glucopyranoside	Gaucher
7	Free and total *N*-acetylneuraminic acid	*N*-acetylneuraminic acid (NANA)	Infantile sialic acid storage disorder (ISSD)

Table 3 Enzyme activity in affected LSD cases having NIHF

Disease name	Enzyme	Sample types			No. of patients ($n = 7$)
		CVS[a]	AF[a]	POC[a]	
Mucopolysaccharidosis					
Hurler disease (MPS-I)	α-Iduronidase	–	7.5 ($n = 1$)	7.9 ($n = 1$)	$n = 2$
Sly syndrome (MPS-VII)	β-Glucuronidase	–	UD ($n = 1$)	0.6 ($n = 1$)	$n = 2$
Sphingolipidosis					
Gaucher's disease	β-Glucosidase	47.46	–	–	$n = 1$
Niemann-Pick A (NPD-A)	Sphingomyelinase	–	3.0	–	$n = 1$
Mucolipidosis					
Mucolipidosis-II	β-Glucuronidase	–	11.9	–	$n = 1$
	Hexosaminidase-total	–	45.9	–	
	β-Galactosidase	–	37.5	–	

UD undetectable, *CVS* chorionic villous sample, *AF* amniotic fluid, *POC* products of conception
[a] All values are in nmol/h/mg protein

Table 4 Normal values of lysosomal enzymes in cultured CVS and cultured AF/POC

Enzymes	Enzyme activity (Sheth et al. 2014)	
	Cultured CVS[a]	Cultured AF/POC[a]
α-Iduronidase	19.27–93.4	85.5–156.3
β-Glucuronidase	26.5–149.6	50.07–197.1
β-Glucosidase	115–409	118–584.8
Sphingomyelinase	13.3–18.8	17.0–69.4
Hexosaminidase-total	4,507–15,473.2	4,487.0–16,286.2
β-Galactosidase	150–644	296–1,195

[a] All values are in nmol/h/mg protein

etiology and as a result almost one-third of the referred patients were found to have LSDs as an underlying cause.

Till date, around 14 different LSDs are known to be associated with NIHF and congenital ascites, with the highest number being associated with mucopolysaccharide disorders followed by sphingolipidosis and lysosomal transporter defects (Cheng et al. 2003). Vianey-Saban and colleagues have carried out a large study of IEM and have shown that 108 fetuses of 1,700 pregnancies with NIHF after exclusion of all causes were found to be affected by LSDs (6.3%) with Sly syndrome as the most common LSD. A present study shows that the highest number of fetuses was found to be affected with MPS-1 and MPS-VII followed by Gaucher, NPD-A, and I-cell disease. The current study has not covered Niemann-Pick disease type C, Wolman, and Farber disease, which is the major limitation of the study. Nonetheless, the overall occurrences of storage disorders in NIHF are in the same order as reported in a large series of data (Whybra et al. 2012). In a tertiary center from North India, Verma and his group (2012) had also incidentally diagnosed one case of Hurler syndrome during fetal autopsy that died in utero at 26 weeks of gestation due to NIHF. Thus, detection of Hurler syndrome in the present study and earlier reports further support the association of NIHF with Hurler syndrome.

Morquio syndrome and sialidosis are also found to be associated with NIHF (Applegarth et al. 1987) but none were detected in the present study.

The exact mechanism of NIHF and LSDs is controversial. The best explicable hypothesis is obstruction of venous blood return resulting from visceromegaly and decreased erythropoiesis leading to anemia with/without hypoproteinemia. There lies a great phenotypic variability among presentation of LSDs. Hydrops fetalis manifests a severe phenotype in Gaucher's disease with the 84GG mutation in *GBA* gene which portrayed as a collodion baby whereas NPD-A does not manifest with NIHF even with two knockout mutations. The effect in the latter could more likely be due to an epigenetic factor/s or gene modifiers (Burin et al. 2004).

There also have been cases of transient NIHF and LSDs, mostly associated with GM1 gangliosidosis, MPS-IVA, MPS-VII, and Niemann-Pick disease type C (Whybra et al. 2012). In a growing list of LSDs and NIHF, more numbers of LSDs are likely to be missed in transient NIHF. Such pregnancies should be investigated or followed up postnatally to know the exact incidence associated with this condition. Recently, Ota et al. (2016) followed up NIHF and merely 33% of the fetuses survived at 1 year pointing towards the possibility of some metabolic disorder that might have been missed in the study.

During the antenatal period, signs like hepatosplenomegaly, hypoplastic lungs, and milky ascitic fluid besides congenital ascites are a clue to LSDs and careful fetal sonography can aid the diagnosis (Daneman et al. 1983). Staretz-Chacham and colleagues (2009) have proposed that dysmorphic facies, irregularity of the epiphyses, and coarse trabeculations of the long bones associated with NIHF corroborate to the diagnosis of LSD. Placental histology in cases with hydrops or ascites at birth may be very helpful in providing the diagnosis of storage diseases (Parks 2015).

High incidence of LSDs in the current study demands more awareness regarding this subgroup of IEM among fetal medicine experts. It can also be inferred that Hurler syndrome and Sly syndrome are the first choices of investigation in a pregnancy associated with NIHF among inborn errors of metabolism in the Indian population.

Moreover, economic and accurate prenatal diagnosis of LSD is a major unmet need for low-middle-income countries like ours which would facilitate consideration of therapies before the occurrence of irreversible complications. The major limitation of the current study was the inability to perform enzymes for all known LSDs, especially in familial NIHF and the history of consanguinity which might have helped us to offer a definitive diagnosis to the patients and provide a further increase in the diagnostic yield.

Thus we conclude that correct diagnosis of NIHF aids in the management of lysosomal storage disorders by newer available enzyme replacement therapies and the genetic counseling in the subsequent pregnancy. This study emphasizes the fact that incidences of LSDs, specifically MPS-I, are likely to be higher than published in the reported studies, predominantly with a history of recurrence NIHF, with Hurler and Sly syndromes being among the common causes in Indian population. The differential diagnosis of LSDs needs to be considered for transient forms of ascites and postnatal follow-up remains obligatory for such patients.

Acknowledgment We sincerely thank the patients and their families for their cooperation and for consenting to investigations. The authors also thank Dr. Sunil Trivedi for critical reading of the manuscript.

Synopsis

A subset of inborn errors of metabolism is a noteworthy cause for recurrent nonimmune fetal hydrops, with Hurler and Sly syndromes being among the common causes in Indian population.

Conflict of Interests

Jayesh Sheth, Mehul Mistri, Krati Shah, Mayank Chaudhary, Koumudi Godbole, and Frenny Sheth declare that they have no conflict of interests (financial or nonfinancial).

Consent

Informed written consent was obtained from all the participants for publication of their clinical details and/or clinical images. A copy of the written consent is available for review by the editor of this journal.

Ethics

- Present study under submission has been approved by the institutional ethics committee [FRIGE's Institute of Human Genetics] wide approval number FRIGE/IEC/5/2010 dated 7th March, 2010. This process is in accordance with the Helsinki Declaration.
- An informed consent was obtained from the parents before enrolling for the investigations [this was in accordance with the requirement of the institutional ethics committee].
- An informed consent for publication was also obtained from the individuals included in the submission [this was in accordance with the requirement of the institutional ethics committee].

Authors' Contributions

Planned and designed the experiments: JS, MM. Clinical analysis: KS, KG, MC. Enzyme and molecular analysis: JS, MM. Wrote the first draft of the manuscript: KS and FS. Made critical revisions and approved final version: KS, JS, and FS. All authors reviewed and approved of the final manuscript.

Funding

No funding was received for this part of the study.

References

Applegarth DA, Toone JR, Wilson RD et al (1987) Morquio disease presenting as hydrops fetalis and enzyme analysis of chorionic villus tissue in a subsequent pregnancy. Pediatr Pathol Affil Int Paediatr Pathol Assoc 7:593–599

Bellini C, Hennekam RCM, Fulcheri E et al (2009) Etiology of non-immune hydrops fetalis: a systematic review. Am J Med Genet A 149A:844–851. doi:10.1002/ajmg.a.32655

Burin MG, Scholz AP, Gus R et al (2004) Investigation of lysosomal storage diseases in nonimmune hydrops fetalis. Prenat Diagn 24: 653–657. doi:10.1002/pd.967

Cheng Y, Verp MS, Knutel T, Hibbard JU (2003) Mucopolysaccharidosis type VII as a cause of recurrent non-immune hydrops fetalis. J Perinat Med 31:535–537. doi:10.1515/JPM.2003.083

Daneman A, Stringer D, Reilly BJ (1983) Neonatal ascites due to lysosomal storage disease. Radiology 149(2):463–467

Gimovsky AC, Luzi P, Berghella V (2015) Lysosomal storage disease as an etiology of nonimmune hydrops. Am J Obstet Gynecol 212:281–290. doi:10.1016/j.ajog.2014.10.007

Ismail KM, Martin WL, Ghosh S et al (2001) Etiology and outcome of hydrops fetalis. J Matern Fetal Med 10:175–181

Machin GA (1989) Hydrops revisited: literature review of 1,414 cases published in the 1980s. Am J Med Genet 34:366–390. doi:10.1002/ajmg.1320340313

Ota S, Sahara J, Mabuchi A et al (2016) Perinatal and one-year outcomes of non-immune hydrops fetalis by etiology and age at diagnosis. J Obstet Gynaecol Res 42:385–391. doi:10.1111/jog.12922

Parks WT (2015) A pathologist's approach to nonimmune hydrops. J Fetal Med 2:143–149. doi:10.1007/s40556-015-0055-x

Sheth J, Mistri M, Sheth F, Datar C, Godbole K, Kamate M, Patil K (2014) Prenatal diagnosis of lysosomal storage disorders by enzymes study using chorionic villus and amniotic fluid. J Fetal Med 1:17. doi:10.1007/s40556-014-0001-3

Sheth J, Patel P, Sheth F, Shah R (2004) Lysosomal storage disorders. Indian Pediatr 41:260–265

Society for Maternal-Fetal Medicine (SMFM), Norton ME, Chauhan SP, Dashe JS (2015) Society for maternal-fetal medicine (SMFM) clinical guideline #7: nonimmune hydrops fetalis. Am J Obstet Gynecol 212:127–139. doi:10.1016/j.ajog.2014.12.018

Staretz-Chacham O, Lang TC, LaMarca ME et al (2009) Lysosomal storage disorders in the newborn. Pediatr 123:1191–1207. doi:10.1542/peds.2008-0635

Swain S, Cameron AD, McNay MB, Howatson AG (1999) Prenatal diagnosis and management of nonimmune hydrops fetalis. Aust N Z J Obstet Gynaecol 39:285–290

Verma PK, Ranganath P, Dalal AB, Phadke SR (2012) Spectrum of lysosomal storage disorders at a medical genetics center in northern India. Indian Pediatr 49:799–804

Vianey-Saban C, Acquaviva C, Cheillan D et al (2016) Antenatal manifestations of inborn errors of metabolism: biological diagnosis. J Inherit Metab Dis 39:611. doi:10.1007/s10545-016-9947-8

Whybra C, Mengel E, Russo A et al (2012) Lysosomal storage disorder in non-immunological hydrops fetalis (NIHF): more common than assumed? Report of four cases with transient NIHF and a review of the literature. Orphanet J Rare Dis 7:86. doi:10.1186/1750-1172-7-86

JIMD Reports
DOI 10.1007/8904_2016_25

RESEARCH REPORT

The Risk of Fatty Acid Oxidation Disorders and Organic Acidemias in Children with Normal Newborn Screening

Callum Wilson • Detlef Knoll • Mark de Hora • Campbell Kyle • Emma Glamuzina • Dianne Webster

Received: 02 October 2016 / Revised: 13 November 2016 / Accepted: 15 November 2016 / Published online: 08 December 2016

Abstract New Zealand has undertaken expanded newborn screening since 2006. During that period there have been no reported cases of fatty acid oxidation disorders or organic acidemias that have been diagnosed clinically that the screening programme missed. However there may have been patients that presented clinically that were not diagnosed correctly or notified.

In order to investigate the false-negative screening rate a case-control study was undertaken whereby the clinical coding data and relevant medical records were reviewed for 150 controls and 525 cases. The cases had normal newborn screening but with key analytes and/or ratios just below the notification level for individual disorders and thus in theory were most at risk of having metabolic disease.

Two cases had medical histories suggestive of metabolic disease and thus could represent a false-negative screen. One of these had marginally elevated octanoyl carnitine levels and thus possible medium-chain acyl Co-A dehydrogenase deficiency (MCADD) while the other had elevated isovaleryl carnitine and thus may have been a case of isovaleric acidemia (IVA). However, subsequent molecular analysis revealed that the diagnosis of MCADD and IVA was unlikely.

Despite relatively high cut-offs the New Zealand Newborn Metabolic Screening Programme does not appear to have missed any confirmed cases of fatty acid oxidation disorders and organic acidemias in its first 8 years of expanded newborn screening. This would suggest a similar low false-negative screening rate in centres with comparable screening protocols and would indicate that the risk of fatty acid oxidation disorders and classical organic acidemias in children who had normal newborn screening is low.

Communicated by: Jerry Vockley, M.D., Ph.D.

C. Wilson (✉) · E. Glamuzina
National Metabolic Service, Starship Children's Hospital, PO Box 92024, Auckland 1142, New Zealand
e-mail: callumw@adhb.govt.nz

D. Knoll
Newborn Metabolic Screening Unit, Auckland City Hospital, Auckland, New Zealand

M. de Hora · D. Webster
Newborn Metabolic Screening Programme, LabPlus, Auckland City Hospital, Auckland, New Zealand

C. Kyle
LabPlus, Auckland City Hospital, Auckland, New Zealand

Introduction

Expanded newborn screening (ENBS) refers to the early detection of disorders of intermediary metabolism by the measurement of acylcarnitines and amino acids in dried blood spots. By focusing on key analytes and ratios, 20 plus potentially clinically devastating diseases can be diagnosed and treated (Chace et al. 2003; Wilcken et al. 2009). A highly specific test is required in order to minimise the laboratory and clinical cost and workload, and more importantly family stress, involved in the follow-up of false positives (Schmidt et al. 2012). Screening laboratories have thus adopted particular key analytes and ratios that are generally accepted to offer the highest screening sensitivity, specificity and positive predictive value. The analyte cut-offs are similar between programmes albeit with some local variation in screening laboratories internationally (McHugh et al. 2011).

For each analyte there are children who at the time of screening had levels just below the cut-off and thus were never seen or at least never offered a secondary test and

others who were just above the cut-off and were thus notified to the local clinical metabolic service for follow-up, investigation and treatment. Children in the former group should be those that are most at risk of having false screen-negative metabolic disease.

The New Zealand newborn metabolic screening programme (NMSP) is responsible for the newborn screening of all children born in New Zealand. Testing occurs on days 2–3 and on average it takes 4–5 days for the samples to be transported and analysed in the screening laboratory. The NMSP has close to 100% coverage. ENBS was established in 2006 and over 20 metabolic diseases are screened for.

The NMSP has always adopted relatively high analyte cut-offs (https://www.clir-r4s.org/PartTools/tarCutComp.aspx?guiPartID=188). However apart from one child with asymptomatic carnitine uptake disorder who was diagnosed after a younger sibling was diagnosed, and one child with tyrosinaemia type 1, whose tyrosine was below the cut-off, the NMSP and the New Zealand National Metabolic Service are not aware of any known false screen-negative metabolic disease cases. Likewise, the two New Zealand biochemical genetics laboratories, both of whom have weekly teleconference meetings with the NMSP, have not diagnosed any new cases of fatty acid oxidation disorders (FAODs) or organic acidemia (OA) that were missed by ENBS. Despite this there may still be patients who have presented to hospital with signs and symptoms caused by underlying metabolic disease who remain undiagnosed.

For many years infants born in New Zealand have been assigned a unique health number at birth. This number is used on the newborn screening sample and for all subsequent healthcare episodes, hence it is relatively straightforward to correlate screening results with medical records.

This possibility, along with the ongoing process of reviewing the laboratory screening protocols for each condition, underlined the uncertainty regarding the risk of metabolic disease in those patients who had levels of screening analytes just below the cut-off and whom could be most at risk of a false-negative screen. The purpose of this study was to investigate the outcome in regard to metabolic disease signs and symptoms of children in that cohort and thus estimate the incidence of FAODs and OAs in those children with normal ENBS.

Study Methodology

A retrospective, case-control, observational analysis was performed with investigators blinded to case or control group through the random allocation of study numbers. The primary outcome measure was the prevalence of signs and/or symptoms suggestive of metabolic disease.

Clinical coding data for all hospital attendances or deaths were obtained from the New Zealand Ministry of Health for both cases and controls (as coded by the International Statistical Classification of Diseases and Related Health Problems, Tenth Revision, Australian Modification, ICD-10-AM). Coding criteria considered consistent with FAODs or OA included hypoglycaemia, lethargy, vomiting, seizures, coma, metabolic acidosis, hepatomegaly, increased transaminases, increased CK, muscle weakness, jaundice, cardiac arrhythmias, cardiomyopathy and unexplained death. Study numbers were noted and the hospital medical notes were reviewed for these admissions, allowing classification into either likely metabolic disease or no evidence of metabolic disease. Groups were then unblinded for analysis.

Newborn screening dried blood spot acylcarnitine profiles, the majority collected on days 2 and 3 of life, for both cases and control groups were measured using flow injection electrospray-tandem mass spectrometry.

Cases and controls were chosen from approximately 460,000 children born between December 2006 and December 2014 who weighed between 2.5 and 4.5 kg, were not premature (more than 37-week gestation) and whose initial screening samples had not come from a neonatal intensive care unit. Approximately 100 cases were chosen from each of six potential disease groups: children with possible (a) methylmalonic/propionic acidemia (MMA/PA), (b) isovaleric acidemia (IVA), (c) medium-chain acyl Co-A dehydrogenase deficiency (MCADD), (d) carnitine uptake deficiency (CUD), (e) carnitine-acylcarnitine transporter deficiency (CACT), carnitine palmitoyl transferase deficiency type II (CPTII), and (f) carnitine palmitoyl transferase deficiency type I (CPTI). The cases were identified by having both the ENBS key analyte and related analyte ratio/s just below (or just above in the case of CPT1) and closest to the cut-off for being classified as a positive screen at the time of screening. This case cohort was chosen as they were screen negative and yet were the most likely biochemically to have metabolic disease.

The analytes were, respectively, in group (a) C3: 7.5–15.5 μmol/L with the C3/C2 ratio 0.25–0.46; (b) C5: 0.7–1.5 μmol/L with the C5/C0 ratio 0.01–0.1; (c) C8: 0.60–0.93 μmol/L with the C8/C2 $\geq$0.02; (d) C0: 2–5 μmol/L; (e) C16: 11–14.75 μmol/L with the (C16 + C18.1)/C2 ratio 0.2–0.5; and (f) C0: 50–160 μmol/L with the C0/(C16 + C18) ratio 31–77 (Table 1).

The numbers in each group did not equal 100 but were as close to this as possible while also including all the patients that met the above criteria. Often there was a group of cases with exactly the same ENBS biochemistry for the particular analyte and/or ratio and one had to either include or exclude them all in order to get the number in the group closest to 100. In group g only 56 patients were included as expanding the criteria recruited very large numbers of patients. There were

Table 1 Key analyte level and ratio for cases

Disease	Analyte (μmol/L)	Ratio	Current NZ cut-off[a]	International 50%ile cut-off[b]	Number
MMA, PA	C3: 7.5–15.5	C3/C2: 0.25–0.46	C3 ≥5 and C3/C2 ≥0.25	C3 ≥5.35, C3/C2 ≥0.22	108
IVA	C5: 0.7–1.5	C5/C0 0.01–0.1	C5 ≥1.0	C5 ≥1.2	90
MCAD	C8: 0.60–0.93	C8/C2: ≥0.02	C8 ≥0.8 or C8 ≥0.6 and C8/C2 ≥0.04	C8 ≥0.32, C8/C2 ≥0.04	94
CUD	C0: 2–5.1		C0 ≤5	C0 ≤8	94
CPT II, CACT	C16: 11–14.75	(C16 + C18.1)/C2: 0.2–0.5	C16 ≥12.4	C16 ≥7	83
CPT I	C0: 50–160	C0/(C16 + C18): 31–77	C0 ≥122, and C0 (C16 + C18) ≥70	C0 ≥124	56

[a] These cut-offs have been slightly modified over the duration of screening and thus a small number of patients who may not have been screen positive at the time of screening would be screen positive now
[b] https://www.clir-r4s.org/PartTools/tarCutComp.aspx?guiPartID=188

in total 525 cases. Over the duration of the screening programme the criteria for a positive screen has evolved and thus a very small number of cases that at the time were screen negative would be considered screen positive now.

None of the cases or families had been seen by either the national metabolic or the local paediatric clinical services in regard to their newborn screening results. In some cases, especially with C3 and low CO the infant's initial screen had indicated, as per the NMSP protocol, a need for a second follow-up dried blood spot, and this had been performed. The resultant level was not within the notification range.

The control group were a selection of 150 randomly chosen patients with normal newborn screening who had the analytes between the 25th and 75th centiles.

C14.1, corresponding to the disease very-long-chain acyl Co-A dehydrogenase deficiency (VLCADD), was not included in this study as it was the subject of an extensive previous study (Ryder et al. 2016). C5DC, the key analyte for glutaric acidemia type 1 (GA1), was not included as there was a clear bimodal distribution with a very small group of GA1 patients who had very high levels of glutaryl carnitine (≥0.7 μmol/L) and the rest having normal levels (≤0.45 μmol/L) with only five patients having levels of 0.45–0.7 μmol/L. C5OH, the analyte for 3-methylcrotonyl carboxylase deficiency and related disorders, was not included as the NMSP no longer screens for these conditions due to the clinical uncertainty regarding a positive screening result.

The intracellular cobalamin defects were not specifically investigated in this study as the NMSP is currently assessing the use of homocysteine rather than methionine, as well as C3, for the screening of these conditions.

Results

Of the 525 cases, two had medical records that revealed admissions to hospital with events that were suggestive of an underlying metabolic disease.

Patient A had newborn screening C8 of 0.74 μmol/L and a C8/C2 ratio of 0.03 at day 2 screening (cut-off for positive screen C8 ≥0.8 μmol/L or C8 ≥0.6 μmol/L and C8/C2 ≥0.04). The patient presented aged 17 months after 2 days of upper respiratory tract viral symptoms and poor feeding. They had fed poorly the previous evening and were found the following morning lethargic and hypotonic. The admission blood sugar was 1.7 mmol/L (normal 3.5–5.4 mmol/L) with an appropriately elevated beta-hydroxybutyrate of 3.7 mmol/L. They were commenced on IV 10% dextrose and discharged the following day after a normal meal. An acylcarnitine profile revealed a slightly elevated C8 of 0.3 μmol/L (normal 0.1–0.2 μmol/L) with the laboratory commenting that it was not typical of MCADD but may reflect an MCADD carrier. No follow-up of this was made. The child had two subsequent hospital visits with viral vomiting illnesses and poor oral intake. During these events the child had been given carbohydrate drinks by the parents and was not hypoglycaemic. Sequencing of exons 1–12 of the ACADM gene as well as the intronic areas immediately bordering the exons along with deletion/duplication analysis from DNA obtained from the original dried blood spot revealed one copy of the common c.985A≥G (p.Lys329Glu) mutation with no other abnormality identified.

Patient B had a screening C5 of 0.9 μmol/L and a C5/C0 of 0.01 on day 3 of life (positive screen C5 ≥1.0 μmol/L). There were no other acylcarnitine abnormalities. At 4 months of age the child was found unresponsive in bed and required cardiopulmonary resuscitation. The previous day they had a vomiting illness with poor oral intake. Upon arrival to hospital they were hypotensive and unresponsive with a marked metabolic acidosis and moderately raised liver function tests. An MRI brain showed widespread severe ischemic changes. The child was initially ventilated but due to signs of brain death this was discontinued and the child died that evening. A postmortem and metabolic investigations were not performed. Sequencing of all 12

exons and flanking intronic regions of the isovaleryl Co-A dehydrogenase (IVD) gene from DNA obtained from the original dried blood spot revealed no mutations.

One of the control patients had a medical history suggestive of a possible FAOD. The baby presented in the early neonatal period with hypoglycaemia and required IV 10% dextrose. The baby had mild left ventricular hypertrophy. Both the hypoglycaemia and the hypertrophy resolved over the next few days and it was felt that they had transient hyperinsulinism. There was no maternal diabetes.

Discussion

Expanded newborn screening has been undertaken internationally for nearly 20 years and there are numerous reports from screening centres of their diagnostic results. Few screening services have specifically reported their experience with missed cases (Estrella et al. 2014; Wilcken 2013).

Since commencing ENBS in late 2006, the NMSP has diagnosed 67 cases of FAODs or OAs (Table 2). In addition, there have been five cases of long-chain fat disorders (three CACT deficiency, two VLCADD) and four cases of holocarboxylase synthase deficiency that presented clinically on day 1 of life, prior to newborn screening. One of the CACT cases and both the VLCADD cases died in the first few days of life. The service also had one case of tyrosinaemia type I who presented with severe liver disease at a 3 months of age and had a normal tyrosine level at the time of screening and was thus missed by the ENBS. There has been one missed asymptomatic case of CUD. Other than these, there have been no known missed cases in New Zealand.

The potential high local incidence of false-positive cases in diseases such as of VLCADD, CPT-1, 3-MCC, IVA, citrulinaemia and maternal CUD (Ensenauer et al. 2004; Vijay et al. 2006; Glamuzina et al. 2011; Ryder et al. 2016; Rips et al. 2016) and the local workforce capacity particularly in the first few years of that contributed to the NMSP adopting relatively high cut-off levels. This results in less work for the screening laboratory, fewer second tests and less false-positive cases, thus limiting unnecessary stressful notifications to families. However higher cut-offs bring the concern that clinically significant cases will be missed.

Table 2 Cases of FAOD and OAs diagnosed by New Zealand newborn screening (number screened approximately 460,000)

	Condition	Case count
Fatty acid oxidation	MCAD	28
	VLCAD	11
	CUD (maternal)	5
	CPT-I	3
	MADD	2
	CUD	1
Organic acidemia	IVA	5
	3-MCC	4
	MMA	3
	GA-I	3
	PA	2

Screening for the aminoacidopathies maple syrup urine disease, homocystinuria and tyrosinaemia using leucine/isoleucine, methionine and tyrosine, respectively, is known to be problematic with high rates of false-positive screening and missed cases being reported (Estrella et al. 2014; Naughten et al. 1998). In fact many patients with these conditions can have normal metabolites at the time of newborn screening (https://www.clir-r4s.org/ProjTools/DiseaseRangeComp.aspx) and thus these conditions were not part of this study. The NMSP plans to improve its screening for homocystinuria and tyrosinaemia type I by using total homocysteine and succinylacetone as key analytes, respectively.

This study investigates whether there have been any false-negative screening cases presenting with FAODs and OAs since New Zealand commenced ENBS in 2006. There were only two cases who presented with possible metabolic disease. Case A was a possible MCADD presentation. The baby/child had a typical clinical MCADD event but with significant ketosis. The latter is unusual but not unknown in MCADD (Christodoulou et al. 1995). They did have an acylcarnitine profile at the time suggestive of a possible 'MCADD carrier state'. They are now being treated with an emergency plan. Molecular analysis revealed only a carrier state and thus they are not likely to represent true MCADD. Case B had borderline ENBS levels of C5, the marker for IVA, and died after a short illness at 4 months. This was the only case in the cohort that died or suffered serious morbidity. While the clinical details were suggestive of IVA, the lack of specific metabolic investigations at the time of death and the absence of any disease-causing mutations in the *IVD* gene made the diagnosis of IVA unlikely. IVA is a difficult disease for screening laboratories as there are a number of relatively common variants with elevated screening levels who are at very low or no risk of clinical disease (Ensenauer et al. 2004). C5 is also elevated in the very rare disease 2-methylbutyryl-CoA dehydrogenase deficiency but this does not present with a severe hepatic metabolic decompensation as seen in Case B and thus seems unlikely.

A limitation of this study is that there may be cases who had metabolic disease signs and symptoms who were not captured in the analysis as they presented to their general

practitioners (family doctors) and/or private paediatrician and not the public hospital. However in New Zealand, any children with significant disease would be seen at a public hospital and have ICD-10-AM coding data sent to the Ministry of Health. Likewise any patient who had metabolic disease diagnosed would be known to the metabolic clinical service and/or the two biochemical genetics laboratories and thus be known to the investigators of this study. A further limitation is that very unusual and/or chronic presentations of these conditions may not have been captured by this study. It is also possible that milder forms of these conditions may present in later childhood or adulthood and thus would not yet be identified by this study. However, newborn screening in New Zealand aims to only diagnose patients whereby treatment makes a difference to outcome in early life. There is a small chance that patients may have emigrated from New Zealand and presented clinically with metabolic disease although it would seem likely that the NMSP would have been notified.

This study did not include premature, NICU and/or low-birth -weight babies as these children frequently have ongoing health issues and it was felt that including them would make the analysis of this study difficult. There is thus the possibility that they could have had metabolic disease missed by screening although neither the metabolic laboratory nor the clinical metabolic service is aware of such cases.

The only missed case of FAOD by the NMSP was a child who at day 2 ENBS had a C0 of 8.3 μmol/L, above our cut-off of 5 μmol/L. She was however subsequently diagnosed with CUD, after the family had moved to Australia and the screening service there diagnosed, by ENBS, the disorder in a younger sibling who had a newborn screening C0 of 3 μmol/L. The older child was asymptomatic and interestingly a review of her initial screening parameters showed that even using the Region 4 post-analytical tool (https://www.clir-r4s.org/PostAlyt-Tools/CondScoreSingle.aspx?pcID=1783) for CUD she would have been missed with a profile of 7, a score not informative for CUD. CUD is a difficult disease for a screening service as affected babies may have relatively high metabolites and thus be missed, there are a significant number of maternal cases diagnosed and the condition itself is likely to be benign in the majority of patients (Rasmussen et al. 2014). This study reflects the historic practice of the NMSP using a low free carnitine (C0) alone to screen for CUD. This is now known to be a less-than-optimal analyte by itself and the local experience of the NMSP is that a very low CO is more likely to reflect maternal CUD. The service has now adopted what is hoped to be a more sensitive and specific set of analytes using a combination of low C0, C3 and C16. Thus the results from this study regarding C0 and CUD are less reliable than for the other FAODs.

While not a focus of this study the number of false-positive cases diagnosed by the NZNMS is difficult to estimate as it depends on what one defines as a case. The relatively high cut-offs have resulted in the National Metabolic Service seeing very few screen-positive patients who based on follow-up biochemistry, enzymology and molecular have been subsequently shown to be a false positive. However the majority of the 32 patients with confirmed VLCADs, CUDs, CPT Is, IVAs and 3-MCCs have remained asymptomatic and it is possible, even likely, that many will remain so. This could be due to the treatment although apart from three patients with symptomatic VLCAD they receive a normal diet and only have an 'emergency plan' for times of illness.

It is essential that ENBS laboratories regularly audit their results, in particular the possibility of false-negative cases, and adjust their screening cut-off criteria accordingly. What is more debatable is whether the advantages of far fewer false-positive cases outweigh the harm of missing a small number of cases. This study along with the experience of the clinical NZNMS suggests that ENBS for clinically significant disorders of fatty acid and organic acid metabolism in New Zealand is highly sensitive as there are few missed cases. This is also likely to be the case in screening centres internationally where cut-offs similar to or more sensitive than those in New Zealand are used. ENBS however doesn't detect all metabolic disorders and there are some FAODs and OA that are not screened for. Accordingly, if clinically indicated, the appropriate diagnostic metabolic investigations and treatment should be undertaken even if the newborn screening was normal.

Synopsis

An audit of the medical records of the most at risk of those who were newborn screen negative suggests that New Zealand Newborn Metabolic Screening service has not missed any cases of clinically significant metabolic disease.

Compliance with Ethics Guidelines

Dr. Callum Wilson, Mr. Detlef Knoll, Mr. Mark de Hora, Dr. Campbell Kyle, Dr. Emma Glamuzina, and Dr. Dianne Webster declare that they have no conflict of interest.

All procedures followed were in accordance with the ethical standards of the responsible committee on human experimentation (institutional and national) and with the Helsinki Declaration of 1975, as revised in 2000.

The study was anonymous and informed consent was not required. No identifying information about patients is included in this chapter. The study received approval from

the NZ Ministry of Health National Screening Unit (NSU), the National Health and Disability Ethics Committee and the Auckland District Health Board Research Committee.

Dr. Callum Wilson designed the study, obtained the ethical approval, helped with the initial collection and analysis of medical data and wrote the initial manuscript; Mr. Detlef Knoll, Mr. Mark de Hora and Dr. Dianne Webster collected and analysed the newborn screening data. Dr. Campbell Kyle and Dr. Emma Glamuzina helped with collection and analysis of the medical data. All the authors contributed to the final manuscript.

Dr. Callum Wilson serves as guarantor for this chapter and accepts full responsibility for the work.

References

Chace DH, Kalas TA, Naylor EW (2003) Use of tandem mass spectrometry for multianalyte screening of dried blood specimens from newborns. Clin Chem 49:1797–1817

Christodoulou J, Hoare J, Hammond J, Ip WC, Wilcken B (1995) Neonatal onset of medium-chain acyl-coenzyme A dehydrogenase deficiency with confusing biochemical features. J Pediatr 126:65–68

Ensenauer R, Vockley J, Willard JM et al (2004) A common mutation is associated with a mild, potentially asymptomatic phenotype in patients with isovaleric acidemia diagnosed by newborn screening. Am J Hum Genet 75:1136–1142

Estrella J, Wilcken B, Carpenter K, Bhattacharya K, Tchan M, Wiley V (2014) Expanded newborn screening in New South Wales: missed cases. J Inherit Metab Dis 237:881–887

Glamuzina E, Marquis-Nicholson R, Knoll D, Love DR, Wilson C (2011) Citrullinaemia type I: a common mutation in the Pacific Island population. J Paediatr Child Health 47:262–265

McHugh D, Cameron CA, Abdenur JE et al (2011) Clinical validation of cutoff target ranges in newborn screening of metabolic disorders by tandem mass spectrometry: a worldwide collaborative project. Genet Med 13:230–254

Naughten ER, Yap S, Mayne PD (1998) Newborn screening for homocystinuria: Irish and world experience. Eur J Pediatr 157: S84–S87

Rasmussen J, Køber L, Lund AM, Nielsen OW (2014) Primary Carnitine deficiency in the Faroe Islands: health and cardiac status in 76 adult patients diagnosed by screening. J Inherit Metab Dis 37:223–223

Rips J, Almashanu S, Mandel H et al (2016) Primary and maternal 3-methylcrotonyl-CoA carboxylase deficiency: insights from the Israel newborn screening program. J Inherit Metab Dis 39:211–217

Ryder B, Knoll D, Love DR et al (2016) The natural history of elevated tetradecenoyl-L-carnitine detected by newborn screening in New Zealand: implications for very long chain acyl-CoA dehydrogenase deficiency screening and treatment. J Inherit Metab Dis (in press)

Schmidt JL, Castellanos-Brown K, Childress S et al (2012) The impact of false-positive newborn screening results on families: a qualitative study. Genet Med 14:76–80

Vijay S, Patterson A, Olpin S et al (2006) Carnitine transporter defect: diagnosis in asymptomatic adult women following analysis of acylcarnitines in their newborn infants. J Inherit Metab Dis 29:627–630

Wilcken B, Haas M, Joy P et al (2009) Expanded newborn screening: outcome in screened and unscreened patients at age 6 years. Pediatrics 124:241–248

Wilcken B (2013) Newborn screening: gaps in the evidence. Science 342:197–198

JIMD Reports
DOI 10.1007/8904_2016_26

RESEARCH REPORT

Clinical and Mutational Characterizations of Ten Indian Patients with Beta-Ketothiolase Deficiency

Elsayed Abdelkreem · Radha Rama Devi Akella · Usha Dave · Sudhir Sane · Hiroki Otsuka · Hideo Sasai · Yuka Aoyama · Mina Nakama · Hidenori Ohnishi · Shaimaa Mahmoud · Mohamed Abd El Aal · Toshiyuki Fukao

Received: 28 July 2016 / Revised: 13 November 2016 / Accepted: 16 November 2016 / Published online: 08 December 2016

Abstract Beta-ketothiolase deficiency (mitochondrial acetoacetyl-CoA thiolase (T2) deficiency) is an inherited disease of isoleucine catabolism and ketone body utilization caused by *ACAT1* mutations. We identified ten Indian patients who manifested with ketoacidotic episodes of variable severity. The patients showed increased urinary excretion of isoleucine-catabolic intermediates: 2-methyl-3-hydroxybutyrate, 2-methylacetoacetate, and tiglylglycine. Six patients had a favorable outcome, one died, and three developed neurodevelopmental sequela. Mutational analysis revealed a common (p.Met193Arg) and four novel (p.Ile323Thr, p.Ala215Asn, c.1012_1015dup, and c.730 +1G>A) *ACAT1* mutations. Transient expression analyses of wild-type and mutant cDNA were performed at 30, 37, and 40°C. A p.Ile323Thr mutant T2 was detected with relative enzyme activity and protein amount of 20% and 25%, respectively, compared with wild type at 37°C; it was more prevalent at 30°C but ablated at 40°C. These findings showed that p.Ile323Thr had a significant residual T2 activity with temperature-sensitive instability. Neither residual enzymatic activity nor mutant T2 protein was identified in p.Met193Arg, p.Ala215Asn, and c.1012_1015dup mutations using supernatants; however, these mutant T2 proteins were detected in insoluble pellets by immunoblot analysis. Expression analyses confirmed pathogenicity of these mutations. T2 deficiency has a likely high incidence in India and p.Met193Arg may be a common mutation in the Indian population.

Communicated by: Michael J Bennett, PhD

E. Abdelkreem · H. Otsuka · H. Sasai · H. Ohnishi · T. Fukao (✉)
Department of Pediatrics, Graduate School of Medicine, Gifu University, 1-1 Yanagido, Gifu 501-1194, Japan
e-mail: toshi-gif@umin.net

E. Abdelkreem · S. Mahmoud · M. Abd El Aal
Department of Pediatrics, Faculty of Medicine, Sohag University, Sohag, Egypt

R.R.D. Akella
Department of Clinical Genetics and Metabolic Medicine, Rainbow Hospital for Women and Children, Hyderabad, India

U. Dave
MILS International India, Mumbai, India

S. Sane
Department of Pediatrics, Jupiter Life Line Hospital, Thane, Maharashtra, India

Y. Aoyama
Education and Training Center of Medical Technology, Chubu University, Aichi, Japan

M. Nakama · T. Fukao
Division of Clinical Genetics, Gifu University Hospital, Gifu, Japan

Abbreviations

2MAA	2-Methylacetoacetate
2M3HB	2-Methyl-3-hydroxybutyrate
SCOT	Succinyl-CoA:3-oxoacid CoA transferase
TIG	Tiglylglycine
T2	Mitochondrial acetoacetyl-CoA thiolase

Introduction

Beta-ketothiolase deficiency, also referred to as mitochondrial acetoacetyl-CoA thiolase (T2) (EC 2.3.1.9, gene symbol *ACAT1*) deficiency (Online Mendelian Inheritance in Man [OMIM] 203750, 607809), is an autosomal recessive disease of isoleucine catabolism and ketone body utilization (Fukao et al. 2014; Hori et al. 2015). Since the first description of T2 deficiency in 1971, more than 100

patients with the condition have been identified worldwide with no ethnic predisposition (Abdelkreem et al. 2016). The clinical hallmark of this disease is recurrent ketoacidotic episodes, between which patients usually have no symptoms. T2 deficiency is marked with increased urinary excretion of the isoleucine catabolic intermediates 2-methyl-3-hydroxybutyrate (2M3HB), 2-methylacetoacetate (2MAA), and tiglylglycine (TIG). The clinical severity of T2 deficiency varies among patients, with some reports of atypical clinical/biochemical presentations. Information extrapolated from follow-up studies of patients with T2 deficiency suggests that a favorable outcome is usually anticipated unless a ketoacidotic episode gives rise to fatal or irreversible, predominantly neurological, complications (Fukao et al. 2014; Abdelkreem et al. 2016).

The human *ACAT1* gene is located at chromosome 11q22.3–23.1. It spans approximately 27 kb and contains 12 exons and 11 introns. T2 cDNA is about 1.5 kb long and encodes a precursor protein of 427 amino acids, including a 33-amino-acid leader polypeptide (Fukao et al. 1990). Mutations in the *ACAT1* gene are highly heterogeneous; to date, more than 70 mutations have been identified (Fukao et al. 2010; unpublished data). Apart from the p.Arg208* mutation that was detected in Vietnamese patients with T2 deficiency, no other common *ACAT1* mutations were identified before this study (Abdelkreem et al. 2016).

There are few studies on T2 deficiency in India. Some cases were detected by urinary organic acid analysis, but the diagnosis was not confirmed by an enzyme assay or mutational analysis except for only one case (Dave Usha and Das Bibhu 2010; Akella et al. 2014). In this study, we report on ten Indians with T2 deficiency, describe their clinical and molecular features, and characterize four *ACAT1* mutations.

Patients and Methods

Patients

The ten Indian patients, who were not related to each other, presented with ketoacidotic episodes of variable severity (Table 1). Most were from Hyderabad and were of Hindu heritage. Suspicion of T2 deficiency in the patients was based on increased urinary excretion of 2M3HB, 2MAA, and TIG, and increased C5:1 carnitine and C5-OH carnitine in the blood acylcarnitine profile; data of urinary organic acid profiles were available for all patients, whereas that of blood acylcarnitine were available for only six patients. Among the ten patients, one patient, GK108, died during his presenting ketoacidotic episode at 11 months of age; GK98 experienced only one ketoacidotic episode at 4 months of age, which has been complicated with severe neurodevelopmental regression and convulsions; GK109 and GK113 both suffered modest developmental delays after their second ketoacidotic episodes; and the others, in contrast, have achieved age-appropriate development to date.

Ethical Considerations

This study was approved by the Ethical Committee of the Graduate School of Medicine, Gifu University, Japan, and was carried out in accordance with the principles contained within the Declaration of Helsinki. Informed consents were obtained from all patients or their parents for being included in the study.

Mutation Analysis

Genomic DNA was extracted and purified from patients' blood using a SepaGene kit (EIDIA, Tokyo, Japan) according to the manufacturer's directions. The 12 *ACAT1* exons, with their intron boundaries, were amplified by PCR using formerly designed primer pairs and conditions (Fukao et al. 1998). The 12 amplified fragments were sequenced using a BigDye® Terminator v1.1 cycle sequencing kit (Applied Biosystems, Foster City, CA, USA) and an ABI PRISM 3130XL genetic analyzer (Applied Biosystems) according to the manufacturer's directions. We used the genomic *ACAT1* sequence (GenBank accession NG_009888.1) as a reference.

Transient Expression Analyses

Transient expression analyses of T2 cDNA were performed using a pCAGGS eukaryote expression vector, as previously described (Niwa et al. 1991; Fukao et al. 1998; Zhang et al. 2004). Briefly, we used a Kod-Plus-Mutagenesis Kit® (Tyobo Co., Osaka, Japan) to construct four full-length mutant cDNA: p.Met193Arg, p.Ile323Thr, p.Ala215Asn, and c.1012_1015dup. Wild-type and mutant constructs were transfected via Lipofectamine2000® (Invitrogen, San Diego, CA, USA) into 5×10^5 SV40-transformed T2-deficient fibroblasts and cultured at 37°C. After 24 h, cells were incubated at 30, 37, and 40°C for another 48 h. Thereafter, cells were harvested and kept at −80°C until use. Cells were freeze-thawed and sonicated in 50 mM sodium phosphate (pH 8.0) and 0.1% Triton X-100 followed by centrifugation at 10,000×g for 10 min.

Using supernatants from cell extracts, we spectrophotometrically monitored the decrease of acetoacetyl-CoA absorbance at 303 nm, which is the result of thiolysis of acetoacetyl-CoA to acetyl-CoA. We measured the difference of thiolase activity in the absence and the presence of potassium ions, which specifically stimulate T2; such a difference represents T2 activity (Fukao et al. 1998; Zhang et al. 2004). The average of three independent experiments

Table 1 Clinical, biochemical, and molecular summary of Indian patients with beta-ketothiolase deficiency

			The first crisis											Prognosis			Mutations	
ID	Consanguinity	Sex	Age at onset	Preceding illness	pH	HCO_3	BE	Glucose	NH_3	Ketonuria	Unconsciousness (No. of days)	Mechanical ventilation	Peritoneal dialysis	No. of crises	Present age	Development outcome		
GK94	+	M	10 months	Fever, cough	6.89	3.3	−28	1.4	22	>80 mg/dl	Coma (4)			1	5.5 year	Good	c.253_255del (p.Glu85del)	c.253_255del (p.Glu85del)
GK98	–	M	4 months		6.8		−30	4.5	37	++++	Coma (7)	+	+	1	3.5 year	Impaired	c.578T>G (p.Met193Arg)	c.578T>G (p.Met193Arg)
GK99	–	M	14 months	Fever, cough	6.9	3.2	−28	1.8		160 mg/dl	Coma (2)	+	+	1	3 year	Good	c.578T>G (p.Met193Arg)	c.578T>G (p.Met193Arg)
GK108	+	F	11 months	Vomiting	6.9	7.2	−22.5				Coma (1)	+		1	Died at 11 month		c.578T>G (p.Met193Arg)	c.578T>G (p.Met193Arg)
GK109	–	M	9 months	Cough	6.8	1.9	−30.5	12.3	116	++++	Coma (1)	+	+	2	2 year	Impaired	c.1012_1015dup	c.1012_1015dup
GK110	+	F	11 months		7	2.4	−28	14.7	42	160 mg/dl	Coma (3)			1	2 year	Good	c.730+1G>A	c.730+1G>A
GK111	–	M	6 months	Fever, cough	7.1	2.4		3.8	49	>80 mg/dl	Coma (4)	+		1	1.5 year	Good	c.578T>G (p.Met193Arg)	c.968T>C (p.Ile323Thr)
GK112	+	F	7 months	Fever, cough	7.15	20	−8		50	+++	lethargy (3)	+		3	2.5 year	Good	c.1124A>G	c.1124A>G
GK113	+	M	12 months	Fever, cough	7.1						Coma (6)			2	2.5 year	Impaired	c.643_644delinsAA (p.Ala215Asn)	c.643_644delinsAA (p.Ala215Asn)
GK114	–	M	19 months	Fever, cough	6.9	3				50 mg/dl	Coma (1)	+	+	1	3 year	Good	c.578T>G (p.Met193Arg)	c.578T>G (p.Met193Arg)

Values for pH, HCO_3, BE, and glucose are shown in mmol/L, whereas NH_3 is in μmol/L. These patients were diagnosed between 2011 and 2016. All patients were from Hyderabad except GK109 and GK112, who were from Mumbai. Patients' development was assessed using the Denver II test (http://denverii.com)

was calculated. In addition, both supernatants and pellets of cell extracts were subjected to immunoblot analysis as described (Fukao et al. 1997, 1998). The first antibody was a mixture of an anti-T2 antibody and anti-succinyl-CoA:3-oxoacid CoA transferase (SCOT) antibody, as previously described (Fukao et al. 1997).

Results

Mutation Analysis

We identified four novel *ACAT1* mutations: c.968T>C (p.Ile323Thr), c.643_644delinsAA (p.Ala215Asn), c.1012_1015dup, and c.730+1G>A. c.578T>G (p.Met193Arg) was the most common mutation, representing 45% of all identified mutant alleles (Table 1).

Transient Expression Analysis

As shown in Fig. 1a, expression of wild-type T2 cDNA produced high-potassium ion-activated acetoacetyl-CoA thiolase activity, which represents T2 activity, whereas that of mock cDNA yielded no detectable T2 enzyme activity at various temperatures. The p.Ile323Thr mutation retained some residual T2 activity, nearly 20%, compared with the wild type, through expression at 37°C. At 30°C, such activity increased to 40%, whereas it was completely ablated at 40°C. Conversely, p.Met193Arg, p.Ala215Asn, and c.1012_1015dup mutations showed no detectable T2 activity through expression under the different temperatures.

In immunoblot analysis of supernatants (Fig. 1b), serial dilution samples extracted from the wild type were applied to evaluate relative amounts of mutant T2 proteins in comparison with that of the wild type. p.Ile323Thr mutant T2 protein was detected through expression at 30 and 37°C but not 40°C. Relative amounts of p.Ile323Thr mutant T2 protein, compared with the wild type, were estimated to be 40% and 20% at 30°C and 37°C, respectively. p.Met193Arg, p.Ala215Asn, and c.1012_1015dup mutant T2 proteins were not observed using supernatants through expression at the designed temperatures; however, these mutant proteins were clearly identified using pellet fractions, with notably faster electrophoretic mobility of the latter mutant protein (Fig. 1c).

Estimated Incidence

The ten Indian patients with T2 deficiency manifested with ketoacidotic episodes between 2011 and 2016. Eight patients were from Hyderabad, which is located in Southern India, covers 650 km^2, and has a population of about 10 million. The birth rate in this area is about 200,000 newborns/year. These eight patients and the previously reported T2-deficient case (GK95), who also was from Hyderabad (Akella et al. 2014), were born between 2010 and 2014. Accordingly, if these nine patients represented all T2-deficient patients during these 5 years in Hyderabad, the incidence of T2 deficiency would be about 1 in 111,000 newborns in this area (9 T2-deficient patients/200,000 × 5 years). This estimated figure is strikingly greater than the highest ever reported incidence of T2 deficiency, which is 1 per 232,000 newborns in Minnesota, USA, between January 2001 and November 2010 (Sarafoglou et al. 2011). As it is possible that other T2-deficient patients died or suffered mild episodes without being diagnosed (Abdelkreem et al. 2016), the actual incidence of T2 deficiency in Hyderabad from 2010 to 2014 may be even higher.

Discussion

ACAT1 mutations are highly diverse, with more than 70 different mutations having been identified to date, and with only a few common mutations (Fukao et al. 2010; Hori et al. 2015). p.Met193Arg accounts for about half the identified mutant alleles in Indian patients with T2 deficiency, suggesting a founder effect in this Indian region. p.Met193Arg is the second most common *ACAT1* mutation after p.Arg208*; the latter mutation represents 87% of T2 mutant alleles in Vietnamese (Fukao et al. 2010). Patients homozygous for p.Met193Arg have, in general, typical clinical and biochemical manifestations of T2 deficiency, although clinical severity and outcome vary. Potentially common *ACAT1* mutations that have yet to be identified could be revealed through the ongoing recognition of more patients with T2 deficiency, particularly in populations with a high rate of consanguineous marriage.

Among the four novel *ACAT1* mutations identified in the current study, c.730+1G>A is an apparent disease-causing mutation because it affects a highly conserved point at the splice donor site of intron 7; aberrant splicing usually ensues as a consequence of decreasing the Shapiro and Senapathy score by c.730+1G>A mutation from 72 to 55 at that splice site (Shapiro and Senapathy 1987). We performed transient expression analysis to confirm that the two novel missense mutations, p.Ile323Thr and p.Ala215Asn, are pathogenic. p.Met193Arg mutation was included as its enzyme activity was analyzed by expression at only 37°C (Akella et al. 2014). c.1012_1015dup is another plausibly detrimental mutation. It causes a frame shift that replaces aspartic acid at position 339 with glutamic acid and inserts a premature stop codon at position 355 of the new reading frame (p.Asp339GlufsTer17). We also studied this mutation

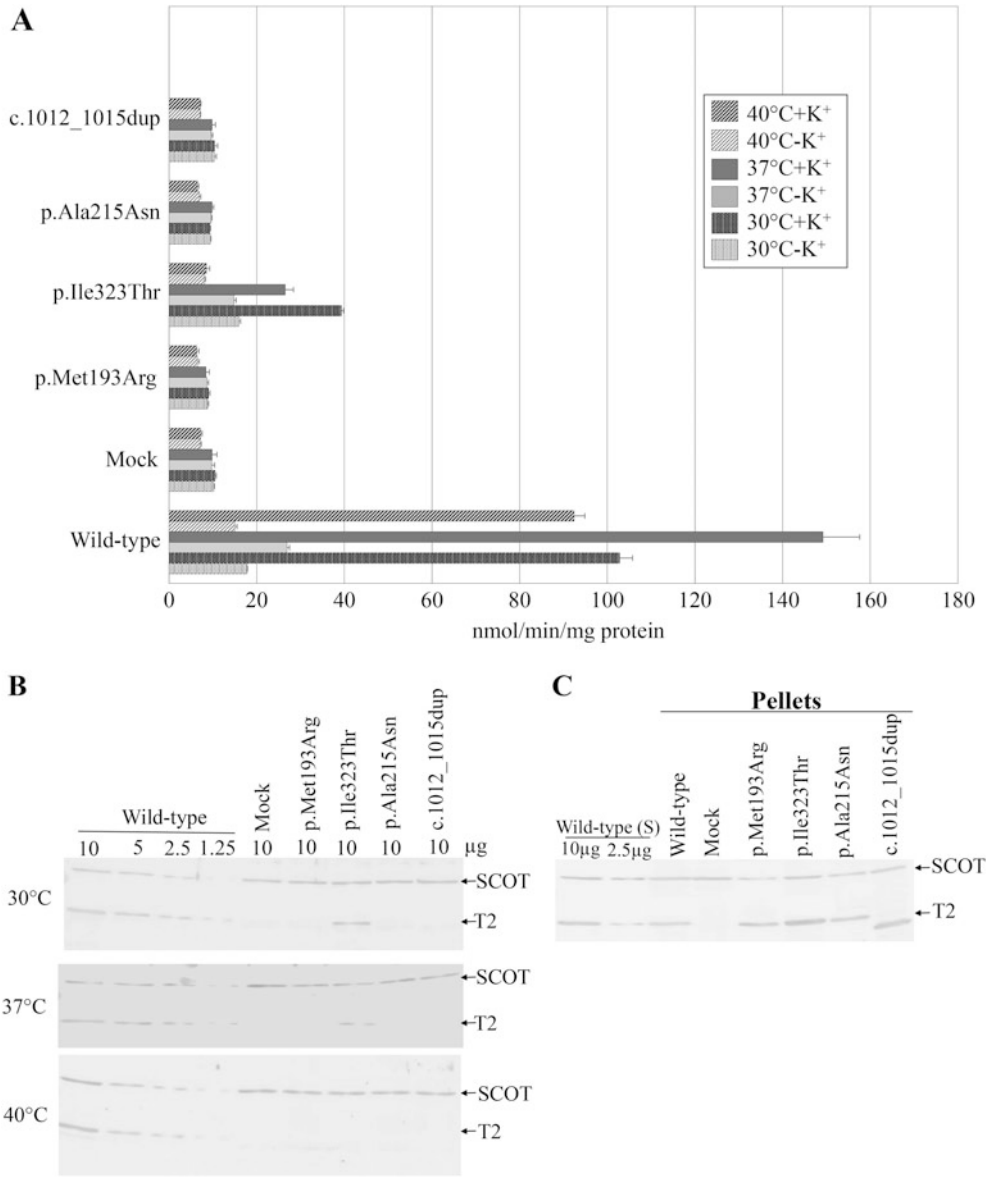

Fig. 1 Transient expression analyses of mutant cDNA. Wild-type and mutant constructs were transfected using Lipofectamine2000® into 5×10^5 SV40-transformed T2-deficient fibroblasts. After incubation at 37°C for 24 h, cells were incubated at 30, 37, and 40°C for 48 h. (**a**) Potassium ion-activated acetoacetyl-CoA thiolase assay. Mean values of acetoacetyl-CoA thiolase activity measured in supernatants of cell extracts in the absence and the presence of potassium ions are shown together with the standard errors of three independent experiments. (**b**) Immunoblot analyses of supernatants. A mixture of an anti-T2 and anti-SCOT was used as the first antibody. Applied protein amounts are shown (in µg) above the lanes. (**c**) Immunoblot analyses of pellets. S indicates supernatant of the wild type that was used in amounts shown above the lanes. Pellets from samples corresponding to 10 µg of supernatant protein were applied. *SCOT* succinyl-CoA:3-oxoacid CoA transferase, *T2* mitochondrial acetoacetyl-CoA thiolase

to elucidate the electrophoretic characters of its mutant protein. The pathogenic effect of the p.Glu85del mutation on T2 enzyme activity was previously demonstrated (Fukao et al. 2002), whereas c.1124A>G was shown to induce a cryptic splice donor site within exon 11 that results in aberrant splicing (Fukao et al. 2008).

The results of T2 enzyme assay and immunoblot analysis clearly showed that p.Ile323Thr mutant T2 protein has a significant residual T2 activity and is unstable in a temperature-sensitive manner, being more prevalent by expression at lower temperatures (30°C > 37°C > 40°C). The other mutant proteins, p.Met193Arg, p.Ala215Asn, and c.1012_1015dup, were not detected in supernatant fractions even at 30°C, suggesting that they are very unstable mutant proteins. The incubation temperature affects posttranslational modifications of protein structure, including protein folding and stability. Incubation at a lower temperature during expression may considerably stabilize mutant T2

proteins (Sakurai et al. 2007). This temperature-sensitive phenomenon was previously described in several *ACAT1* mutations, such as p.Ala132Gly, p.Gln145Glu, p.Glu215-del, p.Glu252del, and p.Thr297Met (Fukao et al. 2001; Zhang et al. 2004; Sakurai et al. 2007).

To further study the effects of mutations on protein solubility, we examined not only supernatants used for the enzyme assay but also pellets of cell extracts. Insoluble mutant T2 proteins p.Ala215Asn, p.Met193Arg, and c.1012_1015dup were detected only in pellets. These three mutations appear to have drastic effects on T2 protein structure, like p.Ala333Pro, which was also identified only in pellets (Fukao et al. 1998). Although having no residual enzymatic activities, some mutant T2 proteins are soluble. For example, p.Gly152Ala and p.Asn158Asp were detected by expression at 30°C, whereas others, such as p. Arg208Gln, p.Tyr219His, and p.Asn282His, could be identified in supernatants by expression not only at 37°C but also at 40°C (Zhang et al. 2004; Sakurai et al. 2007).

A distinction between genetic mutations based on their residual enzymatic activities may become important for some prospective therapeutic modalities. Molecular chaperones, polypeptide unfoldases, can specifically recognize and proofread three-dimensional structures of misfolded/aggregated proteins and convert them into degradable or rehabilitated, potentially functional, proteins. Stimulation of the latter mechanism using various pharmacological agents may favorably affect functions of misfolded mutant proteins if they have residual enzymatic activities, offering potential hope for a variety of yet untreatable genetic diseases (West et al. 2012; Muntau et al. 2014; Finka et al. 2016). The clinical course of T2-deficient patients whose mutations have some residual enzyme activity, such as GK111 here, does not differ from those whose mutations have no enzymatic activity (Fukao et al. 2001). Such lack of genotype-phenotype correlation precludes the use of unfoldases as a potential therapy for T2 deficiency.

In conclusion, we confirmed T2 deficiency at the molecular level in ten new patients from India and characterized their *ACAT1* mutations. T2 deficiency has a likely high incidence in India and p.Met193Arg may be a common mutation in the Indian population.

Acknowledgments The authors thank the Cultural Affairs and Missions Sector, Egyptian Ministry of Higher Education, for providing a scholarship to study beta-ketothiolase deficiency. The authors also thank N. Sakaguchi for her indispensable technical assistance.

Funding This work was supported in part by a Grant-in-Aid for Scientific Research from the Ministry of Education, Culture, Sports, Science and Technology of Japan [grant numbers 26114708, 24591505, 16K09962, 15K01693]; Health and Labour Science Research Grants for Research on Intractable Diseases from the Ministry of Health, Labour and Welfare of Japan; and the Practical Research Project for Rare/Intractable Diseases from Japan Agency for Medical Research and Development (AMED).

Synopsis

Beta-ketothiolase (T2) deficiency has a likely high incidence in India where p.Met193Arg may be a common mutation.

Compliance with Ethics Guidelines

Conflict of Interest

Toshiyuki Fukao has received a Grant-in-Aid for Scientific Research from the Ministry of Education, Culture, Sports, Science and Technology of Japan [grant numbers 26114708, 24591505, 16K09962]; Health and Labour Science Research Grants for Research on Intractable Diseases from the Ministry of Health, Labour and Welfare of Japan; and the Practical Research Project for Rare/Intractable Diseases from Japan Agency for Medical Research and Development (AMED).

Yuka Aoyama has received a Grant-in-Aid for Scientific Research from the Ministry of Education, Culture, Sports, Science and Technology of Japan [grant number 15K01693].

Elsayed Abdelkreem, Radha Rama Devi Akella, Usha Dave, Sudhir Sane, Hiroki Otsuka, Hideo Sasai, Mina Nakama, Hidenori Ohnishi, Shaimaa Mahmoud, and Mohamed Abd El Aal declare that they have no conflict of interest.

Informed Consent

All procedures followed were in accordance with the ethical standards of the responsible committee on human experimentation (institutional and national) and with the Helsinki Declaration of 1975, as revised in 2000. Informed consents were obtained from all patients or their parents for being included in the study.

Details of the Contributions of Individual Authors

Elsayed Abdelkreem, Hiroki Otsuka, Hideo Sasai, Yuka Aoyama, and Mina Nakama collected data, performed mutational and expression analyses, and drafted the first version of the manuscript. Radha Rama Devi Akella, Usha Dave, and Sudhir Sane were involved in clinical management of patients and critically reviewed the manuscript. Hidenori Ohnishi, Shaimaa Mahmoud, and Mohamed Abd El Aal critically reviewed and revised the manuscript, and approved the final version as submitted. Toshiyuki Fukao

initiated and supervised this study, reviewed and revised the manuscript, and approved the final version as submitted. All authors approved the final manuscript as submitted and agree to be accountable for all aspects of the work. All authors confirm the absence of previous similar or simultaneous publications.

References

Abdelkreem E, Otsuka H, Sasai H et al (2016) Beta-ketothiolase deficiency: resolving challenges in diagnosis. J Inborn Errors Metab Screen 4:1–9

Akella RR, Aoyama Y, Mori C, Lingappa L, Cariappa R, Fukao T (2014) Metabolic encephalopathy in beta-ketothiolase deficiency: the first report from India. Brain Dev 36:537–540

Dave Usha P, Das Bibhu R (2010) Newborn screening – from "Guthrie age to Genomic age". J Obstet Gynaecol India 60:210–214

Finka A, Mattoo RU, Goloubinoff P (2016) Experimental milestones in the discovery of molecular chaperones as polypeptide unfolding enzymes. Annu Rev Biochem 85:715–742

Fukao T, Yamaguchi S, Kano M et al (1990) Molecular cloning and sequence of the complementary DNA encoding human mitochondrial acetoacetyl-coenzyme A thiolase and study of the variant enzymes in cultured fibroblasts from patients with 3-ketothiolase deficiency. J Clin Invest 86:2086–2092

Fukao T, Song XQ, Mitchell GA et al (1997) Enzymes of ketone body utilization in human tissues: protein and messenger RNA levels of succinylcoenzyme A (CoA):3 ketoacid CoA transferase and mitochondrial and cytosolic acetoacetylCoA thiolases. Pediatr Res 42:498–502

Fukao T, Nakamura H, Song XQ et al (1998) Characterization of N93S, I312T, and A333P missense mutations in two Japanese families with mitochondrial acetoacetyl-CoA thiolase deficiency. Hum Mutat 12:245–254

Fukao T, Scriver CR, Kondo N, T2 Collaborative Working Group (2001) The clinical phenotype and outcome of mitochondrial acetoacetyl-CoA thiolase deficiency (beta-ketothiolase or T2 deficiency) in 26 enzymatically proved and mutation-defined patients. Mol Genet Metab 72:109–114

Fukao T, Nakamura H, Nakamura K et al (2002) Characterization of 6 mutations in 5 Spanish patients with mitochondrial acetoacetyl-CoA thiolase deficiency: effects of amino acid substitutions on tertiary structure. Mol Genet Metab 75:235–243

Fukao T, Boneh A, Aoki Y, Kondo N (2008) A novel single-base substitution (c.1124A>G) that activates a 5-base upstream cryptic splice donor site within exon 11 in the human mitochondrial acetoacetyl-CoA thiolase gene. Mol Genet Metab 94:417–421

Fukao T, Nguyen HT, Nguyen NT et al (2010) A common mutation, R208X, identified in Vietnamese patients with mitochondrial acetoacetyl-CoA thiolase (T2) deficiency. Mol Genet Metab 100:37–41

Fukao T, Mitchell G, Sass JO, Hori T, Orii K, Aoyama Y (2014) Ketone body metabolism and its defects. J Inherit Metab Dis 37:541–551

Hori T, Yamaguchi S, Shinkaku H et al (2015) Inborn errors of ketone body utilization. Pediatr Int 57:41–48

Muntau AC, Leandro J, Staudigl M, Mayer F, Gersting SW (2014) Innovative strategies to treat protein misfolding in inborn errors of metabolism: pharmacological chaperones and proteostasis regulators. J Inherit Metab Dis 37:505–523

Niwa H, Yamamura K, Miyazaki J (1991) Efficient selection for high-expression transfectants with a novel eukaryotic vector. Gene 108:193–199

Sakurai S, Fukao T, Haapalainen AM et al (2007) Kinetic and expression analyses of seven novel mutations in mitochondrial acetoacetyl-CoA thiolase (T2): identification of a Km mutant and an analysis of the mutational sites in the structure. Mol Genet Metab 90:370–378

Sarafoglou K, Matern D, Redlinger-Grosse K et al (2011) Siblings with mitochondrial acetoacetyl-CoA thiolase deficiency not identified by newborn screening. Pediatrics 128:e246–e250

Shapiro MB, Senapathy P (1987) RNA splice junctions of different classes of eukaryotes: sequence statistics and functional implications in gene expression. Nucleic Acids Res 15:7155–7174

West JD, Wang Y, Morano KA (2012) Small molecule activators of the heat shock response: chemical properties, molecular targets, and therapeutic promise. Chem Res Toxicol 25:2036–2053

Zhang GX, Fukao T, Rolland MO et al (2004) Mitochondrial acetoacetyl-CoA thiolase (T2) deficiency: T2-deficient patients with "mild" mutation(s) were previously misinterpreted as normal by the coupled assay with tiglyl-CoA. Pediatr Res 56:60–64

JIMD Reports
DOI 10.1007/8904_2016_29

CASE REPORT

Atypical Presentation and Treatment Response in a Child with Familial Hypercholesterolemia Having a Novel LDLR Mutation

S. Varma • A.D. McIntyre • R.A. Hegele

Received: 09 September 2016 / Revised: 16 November 2016 / Accepted: 17 November 2016 / Published online: 09 December 2016

Abstract Familial hypercholesterolemia (FH) is an autosomal codominantly inherited disease. The severity of clinical presentation depends on the zygosity of the mutations in the *LDLR*, *APOB*, or *PCSK9* genes. The homozygous form (HoFH) is associated with high mortality rate by third decade of life, while individuals with HeFH begin to suffer from premature cardiovascular disease in fourth or fifth decade of life. Statin drugs have helped to improve the biochemical profile and life expectancy in HeFH, while they are only minimally effective in HoFH. LDL apheresis remains an effective treatment option in HoFH, though limited by its availability and affordability issues. We present the case that highlights a few novel aspects of clinical and genetic heterogeneity in FH, wherein a child presented with features of both HeFH and HoFH. His clinical picture was that of HoFH; however he responded well clinically and biochemically to pharmacologic treatment only. DNA sequencing showed a novel heterozygous rare splicing variant in the LDLR gene in addition to a relatively high polygenic trait score comprised of LDL-C raising alleles from common polymorphic sites. Interestingly his normolipemic mother showed the same heterozygous mutation. Thus this novel splicing variant in LDLR showed nonclassical co-segregation with the disease phenotype and was associated with a high polygenic trait score comprised of common LDL-C raising polymorphic alleles in the affected proband. Thus it indicates the phenotypic heterogeneity of FH and suggests that secondary causes, such as polygenic factors and possibly as yet undetermined genetic or environmental factors, can exacerbate the metabolic phenotype in an individual who is genotypically heterozygous for FH.

Abbreviations

ApoA	Apolipoprotein A
ApoB	Apolipoprotein B
FH	Familial hypercholesterolemia
HDL	High-density lipoproteins
HeFH	Heterozygous familial hypercholesterolemia
HoFH	Homozygous familial hypercholesterolemia
LDL-C	Low-density lipoprotein cholesterol
TG	Triglycerides

Introduction

Familial hypercholesterolemia (FH) is a rare and life-threatening disease. FH is classically an autosomal codominant disorder: heterozygous FH (HeFH), due to a single mutant allele, has a population prevalence of ~1:250, while the clinically more severe homozygous FH (HoFH) due to bi-allelic mutations has a population prevalence estimated between 1 in 160,000 and 300,000 (Cuchel et al. 2014). Though the categorization as HoFH or HeFH is based on clinical and genetic parameters there is not a linear genotype-phenotype correlation in FH. Both HeFH and

Communicated by: Robert Steiner

S. Varma
Department of Pediatrics, All India Institute of Medical Sciences, New Delhi, India

S. Varma (✉)
Service of Pediatric Gastroenterology and Hepatology, Cliniques Universitaires St Luc, Brussels, Belgium
e-mail: varma.sharat@yahoo.com

A.D. McIntyre · R.A. Hegele
Robarts Research Institute and Department of Medicine, Schulich School of Medicine, Western University, London, ON, Canada N6A 5B7

HoFH are characterized by xanthomas, elevated cholesterol levels, and premature atherosclerotic cardiovascular disease (CVD), although levels of low-density lipoprotein (LDL) cholesterol are elevated to a much greater degree in HoFH (up to tenfold normal) compared to HeFH (up to fourfold normal). Both HeFH and HoFH can result from one or two rare mutations, respectively, in *LDLR*, *APOB*, and *PCSK9* genes. In contrast, carriers of one mutant allele of the *LDLRAP1* gene have no phenotype: HoFH is expressed phenotypically only in individuals with two rare mutations in the *LDLRAP1* gene (Cuchel et al. 2014). Interestingly, with increased genetic analysis, there is clearly some phenotypic overlap between certain individuals who genetically would be considered to have HeFH or HoFH based on molecular genetic criteria alone.

If left untreated HoFH has been reported to be almost universally fatal by the second or third decade of life, while individuals with HeFH begin to suffer from premature CVD in the fourth or fifth decade of life. Statin drugs have helped to normalize life expectancy in HeFH, while they are only minimally effective in HoFH (Cuchel et al. 2014; Marais et al. 2002; Gagne et al. 2002). The mainstay of treatment in HoFH has been weekly or biweekly plasmapheresis or selective LDL apheresis. Newer treatments recently approved or under development, including gene therapy, are providing new hope for children and young adults afflicted with HoFH (Cuchel et al. 2014). Given the proven ability of various LDL-lowering treatments to alter disease course and extend life, it is imperative to diagnose FH early and to begin appropriate management (Wiegman et al. 2015). Also the clinical presentation of HeFH and HoFH can represent a continuum; while genetic confirmation though beneficial has its own drawbacks in lacking a robust genotype-phenotype correlate (Cuchel et al. 2014; Soutar and Naoumova 2007; Talmud et al. 2013).

Case Report

We present an 18-month-old boy, born to non-consanguineous parents who presented with diffuse cutaneous xanthomas especially over the hands, legs, and face while the rest of clinical examination was unremarkable (Fig. 1). His blood examination (Table 1) revealed elevated total cholesterol level. Further lipid analysis showed elevations in both LDL cholesterol (LDL-C) and triglycerides (TG), with decreased high-density lipoprotein cholesterol (HDL-C). Apolipoprotein A-1 (apo A-1) level was decreased while apolipoprotein B (Apo B) level was increased. Based on the impressive xanthomatosis and very high LDL-C for age, a provisional diagnosis of HoFH was made, as he satisfied essentially all the diagnostic criteria (Cuchel et al. 2014; Wiegman et al. 2015). Causes for secondary

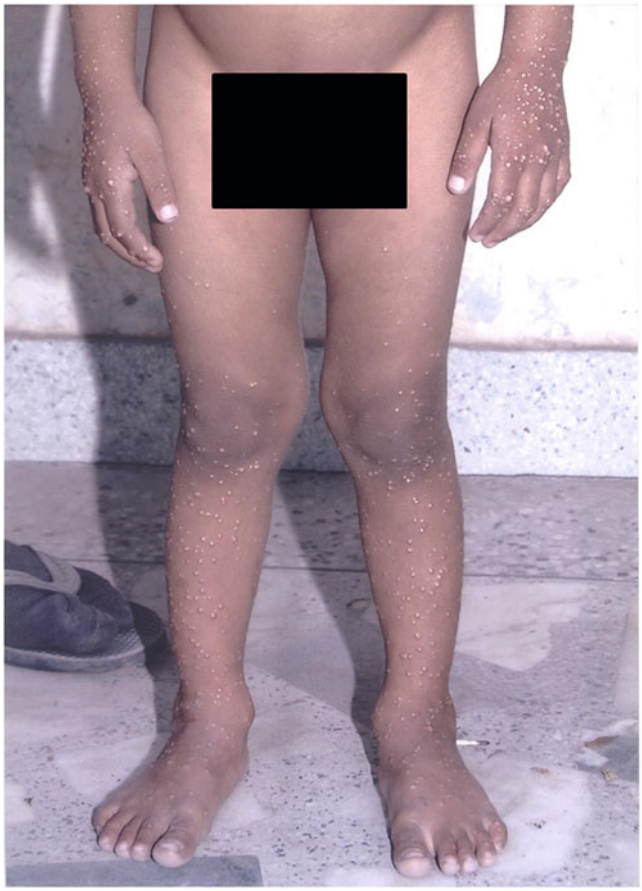

Fig. 1 Cutaneous xanthomas seen the child (index case)

hypercholesterolemia including nephrotic syndrome, hypothyroidism, primary biliary disease, and liver dysfunction were ruled out. Other diagnostic considerations included sitosterolemia, lipoprotein lipase deficiency, lysosomal acid lipase deficiency (cholesterol ester storage disease – CESD), apo A-1 or apo C-2 deficiency, apo E variant or E2/E2 homozygosity (type III hyperlipoproteinemia), and LCAT deficiency. Echocardiography and carotid ultrasound to assess intimal thickness measurement were both normal. He was started on a low plant sterol diet and statin treatment. Subsequently ezetimibe and cholestyramine were added. With this treatment his xanthomas and lipid profile showed substantial improvement (Tables 1 and 2) over the next one and a half years until his last consultation.

The patient and his parents underwent targeted next-generation DNA sequencing (Hegele et al. 2015), which found that the patient and his mother were each heterozygous for a novel insertion/deletion mutation in the LDLR gene, namely in +8 delCGGGGCCAGGG in intron 4. DNA sequence analysis of other candidate genes in monogenic dyslipidemia, including *APOB*, *PCSK9*, *LDLRAP1* (*ARH*), *ABCG5*, *ABCG8*, *LIPA(CESD)*, *APOA1, APOE, APOC2*, and *LCAT*, revealed no other rare and

Table 1 Lipid profile at baseline (at the time of diagnosis) and after 18 months of therapy with statin and ezetimibe

	Normal	Pretreatment	Posttreatment	Change with treatment
Total cholesterol (mg/dl)	<200	403	297	−26.3%
Triglycerides (mg/dl)	<150	211	200	−5.2%
HDL cholesterol (mg/dl)	<40	9	11	+22.2%
LDL cholesterol (mg/dl)	<130	352	249	−29.3%
VLDL cholesterol (mg/dl)	10–30	42	37	−11.9%
Apo A-I (mg/dl)	120–176	80	75	−6.2%
Apo B (mg/dl)	63–114	166	140	−15.6%

HDL high-density lipoprotein, *LDL* low-density lipoprotein, *VLDL* very-low-density lipoprotein, *apo* apolipoprotein

Table 2 Lipid profile of parents as part of reverse cascade screening

	Normal	Mother	Father
Total cholesterol (mg/dl)	<200	162	203
Triglycerides (mg/dl)	<150	115	219
HDL cholesterol (mg/dl)	<40	41	41
LDL cholesterol (mg/dl)	<130	98	118.2
VLDL cholesterol (mg/dl)	10–30	23	43.8

HDL high-density lipoprotein, *LDL* low-density lipoprotein, *VLDL* very-low-density lipoprotein, *apo* apolipoprotein

potentially disease-causing variants. The patient was also found to have a high polygenic trait-raising score for LDL-C comprised of multiple small-effect SNPs (15/20), meaning that only ~8% of people would have a higher burden of polygenic effects to raise LDL-C. The findings were interesting in that the patient's mother was not markedly dyslipidemic. Additional genetic studies, including multiplex ligation primer amplification to detect large-scale copy-number variation of the LDLR gene, were normal in the family. Using the Rogan method, bioinformatics based analysis of the impact of the detected mutation on the RNA splicing revealed that it was highly deleterious. The mutation abolished a natural RNA splicing site and it was predicted that a cryptic isoform would be created 60 base pairs downstream and this would result in an increase in the binding by 3321.8%. By contrast the RT-PCR analysis of the *LDLR* RNA from peripheral blood leucocytes showed no evidence of splicing defects in the proband or parents.

Discussion

This case description highlights a few novel aspects of clinical and genetic heterogeneity in FH. The child presented with a clinical picture suggesting HoFH; however, he responded well clinically and biochemically to pharmacologic treatment only, indicating that he has a phenotype with features of both HeFH and HoFH. DNA sequencing of known candidate genes showed a novel heterozygous rare splicing variant in the *LDLR* gene in addition to a relatively high polygenic trait score comprised of LDL-C-raising alleles from common polymorphic sites. It is of interest that his essentially normolipemic mother is heterozygous for the same *LDLR* mutation. Thus this novel splicing variant in *LDLR* showed nonclassical co-segregation with the disease phenotype. The only probable explanatory factor being a high polygenic trait score comprised of common LDL-C-raising polymorphic alleles. Additionally there may be parental allele-of-origin epigenetic influences or perhaps an oligogenic interaction involving a novel mutation in new genes that has not yet been associated with lipid metabolism. While this might be resolved by whole-genome or whole-exome sequencing, it would be challenging to ascertain a single potentially causative interacting novel secondary factor from the whole genome of a single individual.

This case indicates the phenotypic heterogeneity of FH and suggests that secondary causes, such as polygenic factors and possibly as yet undetermined genetic or environmental factors, can exacerbate the metabolic phenotype in an individual who is genotypically heterozygous for FH.

Author Contributions

Varma S: (a) Physician involved in patient care, (b) planning, (c) drafting the chapter.

McIntyre AD and Hegele RA: (a) Design and conduct of genetic tests, (b) revising the chapter manuscript.

Conflict of Interest

Varma Sharat, McIntyre Adam, and Hegele Rob declare that they have no conflict of interest.

Compliance with Ethics Guidelines

All procedures followed were in accordance with the ethical standards of the responsible committee (institutional and national) and with the Helsinki Declaration of 1975, as revised in 2000. Informed consent was obtained from parents of the child for genetic testing and publication of the scientific results.

References

Cuchel M, Bruckert E, Ginsberg HN, Raal FJ, Santos RD, Hegele RA et al (2014) Homozygous familial hypercholesterolaemia: new insights and guidance for clinicians to improve detection and clinical management. A position paper from the Consensus Panel on Familial Hypercholesterolaemia of the European Atherosclerosis Society. Eur Heart J 35(32):2146–2157

Gagne C, Gaudet D, Bruckert E (2002) Efficacy and safety of ezetimibe coadministered with atorvastatin or simvastatin in patients with homozygous familial hypercholesterolemia. Circulation 105(21):2469–2475

Hegele RA, Ban MR, Cao H, McIntyre AD, Robinson JF, Wang J (2015) Targeted next-generation sequencing in monogenic dyslipidemias. Curr Opin Lipidol 26(2):103–113

Marais AD, Blom DJ, Firth JC (2002) Statins in homozygous familial hypercholesterolemia. Curr Atheroscler Rep 4(1):19–25

Soutar AK, Naoumova RP (2007) Mechanisms of disease: genetic causes of familial hypercholesterolemia. Nat Clin Pract Cardiovasc Med 4(4):214–225

Talmud PJ, Shah S, Whittall R, Futema M, Howard P, Cooper JA et al (2013) Use of low-density lipoprotein cholesterol gene score to distinguish patients with polygenic and monogenic familial hypercholesterolaemia: a case-control study. Lancet 381 (9874):1293–1301

Wiegman A, Gidding SS, Watts GF, Chapman MJ, Ginsberg HN, Cuchel M et al (2015) Familial hypercholesterolaemia in children and adolescents: gaining decades of life by optimizing detection and treatment. Eur Heart J 36(36):2425–2437

JIMD Reports
DOI 10.1007/8904_2016_22

RESEARCH REPORT

Development of a Tandem Mass Spectrometry Method for Rapid Measurement of Medium- and Very-Long-Chain Acyl-CoA Dehydrogenase Activity in Fibroblasts

Damien Bouvier · Christine Vianey-Saban · Séverine Ruet · Cécile Acquaviva

Received: 19 July 2016 / Revised: 07 November 2016 / Accepted: 09 November 2016 / Published online: 10 December 2016

Abstract Mitochondrial fatty acid oxidation is a vital biochemical process for energy metabolism. Among the known fatty-acid metabolism disorders, very-long-chain acyl-CoA dehydrogenase (VLCAD) deficiency and medium-chain acyl-CoA dehydrogenase (MCAD) deficiency count among the most frequent. Both are potentially very serious diseases as they carry a risk of severe neurological post-crisis sequelae, and even sudden death. Diagnosis relies on plasma acylcarnitine profile analysis and urine organic acid analysis, followed by genetic testing to confirm diagnosis. However, in some cases, it is crucial to run a specific diagnostic assay for enzyme activity, which is generally performed in leukocytes or fibroblasts. The aim of this study was to address this need, first by developing a MCAD and VLCAD enzyme activity-specific diagnostic assay in fibroblasts (by measuring the reaction products, i.e. enoyl-CoA) via a rapid LC–MS/MS-based technique, and then by testing MCAD-deficient patients ($n = 6$), VLCAD-deficient patients ($n = 10$), and control patients ($n = 12$). MCAD activity was significantly different in the MCAD-deficiency (MCADD) group (mean = 0.07 nmol C8:1 formed/min/mg protein) compared to the control group (mean = 0.36 nmol C8:1 formed/min/mg protein). All MCADD patients showed less than 35% residual MCAD activity. VLCAD activity was significantly decreased in the VLCADD group (mean = 0.06 nmol C16:1 formed/min/mg protein) compared to the control group (mean = 0.86 nmol C16:1 formed/min/mg protein, respectively). All VLCADD patients showed less than 35% residual VLCAD activity. This technique allowed also to confirm that a novel *ACADVL* gene mutation (c.1400T>C) is responsible for a defective VLCAD activity (residual activity at 10%).

Abbreviations

ETF	Electron Transfer Flavoprotein
FA	Fatty acids
FAD	Flavin adenine dinucleotide
HPLC	High-performance liquid chromatography
MCAD	Medium-chain acyl-CoA dehydrogenase
MCADD	MCAD deficiency
MES	2-(*N*-morpholino)ethanesulfonic acid
OMIM	Online Mendelian Inheritance in Man
VLCAD	Very-long-chain acyl-CoA dehydrogenase
VLCADD	VLCAD deficiency

Introduction

Mitochondrial fatty acid (FA) oxidation is essential for energy production (Houten and Wanders 2010), and a

Communicated by: Cornelis Jakobs

D. Bouvier
Service de Biochimie Médicale, Centre de Biologie, CHU Gabriel-Montpied, rue Montalembert, 63000 Clermont-Ferrand, France

D. Bouvier
Retinoids, Reproduction Developmental Diseases, School of Medicine, Clermont Université, Université d'Auvergne, EA7281, 63000 Clermont-Ferrand, France

C. Vianey-Saban · S. Ruet
Service Maladies Héréditaires du Métabolisme et Dépistage Néonatal, Centre de Biologie et de Pathologie Est, CHU Lyon, INSERM U1060 CarMeN, 69500 Bron, France

C. Acquaviva (✉)
Service Maladies Héréditaires du Métabolisme et Dépistage Néonatal, Centre de Biologie et de Pathologie Est, CHU Lyon, UMR 5305 CNRS/UCBL, 69500 Bron, France
e-mail: cecile.acquaviva-bourdain@chu-lyon.fr

deficiency in the process leads to inability to utilize FA, often resulting in fasting hypoketotic hypoglycemia. Of the 24 known fatty-acid metabolism disorders, autosomal-recessive deficiencies in very-long-chain acyl-CoA dehydrogenase (VLCAD, EC1.3.8.9) (OMIM 609575) and medium-chain acyl-CoA dehydrogenase (MCAD, EC1.3.8.7) (OMIM 201450) count among the more frequent. Both enzymes catalyze the first step of the mitochondrial FA oxidation cycle leading to dehydrogenation of acyl-CoA to enoyl-CoA (Houten and Wanders 2010; Wanders et al. 1999). This step requires flavin adenine dinucleotide (FAD) bound to Electron Transfer Flavoprotein (ETF), which is then reduced into FADH2. VLCAD is bound to the inner mitochondrial membrane whereas MCAD is a matrix enzyme (Houten and Wanders 2010; Wanders et al. 1999). MCAD acts on medium-chain FA (4–14 carbon atoms, optimum activity with 6-carbon atoms). VLCAD acts on long-chain FA (12–22 carbon atoms, optimum activity with 16-carbon atoms) (Hashimoto 1992). Clinical presentation of VLCAD deficiency (VLCADD) may include cardiomyopathy, encephalopathy, hypoglycemia, and rhabdomyolysis (Arnold et al. 2009). MCAD deficiency (MCADD) is associated with hypoketotic hypoglycemia, hepatic symptoms that are predominantly related to intercurrent illnesses or prolonged fasting. Sudden death related to heartbeat disorders may also occur in adults (Feillet et al. 2012).

For VLCADD and MCADD, diagnosis is first suspected by plasma acylcarnitine and urine organic acid analyses, and has to be confirmed by molecular biology (Feillet et al. 2012; Vianey-Saban et al. 1998).

MCADD management specifies that enzyme activity must confirm diagnosis if molecular biology is not contributory. In addition, as a *post mortem* plasma acylcarnitine profile is very difficult to interpret, an enzyme activity assay can prove important in the exploration of sudden death (Feillet et al. 2012).

Strategy is similar for VLCADD where an enzyme activity assay may be even more valuable given the heterogeneity of *ACADVL* gene mutations (Vianey-Saban et al. 1998).

A method that measures the production of octenoyl-CoA (C8:1-CoA) (after addition of octanoyl-CoA as substrate) or hexadecenoyl-CoA (C16:1-CoA) (after addition of palmitoyl-CoA as substrate) by tandem mass spectrometry in lymphocytes was published (Tajima et al. 2008; ter Veld et al. 2009). The method uses ferrocenium hexafluorophosphate, an artificial electron acceptor for MCAD or VLCAD, to specifically determine MCAD and VLCAD activity within a day, but has never been further developed for analysis in fibroblasts.

Methods

Patients

Skin fibroblasts (75 cm^2 flask per strain, i.e. around 6.10^6 cells) grown in Ham's culture medium added with 12% fetal calf serum are harvested at confluence (Centre de Biotechnologie Cellulaire, Hospices Civils de Lyon, Bron). After trypsinization, washing in phosphate-buffered saline (PBS) and aspirating the supernatant, dry-harvested fibroblast pellets (12 controls, 10 known VLCAD-deficient patients, 6 known MCAD-deficient patients) were frozen at −80°C for storage.

The pellets were then resuspended with 300 µL of ammonium acetate (10 mM, pH = 8) and sonicated, in ice, for three × 15 sec bursts at 30 sec intervals.

Tests were also carried out in control-sample fibroblasts to evaluate analytical performance.

Reagents

Ammonium acetate and 2-(*N*-morpholino)ethanesulfonic acid (MES) were purchased from Merck (Darmstadt, Germany). Acetonitrile, octanoyl-CoA (C8:0), hexadecenoyl-CoA (C16:0), and ferrocenium hexafluorophosphate were obtained from Sigma-Aldrich (Deisenhofen, Germany).

Protein Assay

The total protein assay in sonicated fibroblast homogenates was performed in a 1:20 dilution on an ABX Pentra400® benchtop analyzer (Horiba Medical) using a colorimetric technique based on the bicinchoninic acid method (Thermo Scientific, Rockford, USA).

Procedures

Sonicated fibroblast homogenates, adjusted to a protein concentration of 0.2 g/L with ammonium acetate 10 mM, pH = 8, were diluted (1:1 V/V) in ferrocenium hexafluorophosphate solution (400 µM, pH = 8) to a final volume of 100 µL. The enzymatic reaction was started at 37°C by adding the substrate in MES buffer (20 mM, pH = 6): 4 µL of C8:0 (5 mM) to assay MCAD activity; 4 µL of C16:0 (5 mM) to assay VLCAD activity. After 15 min incubation, the reaction was stopped by adding 100 µL of ice-cold acetonitrile. A T0 timepoint measure was taken for each condition by simultaneously adding substrate and acetonitrile. After centrifugation at 14,000 g for 8 min at 4°C, the supernatant was transferred to autosampler vials with inserts for HPLC–mass spectrometry.

The analyte samples were injected (20 μL for the MCAD assay, 5 μL for the VLCAD assay) and chromatographic separation was carried out using a C18 Uptisphere column (50×2.1 mm, particle size: 3 μm) (Interchim, Montluçon, France). Flowrate was 200 μL/min. Eluent was a 70:30 (V/V) mixture (for MCAD assay) or 45:55 (V/V) mixture (for VLCAD assay) of ammonium acetate (10 mM, pH = 8) and acetonitrile. After chromatographic separation, the samples were analyzed by electrospray ionization–tandem mass spectrometry (ESI-MS/MS, Api 3200, Sciex, Les Ulis, France) in positive ion mode. The products derived directly from the MCAD-catalyzed reaction, i.e. octenoyl-CoA (C8:1), and the VLCAD-catalyzed reaction, i.e. hexadecenoyl-CoA (C16:1), were quantified. The products of the second step in the FA oxidation process were also assayed, i.e. 3-hydroxyoctanoyl-CoA (C8OH) and 3-hydroxypalmitoyl-CoA (C16OH), respectively. The product ions were studied in multiple reaction monitoring (MRM) mode, with each transition corresponding to substrate (C8:0 *m/z* 894.2>387.3, and C16:0 *m/z* 1006.4>499.4) or to products of the enzymatic reaction (C8:1 *m/z* 892.2>385.3, and C8OH *m/z* 910.2>403.3 or C16:1 *m/z* 1004.4>497.4 and C16OH *m/z* 1022.4>515.4). Working up from the peak areas obtained, the quantities of reaction products were calculated from substrate area at timepoint T0. As C8:1, C16:1, C8OH, and C16OH are not commercially available, response of the substrate and response of the enzymatic reaction products were considered identical.

Expression of Results

Enzymatic activities are expressed in nmol C8:1 (MCAD) or C16:1 (VLCAD) formed per minute per mg of proteins. For patients with MCADD or VLCADD, residual activity was evaluated as a ratio of the activity level of the control enzyme, i.e. VLCAD for MCAD-deficient patients and MCAD for VLCAD-deficient patients. The MCAD-to-VLCAD or VLCAD-to-MCAD ratios are then normalized by the mean of the ratios of the control group tested in the same experiment, thus giving (MCAD-to-VLCAD)-to-control and (VLCAD-to-MCAD)-to-control ratios.

Statistical Analysis

Group-wise results (control, MCADD, VLCADD) for MCAD or VLCAD enzymatic activity are reported as means (SD; $CI_{95\%}$). Between-group comparisons (control, MCADD, VLCADD) of MCAD (or VLCAD) activity were performed by one-way ANOVA, followed by a Tukey's post hoc test for pairwise comparisons between significantly different groups. All statistical analyses were performed using GraphPad® Prism 5 software. Statistical significance was set at $p < 0.05$.

Results

Optimization of the Method

The final selected analytical parameters were set as follows: protein concentration = 0.1 g/L, incubation time = 15 min, ferrocenium hexafluorophosphate concentration = 200 μM, final substrate (C8 or C16) concentration = 0.2 mmol/L.

Intra-assay coefficient of variation (CV) assessed via 10 repeated measures on the same control cell line was 4.3% (mean 0.47 nmol/min/mg protein) for MCAD activity and 10.8% (mean 0.74 nmol/min/mg protein) for VLCAD activity. Inter-assay CV assessed via 5 measurements carried out over 5 days on the same control cell line was 19% (mean 0.41 nmol/min/mg protein) for MCAD activity and 31% (mean 0.92 nmol/min/mg protein) for VLCAD activity.

Figure 1 illustrates chromatograms obtained in MRM mode for a patient with MCADD (Fig. 1a) or VLCADD (Fig. 1b), compared to a control patient with a decrease in signal intensity for the products C8:1 or C16:1 and C8OH or C16OH without concomitant change in signal intensity for substrate C8 or C16 (in surplus).

Population Studied

Three patient groups were studied: a group of 12 control patients, a group of 10 previously diagnosed VLCAD-deficient patients (P1–P10), and a group of six previously diagnosed MCAD-deficient patients (P11–P16). For each patient, MCAD and VLCAD activity assays were performed in duplicate within a same series and over two independent experimental runs.

Key clinical data on patients P1–P16 are reported in Table 1. All enzyme deficiencies were confirmed by molecular biology except for patient P11 who was only heterozygous for the frequent c.985A>G mutation. Diagnosis was confirmed for this patient by an enzymatic activity assay using ETF as electron acceptor (Bertrand et al. 1992). All the identified mutations (Table 1) have been described as deleterious in the literature and/or by predictions software (Alamut®, Interactive biosoftware).

Enzymatic Activities in the Study Population

Mean MCAD activity in the control group was 0.36 nmol C8:1 formed/min/mg protein (SD: 0.07; $CI_{95\%}$: 0.31–0.40). Mean MCAD activity in known VLCAD-deficient patients was 0.30 nmol C8:1 formed/min/mg protein (SD: 0.09; $CI_{95\%}$: 0.25–0.35). Mean MCAD activity in known MCAD-deficient patients was 0.07 nmol C8:1 formed/min/mg protein (SD: 0.08; $CI_{95\%}$: 0.00–0.13), which is significantly different to the control and "VLCAD-deficiency" groups ($p < 0.0001$) (Fig. 2a).

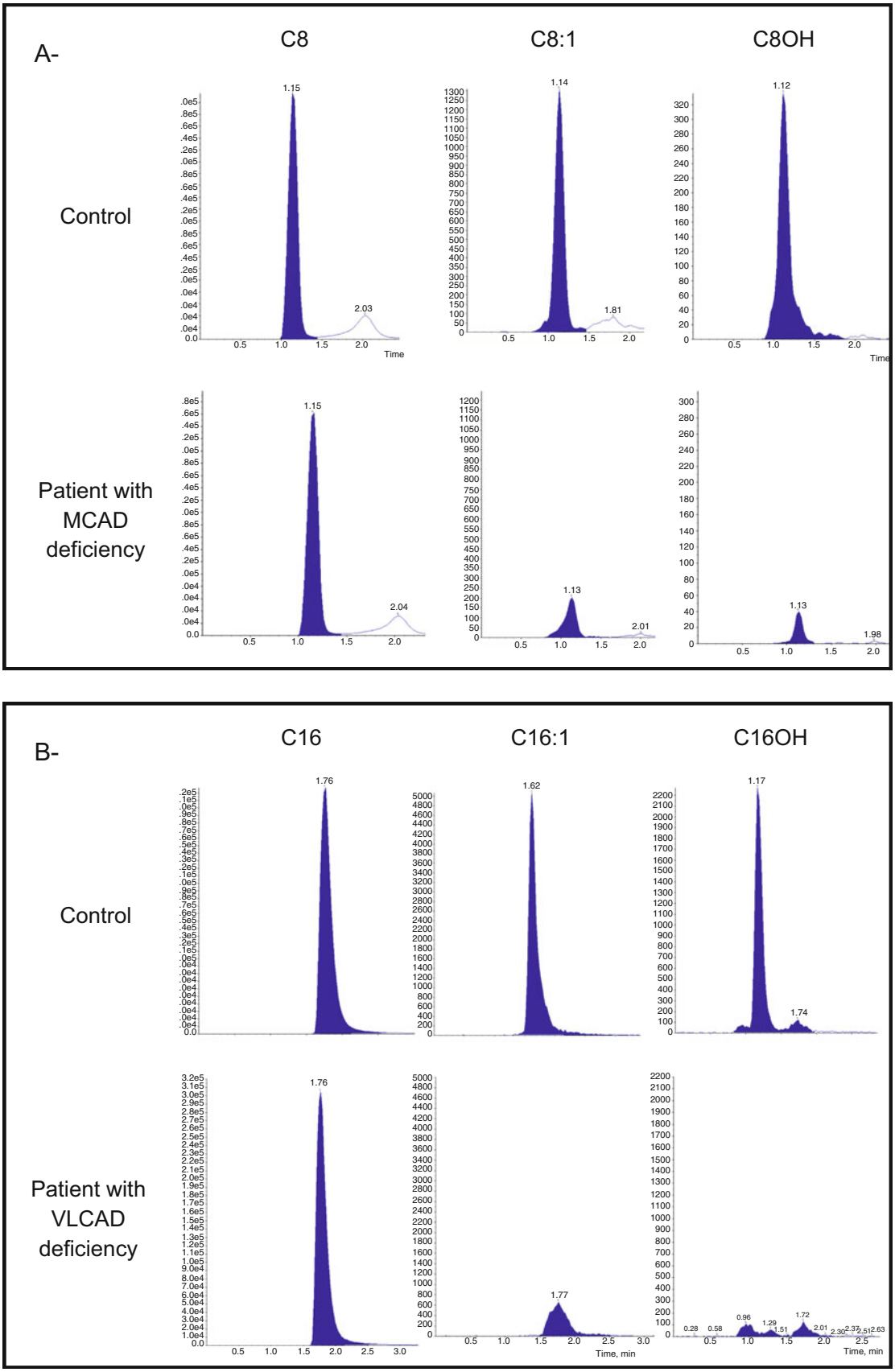

Fig. 1 MRM-mode chromatograms obtained after MCAD (**a**) and VLCAD (**b**) enzyme reactions. For each molecule, peaks are shown at identical scale between control patient and known MCAD-deficient (**a**) or known VLCAD-deficient (**b**) patient. (**a**) Substrate octanoyl-CoA (C8) and products octenoyl-CoA (C8:1) and 3-hydroxyoctanoyl-CoA (C8OH) were assayed. (**b**) Substrate palmitoyl-CoA (C16) and products

Mean VLCAD activity in the control group was 0.86 nmol C16:1 formed/min/mg protein (SD: 0.028; $CI_{95\%}$: 0.68–1.04). Mean VLCAD activity in known MCAD-deficient patients was 0.73 nmol C16:1 formed/min/mg protein (SD: 0.49; $CI_{95\%}$: 0.35–1.11). Mean VLCAD activity in known VLCAD-deficient patients was 0.06 nmol C16:1 formed/min/mg protein (SD: 0.07; $CI_{95\%}$: 0.02–0.10), which is significantly different to the control and "MCAD-deficiency" groups ($p < 0.0001$) (Fig. 2b).

All the known VLCADD and MCADD patients showed less than 35% residual VLCAD or MCAD activity (Table 1).

Discussion

MCADD and VLCADD are autosomal-recessive inborn errors of metabolism. Diagnosis is first suggested by plasma acylcarnitine profile analysis and urine organic acid analysis, and generally has to be confirmed by molecular biology. But sometimes a specific MCAD and VLCAD enzyme activity assay may prove necessary in cases involving non-contributive genetics or cases where patients refuse consent for genetic testing. In this context we developed a tandem mass spectrometry assay of MCAD/VLCAD activity in fibroblasts.

We first optimized the technique originally developed by Tajima et al. (2008) and ter Veld et al. (2009) in lymphocytes. Wanders et al. (2010) also used the ferrocenium hexafluorophosphate in a HPLC coupled to UV-detection assay of MCAD/VLCAD activity in fibroblasts. Although we ultimately retained the same ferrocenium hexafluorophosphate concentration (200 μM) and the same amount of substrate (20 nmol) as the original method, we opted for a 15 min incubation time at 37°C (instead of 5 min originally) and a 0.1 g/L protein concentration (instead of 0.03 g/L originally). Analytical performances for VLCAD activity are weaker than for MCAD activity, while the CVs remain acceptable for a tandem mass spectrometry technique. This can be explained by the fact that VLCAD is a membrane bound enzyme and therefore offers more random substrate availability than MCAD which is a matrix-soluble enzyme, despite the sonication step.

We applied this new method to analyze fibroblasts from MCAD-deficient or VLCAD-deficient patients. The activity of the deficient enzyme was significantly lower in the corresponding patient groups. Each individual patient with MCADD or VLCADD showed a significant decrease in the corresponding enzyme activity.

However, three particular cases draw our attention.

In patient P1, who died at day 2 of life with only post mortem organic acid profile evocative of long-chain FAO defect, two mutations were identified in *ACADVL* gene. Mutation c.1837C>T (p.Arg613Trp) has previously been described in the literature (Souri et al. 1996). The second substitution, c.1400T>C (p.Ile467Thr), has never been described (zero Pubmed, Ensembl, Clinvar, or ExAc Browser hits) and was classified as intermediate-severity by the prediction software. Both c.1837C>T and c.1400T>C mutations were properly segregated in the parents. The enzyme activity assay demonstrates its full utility in this case and enables diagnosis to be confirmed with a mean 10% residual VLCAD activity.

For patient P11, presenting with MCADD of good prognosis, only one heterozygous mutation was identified in *ACADM* gene. No other mutation was found in exons and flanking intronic regions of the second allele. The MCAD residual activity of 8% confirms plasma acylcarnitine and urine organic acid analyses. This method is easier and shorter to achieve than the previous method using ETF (Bertrand et al. 1992).

For patient P13, presenting with MCADD of good prognosis, two mutations were identified in the *ACADM* gene, both of which have been described in the literature (McKinney et al. 2004, Waddell et al. 2006). Mutation c.127G>A (p.Glu43Lys) has been described in homozygous state in a patient who also presented a mutation in heterozygous state on the gene coding for SCAD (McKinney et al. 2004). Mutation c.617G>A, which leads to substitution of a positively charged side-chain amino acid (arginine) at position 206 by a same-family amino acid (histidine), has been described in a compound heterozygous c.617G>A/c.985A>G patient (Waddell et al. 2006). Both mutations are classified as intermediate-severity by prediction software, which is an understandable conclusion given how c.617G>A is a conservative mutation. The enzyme activity assay demonstrates its utility and enables diagnosis to be confirmed with a mean 33% residual MCAD activity compared to controls. French consensus guidelines on diagnostic screening have set the confirmatory cut-off as less than 25% residual activity (Feillet et al. 2012). However, the guidelines were put together based on results obtained with the reference technique using ETF in fluorescence analysis, and it is now time to redefine a new threshold (possibly 35%) with this technique. Furthermore, the clinical picture and type of mutations point towards a moderate form of MCAD deficiency and explain why residual activity was found to be around 33%. Analysis of other patients is needed to define this new threshold.

Fig. 1 (continued) hexadecenoyl-CoA (C16:1) and 3-hydroxypalmitoyl-CoA (C16OH) were assayed

Table 1 Main clinical and genetic data, and residual activities of the 6 MCAD-deficient and the 10 VLCAD-deficient patients

		Clinical data				Molecular diagnostics			
	Patient	Related parents	Age of first symptoms	Symptoms	Evolution	Gene	Protein	MCAD residual activity (%)	VLCAD residual activity (%)
VLCADD	P1	No	2 days	Hypotonia, malaise and sudden death	Sudden death	c.1400T>C/c.1837C>T	p.Ile467Thr/p.Arg613Trp	/	10
	P2	Yes	1 year	Sleepiness during infections	Good with diet	c.899T>C/c.899T>C	p.Met300Thr/p.Met300Thr	/	4
	P3	No	2 days	Neurological distress	Good with diet	c.364A>G/c.1614C>A	p.Asn122Asp/p.Ala539Asp	/	3
	P4	Yes	2 days	Hypotonia, liver failure, hypertrophic cardiomyopathy, hypoglycemia	Death at 3 months	c.1679-6G>A/c.1679-6G>A	Splicing error	/	11
	P5	Yes	3 days	Sleepiness, hypotonia, hepatomegaly, metabolic acidosis, hyperlactacidemia, hyperammonemia	Death at 3 weeks	c.541C>T/c.541 C>T	p.His181Tyr/p.His181Tyr	/	7
	P6	No	40 years	Rhabdomyolysis in the effort	Good with diet	c.779C>T/c.1443A>T	p.Thr260Met/p.Gly481Gly	/	34
	P7	No	Neonatal	Hypoketotic hypoglycemia	Good with diet	c.779C>T/c.842C>A	p.Thr260Met/p.Ala281Asp	/	1
	P8	Yes	9 years	Exercise intolerance with cramps and myoglobinuria triggered by fasting and cold	Good with diet	c.1500_1502del/c.1500_1502del	p.Leu502del/p.Leu502del	/	7
	P9	No	Neonatal	Hypotonia, hypoglycemia	Death	c.777_778dup/c.777_778dup	p.Val261ArgfsX16/p.Val261ArgfsX16	/	0
	P10	No	1 year	Hypoglycemia	Good with diet	c.1837C>T/c.1837C>T	p.Arg613Trp/p.Arg613Trp	/	24
MCADD	P11	No	2 weeks	Convulsions	Good with diet	c.985A>G/[a]	p.Lys329Glu/[a]	8	/
	P12	No	3 days	Hypotonia, hypoglycemia, metabolic acidosis, hyperlactacidemia	Death	c.985A>G/c.468+1G>A	p.Lys329Glu/Splice	18	/
	P13	No	Neonatal	Hypotonia, hypoglycemia	Good with diet	c.127G>A/c.617G>A	p.Glu43Lys/p.Arg206His	33	/
	P14	No	8 months	Neurological distress, hypoglycemia	Good with diet	c.985A>G/c.985 A>G	p.Lys329Glu/p.Lys329Glu	24	/
	P15	No	15 months	Sleepiness, coma, hypoglycemia	Good with diet	c.985A>G/c.985 A>G	p.Lys329Glu/p.Lys329Glu	11	/
	P16	No	3 days	Convulsions, hypoglycemia	Lost for follow-up	c.872T>G/c.985A>G	p. Leu291X/p.Lys329Glu	11	/

For each patient, enzymatic reaction was performed in duplicate over two independent experiments. The activity (in nmol of product formed (C8:1 for MCAD activity, C16:1 for VLCAD activity)/min/mg protein) of the deficient enzyme (MCAD or VLCAD) was ratioed to the activity of the control enzyme (VLCAD or MCAD), and this ratio was then normalized by the mean control-group ratio to give a residual activity in %

[a] No mutation found in exons and flanking intronic regions

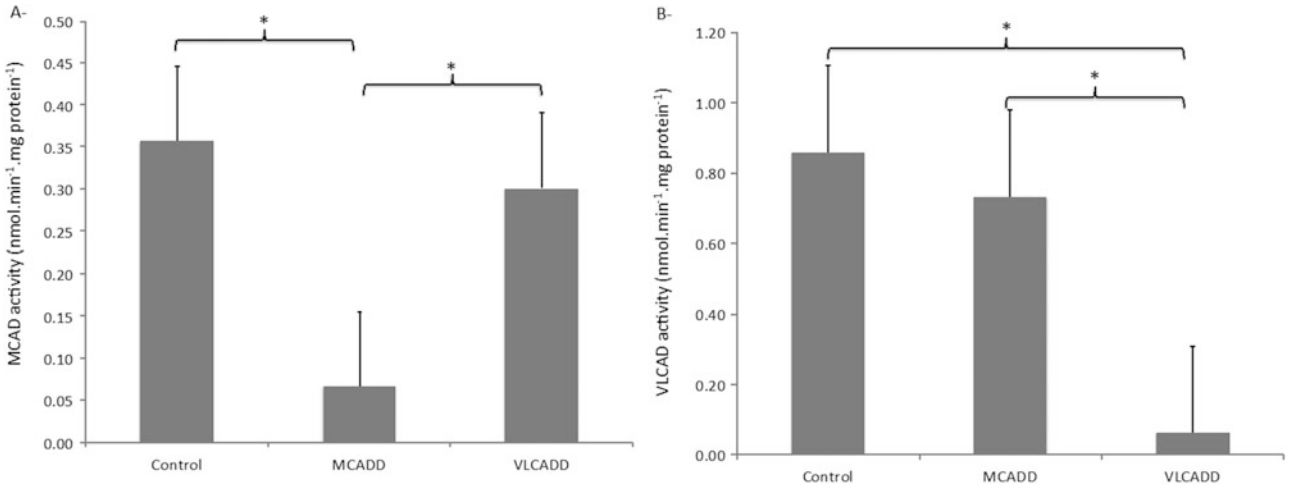

Fig. 2 Mean MCAD (**a**) and VLCAD (**b**) enzyme activities per patient group: control patients ($n = 12$), known VLCAD-deficient patients ($n = 10$) (VLCADD) and known MCAD-deficient patients ($n = 6$) (MCADD). For each patient, enzymatic reaction was performed in duplicate over two independent experiments. *$p < 0.0001$

Conclusion

The tandem mass spectrometry assay of MCAD/VLCAD activity in fibroblasts developed here offers powerful selective diagnostic screening of MCAD-deficient and VLCAD-deficient patients.

Acknowledgments The authors thank A.T.T. (Auvergne Traduction Technique®) for proofreading the manuscript.

Take-Home Message

The reader will learn about the usefulness of MCAD and VLCAD activity measurement and the performance of the method developed in fibroblasts.

Conflict of Interest

Damien Bouvier, Christine Vianey-Saban, Séverine Ruet, and Cécile Acquaviva declare that they have no conflict of interest.

Compliance with ethics guidelines: Informed consent was obtained from all patients for being included in the study.

Authors Contribution

Damien Bouvier and Severine Ruet have performed technical part of the study.

Damien Bouvier, Christine Vianey-Saban, Severine Ruet, and Cécile Acquaviva have performed analysis and interpretation of the data.

Damien Bouvier drafted the article.

Christine Vianey-Saban and Cécile Acquaviva revised the article.

References

Arnold GL, Van Hove J, Freedenberg D et al (2009) A Delphi clinical practice protocol for the management of very long chain acyl-CoA dehydrogenase deficiency. Mol Genet Metab 96(3): 85–90

Bertrand C, Dumoulin R, Divry P, Mathieu M, Vianey-Saban C (1992) Purification of electron transfer flavoprotein from pig liver mitochondria and its application to the diagnosis of deficiencies of acyl-CoA dehydrogenases in human fibroblasts. Clin Chim Acta 210(1-2):75–91

Feillet F, Ogier H, Cheillan D et al (2012) Medium-chain acyl-CoA-dehydrogenase (MCAD) deficiency: french consensus for neonatal screening, diagnosis, and management. Arch Pediatr 19(2): 184–193

Hashimoto T (1992) Peroxisomal and mitochondrial enzymes. Prog Clin Biol Res 375:19–32

Houten SM, Wanders RJA (2010) A general introduction to the biochemistry of mitochondrial fatty acid β-oxidation. J Inherit Metab Dis 33:469–477

McKinney JT, Longo N, Hahn SH et al (2004) Rapid, comprehensive screening of the human medium chain acyl-CoA dehydrogenase gene. Mol Genet Metab 82(2):112–120

Souri M, Aoyama T, Orii K, Yamaguchi S, Hashimoto T (1996) Mutation analysis of very-long-chain acyl-coenzyme A dehydrogenase (VLCAD) deficiency: identification and characterization of mutant VLCAD cDNAs from four patients. Am J Hum Genet 58(1):97–106

Tajima G, Sakura N, Shirao K et al (2008) Development of a new enzymatic diagnosis method for very-long-chain Acyl-CoA dehydrogenase deficiency by detecting 2-hexadecenoyl-CoA production and its application in tandem mass spectrometry-based selective screening and newborn screening in Japan. Pediatr Res 64(6):667–672

ter Veld F, Mueller M, Kramer S et al (2009) A novel tandem mass spectrometry method for rapid confirmation of medium- and very long-chain acyl-CoA dehydrogenase deficiency in newborns. PLoS One 4:e6449

Vianey-Saban C, Divry P, Brivet M et al (1998) Mitochondrial very-long-chain acyl-coenzyme A dehydrogenase deficiency: clinical characteristics and diagnostic considerations in 30 patients. Clin Chim Acta 269(1):43–62

Waddell L, Wiley V, Carpenter K et al (2006) Medium-chain acyl-CoA dehydrogenase deficiency: genotype-biochemical phenotype correlations. Mol Genet Metab 87(1):32–39

Wanders RJ, Vreken P, den Boer ME, Wijburg FA, van Gennip AH, IJlst L (1999) Disorders of mitochondrial fatty acyl-CoA beta-oxidation. J Inherit Metab Dis 22(4):442–487

Wanders RJ, Ruiter JP, IJLst L, Waterham HR, Houten SM (2010) The enzymology of mitochondrial fatty acid beta-oxidation and its application to follow-up analysis of positive neonatal screening results. J Inherit Metab Dis 33(5):479–494

JIMD Reports
DOI 10.1007/8904_2016_27

RESEARCH REPORT

Analysis of Melanin-like Pigment Synthesized from Homogentisic Acid, with or without Tyrosine, and Its Implications in Alkaptonuria

Adam M. Taylor • Koen P. Vercruysse

Received: 28 August 2016 / Revised: 02 November 2016 / Accepted: 16 November 2016 / Published online: 10 December 2016

Abstract Alkaptonuria is an iconic disease used by Archibald Garrod to demonstrate the theory of "inborn errors of metabolism". AKU knowledge has advanced in recent years: development of an in vitro model, discovery of murine models and advances in understanding bone and cartilage phenotypes and arthropathy in AKU. These discoveries have aided in a new clinical trial into nitisinone. However, there are still knowledge gaps surrounding the pigment in AKU and the pigmentation process. We demonstrate an advance in the understanding in the kinetics and chemistry of the polymerisation of homogentisic acid (HGA) into its pigment using size-exclusion chromatography and IR spectroscopy. We compared the properties of HGA-based pigments that were freshly prepared to those stored in solution for 2 years. Our results demonstrate the importance of pH in the polymerisation process and that colour change seen in solution (analogous to AKU patient urine) is not initially due to presence of ochronotic pigment but the quinone intermediary. In addition, we observed that pigment formation from HGA can occur in the presence of tyrosine, without the inclusion of this tyrosine into the pigment. These observations have positive implications for patients with alkaptonuria; an increased understanding of the pigment polymer chemistry, the presence of an intermediary and their kinetics present more therapeutic opportunities for treating the condition, including preventing the pigment from forming, binding or reversing established pigmentation. AKU patients treated with nitisinone show elevated tyrosine levels causing side effects such as corneal opacities; our data demonstrates that elevated tyrosine levels should not contribute or add to the ochronotic pigment burden in these patients.

Communicated by: Ina Knerr, MD

Electronic supplementary material: The online version of this chapter (doi:10.1007/8904_2016_27) contains supplementary material, which is available to authorized users.

A.M. Taylor (✉)
Faculty of Health and Medicine, Lancaster Medical School, Lancaster University, Bailrigg, Lancaster LA1 4YW, UK
e-mail: a.m.taylor@lancaster.ac.uk

K.P. Vercruysse
Department of Chemistry, Tennessee State University, Nashville, TN 37209, USA

Introduction

Alkaptonuria (AKU) is a rare autosomal recessive condition which results from a single-enzyme deficiency on the tyrosine metabolic pathway (Mistry et al. 2013). This enzyme, homogentisate 1,2-dioxygenase (HGD), is responsible for cleaving the benzene ring of homogentisic acid (HGA). However, in AKU patients the deficiency of this enzyme results in systemic elevation of HGA. This systemic elevation occurs even though the kidneys excrete gram quantities of HGA per day in urine. The presence of HGA in gram quantities results in darkening of urine over time or upon addition of alkali substances – this is the first clinic symptom in the triad that are typical of AKU. Regardless of the excretion of gram quantities, the systemic elevation of HGA leads to polymerisation of the HGA monomer in collagenous tissues. This polymerisation leads to darkening, termed ochronosis – the second of the clinical triad. Overtime the ochronosis leads to ochronotic osteoarthropathy, the final clinical symptom, leading to the need for joint replacement, often multiple joint replacements in

AKU patients. The darkening of urine is present from birth; ochronosis is believed to begin in the third decade of life with ochronotic osteoarthropathy presenting late in the fourth and fifth decades of life (Taylor et al. 2011).

AKU holds a unique place in medical history as one of the diseases that Garrod used to describe "inborn errors of metabolism". In more recent years the defective gene has been mapped and cloned (Pollak et al. 1993; Zatkova 2011). An in vitro model and a mouse model are also available to aid in understanding the progression of the disease and screening of therapeutic agents (Preston et al. 2014; Taylor et al. 2012; Tinti et al. 2011). Although advances have been made in understanding AKU there is one area that is still somewhat lacking: the analysis and understanding of what occurs to HGA and the chemical changes that occur as it polymerises that may enable or determine how the pigment interacts with the cells and extracellular matrices of AKU patients' tissues.

The histological reaction of HGA and its polymeric derivative with Schmorl's reagent show identical staining properties to tyrosine and melanin (Tinti et al. 2011). The conversion of L-tyrosine to its L-3,4-dihydroxyphenylalanine (L-DOPA) intermediary and melanin is catalysed by tyrosinase and it has been proposed that this could also be involved in the conversion of HGA to its quinone intermediary and subsequent ochronotic pigment (Taylor et al. 2016a, b). L-Tyrosine is converted into L-DOPA, which is then converted into an *o*-quinone, L-DOPA-quinone. Both reactions are catalysed by tyrosinase and the oxidations of L-tyrosine to L-DOPA and to melanin pigment follow each other consecutively (Goldfeder et al. 2013). The *o*-quinone form of L-DOPA, via a series of steps, self-polymerises (non-enzymatically) to form melanin (Faccio 2012; Sonmez 2011). The oxidation pathway of HGA into ochronotic pigment is presumed to be similar to the L-tyrosine–L-DOPA–melanin pathway (Roberts et al. 2015). HGA is somewhat similar to L-DOPA as L-DOPA is an *o*-diphenolic compound and HGA is a *p*-diphenolic compound (Rosa 2011). HGA can oxidize into the *p*-quinone molecule, benzoquinone acetic acid (BQA), before going on to polymerise as the ochronotic pigment (Roberts et al. 2015) (see supplementary Fig. 1). This study set out to examine the polymerisation of HGA to melanin-like pigment and to try to understand its chemical composition. A further objective was to examine if in the polymerisation of HGA pigment L-tyrosine could be incorporated into the pigment molecule.

Materials and Methods

Homogentisic acid (HGA), tyrosine sodium chloride and molecular grade water were all purchased from Sigma Aldrich, UK. All other chemicals used were of analytical grade.

The following solutions were prepared:

Solution 1: 2 mL with HGA at 50 mg/mL and NaOH at 0.25M.

Solution 2: 2.5 mL with HGA at 40 mg/mL, tyrosine at 0.2M and NaOH at 0.2M.

Solution 3: 0.55 mL with HGA at 91 mg/mL.

Solution 4: 0.55 mL with HGA at 91 mg/mL and NaOH at 0.1M.

Solution 5: 0.55 mL with HGA at 91 mg/mL solution of HGA and NaOH at 1M.

Solutions 1 and 2 were placed in sealed vials and left on a laboratory bench for 2 years before being subjected to analysis. At the time of analysis 200 µL aliquots of each solution were removed and subjected to the following. The aliquots were diluted with 20 mL distilled water and dialysed using Spectrum Spectra/Por RC dialysis membranes with molecular weight cut-off of 3.5 kDa obtained from Fisher Scientific (Suwanee, GA, USA) against water (up to 3.5 L) for 3 days with up to four changes of water each day. Following dialysis a 400 µL aliquot was diluted with 600 µL chromatography solvent, centrifuged and analysed by size-exclusion chromatography (SEC). The dialysed mixtures were kept at −20°C for 6 h and dried for 3 days using a Labconco FreeZone Plus 4.5 L benchtop freeze-dry system obtained from Fisher Scientific (Suwanee, GA, USA). This yielded pigment samples #1 and #2. Solutions 3–5 were kept on the lab bench at room temperature. Over the course of 10 days, 5 µL aliquots were diluted 1,000-fold with solvent for size-exclusion chromatography, centrifuged and analysed by size-exclusion chromatography. After 10 days of standing at room temperature, solution 5 was dialysed and dried as outlined for solutions 1 and 2, yielding pigment sample #5.

Size-Exclusion Chromatography (SEC)

SEC analyses were performed on a Breeze 2 HPLC system equipped with two 1500 series HPLC pumps and a model 2998 Photodiode array detector from Waters, Co (Milford, MA, USA). Analyses were performed using an Ultrahydrogel 500 column (300 × 7.8 mm) obtained from Waters, Co (Milford, MA, USA) in isocratic fashion using a mixture of 25 mM Na acetate:methanol:acetic acid (90:10:0.05% v/v) as solvent. Analyses were performed at room temperature and 20 µL of sample was injected.

FT-IR Spectral Analysis

FT-IR spectroscopic scans were made using the NicoletiS10 instrument equipped with the SmartiTR Basic accessory from ThermoScientific (Waltham, MA). Scans were taken

with a resolution of 4 cm^{-1} between 650 and 4,000 cm^{-1} at room temperature using a KBr beam splitter and DTGS KBr detector. Each spectrum represents the accumulation of 32 scans.

Results

Macroscopic examination of the mixtures showed that solutions 1, 2 and 5 were dark black with no light able to pass through the samples, while solution 4 had turned dark orange. Solution 3 had maintained the light yellow colour it had at the start of the experiment. The aliquots from solutions 1, 2 and 5 did not show any precipitations upon dilution for size-exclusion chromatography analysis or during the dialysis process; the solutions maintained a dark-brown to black colouration. However, during the freezing process of the dialysed mixtures a phase separation occurred. The frozen mixtures displayed a heterogeneous colouration. They had a central core of black ice surrounded by clear-coloured ice. Upon freeze-drying, flaky to powdery dark-brown material was obtained, but the sides of the plastic tubes that contained the dialysed mixtures during the freeze-drying process were stained with rings of dark-brown material.

Figure 1 illustrates the SEC profile of a diluted aliquot from solution 5 after 48-h reaction at room temperature. In SEC analyses, molecules are separated on the basis of differences in hydrodynamic volume (often related to the molecular mass of the molecule); the lower the retention time, the higher the hydrodynamic volume of the analyte. In our SEC analyses, the lower limit of exclusion, as determined by the injection of water, was about 15 min. Peaks with a retention time lower than 15 min are high-molecular-mass compounds, while peaks with retention times of 15 min or higher are low-molecular-mass compounds. HGA was determined to have a retention time of about 21 min in our SEC analyses. Following reaction between HGA and NaOH in solution 5, a new peak emerged with a retention time of about 12.4 min and with absorbance in the UV and visible range of the electromagnetic spectrum. This peak was presumed to correspond to the pigment generated from HGA. Kinetic monitoring of the area under the curve (AUC) of the peak corresponding to HGA and the new peak with retention time of about 12.4 min obtained through SEC analyses of diluted aliquots from solution 5 indicated that near all HGA reacted away within 10 days and the amount of high-molecular-mass pigment increased steadily over this period (results not shown). SEC analyses revealed that no pigment was generated in solutions 3 and 4 (though a change in colour was observed) and that the concentration of HGA did not change significantly over the course of 10 days (results not shown). The change in colour observed in solution 4 was attributed to pH effects on HGA and possible oxidation to the quinone form of HGA. SEC analyses of diluted aliquots from dialysed solutions 1 and 2 yielded peaks with retention times around 12.4 min and no peaks corresponding to HGA (results not shown). Figure 2 illustrates the UV-Vis profiles of the peak corresponding to the HGA-derived pigment observed in the SEC analyses of purified solutions 1, 2 and 5. All three samples had similar UV-Vis absorbance profiles: strong absorbance in the UV range and modest absorbance in the visible range. Figure 3

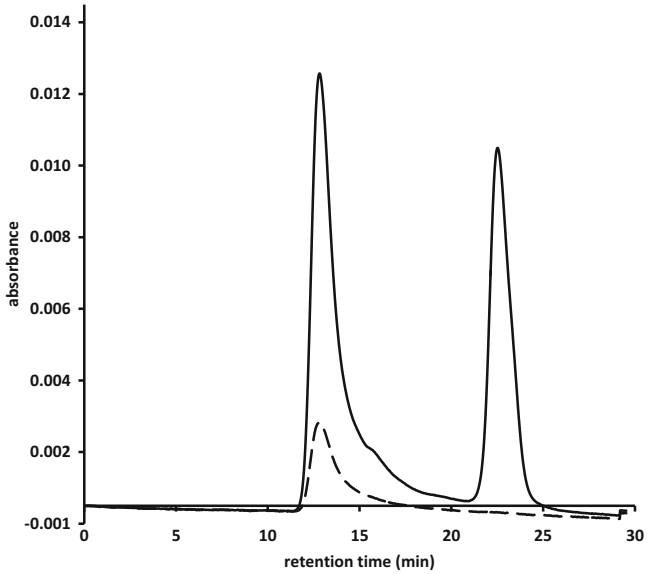

Fig. 1: SEC profile viewed at 290 nm (*solid line*) and 400 nm (*dashed line*) of a diluted aliquot from solution 5 after 48-h reaction at room temperature

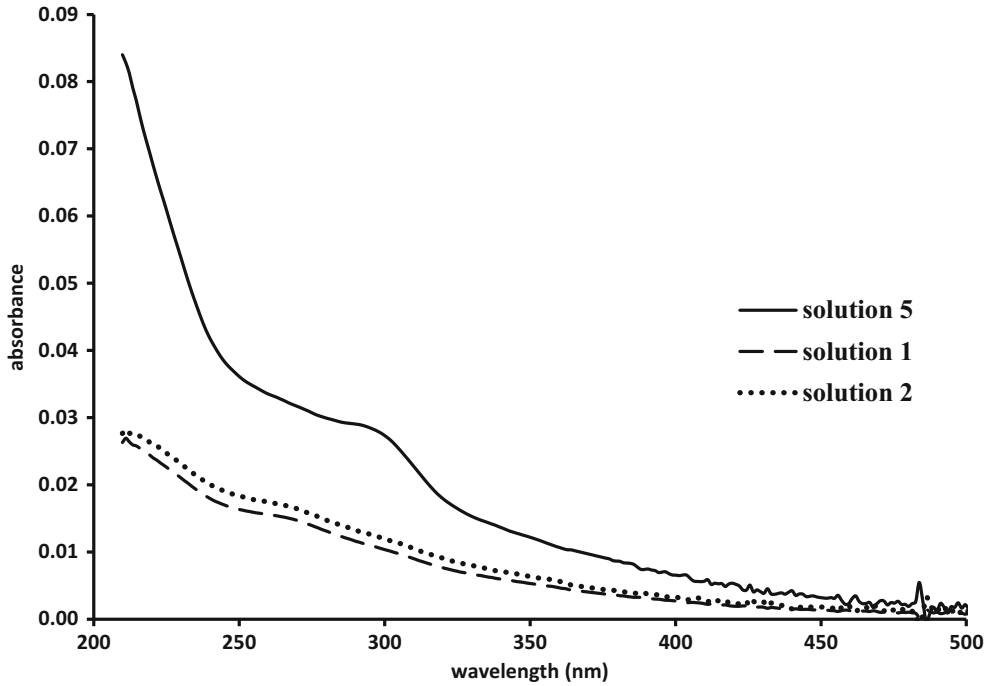

Fig. 2: UV-Vis spectra of the peak with retention time of about 12.4 min of the SEC analysis of solution 1 (*dashed line*), solution 2 (*dotted line*) and solution 5 (*solid line*)

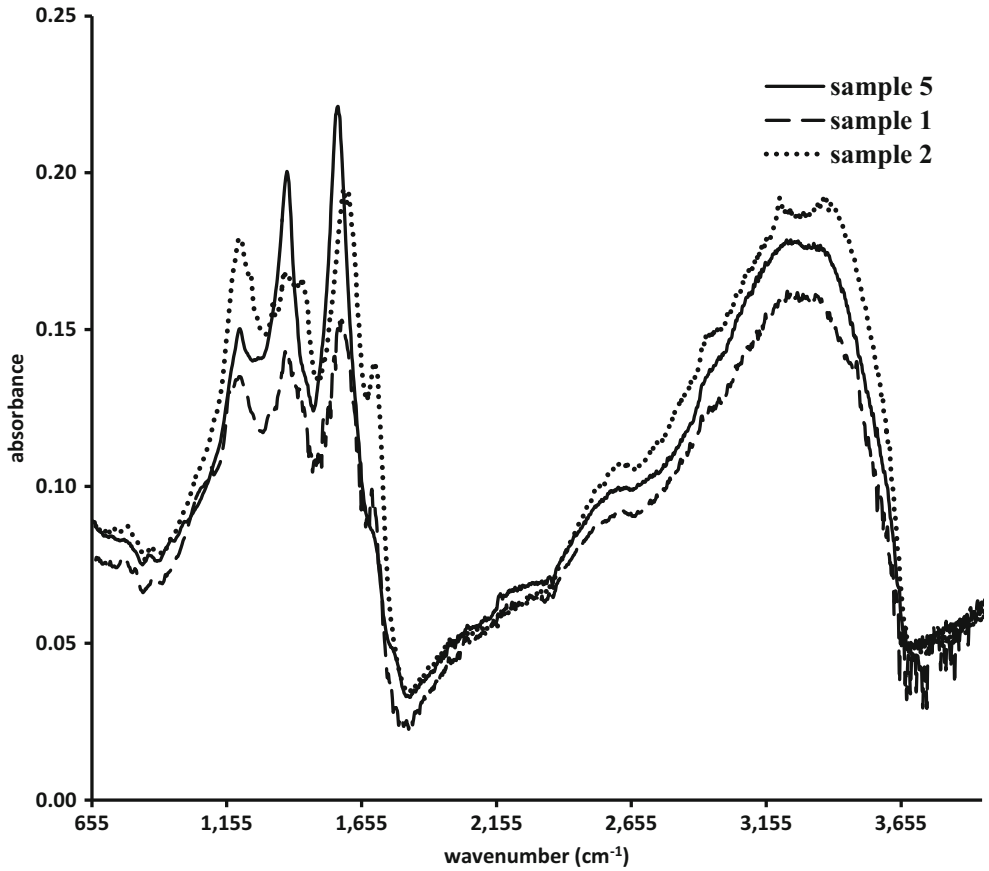

Fig. 3: FT-IR spectra obtained of pigment samples 1 (*dashed line*), 2 (*dotted line*) and 5 (*solid line*)

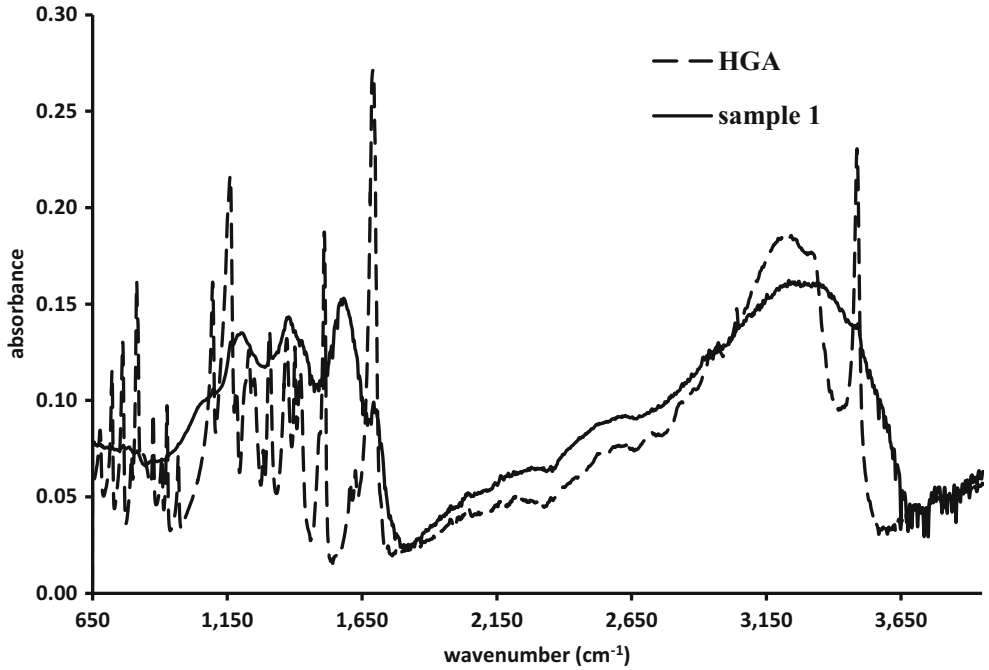

Fig. 4: FT-IR spectra of dried pigment from solution 1 (*black line*) and HGA (*dashed line*)

illustrates an overlay of the FT-IR spectra obtained of pigment samples 1, 2 and 5. The FT-IR spectra of the three pigment samples are qualitatively identical to each other. This suggests that the pigment left standing for 2 years did not undergo any significant chemical alterations compared to freshly prepared pigment materials. Figure 4 illustrates an overlay of the FT-IR spectra obtained of the dialysed and dried pigment from solution 1 and HGA.

The dried pigment samples can be redissolved in water and an attempt was made to take an NMR spectrum of pigment sample 1 by dissolving about 15 mg in 0.7 mL D_2O. The attempt failed as no signals were obtained in the ^{1}H or ^{13}C scans. It was observed that the pigment material had precipitated during the NMR analysis and this was attributed to the cooler temperature of the NMR core environment. This constituted a second observation that some physical instability occurs when pigment solutions are cooled off below ambient temperatures.

Discussion

The polymerisation of HGA monomer is well defined in the scientific literature; however little is known about how HGA pigment molecules interact with each other or with other biomolecules that are present in solutions or more importantly biological matrices. Furthermore, little is known about the kinetics of the reaction and the conversion of HGA to its intermediary and finally the ochronotic pigment seen in AKU occurs. This study is the first to examine aged ochronotic pigment formed from HGA and to examine the kinetics of the polymerisation of HGA to pigment using SEC. Our observations suggest that, when studying the formation of pigment from HGA, merely monitoring change in absorbance may be misleading as changes in colour without formation of pigment can occur. Our SEC analyses confirmed that a high-molecular-mass pigment was generated in solutions 1, 2 and 5 and that the colour of these samples was not due to a low-molecular-mass chromophore. SEC analyses of solution 5 at intermediate stages did not show any other peaks than those corresponding to pigment or HGA. If other intermediates were generated in the reaction between HGA and NaOH they may have had a short lifetime. Our kinetic studies indicate that no to very little pigment formation occurred when HGA was kept in water or in a 0.1M NaOH environment and that almost 100% of the HGA reacted away within 10 days when present in a 1M NaOH environment. This strongly suggests that for HGA to polymerise into its pigment, an alkalinity threshold needs to be surpassed for the HGA molecules to be activated. Any enzyme or other biomolecule responsible for the in vivo formation of pigment from HGA probably needs to act as a base catalyst in addition to being an oxidase.

In the ochronosis process in AKU the polymer is suggested to be present in urine in solution giving a darkened colour, particularly at alkali pH; although this is not damaging to AKU patients the detrimental effects of

ochronosis are seen in later life where the ochronosis is widely seen in joint tissues, bound to collagen fibres (Taylor et al. 2010). The UV absorbance of the pigment of solution 5 appeared to be relatively stronger than the UV absorbance of the pigment in solutions 1 or 2. This difference in UV-Vis spectra may reflect a physical difference between the samples, as FT-IR analyses of the pigments 1, 2 and 5 did not reveal any chemical differences between the samples. As solutions 1 and 2 were left standing for 2 years, we envision that more aggregation, possibly through π-π stacking interactions between the aromatic units of the pigment molecules, could have occurred. Overall, the UV-Vis spectra are similar to the UV-Vis spectrum of the HGA-based pigment reported before (Menon et al. 1991).

Whilst the association of pigment with collagen or other collagen-associated proteins has been shown, it is still not clear exactly what atoms are bound together between the biological matrices and HGA and/or its polymer (Chow et al. 2011). One of the major unanswered questions is as to whether the binding of HGA or pigment to the matrix is by HGA which then subsequently polymerises, or if the polymerisation occurs within the space surrounding collagen fibres and it is the BQA intermediary or the ochronotic polymer which first binds to the collagen fibres. Ochronotic cartilage shows a significant decrease in the amount of glycosaminoglycan (GAG) present in the cartilage matrix and it may be the spaces left from the removal of these GAGs that the polymer is filling. Alternatively, GAGs present in the matrix may act as the nucleation sites for HGA or BQA (Taylor et al. 2016a, b). In this context it is worth noting that in a study of the interaction between carbohydrates and proteins, it was observed that carbohydrates favoured interaction with aromatic types of amino acids (Hudson et al. 2015). Alternatively, another such nucleation interaction could occur between the OH group of hydroxyproline and HGA. These hypotheses will be addressed in future research efforts.

The spectrum of sample 2 is qualitatively very similar to the spectra of samples 1 and 5. This suggests that the presence of tyrosine had not altered the pigment formation from HGA in any way. The region of the spectra between wavenumbers 1,000 and 1,700 cm^{-1} is very similar to the FT-IR spectrum obtained from a pigment obtained from HGA under similar conditions (Turick et al. 2002). The spectra of the pigments exhibit a shoulder at a wavenumber of about 1,080 cm^{-1} and broad peaks with wavenumbers of about 1,200, 1,380 and 1,580 cm^{-1}. These absorbances can be attributed to C–H in-plane/out-of-plane deformation, C–O stretching, phenolic OH bending and aromatic C=C bending vibrations, respectively. In addition, a peak at a wavenumber of about 1,700 cm^{-1} can be observed and such a peak is associated with the presence of carbonyl stretching (Turick et al. 2002). Absent in the spectrum of sample 2 are peaks with wavenumbers between 1,500 and 1,540 cm^{-1}. Such peaks have been assigned to amino functionalities in melanin pigments derived from DOPA (Apte et al. 2013; Tu et al. 2009). This further suggests that tyrosine was not built into the pigment sample when mixed with HGA. The overlay of FT-IR spectra of pigment sample 1 and HGA shows that all the typical, well-defined peaks associated with HGA are not present in the pigment sample. An exception to this may be the peak at wavenumber of about 1,690 cm^{-1}. This peak corresponds to the C=O bond of the carboxylic acid functional group. Noticeably absent in the spectrum of sample 1 is the sharp peak at wavenumber of about 3,480 cm^{-1}. This peak represents free, not hydrogen-bonded OH groups and its absence in the spectrum of sample 1 suggests that the phenols of HGA are linked into new chemical bonds or hydrogen-bonded into the new structure. The broad peak at wavenumber of about 3,300 cm^{-1} suggests the presence of hydrogen-bonded OH groups. In addition, the sharp peaks at wavenumbers between 700 and 900 cm^{-1} present in the spectrum of HGA are absent in the spectrum of sample 1. Peaks in that region correspond to aromatic C–H bonds and their absence in the spectrum of the dried sample suggests that in the pigment, aromatic units are linked to each other via C–C or C–O bonds.

Our results demonstrate the absence of distinct tyrosine peaks from the 2-year-old pigment generated in the presence of tyrosine, which is clinically interesting. A current ongoing trial looking at the suitability of nitisinone in AKU patients is looking to be very promising for reducing HGA. However, the major risk in these patients is an increase in plasma tyrosine, leading to corneal opacities and other more severe complications (Ranganath et al. 2016). An absence of detectable tyrosine from the spectra in our study suggests that patients who have established ochronosis will likely not have to worry about the polymerisation of tyrosine and it binding to the already established ochronotic pigment in their tissues. The presence of potentially high-molecular-mass material or nanoparticulate material is also of clinical interest. It has been shown that the pigmented material alters the biomechanical properties of cartilage and is resistant to enzymatic degradation (Taylor et al. 2011). High-molecular-mass pigments, as well as being unable to be broken down, are unlikely to be able to be moved from the cells and tissues of the body, thereby adding pressure for any therapeutic agent to be targeted as early as possible in life prior to any pigment formation or deposition (Taylor et al. 2011). Finally, we show that SEC presents a useful tool for examining the conversion of HGA to intermediaries and pigment polymer and should be used in assessing the effectiveness of antioxidant and anti-polymeric agents

in vitro to gain a greater understanding of HGA pigments and how to inhibit their formation.

Acknowledgements Dr. Adam Taylor would like to acknowledge the Rosetrees Trust for funding. Dr. Vercruysse was in part supported by the Institute for Food, Agricultural and Environmental Research at Tennessee State University.

"Take-Home" Message

Our data shows initial colour change in samples of HGA solution is due to the formation of intermediaries which are not polymerised pigment. C–C and C–O bonds are involved in linking aromatic units in the formation of ochronotic pigment. Tyrosine is not incorporated into ochronotic pigment meaning that patients with elevated plasma tyrosine will not have elevated plasma tyrosine adding or contributing to the pigment burden.

Contribution

Drs. Taylor and Vercruysse have been involved in conception, design, analysis and interpretation of data. Both authors drafted the chapter and revised it critically for important intellectual content.

References

Apte M, Girme G, Bankar A, RaviKumar A, Zinjarde S (2013) 3, 4-dihydroxy-L-phenylalanine-derived melanin from Yarrowia lipolytica mediates the synthesis of silver and gold nanostructures. J Nanobiotechnol 11:1–9

Chow WY, Taylor AM, Reid DG, Gallagher JA, Duer MJ (2011) Collagen atomic scale molecular disorder in ochronotic cartilage from an alkaptonuria patient, observed by solid state NMR. J Inherit Metab Dis 34:1137–1140

Faccio G, Kruus K, Saloheimo M, Thöny-Meyer L (2012) Bacterial tyrosinases and their applications. Process Biochem 47:1749–1760

Goldfeder M, Egozy M, Shuster Ben-Yosef V, Adir N, Fishman A (2013) Changes in tyrosinase specificity by ionic liquids and sodium dodecyl sulfate. Appl Microbiol Biotechnol 97:1953–1961

Hudson KL, Bartlett GJ, Diehl RC et al (2015) Carbohydrate–aromatic interactions in proteins. J Am Chem Soc 137:15152–15160

Menon IA, Persad SD, Haberman HF et al (1991) Characterization of the pigment from homogentisic acid and urine and tissue from an alkaptonuria patient. Biochem Cell Biol 69:269–273

Mistry JB, Bukhari M, Taylor AM (2013) Alkaptonuria. Rare Dis 1: e27475

Pollak MR, Chou YH, Cerda JJ et al (1993) Homozygosity mapping of the gene for alkaptonuria to chromosome 3q2. Nat Genet 5:201–204

Preston AJ, Keenan CM, Sutherland H et al (2014) Ochronotic osteoarthropathy in a mouse model of alkaptonuria, and its inhibition by nitisinone. Ann Rheum Dis 73:284–289

Ranganath LR, Milan AM, Hughes AT et al (2016) Suitability of Nitisinone in Alkaptonuria 1 (SONIA 1): an international, multicentre, randomised, open-label, no-treatment controlled, parallel-group, dose-response study to investigate the effect of once daily nitisinone on 24-h urinary homogentisic acid excretion in patients with alkaptonuria after 4 weeks of treatment. Ann Rheum Dis 75:362–367

Roberts NB, Curtis SA, Milan AM, Ranganath LR (2015) The pigment in alkaptonuria relationship to melanin and other coloured substances: a review of metabolism, composition and chemical analysis. JIMD Rep 24:51–66

Rosa A, Tuberoso CI, Atzeri A, Melis MP, Bifulco E, Dessi MA (2011) Antioxidant profile of strawberry tree honey and its marker homogentisic acid in several models of oxidative stress. Food Chem 129:1045–1053

Sonmez F, Sevmezler S, Atahan A et al (2011) Evaluation of new chalcone derivatives as polyphenol oxidase inhibitors. Bioorg Med Chem Lett 21:7479–7482

Taylor AM, Wilson PJ, Ingrams DR, Helliwell TR, Gallagher JA, Ranganath LR (2010) Calculi and intracellular ochronosis in the submandibular tissues from a patient with alkaptonuria. J Clin Pathol 63:186–188

Taylor AM, Boyde A, Wilson PJ et al (2011) The role of calcified cartilage and subchondral bone in the initiation and progression of ochronotic arthropathy in alkaptonuria. Arthritis Rheum 63:3887–3896

Taylor AM, Preston AJ, Paulk NK et al (2012) Ochronosis in a murine model of alkaptonuria is synonymous to that in the human condition. Osteoarthr Cartil 20:880–886

Taylor AM, Kammath V, Bleakley A (2016a) Tyrosinase, could it be a missing link in ochronosis in alkaptonuria? Med Hypotheses 91:77–80

Taylor AM, Hsueh MF, Ranganath LR et al (2016b) Cartilage biomarkers in the osteoarthropathy of alkaptonuria reveal low turnover and accelerated ageing. Rheumatology. doi:10.1093/rheumatology/kew355

Tinti L, Taylor AM, Santucci A et al (2011) Development of an in vitro model to investigate joint ochronosis in alkaptonuria. Rheumatology (Oxford) 50:271–277

Tu YG, Xie MY, Sun YZ, Tian YG (2009) Structural characterization of melanin from Black-bone silky fowl (Gallus gallus domesticus Brisson). Pigm Cell Melanoma Res 22:134–136

Turick CE, Tisa LS, Caccavo F Jr (2002) Melanin production and use as a soluble electron shuttle for Fe(III) oxide reduction and as a terminal electron acceptor by Shewanella algae BrY. Appl Environ Microbiol 68:2436–2444

Zatkova A (2011) An update on molecular genetics of Alkaptonuria (AKU). J Inherit Metab Dis 34:1127–1136

JIMD Reports
DOI 10.1007/8904_2016_28

RESEARCH REPORT

Bone Health in Classic Galactosemia: Systematic Review and Meta-Analysis

Britt van Erven • Lindsey Welling • Sandra C. van Calcar • Artemis Doulgeraki • François Eyskens • Joanna Gribben • Eileen P. Treacy • Rein Vos • Susan E. Waisbren • M. Estela Rubio-Gozalbo • Annet M. Bosch

Received: 07 June 2016 / Revised: 24 October 2016 / Accepted: 16 November 2016 / Published online: 20 December 2016

Abstract Introduction: Previous studies have reported an association between classic galactosemia (CG) and decreased bone mass. The primary objective of this systematic review with meta-analysis was to determine the extent of bone mineral density (BMD) Z-score reduction. Low BMD was defined as a Z-score ≤ -2 standard deviations (SD). The secondary objective was to evaluate other indicators of bone status through a descriptive analysis.

Methods: Systematic search strategies were developed by an experienced clinical librarian. Selection of relevant manuscripts, risk of bias assessment, and data extraction were performed independently by two investigators.

Results: Four studies were included in the meta-analysis. BMD Z-scores in children and adults with CG measured at the lumbar spine (LBMD; 4 studies; $n = 112$), total hip (HBMD; 2 studies; $n = 58$), and femoral neck (FBMD; 2 studies; $n = 73$) were assessed. Mean BMD Z-scores in the CG population were LBMD −0.70 (95% CI: −0.88, −0.52); HBMD −0.89 (95% CI: −1.14, −0.64); and FBMD −0.63 (95% CI −1.29, 0.02). Results from studies included in the descriptive analysis ($n = 7$) show that vitamin D levels were frequently in the low reference range, whereas serum calcium levels were within reference range.

Communicated by: Alberto B. Burlina, MD

The authors "Britt van Erven" and "Lindsey Welling" are equal first authors.

The authors "M. Estela Rubio-Gozalbo" and "Annet M. Bosch" are equal first authors.

Electronic supplementary material: The online version of this chapter (doi:10.1007/8904_2016_28) contains supplementary material, which is available to authorized users.

B. van Erven · M.E. Rubio-Gozalbo (✉)
Department of Pediatrics and Department of Clinical Genetics, Maastricht University Medical Center, PO Box 5800, 6202 Maastricht, The Netherlands
e-mail: estela.rubio@mumc.nl

L. Welling · A.M. Bosch
Department of Pediatrics, Academic Medical Center, Emma Children's Hospital, University of Amsterdam, Amsterdam, The Netherlands

S.C. van Calcar
Department of Molecular and Medical Genetics, School of Medicine, Oregon Health and Science University, Portland, Oregon, USA

A. Doulgeraki
Department of Bone and Mineral Metabolism, Institute of Child Health, Agia Sophia Children's Hospital, Athens, Greece

F. Eyskens
Department of Metabolic Disorders in Children, Antwerp University Hospital UZA, Edegem, Belgium

F. Eyskens
Center of Inherited Metabolic Diseases, Metabolic Lab PCMA, Wilrijk, Belgium

J. Gribben
Nutrition & Dietetics Department, Guy's & St. Thomas' NHS Foundation Trust, London, UK

E.P. Treacy
Mater Misericordiae University Hospital, Trinity College Dublin, Dublin, Ireland

E.P. Treacy
University College Dublin, Dublin, Ireland

R. Vos
Department of Methodology and Statistics, Faculty of Health, Medicine and Life Sciences, Maastricht University, Maastricht, The Netherlands

R. Vos
CAPHRI School for Public Health and Primary Care, Maastricht University Medical Center, Maastricht, The Netherlands

S.E. Waisbren
Division of Genetics and Genomics, Boston Children's Hospital and Harvard Medical School, Boston, MA, USA

Conclusion: The mean BMD Z-score in the CG population is −0.7, which is lower than in the general population, though still within two SD of the reference mean of zero. This indicates that bone health is mildly affected in CG and that more patients, compared to the general population, are at risk for a BMD Z-score ≤−2 SD. In conclusion, clinicians should ensure appropriate preventive and therapeutic measures for CG patients.

Introduction

Classic galactosemia (CG, MIM 230400), a genetic disorder of galactose metabolism due to deficiency of galactose-1-phosphate uridyltransferase (GALT; EC 2.7.7.12), is characterized by the occurrence of late complications in spite of early diagnosis and lifelong dietary treatment. The first report of an association between CG and decreased bone mass dates back to 1993 (Kaufman et al. 1993) and a bone mineral density (BMD) Z-score more than two standard deviations (SD) below the mean was found in 25–30% of adult patients (Waisbren et al. 2012; Batey et al. 2013). Thorough evaluation of the frequency and severity of impaired bone health in CG patients, compared to the non-galactosemia population, is crucial for determining its extent and relevance for patient care.

CG patients could be at risk for compromised bone health due to diet restrictions, ovarian insufficiency in women, limited physical activity in some cases, and possibly unknown intrinsic factors associated with the disease. Sufficient intake of calories, protein, and micronutrients is essential for acquiring an optimal bone mass, and the lifelong galactose restriction may predispose patients to nutritional deficiencies (Wiesmann et al. 1995; Rutherford et al. 2002; El-Bassyouni et al. 2006; Waisbren et al. 2012). Furthermore, ovarian damage resulting in low estrogen concentrations is present in over 80% of female patients with CG (Fridovich-Keil et al. 2011), which increases their susceptibility to the development of low bone mass. Remarkably, supplementation of calcium, vitamins, and estrogen only seems to partially improve bone mass (Kaufman et al. 1993; Renner et al. 1999; Panis et al. 2006), which may point to the presence of an underlying intrinsic bone defect. Aberrant glycosylation of collagen and other glycoproteins related to bone metabolism, which is also seen in patients with other glycosylation defects such as phosphomannomutase 2 deficiency (PMM2-CDG) (Bons et al. 2008), has been suggested as a potential intrinsic abnormality (Kaufman et al. 1993; Coss et al. 2013) and the decreased IGF-I and IGFBP-3 concentrations that are found in patients might reflect this (Panis et al. 2007). Furthermore, reduced physical activity due to motor abnormalities (Rubio-Agusti et al. 2013) and cognitive impairment (Schweitzer et al. 1993; Rasmussen et al. 1996; Shield et al. 2000; Hoffmann et al. 2011) may affect bone health as well. Clinical practice, focused on reducing the risk of impaired bone health in those with CG, includes routine monitoring of BMD, which is an important determinant of bone strength and has predictive value in assessing fracture risk (Marchall et al. 1996), and optimization of exogenous factors affecting bone mass (nutrition, estrogen concentrations, physical activity) (Van Erven et al. 2014).

The primary aim of our study is to evaluate the extent of impaired bone health in patients with CG, and the need of monitoring and treatment. Few studies assessing bone health in CG are published. These studies have small patient sample sizes, and results vary from one study to another. As the current conjecture of low BMD in CG is based on single studies, further evaluation is needed to confirm the validity of this hypothesis (Haidich 2010). Meta-analysis is the most commonly used statistical technique to pool results from two or more separate studies. The added value of a meta-analysis may include increased power and improved precision of the results. Therefore, we performed a systematic review with meta-analysis of BMD in children and adults with CG. As recommended by the International Society for Clinical Densitometry (ISCD), low BMD is defined here as a BMD Z-score ≤−2.0 SD (Schousboe et al. 2013; Gordon et al. 2014). We also explored the usefulness of other indicators of bone status as potential diagnostic or monitoring tools.

Methods

Research Question

The primary outcome for our meta-analysis was bone mass reported as BMD (areal BMD), either as Z-score or as absolute measurement, assessed with dual-energy X-ray absorptiometry (DXA) since this is the preferred tool for evaluating BMD/bone mass in both children and adults (Schousboe et al. 2013; Gordon et al. 2014). BMD is a major determinant of bone strength and its assessment is considered the cornerstone in the diagnostics of low bone mass (Kanis et al. 2013). Only areal BMD measurements were included in the analysis since these are most commonly used in clinical practice; results of estimated volumetric BMD were not included.

The secondary outcomes for our systematic review, reported in a descriptive way, were bone mineral content (BMC), and parameters involved in bone metabolism such

as vitamins, minerals, hormones, bone turnover markers (BTM), and fracture risk.

Inclusion and Exclusion Criteria for Study Selection

We included all original studies (cross-sectional study design, randomized controlled trial [RCT], cohort study, case-control study) as well as conference abstracts on bone health in children and adults with CG. If there was (potential) overlap between study cohorts, only the first/original article was included. Articles in a language other than English, and animal and cell studies were excluded.

Search Strategy

A computerized literature search was conducted in MEDLINE, EMBASE, and the Cochrane Library by one of the investigators (LW) and a trained clinical librarian from University of Amsterdam (see Supplementary data S1, Search strategies). Databases were searched initially in February 2015 and a final search was completed in July 2015 to ensure the inclusion of recently published articles. No limits were used in these searches.

Study Selection

Titles and abstracts generated by literature searches were screened by two separate researchers (BvE and LW) to select potentially eligible studies. Studies not relating to the research question were excluded. Selected conference abstracts and full text articles of selected studies were independently reviewed by two authors (BvE and LW) for inclusion in the systematic review. In case of exclusion, the reason was reported. Additionally, reference lists from included trials and excluded narrative or systematic reviews were hand-searched to identify additional relevant studies. Consensus was reached between the two authors regarding the eligibility assessments.

Data Extraction

Data were extracted by two separate researchers (BvE and LW) according to predefined criteria (see Supplementary data S2a and S2b, Summary of evidence tables). Outcome measures of interest were BMD at any site measured with DXA; BMC; incidence of fractures; BTM reflecting bone formation (bone-specific alkaline phosphatase, under-carboxylated osteocalcin [ucOC], carboxylated osteocalcin [cOC]), bone resorption (N-terminal telopeptide, C-terminal telopeptide) or bone modeling (insulin-like growth factor-1 [IGF-1]); and vitamins (vitamin D), minerals (calcium), and hormones (estradiol, parathormone) important for bone metabolism.

Data Collection Processes

If a mean BMD Z-score and/or standard deviation (SD) was not reported for the entire cohort in an article, the authors were requested to share either these variables together with mean age at testing and SD or individual patient data (IPD). IPD included individual mean BMD Z-score with SD, age at testing, and gender. The corresponding author was contacted first, and if there was no reply within 4 weeks, one of the other authors was contacted.

Individual Patient Data Integrity

IPD were checked for integrity by reviewing completeness; in case of incompleteness the data were not included in the systematic review. If more data were received from the authors than originally published, these were only included if patient characteristics matched those from the original article. In case of any discrepancies, the authors were contacted.

Assessment of Quality and Risk of Bias in Individual Studies

Quality appraisal and assessment of bias were performed with an appropriate checklist from the "Scottish Intercollegiate Guidelines Network" (SIGN), if available (available for RCT, non-RCT, cohort study, case-control study). Quality appraisal and risk of bias analysis were performed and discussed by two independent investigators (BvE and LW). Articles were appraised as low, acceptable, or high quality; those assessed as low quality were excluded from the review.

Data Analysis

We performed a meta-analysis of BMD to evaluate whether the mean BMD Z-score in the CG population differs from normative data (a mean BMD Z-score of zero in the general population). We used Review Manager 5.3 version 5.3.5 for the analysis. The inverse-variance method was used to pool study data, and the individual effect sizes were weighted according to the reciprocal of their variance (Deeks et al. 2010). I^2 was used as a measure of heterogeneity (The Cochrane Collaboration 2011). The p-value used to reject the null hypothesis of homogeneity was 0.1 (p-value of Q; Q = chi squared statistic). In case of low heterogeneity (0–30%) a fixed effects model was used to pool data. In case of moderate-to-high heterogeneity (30–100%), both fixed and random effects models were applied, resulting in a sensitivity analysis with description of differences between the fixed and random effects models and selection of the most appropriate model. Aggregate data and IPD were analyzed together using a two-stage approach: for

IPD, a mean BMD Z-score and SD were calculated first, and were then included in the next step as aggregate data. BMD Z-scores were pooled based on the measurement site (lumbar spine, total hip, femoral neck, and total body). For the overall effect size, a p-value of 0.05 was considered statistically significant. Yet, in case of multiple testing, adjustment for Bonferroni correction was applied.

In order to assess clinical relevance of the mean BMD Z-score of the CG population, the normal distribution was used to find the percentiles of Z-scores, and thus the estimated proportion of patients with a BMD Z-score ≤ -2 SD (low bone mass) using SPSS version 23. For this, two approaches were used, one with the SD of normative data (mean of zero, SD 1), another with the SD of the mean calculated in our meta-analysis.

The secondary outcome measures (BMC, minerals, vitamins, hormones, and BTM) were presented in a descriptive manner.

Results

Study Selection

The literature search identified 138 potential publications of which 94 remained after removing duplicates ($n = 44$). After screening the titles and abstracts of the unique publications, 71 were excluded because they did not relate to the research question. Detailed evaluation of the 23 selected publications led to the exclusion of 10 studies for various reasons (see Fig. 1: Flow diagram selection process).

For the meta-analysis, eight studies were selected because they encompassed BMD measurements. Only one of these studies reported all data required for inclusion (Panis et al. 2004); the authors of the other seven studies were contacted for additional information. Three authors provided the required data at request (Waisbren et al. 2012; Tan et al. 2014; Doulgeraki et al. 2014) (Supplementary data S3, Data collection process). Accordingly, a total of four articles were included in our meta-analysis on BMD.

A total of seven studies reported on our secondary outcome measures and were therefore included in the descriptive analysis.

The complete study selection process is presented as a flow diagram, separately for the meta-analysis and the descriptive analysis (Fig. 1a, b).

Included Studies

Characteristics of the studies included in the meta-analysis or descriptive analysis are presented in Supplementary data

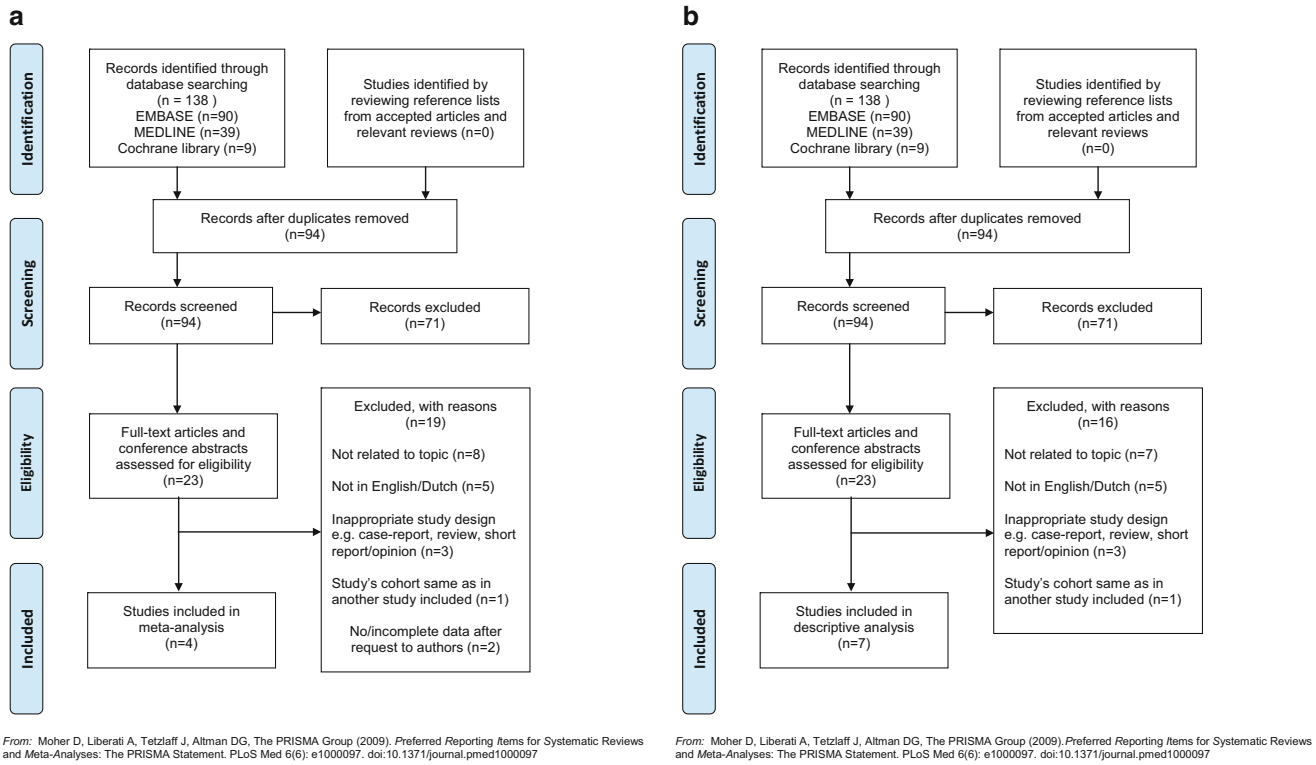

Fig. 1 (**a**) Flow diagram selection process meta-analysis; (**b**) flow diagram selection process descriptive analysis

S2a and S2b, Summary of evidence tables. Age of the patients in the included studies ranged from 2.5 to 59 years.

Individual Patient Data Integrity

No issues with IPD integrity were detected.

Assessment of Quality and Risk of Bias in Individual Studies

A quality appraisal with the standardized checklist was applicable for only one study, a randomized controlled trial (Panis et al. 2006). The paper was graded high quality as defined by the risk of bias checklist for randomized controlled trial of SIGN.

Meta-Analysis on BMD in Classic Galactosemia Patients

Four studies (three cross-sectional studies and one retrospective case series) were included in this meta-analysis of BMD Z-score (Panis et al. 2004; Waisbren et al. 2012; Tan et al. 2014; Doulgeraki et al. 2014). Panis et al. (2004) assessed 40 patients with a mean age of 8.9 years (range 3.0–17.3). Waisbren et al. (2012) evaluated BMD in 33 patients with a mean age of 32.6 years (range 18–59). Doulgeraki et al. (2014) reported BMD Z-scores of 14 patients with a mean age of 13.16 years (range 6.17–16.58 years). Tan et al. (2014) provided the individual patient data reported in their conference abstract as well as additional new data ($n = 5$). The mean age in these 25 patients was 13.5 years (range 5–41 years). Mean BMD Z-scores were calculated and are presented in Supplementary Data S2a.

Complete Cohort (Children and Adults)

A total of 112 CG patients assessed in four studies were included in this part of the meta-analysis. At the site of the lumbar spine, a mean BMD Z-score of −0.70 (95% CI: −0.88, −0.52) was found (Panis et al. 2004; Waisbren et al. 2012; Tan et al. 2014; Doulgeraki et al. 2014). Heterogeneity was zero ($I^2 = 0\%$); a fixed effects model was used. The overall effect was statistically significant ($p < 0.00001$) when compared to the mean of normative data (BMD Z-score of zero). One of the studies crossed the line of no effect (Fig. 2).

In 58 pooled patients included in two studies, mean total hip BMD Z-score was −0.89 (95% CI: −1.14, −0.64) (Waisbren et al. 2012; Tan et al. 2014). Heterogeneity was zero ($I^2 = 0\%$); a fixed effects model was used. The overall effect was significantly different from the mean of normative data ($p < 0.00001$) and none of the studies crossed the line of no effect (Fig. 3).

At the site of the femoral neck, 73 CG patients from 2 studies were pooled (Panis et al. 2004; Waisbren et al. 2012). The heterogeneity was high ($I^2 = 91\%$), leading to determination of the mean BMD Z-score with both fixed and random effects models (Figs. 4 and 5, respectively). A mean BMD Z-score of −0.63 was found with both models, with a difference in 95% confidence interval (95% CI fixed effects model: −0.83, 0.44; 95% CI random effects model: −1.29, 0.02). As heterogeneity was very high and both studies are of adequate quality with comparable cohort sizes, it was chosen to base conclusions on the results of the random effects model. Even though both studies did not cross the line of no effect, the overall effect was not significantly different from the mean of normative data when using the random effects model ($p = 0.06$) (Fig. 5).

Children with CG

In pooled data from 76 children from three studies, mean lumbar spine BMD Z-score was −0.64 (95% CI: −0.84, −0.43) (Panis et al. 2004; Tan et al. 2014; Doulgeraki et al. 2014). Heterogeneity was zero ($I^2 = 0\%$); a fixed effects model was used. This was overall significantly different from the mean of normative data ($p < 0.00001$). One study crossed the line of no effect (same study as in lumbar spine BMD Z-score analysis of the entire patient group) (Fig. 6).

Adults with CG

In pooled data from 36 adults with CG included in two studies, mean lumbar spine BMD Z-score was −0.94 (95% CI: −1.30, −0.57) (Waisbren et al. 2012; Tan et al. 2014). Heterogeneity was zero ($I^2 = 0\%$); a fixed effects model

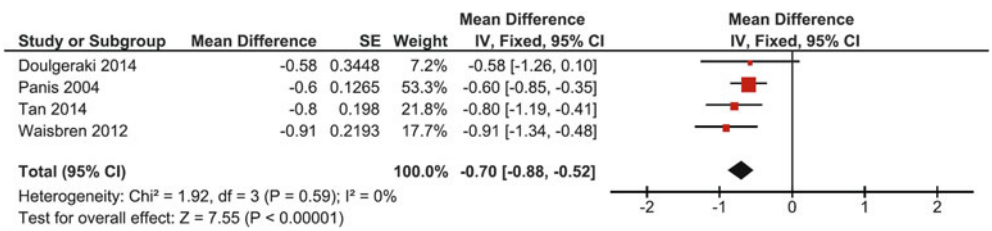

Fig. 2 Forest plot of lumbar spine BMD Z-score in complete CG cohort

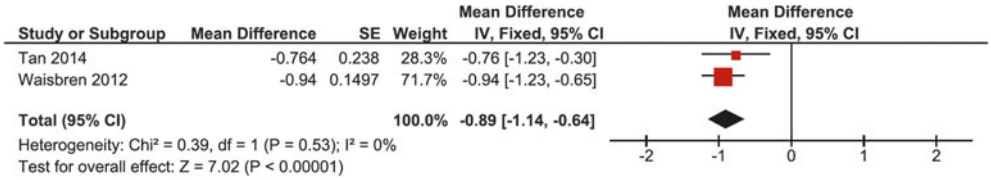

Fig. 3 Forest plot of total hip BMD Z-score of the complete CG cohort

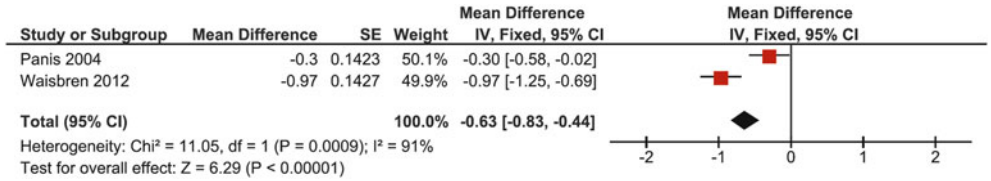

Fig. 4 Forest plot of femoral neck BMD Z-score in complete CG cohort (fixed effects model)

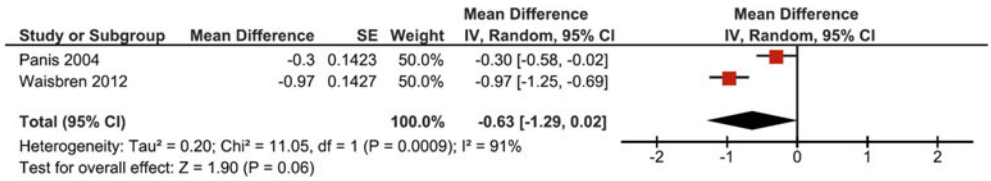

Fig. 5 Forest plot of femoral neck BMD Z-score in complete CG cohort (random effects model)

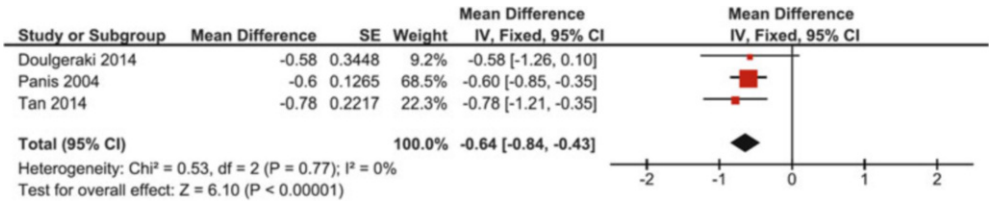

Fig. 6 Forest plot of lumbar spine BMD Z-score in children with CG

was used. The overall effect was statistically significant from the mean of normative data ($p < 0.00001$), and none of the studies crossed the line of no effect (Fig. 7).

Mean BMD Z-score at the total hip in this group of adults was −0.91 (95% CI: −1.20, −0.63) (Waisbren et al. 2012; Tan et al. 2014). Heterogeneity was zero ($I^2 = 0\%$); a fixed effects model was used. One study crossed the no-effect line, but the overall effect was significantly different from the mean of normative data ($p < 0.00001$) (Fig. 8).

We could not perform a subgroup analysis on BMD Z-scores for adult males and adult females separately since one study included data on only one or two patients.

Clinical Relevance

The normal distribution was used to find the percentiles of Z-scores, and thus the estimated proportion of patients with a BMD Z-score ≤−2 SD (low bone mass). Two approaches were used: one with an SD of 1.9 (resulting from the 95% CI of the calculated mean lumbar spine BMD Z-score of −0.7 in the complete CG group) and another with an SD of 1.0 (according to the normal distribution curve of BMD in the general population). Accordingly, 10–25% of CG patients are estimated to be at risk for a BMD Z-score ≤−2 SD, and thus a low bone mass, whereas this is only 2.3% in the general population (normally distributed parameter).

Descriptive Analysis

Bone Mineral Content

Another indicator of bone health is BMC, which reflects other aspects of bone mass acquirement than BMD and might therefore be of additional value in children (Mølgaard et al. 1997). BMC of femoral neck, lumbar

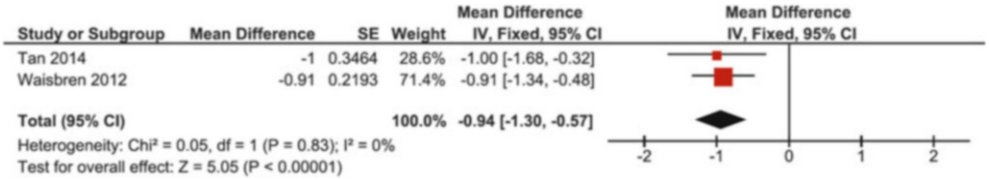

Fig. 7 Forest plot of lumbar spine BMD Z-score in adults with CG

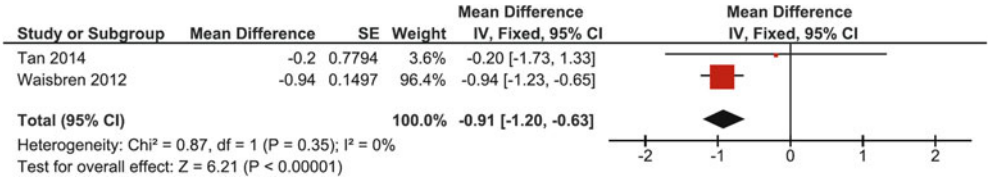

Fig. 8 Forest plot of total hip BMD Z-score in adults with CG

spine, and total body was assessed in a single study by Panis et al. (2006) (40 patients, age range 3–17 years) (Panis et al. 2006). In this randomized controlled trial, in which the effect of supplementation of calcium, vitamin K1, and vitamin D3 on bone health was studied, baseline measurements of BMC Z-scores in 40 children with CG (age 3–17 years) were conducted. Mean BMC Z-scores (varying between −0.3 and −1.1 for different subgroups) were lower than in controls.

Vitamins, Minerals, and Hormones

Six studies evaluated vitamin D status in CG patients (n = 197) (Rubio-Gozalbo et al. 2002; Panis et al. 2004; Gajewska et al. 2006; Gajewska et al. 2008; Sirrs et al. 2010; Waisbren et al. 2012). One study assessed 1,25-OH-D concentrations only (Panis et al. 2004), four measured 25-OH-D only, and one evaluated both (Rubio-Gozalbo et al. 2002). The studies varied with regard to vitamin D reference ranges and units, and in some the specified range of desired vitamin D concentrations was not stated. Two studies in adults with CG reported that most patients had levels in the low reference range (Sirrs et al. 2010; Waisbren et al. 2012). Compliance to vitamin D supplements differed between the two cohorts. The remaining four studies, performed in children with CG, found vitamin D levels to be within reference range.

Four studies with a total of 148 patients assessed serum calcium levels (Rubio-Gozalbo et al. 2002; Panis et al. 2004; Gajewska et al. 2006; Gajewska et al. 2008). In all studies calcium levels were found to be within reference range. Rubio-Gozalbo et al. (2002) found no correlation between BMD results and calcium intake in their cohort of children with CG (Rubio-Gozalbo et al. 2002).

Parathormone was also measured in the studies by Rubio-Gozalbo et al. (2002) and Panis et al. (2004) and revealed values within reference range. Only one study measured 17-beta-estradiol levels in a cohort of 40 children aged 3–17.3 years (mean age 8.9 years) (Panis et al. 2004). Mean levels did not differ from reference values.

Bone Turnover Markers

Four cross-sectional studies examined BTM in CG patients (Rubio-Gozalbo et al. 2002; Panis et al. 2004; Gajewska et al. 2006; Gajewska et al. 2008): three studies included children only (<18 years) and one study included patients up to 20 years. A total of 148 patients were included in these studies (range 11–62 patients/study). There were no studies reporting on markers of bone status in adult patients.

Carboxy-terminal telopeptide of type 1 collagen, measured in all four studies, was found to be significantly reduced in children but not in adolescents when compared to controls. Panis et al. (2004) found it to be inversely correlated with BMD Z-score of the femoral neck and lumbar spine (Panis et al. 2004). Amino-terminal telopeptide of type I collagen levels were measured in two study cohorts and levels were found to be significantly low in both cohorts of CG children (Rubio-Gozalbo et al. 2002; Panis et al. 2004). Gajewska et al. (2008) reported about 30% higher values of bone-specific alkaline phosphatase in adolescents than in controls (Gajewska et al. 2008), whereas normal values were found in children. In addition, Gajewska et al. found increased osteocalcin (OC; sum of carboxylated [cOC] and under-carboxylated osteocalcin [ucOC]) levels in adolescents with CG (Gajewska et al. 2008), whereas Panis et al. (2004) reported significantly decreased cOC levels with normal ucOC levels in children (Panis et al. 2004). Normal values of OC (Gajewska et al. 2006; Gajewska et al. 2008) and cOC and ucOC (Rubio-Gozalbo et al. 2002) in children were reported in three

studies. Furthermore, Panis et al. (2004), the only study measuring IGF-1 levels, reported reduced IGF-1 Z-scores in children (Panis et al. 2004) and found that IGF-1 Z-score was a strong positive predictor of femoral neck and lumbar spine BMD.

Fracture History

Waisbren et al. (2012) reported that 45% of 33 patients (mean age 32.6 years, range 18–59) had broken a bone, 6 during childhood and the others at ages 20–46 years (Waisbren et al. 2012).

Discussion

In this systematic review we evaluated bone mass in patients with CG through a meta-analysis of BMD. The results of our meta-analysis indicate that mean bone mass in the CG population, reflected by mean BMD Z-score, is more than a half-standard deviation lower than in the general population. While this is still within two SD of the normative mean, this result indicates that an increased proportion of individuals with CG will have a BMD Z-score ≤ -2 SD, and thus a low bone mass for age, as compared to individuals in the general population. Based on the meta-analysis, estimated prevalence of BMD Z-score ≤ -2 SD in patients with CG is 10–25%, which is higher than in the general population (2.3%). Mean BMD Z-scores in pooled data of adults and children with CG were reduced at all sites (lumbar spine −0.70, total hip −0.89, femoral neck −0.63), of which only the latter was not statistically significant, probably due to heterogeneity between included study cohorts. Findings from our descriptive analysis support the need for improved evaluation and optimization of vitamin D concentrations. Though serum calcium levels were within reference range in all studies that addressed calcium status, ensuring sufficient intake of calcium remains a point of attention in this population. Data on the role of BMC and BTM as other indicators of bone status are very limited and, in the case of BTM, highly ambiguous. Therefore, routine screening of these indicators in CG patients does not seem of additional value at present. Literature on bone mass in CG is scarce and study cohorts are small as a result of the rarity of the disease. This limits the number of studies and patients included in our meta-analysis, which hampers extensive subgroup analyses and solid conclusions. However, this systematic review is currently the most comprehensive study evaluating bone health in CG patients, thereby providing results that are more representative for the whole population of CG patients.

This study was limited in that not all original patient data could be obtained. In addition, data used in this study were all cross-sectional, and conclusions about progression over time must therefore be interpreted with caution. Longitudinal studies following patients in time are needed to enable firm conclusions on this. Moreover, ISCD recommendations for pediatric DXA (Crabtree et al. 2014) were not unanimously followed by the researchers, as they used different sites of measurement and did not take into account the presence of short stature or growth delay, with the exception of only one study (Doulgeraki et al. 2014). Furthermore, data on fracture history were obtained in only one study (Waisbren et al. 2012), though this is required to establish a diagnosis of osteoporosis. Future studies should consider the ISCD recommendations to further improve insights into bone health in CG.

Conclusions

BMD Z-scores in individual CG patients are within two SD of the normative mean in the majority of patients with CG. However, results from our meta-analysis demonstrate that the mean BMD Z-score in the CG population is lower than the mean BMD Z-score in the general population. These results suggest that bone health in general is mildly affected, and that an estimated proportion of 10–25% of patients with CG could be at risk for a low bone mass (BMD Z-score ≤ -2) as compared to the general population. With the currently available literature, which lacks data on fracture prevalence, it is impossible to draw conclusions about osteoporosis risk. Vitamin D levels are low in many patients, emphasizing the need for monitoring of 25(OH) D levels and vitamin D supplementation. Optimization of calcium intake remains important. Evaluation of the importance of other parameters of bone health (BCM, BTM, hormones) was inconclusive due to a limited number of studies with inconsistent results. Concluding, it is important that treating physicians are aware that patients with CG are at risk for having or developing low bone mass, so that patients will be screened and treated appropriately.

Acknowledgements The authors would like to thank the clinical librarian A.G.E. Leenders (Academic Medical Center, Amsterdam, the Netherlands) for developing the search strategies for this review, as well as Dr. M.J. van Kroonenburgh (Maastricht University Medical Center, Department of Nuclear Medicine) for answering queries on the technical aspects of bone mass evaluation.

Take-Home Message

It is important that treating physicians are aware that patients with CG are at risk for having or developing low bone mass, warranting appropriate screening and treatment.

Contributions of Individual Authors

Britt van Erven: conception and design, acquisition of data, analysis and interpretation of data, drafting the chapter, revising the chapter critically for important intellectual content.

Lindsey Welling: conception and design, acquisition of data, analysis and interpretation of data, drafting the chapter, revising the chapter critically for important intellectual content.

Sandra C. van Calcar: analysis and interpretation of data, revising the chapter critically for important intellectual content.

Artemis Doulgeraki: acquisition of data, revising the chapter critically for important intellectual content.

François Eyskens: analysis and interpretation of data, revising the chapter critically for important intellectual content.

Joanna Gribben: acquisition of data, revising the chapter critically for important intellectual content.

Eileen P. Treacy: acquisition of data, revising the chapter critically for important intellectual content.

Rein Vos: statistical design, revising the chapter critically for important intellectual content.

Susan E. Waisbren: acquisition of data, revising the chapter critically for important intellectual content.

M. Estela Rubio-Gozalbo: conception and design, analysis and interpretation of data, drafting the chapter, revising the chapter critically for important intellectual content.

Annet M. Bosch: conception and design, analysis and interpretation of data, drafting the chapter, revising the chapter critically for important intellectual content.

All authors read and approved the manuscript before submission.

Guarantor

M. Estela Rubio-Gozalbo.

Conflict of Interest Statement

Annet M. Bosch is in receipt of research grants from Nutricia and was a member of an advisory board for Nutricia.

Sandra C. van Calcar declares that she has no conflict of interest.

Artemis Doulgeraki declares that she has no conflict of interest.

Britt van Erven declares that she has no conflict of interest.

François Eyskens declares that he has no conflict of interest.

Joanna Gribben declares that she has no conflict of interest.

M. Estela Rubio-Gozalbo declares that she has no conflict of interest.

Eileen P. Treacy declares that she has no conflict of interest.

Rein Vos declares that he has no conflict of interest.

Susan E. Waisbren declares that she has no conflict of interest.

Lindsey Welling declares that she has no conflict of interest.

Details of Funding

No financial support from sponsors was received for the conduct of this research.

Ethics Approval

Not required. This chapter does not contain any interventional studies with human or animal subjects performed by any of the authors.

References

Batey LA, Welt CK, Rohr F et al (2013) Skeletal health in adult patients with classic galactosemia. Osteoporos Int 24:501–509

Bons JA, Michielsen EC, de Boer D et al (2008) A specific immunoprecipitation method for isolating isoforms of insulin-like growth factor binding protein-3 from serum. Clin Chim Acta 387:59–65

Coss KP, Doran PP, Owoeye C et al (2013) Classical Galactosaemia in Ireland: incidence, complications and outcomes of treatment. J Inherit Metab Dis 36:21–27. doi:10.1007/s10545-012-9507-9

Crabtree NJ, Arabi A, Bachrach LK et al (2014) Dual-energy X-ray absorptiometry interpretation and reporting in children and adolescents: the revised 2013 ISCD Pediatric Official Positions. J Clin Densitom 17:225–242. doi:10.1016/j.jocd.2014.01.003

Deeks JJ, Higgins JPT, on behalf of the Statistical Methods Group of The Cochrane Collaboration (2010) Statistical algorithms in Review Manager:5 Retrieved from: http://ims.cochrane.org/revman/documentation/Statistical-methods-in-RevMan-5.pdf. Accessed 24 Oct 2016

Doulgeraki A, Monopolis I, Deligianni D et al (2014) Body composition in young patients with galactose metabolic disorders: a preliminary report. J Pediatr Endocrinol Metab 27:81–86. doi:10.1515/jpem-2013-0161

El-Bassyouni HT, Ashour AM, Ezzat A et al (2006) The effect of diet on antioxidant status in patients with galactosemia. J Med Sci 6:452–457

Fridovich-Keil JL, Gubbels CS, Spencer JB et al (2011) Ovarian function in girls and women with GALT-deficiency galactosemia. J Inherit Metab Dis 34:357–366. doi:10.1007/s10545-010-9221-4

Gajewska J, Ambroszkiewicz J, Radomyska B et al (2008) Serum markers of bone turnover in children and adolescents with classic galactosemia. Adv Med Sci 53:214–220. doi:10.2478/v10039-008-0026-8

Gajewska J, Ambroszkiewicz J, Radomyska B, Laskowska-Klita T (2006) Bone turnover markers in prepubertal children with classical galactosemia. Indian J Gastroenterol 25:221–222

Gordon C, Leonard MB, Zemel BS, International Society for Clinical Densitometry (2014) 2013 Pediatric Position Development Conference: executive summary and reflections. J Clin Densitom 17:219–224

Haidich AB (2010) Meta-analysis in medical research. Hippokratia 14:29–37. doi:10.5005/jp/books/10519

Hoffmann B, Wendel U, Schweitzer-Krantz S (2011) Cross-sectional analysis of speech and cognitive performance in 32 patients with classic galactosemia. J Inherit Metab Dis 34:421–427. doi:10.1007/s10545-011-9297-5

Kanis JA, McCloskey EV, Johansson H et al (2013) European guidance for the diagnosis and management of osteoporosis in postmenopausal women. Osteoporos Int 24:23–57. doi:10.1007/s00198-012-2074-y

Kaufman FR, Loro ML, Azen C et al (1993) Effect of hypogonadism and deficient calcium intake on bone density in patients with galactosemia. J Pediatr 123:365–370

Marchall D, Johnell O, Wedel H (1996) Meta-analysis of how well measures of bone mineral density predict occurrence of osteoporotic fractures. BMJ 18:1254–1259

Mølgaard C, Thomsen BL, Prentice A et al (1997) Whole body bone mineral content in healthy children and adolescents. Arch Dis Child 76:9–15. doi:10.1136/adc.78.4.395b

Panis B, Forget PP, Van Kroonenburgh MJPG et al (2004) Bone metabolism in galactosemia. Bone 35:982–987

Panis B, Gerver W-JM, Rubio-Gozalbo ME (2007) Growth in treated classical galactosemia patients. Eur J Pediatr 166:443–446. doi:10.1007/s00431-006-0255-4

Panis B, Vermeer C, van Kroonenburgh MJPG et al (2006) Effect of calcium, vitamins K1 and D3 on bone in galactosemia. Bone 39:1123–1129. doi:10.1016/j.bone.2006.05.002

Rasmussen RK, Andreassen AB, Stromme P, Hansen TW (1996) Learning disabilities and language pathology in patients with galactosemia. Logoped Phoniatr Vocol 21:157–162. doi:10.3109/14015439609098884

Renner C, Razeghi S, Uberall MA et al (1999) Hormone replacement therapy in galactosaemic twins with ovarian failure and severe osteoporosis. J Inherit Metab Dis 22:194–195

Rubio-Agusti I, Carecchio M, Bhatia KP et al (2013) Movement disorders in adult patients with classical galactosemia. Mov Disord 28:804–810. doi:10.1002/mds.25348

Rubio-Gozalbo ME, Hamming S, van Kroonenburgh MJ et al (2002) Bone mineral density in patients with classic galactosaemia. Arch Dis Child 87:57–60

Rutherford PJ, Davidson DC, Matthai SM (2002) Dietary calcium in galactosaemia. J Hum Nutr Diet 15:39–42

Schousboe J, Shepherd JA, Bilezikian JP, Baim S (2013) Executive summary of the 2013 International Society for Clinical Densitometry Position Development Conference on bone densitometry. J Clin Densitom 16:455–466

Schweitzer S, Shin Y, Jakobs C, Brodehl J (1993) Long-term outcome in 134 patients with galactosaemia. Eur J Pediatr 152:36–43

Shield JP, Wadsworth EJ, MacDonald A et al (2000) The relationship of genotype to cognitive outcome in galactosaemia. Arch Dis Child 83:248–250

Sirrs S, Bosdet T, Branov J, et al. (2010) High prevalence of vitamin D insufficiency in galactosemic adults despite compliance with supplementation. J Inherit Metab Dis 33:S64

Tan C, Stonestreet K, Winstone R, et al. (2014) Management and long-term outcomes of classical galactosaemia-a single centre experience in the UK. Conf Annu Symp Soc Study Inborn Errors Metab SSIEM 2014 Innsbruck Austria Conf Start 20140902 Conf End 20140905 Conf Publ (var.pagings) 37(Suppl 1):S57

The Cochrane Collaboration (2011) Cochrane Handbook for Systematic Reviews of Interventions Version 5.1.0 [updated March 2011]

Van Erven B, Römers MM, Rubio-Gozalbo ME (2014) Revised proposal for the prevention of low bone mass in patients with classic galactosemia. JIMD Rep 17:41–46. doi:10.1007/8904_2014_331.Epub

Waisbren SE, Potter NL, Gordon CM et al (2012) The adult galactosemic phenotype. J Inherit Metab Dis 35:279–286. doi:10.1007/s10545-011-9372-y

Wiesmann UN, Rosé-Beutler B, Schlüchter R (1995) Leguminosae in the diet: the raffinose-stachyose question. Eur J Pediatr 154:93–96. doi:10.1007/BF02143812

JIMD Reports
DOI 10.1007/8904_2016_31

CASE REPORT

Cognitive Development in a Young Child with Mucolipidosis Type IV: A Case Report

Evelyn L. Fisher · Rose A. Sevcik · MaryAnn Romski

Received: 18 August 2016 / Revised: 11 November 2016 / Accepted: 28 November 2016 / Published online: 03 January 2017

Abstract Mucolipidosis Type IV (ML IV) is an autosomal recessive genetic disorder characterized by severe psychomotor impairments and ophthalmologic abnormalities. Reports on the cognitive development of people with ML IV are limited, but suggest that achievement of language and cognitive milestones varies between a 3- and 18-month level. There is also variability in reports of whether people with ML IV make developmental progress, regress, or remain static after infancy. This study examines the longitudinal development of a young child with ML IV who participated in an augmentative and alternative communication (AAC) intervention.

At 26 months, the child displayed significant developmental delays on direct assessment, with the exception of a possible relative strength in receptive language. An examination of adaptive behavior over time indicated improvements in raw scores but declines in standard scores across all domains. She learned to use 13 new words with a speech generating device (SGD) by the end of intervention.

These results add to literature on the clinical manifestations of ML IV and indicate that although children with this disorder have deficits in many domains, they may be most severely affected in gross motor or oral motor development and have a relative strength in receptive language. Moreover, this child made progress in all domains of adaptive functioning, but at a slower pace than typically developing children. She also gained expressive vocabulary in the AAC intervention, and this may have supported her development in other areas.

Communicated by: Maurizio Scarpa, M.D, Ph.D

E.L. Fisher (✉)
Psychology Department, Georgia State University, PO Box 5010, Atlanta, GA 30302, USA
e-mail: Efisher7@student.gsu.edu

R.A. Sevcik · MA. Romski
Georgia State University, PO Box 5010, Atlanta, GA 30302, USA

Introduction

Background

Mucolipidosis Type IV (ML IV) is a lysosomal storage disorder characterized by severe psychomotor impairments and ophthalmologic abnormalities (Amir et al. 1987). It was first described in 1974 by Berman and colleagues (Berman et al. 1974). ML IV affects approximately 1 in 40,000 Ashkenazi Jewish births and is very rare in other populations. The disorder is caused by a mutation in the MCOLN1 gene, which codes for the cation channel protein mucolipin 1(Wakabayashi et al. 2011). The exact mechanism by which the mutation results in the clinical presentation of MLIV is not fully understood, but the disruption in normal cell function due to an absence of mucolipin 1 is believed to cause damage and dysfunction in many systems of the body. As such, a variety of medical comorbidities are characteristic of ML IV. Common digestive complications observed in people with ML IV are achlorhydria and anemia (Geer et al. 2010). Ophthalmologic abnormalities often include corneal opacity and retinal degeneration. Vision in people with MLIV is thought to be close to normal early in life, but impairments are typically severe by the teenage years (Geer et al. 2010). Delayed motor development is often the first cause for concern among parents of children with ML IV. Muscular abnormalities initially present as hypotonia, and often gradually transform into spasticity. The majority of people with ML IV are not able to walk independently (Mucolipidosis type IV 2015). Neuroanatomical studies reveal that people with ML IV

exhibit decreased white matter volume, especially in the cerebellum (Schiffmann et al. 2014).

Reports on the neurodevelopment of people with ML IV are limited in number, and consist predominantly of case studies, as well as a few studies of larger samples. They suggest that motor milestones achieved are usually between a 12- and 15-month level, whereas cognitive milestones achieved may vary between a 3- and 18-month level (Amir et al. 1987). Results of assessments of people with ML IV must be interpreted with great caution, however, due to the difficulty in making valid inferences about cognition from tasks that may be inaccessible to people with severe motor impairments (Martin et al. 2008). There is also variability in reports of whether people with ML IV make developmental progress, regress, or remain static after infancy (Amir et al. 1987; Schiffmann et al. 2014).

The prognosis for speech development is generally poor. Although a few more mildly affected individuals have been identified in the literature, most people with ML IV do not develop speech beyond a few single words, and many have no intelligible speech at all (Amir et al. 1987). Despite severe impairments in speech production, several studies have indicated a relative strength in receptive language, and a few people with ML IV have demonstrated success in learning to use up to 50 sign language words to communicate (Schiffmann et al. 1993). Together, these findings strongly suggest that augmentative and alternative communication, or AAC, is the ideal approach for meeting the communication needs of people with ML IV and supporting quality of life and inclusion for those affected by the disorder. Research suggests that people with severe intellectual disability and/or sensorimotor impairments can successfully learn to communicate using AAC (Romski and Sevcik 2005). AAC modalities include unaided symbols, such as sign language and gesture, as well as aided communication supported by external symbols, such a pictures on a speech generating device (SGD).

The purpose of this case study was to describe the development of a young child with ML IV who participated in a longitudinal parent-coached augmented language intervention study. This case study adds to the literature on clinical manifestations and course of ML IV and provides information on one child's outcome following a specific early intervention technique for addressing the characteristic neurodevelopmental deficits associated with the disorder. We examined her initial developmental profile, change in skills over time, and effect of AAC on her communication skills.

Case Report

Methods

Participant

The child was a Caucasian female. Parents first observed delayed motor development when she was 4 months of age. She was subsequently diagnosed with ML IV after a neurological evaluation and genetic testing. She was referred to the study by the state public early intervention program for infants and toddlers with developmental disabilities and began study participation at 26 months of age. Although the intervention was intended to supplement the clinical services that children received outside of the study, this child did not receive any additional speech-language therapy until after the post-intervention time point. At this point, she began receiving 90 min of speech-language therapy per week in a public co-taught preschool setting. Her hearing and vision were tested prior to study participation. Her hearing acuity was within normal limits and her visual acuity was possibly slightly impaired. In terms of motor skills, she was unable to walk or crawl throughout the duration of the study, and used a stroller for mobility. However, she had sufficient control of upper extremities to independently reach for and press large buttons on an SGD. The child's mother also participated in the study as the primary reporter for most measures and a communication partner. At the time of the study, she had completed a master's degree in special education and was a homemaker. English was the primary language spoken at home, and Hebrew was a secondary language. The household included the child's mother, father, and one brother (age 4 years).

Procedure

The mother–child dyad participated in a randomized controlled trial of parent-coached augmented language interventions for young children with significant developmental delays (Romski et al. 2016). The mother–child dyad was randomly assigned a waitlist period, followed by the Augmented-Input and Output Hybrid (AC-IO) condition. In this condition, children were encouraged to use an SGD to communicate using both adult modeling and prompting. The child received the Tech Talk by Advanced Multi-Media Devices Incorporated (AMDI) as the SGD. The intervention protocol included 24 sessions implemented over

Table 1 Measures administered to the participant

	Time Point	Age	MSEL	VABS	SICD	CDI	CALC	PPVT
T1	Three months pre-intervention	26	×	×	×	×	×	
T2	At start of intervention	29	×	×	×	×	×	
T3	Post-intervention	37			×	×	×	
T4	Three months post-intervention	41			×	[a]	×	
T5	Six months post-intervention	45			×	[a]	×	
T6	Twelve months post-intervention	50		×	×	×	×	×

[a] Measure was administered, but not returned by parent

20 weeks. Each session lasted 30 min, and consisted of three 10 min activities: play, book, and snack. The first 18 intervention sessions were conducted in the Toddler Language Intervention Project Lab at Georgia State University. The final six sessions were conducted in the child's home. Target vocabulary words for the child were chosen collaboratively by the parent and the project's speech-language pathologist. When the child mastered the use of their target vocabulary set, additional words were added to it.

Over the course of the 24 sessions, the parent was taught to implement the components of the intervention and gradually led the intervention sessions. For the first eight sessions, the project's interventionist implemented the intervention while the speech-language pathologist explained the techniques to the parent and answered his or her questions. For sessions 9–10, the parent implemented the intervention during the last 10 min, or snack. For sessions 11–12, the parent implemented the intervention during the last 20 min, or book and snack. Beginning in session 13, the parent led the entire 30 min session, including all three activities. The interventionist continued to coach the parent as needed throughout all of the sessions.

Measures

In order to characterize participants and evaluate the effectiveness of the intervention, the child was assessed at six time points: three months prior to intervention, at the start of intervention, post-intervention, three months post-intervention, six months post-intervention, and twelve months post-intervention. Table 1 lists the assessments and the time of their administration. Standardized assessment measures included the *Mullen Scales of Early Learning* (MSEL) (Mullen 1995), *Vineland Adaptive Behavior Scales, Second Edition* (VABS-II) (Sparrow et al. 2005), *Sequenced Inventory of Communication Development-Revised* (SICD-R) (Hedrick and Prather 1975), *MacArthur-Bates Communication Development Inventory* (CDI) *Words and Gestures* form (Fenson et al. 2006), *Clinical Assessment of Language Comprehension* (CALC) (Miller and Paul 1995), and *Peabody Picture Vocabulary Test, Fourth Edition* (PPVT-4) (Dunn and Dunn 2007). Tests were administered by the project's speech-language pathologist. Interventionists did not administer any assessments in order to avoid potential bias.

In addition to standardized assessment, transcripts of intervention sessions were created using the Systematic Analysis of Language Transcripts (SALT) program (Miller and Chapman 1985) in order to characterize parent and child communication over the course of the intervention (Romski et al. 2010). Trained, reliable transcribers used an event-based coding scheme to document each instance in which a child used a target vocabulary word and the mode in which he or she used it: spoken, augmented, or both spoken and augmented. Communication also was coded as prompted or unprompted.

Finally, parents completed the Parenting Stress Index (PSI) (Abidin 1995) and the Parent Perception of Language Development (PPOLD) (Romski et al. 2011) measures in order to allow the investigators to examine the experiences and views of parents participating in the study.

Results

Initial Developmental Profile

At 26 months, the child performed in the Very Low range ($T \leq 20$) on all domains of the MSEL, with the exception of Receptive Language, which was a relative strength ($T = 37$; AE = 22 months.). Her most severe delays were in Gross Motor ($T \leq 20$; AE = 7 months) and Expressive Language ($T \leq 20$; AE = 7 months), with Fine Motor somewhat less delayed ($T \leq 20$; AE = 13 months). Additionally, the VABS-II indicated Moderately Low abilities across Communication, Daily Living Skills, and Socialization, and Low abilities in Motor skills. At the subdomain level of the VABS-II, her most severe delays

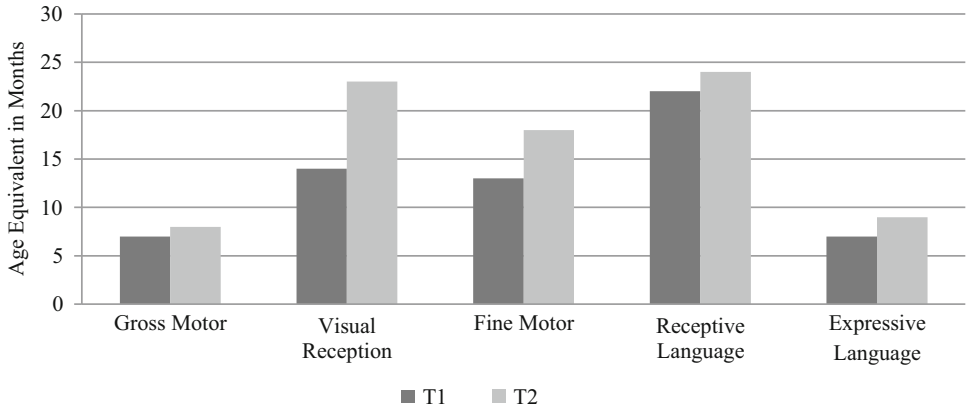

Fig. 1 MSEL at T1 and T2

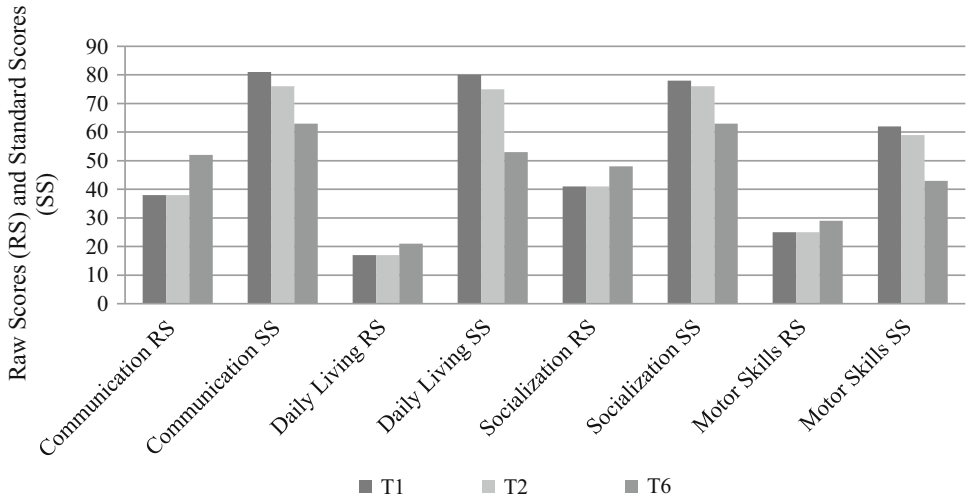

Fig. 2 VABS raw and standard scores at T1, T2, and T6

were again in Gross Motor (*v*-scale score = 6; AE = 5 months) and Expressive Communication (*v*-scale score = 10; AE = 13 months). Fine Motor was also at a similar level (*v*-scale score = 10; AE = 14 months). Her Receptive Communication was somewhat stronger (*v*-scale score = 13; AE = 18 months).

Her SICD performance supported a relative strength in receptive language, which was at the 20-month level, compared to expressive language, which was at the 12-month level. On the CDI, the child's mother reported that she understood 273 words, and was able to say one word (the animal sound baa baa). The Emerging Language Stage section of the CALC, an informal measure of early language comprehension that uses known objects and people, indicated that the child responded to joint attention bids and comprehended familiar object names at baseline.

Change in Skills Over Time

At 29 months, the child continued to exhibit Very Low performance in the Gross Motor, Fine Motor and Expressive Language domains of the MSEL. She demonstrated relative strengths in Receptive Language ($T = 38$; AE = 24 months) and Visual Reception ($T = 34$; AE = 23 months). A comparison of age equivalent MSEL scores at T1 and T2 was conducted in order to examine the child's progress in relation to gains that would be expected, given three months of maturation. This comparison revealed that the child made gains in all areas, though her progress in Gross Motor was minimal (see Fig. 1).

A comparison of the VABS profile at 26 and 29 months and 50 months revealed improvements in raw scores, but declines in Standard Scores across all domains (see Fig. 2).

Table 2 SICD and CDI scores across time points

	T1	T2	T3	T4	T5	T6
SICD						
Receptive	20	20	24	24	24	24
Expressive	12	12	12	12	12	12
CDI						
Words understood	275	282	290	N/A	N/A	290
Words spoken	1	3	16	N/A	N/A	5

Note: SICD scores represent estimated age equivalence in months, CDI scores represent total items endorsed by the parent from a total of 396 possible words

Between 26 and 29 months, Age-equivalent subdomain scores remained identical for Receptive Communication, Expressive Communication, and Fine Motor, and increased mildly in the Gross Motor domain, from 5 to 7 months AE. Age-equivalent score gains between 29 and 50 months were variable (Receptive Communication +12 months; Expressive Communication +4 months; Gross Motor +1 month; Fine Motor −4 months).

Expressive communication scores on the SICD-R remained at the 12-month level throughout the duration of the study. It is important to note that the SICD-R Expressive items specifically focus on vocalizations and speech, and thus progress in the use of an SGD would not be represented on this test. Receptive communication scores shifted from the 20- to the 24-month level at the post intervention time point, and remained at that level for all follow-up assessments. On the CDI, the number of words that the child's mother reported she understood increased gradually from the three months prior to intervention to post intervention time points, and remained stable at the 12-month follow-up. Words spoken also increased from the three months prior to intervention to post intervention time points, but had declined at the 12-month follow-up (see Table 2). In terms of the CALC, at the post intervention time point, two additional skills appeared in the child repertoire: comprehension of action words and comprehension of words for absent person and objects. At the 12-month follow-up, the child correctly identified 23 words by touching pictures, and received a standard score of 63 and an age equivalent score of 26 months on the PPVT-4, consistent with other measures.

Effect of Language Intervention

The observational coding scheme indicated that the child independently produced one manual sign (eat) in the baseline intervention session. In session 24, she independently produced one manual sign (eat) and 13 different augmented words (applesauce, baby, bar, bee, bucket, cheese, cup, out, play, potty, sing, the end, turn page) spontaneously using the SGD. She did not produce any spoken words during either session. The proportion of her utterances that were intelligible increased from 0.43 to 0.85 between session 1 and 24 due to the use of the augmented words. Her type token ratio, an indication of the diversity in the words she produced, decreased slightly, from 0.16 in session 1 to 0.13 in session 24. Finally, the total number of turns she took in communicative exchanges increased from 48 in session 1, to 120 in session 24.

At follow-up appointments, the child was no longer using the SGD in the home environment because the family had chosen to use a combination of manual signs, facial expressions, and vocalizations as a means of communication instead of the SGD. Parents reported to study staff that they found the SGD too cumbersome for their daily lives, but they were interested in exploring iPad apps as a communication system in the future. However, in her preschool environment, the child continued to use an SGD similar to the one used in the study in order to participate in classroom activities.

Parent Questionnaires

The mother's responses on the PSI indicated average to below average levels of parenting stress throughout the entire durations of the study. Changes over time were marginal. The mother's responses to the POLD were similar to other parents in the sample. A comparison of pre and post intervention PPOLD ratings indicated increased perceptions of child success in communicating, but no change in perceptions of the degree of difficulty the child faces when attempting to communicate.

Discussion

These results add to literature on the clinical manifestations of ML IV and indicate that although children with this disorder have deficits across many domains, they may be most severely affected in gross motor and expressive language development. The child reported on in this study displayed significant developmental delays in these areas, but more mild delays relative to peers in receptive language and visual reception at 29 months. The age equivalence scores observed for this child were also somewhat more advanced than those reported in other studies of people with ML IV (Amir et al. 1987; Schiffmann et al. 2014). Possible explanations for this difference include the individual variation in disorder severity and course, the reporting style of the mother, the content of the direct

assessment measures, or the effect of early intervention for the child.

Observations regarding the course of development for the child over the time span of 26–50 months generally suggest progress, though at a slower pace than peers. Consistent increases in skills were apparent on both the MSEL and VABS. Improvements also were observed on the SICD, CDI, and CALC, though not consistently, and no further progress was apparent on these measures after the post-intervention time point. It is difficult to determine whether this suggests a slowing of development, or reflects insufficiency in the measure's ability to capture small changes in the skills of children with developmental disabilities.

She also gained expressive vocabulary via the use of an SGD. This finding is consistent with other studies showing that children with developmental disabilities, including those with complex medical conditions, benefit from language intervention with SGDs (Romski et al. 2008, 2010, 2015). The child's experience expanded her ability to successfully communicate with her family and may have supported her development in other areas. Given the significant motor impairments exhibited in ML IV, the use of an SGD may provide a viable communication approach at a very early age. Optimizing the ability of the individual to participate in social contexts by supporting communication is critical to quality of life among people with developmental disabilities (Sevcik and Romski 2016).

In light of the family's concerns about the SGD being cumbersome, future research in this area might further explore maximizing the convenience and transportability of SGDs. Many improvements have been made in technology in recent years, with the rapidly increasing availability of tablet computer apps for AAC. The child continued to use an SGD at preschool, suggesting that perhaps SGDs are especially valuable in educational environments. This could relate to increased demands on the child or the fact that preschool staff members are less familiar with her compared to her parents, and thus likely to have more difficulty anticipating her needs and interpreting other forms of communication.

Limitations of this report include that it involved only one child with ML IV, and thus the results may not be generalizable to all children with this disorder. It is also important to keep in mind that many issues influence cognitive and linguistic development in children with rare disorders, including both intrinsic and extrinsic factors. Also, our intervention was intensive and focused on parent-implemented intervention so that the child and parent could communicate at home. It may not be feasible for all families. At the same time, Romski et al. 2007 showed that parents were capable of implementing similar intervention with high fidelity to the standardized instructions. Additionally, the very low attrition rate observed in our study (5.6%) indicates that the majority of families were able to complete the intervention program. In conclusion, early language intervention using SGDs that focuses on parent coaching may provide a route for developing communication for children with ML IV.

Acknowledgments We would like to thank the participant and her family. This research was funded by Institute of Education Sciences Grant Number #R324A070122 to MaryAnn Romski.

Synopsis

This longitudinal case study of a child with ML IV suggests that people with this disorder (1) make slowed but measurable developmental progress in early childhood and (2) benefit from augmentative and alternative communication (AAC) interventions.

Author Notes

Contributions of Individual Authors

Evelyn Fisher completed data analysis and drafted the manuscript. Drs. MaryAnn Romski and Rose Sevcik were integrally involved in the conception, design, and implementation of the larger study. They also edited the manuscript and added specific information about the original study and data.

Guarantor Author

Evelyn Fisher serves as the guarantor and accepts responsibility for this work.

Competing Interests

The authors have no competing interests to declare.

Funding

This project was funded by the Institute of Education Sciences, Grant R324A070122 to MaryAnn Romski. The authors confirm independence from the sponsors; the content of this manuscript was not influenced by the sponsors.

Ethics Approval

The study was approved by the Georgia State University Institutional Review Board (IRB), and all procedures were

performed in accordance with the ethical standards of the IRB.

Consent Statement

Informed consent was obtained from a parent of each child included in the study.

References

Abidin RR (1995) Parenting stress index: professional manual, 3rd edn. Pediatric Psychology, Charlottesville

Amir N, Zlotogora J, Bach G (1987) Mucolipidosis type IV: clinical spectrum and natural history. Pediatrics 79(6):953–959

Berman ER, Livni N, Shapira E, Merin S, Levij IS (1974) Congenital corneal clouding with abnormal systemic storage bodies: a new variant of mucolipidosis. J Pediatr 84(4):519–526. doi:10.1016/S0022-3476(74)80671-2

Dunn LM, Dunn DM (2007) Peabody picture vocabulary test, 4th edn. PsycTESTS, San Antonio. doi:10.1037/t15144-000

Fenson L, Marchman VA, Thal DJ, Dale PS, Reznick JS, Bates E (2006) MacArthur-bates communicative development inventories, 2nd edn. PsycTESTS, San Antonio. doi:10.1037/t11538-000

Geer JS, Skinner SA, Goldin E, Holden KR (2010) Mucolipidosis type IV: a subtle pediatric neurodegenerative disorder. Pediatr Neurol 42(3):223–226. doi:10.1016/j.pediatrneurol.2009.10.002

Hedrick D, Prather EM (1975) Sequenced inventory of communication development, Revised edn. Western Psychological Services, Torrence

Martin, H. R., Poe, M. D., Reinhartsen, D., Pretzel, R. E., Roush, J., Rosenberg, A., Escolar, M. L. (2008). Methods for assessing neurodevelopment in lysosomal storage diseases and related disorders: a multidisciplinary perspective. Acta Paediatr 97(457), 69–75. 10.1111/j.1651-2227.2008.00651.x

Miller J, Chapman R (1985) Systematic analysis of language transcripts [computer software]. University of Wisconsin, Madison

Miller JF, Paul R (1995) The clinical assessment of language comprehension. Paul H Brookes Pub Co., Baltimore

Mucolipidosis type IV. (2015) Retrieved August 18, 2015 from http://ghr.nlm.nih.gov/condition/mucolipidosis-type-iv

Mullen EM (1995) Mullen scales of early learning manual (AGS ed). American Guidance Service, Circle Pines

Romski M, Sevcik R (2005) Augmentative communication and early intervention: myths and realities. Infants Young Child Interdiscip J Spec Care Pract 18(3):174–185

Romski M, Sevcik RA, Adamson LB, Cheslock M, Smith A (2007) Parents can implement AAC interventions: ratings of treatment implementation across early language interventions. Early Child Serv Interdiscip J Eff 1(4):249–259

Romski MA, Krupa JH, Cheslock M, Sevcik RA, Adamson LB (2008) Language and communication changes in a child with holoprosecephaly: a case report. Med J Speech Lang Pathol 14:10–19

Romski M, Sevcik RA, Adamson LB, Cheslock M, Smith A, Barker RM, Bakeman R (2010) Randomized comparison of augmented and nonaugmented language interventions for toddlers with developmental delays and their parents. J Speech Lang Hear Res 53(2):350–364

Romski M, Sevcik RA, Adamson LB, Smith A, Cheslock M, Bakemana R (2011) Parent perceptions of the language development of toddlers with developmental delays before and after participation in parent-coached language interventions. Am J Speech Lang Pathol 20(2):111–118. doi:10.1044/1058-0360(2011/09-0087)

Romski M, Sevcik RA, Barton-Hulsey A, Whitmore AS (2015) Early intervention and AAC: what a difference 30 years makes. AAC Augmentative Altern Commun 31(3):181–202. doi:10.3109/07434618.2015.1064163

Romski M, Sevcik R, Adamson L, Barton-Hulsey A, Barker RM, Bakeman R, Whitmore A, Smith A (2016). Parent-implemented language intervention for young children with developmental disabilities, manuscript in preparation

Schiffmann R, Grishchuk Y, Goldin E (1993) Mucolipidosis IV. In: Pagon RA, Adam MP, Ardinger HH, Wallace SE, Amemiya A, Bean LJ, Stephens K (eds) GeneReviews. University of Washington, Seattle Retrieved from http://www.ncbi.nlm.nih.gov/books/NBK1214/

Schiffmann R, Mayfield J, Swift C, Nestrasil I (2014) Quantitative neuroimaging in mucolipidosis type IV. Mol Genet Metabol 111(2):147–151. doi:10.1016/j.ymgme.2013.11.007

Sevcik RA (2016) Romski MA (2016) Examining the science and practice of communication interventions for individuals with severe disabilities. Am J Intellect Dev Disabil 121(2):121–138

Sparrow S, Cicchetti D, Balla D (2005) Vineland adaptive behavior scales: survey form manual, 2nd edn. American Guidance Services, Circle Pines

Wakabayashi K, Gustafson AM, Sidransky E, Goldin E (2011) Minireview: Mucolipidosis type IV: an update. Mol Genet Metabol 104:206–213. doi:10.1016/j.ymgme.2011.06.006

JIMD Reports
DOI 10.1007/8904_2016_36

RESEARCH REPORT

White Matter Microstructure and Subcortical Gray Matter Structure Volumes in Aspartylglucosaminuria; a 5-Year Follow-up Brain MRI Study of an Adolescent with Aspartylglucosaminuria and His Healthy Twin Brother

Tokola Anna • Brandstack Nina • Hakkarainen Antti • Salli Eero • Åberg Laura • Autti Taina

Received: 6 September 2016 / Revised: 6 December 2016 / Accepted: 9 December 2016 / Published online: 10 February 2017

Abstract *Objective*: Aspartylglucosaminuria is an inherited, lysosomal storage disease causing progressive decline in cognitive and motor functions. The aim of this study was to evaluate volumes of subcortical gray matter structures and white matter microstructure in aspartylglucosaminuria in adolescence in a longitudinal study for the first time.

Methods: A boy with aspartylglucosaminuria and his healthy twin brother were imaged twice with a 3.0 T MRI scanner at the ages of 10 and 15 years. Subcortical gray matter structure volumes were measured using an atlas-based automatic method, and diffusion tensor imaging was used to evaluate the white matter microstructure of the corpus callosum and the thalamocortical pulvinar tracts.

Results: The subcortical gray matter structures were smaller at onset and diminished at follow-up in the affected twin, with the exception of the amygdala which was larger and remained the size. The largest difference in volume between the twins was found in the thalami. The total gray and white matter volumes decreased in the affected twin. In diffusion tensor imaging analysis, the fractional anisotropy was decreased at onset in the affected twin compared to the healthy brother in the evaluated tracts. The axial, radial and mean diffusivity values were increased in the affected twin. The difference between the twins increased slightly at follow-up.

Interpretation: The findings suggest that volumetric measurements and diffusion tensor imaging based microstructural analysis may be useful modalities for monitoring disease progression and response to emerging treatment in aspartylglucosaminuria, but further studies with more subjects are necessary to confirm the results.

Communicated by: Nicole Wolf, M.D., Ph.D.

The original version of this chapter was revised: The Acknowledgement and Funding information was included. The erratum to this chapter is available at DOI 10.1007/8904_2017_18

Electronic supplementary material: The online version of this chapter (doi:10.1007/8904_2016_36) contains supplementary material, which is available to authorized users.

T. Anna (✉) · B. Nina · H. Antti · S. Eero · A. Taina
HUS Medical Imaging Center, Radiology, University of Helsinki and Helsinki University Hospital, Helsinki, Finland
e-mail: anna.tokola@hus.fi

Å. Laura
Department of Psychiatry, University of Helsinki and Helsinki University Hospital, Helsinki, Finland

Introduction

Aspartylglucosaminuria (AGU) is an inherited, autosomal recessive, progressive neurodegenerative disease. It belongs to lysosomal storage disorders and manifests with progressive decline in cognitive and motor functions, leading to premature death (Autti et al. 1997). Clumsiness and delayed speech development are usually the first symptoms noted in early childhood. Despite the ongoing disease, children learn new skills up until their teenage years, though more slowly than healthy children. Thereafter, learned skills are gradually lost, resulting in severe intellectual disability and deterioration of motor skills (Arvio and Arvio 2002).

The disease is caused by a mutation of the *AGA* gene located on 4q34.3, resulting in deficient activity of aspartylglucosaminidase, a lysosomal hydrolase enzyme (Saarela et al. 2001). As a result, there is excessive accumulation of uncleaved glycoasparagines in lysosomes and elevated metabolite levels in urine.

There is yet no treatment available to cure or slow down the progression of AGU. Mouse model studies investigating virus-mediated gene therapy and enzyme replacement therapy in AGU have shown some promise (Dunder et al. 2000; Virta et al. 2006). Also, small molecule compounds which may be suitable for chaperone therapy of AGU have been identified in a recent study (Banning et al. 2016). At the moment, objective modalities are needed for indexing illness stage and monitoring response to emerging treatment.

Previous brain magnetic resonance imaging (MRI) studies have revealed a typical combination of findings in AGU, including decreased T2 signal intensity (SI) in the thalami and especially the pulvinar nuclei, high T2 SI in the periventricular white matter (WM), juxtacortical high T2 SI foci and poor differentiation between gray matter (GM) and WM. Also, thin corpus callosum (CC) and some degree of cerebral and/or cerebellar atrophy are found in nearly all patients with AGU (Autti et al. 2008; Tokola et al. 2015).

Modern MRI-based methods provide more detailed information about volumetric and structural changes caused by disease processes. Brain volumes including subcortical GM structure volumes may be calculated using automated or semi-automated methods (Zhang et al. 2001; Fischl et al. 2002; Jenkinson et al. 2012). Diffusion tensor imaging (DTI) allows quantification of tissue architecture through both the degree and directionality of tissue water diffusion within a voxel, and can be used to noninvasively estimate WM tract integrity in vivo (Basser and Pierpaoli 1996).

We evaluated changes in total WM, total GM and subcortical GM structure volumes, and WM microstructure in an adolescent with AGU during a 5-year follow-up to better understand the disease process and find potential tools for indexing the illness stage in AGU. Adolescence is a unique period in the human lifespan, and various morphometric changes occur in the still-developing brain. In AGU, the typical turning point in motor and cognitive development makes this phase intriguing for investigation. Based on the age phase and pathophysiology of the disease, we hypothesized that there is volume reduction of subcortical GM structures and microstructural changes in WM tracts in the affected twin already at onset, and a progression at follow-up was expected.

Materials and Methods

Study Participants

The boy with AGU was born after a full-term twin pregnancy with a cesarean section. The early motor developmental milestones were reached within normal range. He learned to walk at the age of 15 months and had his first words at the age of 18 months. At the age of 3, speech therapy was initiated because of delayed speech. As part of etiological examinations for the developmental delay, a urine sample was collected and revealed increased amounts of aspartylglucosamine. The diagnosis of aspartylglucosaminuria was confirmed at age 5.

At the time of the first examination at 10 years of age, mild problems of coordination and balance were noticed. He was prepubertal. The cognitive performance was at the level of mild mental retardation.

At the time of the second examination at the age of 15 years, problems with coordination and balance were pronounced. Furthermore, dysarthria was observed in speech. The pubertal status was G3-4, P4. In the psychological examination, the cognitive performance had decreased as compared with levels for his age, being at the level of moderate mental retardation. No epileptic seizures had occurred.

The healthy dizygotic twin brother developed normally and had normal school history. His puberty preceded the puberty of the affected twin. He had a sports injury at the age of 14 years causing a small impacted, left-sided temporal skull fracture, which was operated. No persistent intracerebral changes were caused by the injury and the artifacts from the skull fixation material were minor, not causing disruption to the subcortical GM structures or WM tracts evaluated in the study.

The twins were imaged twice with 3.0 T brain MRI during a 5-year follow-up. The first examination was performed at the age of 9.9 years and the second at the age of 15.1 years. As a twin, the control person was age, sex and environment matched and shared around 50% of the genome. Informed consent was obtained from the parents of the twins prior to the study. A clinical neurological examination was performed on the siblings and data on their medical history was collected from the parents and medical records. No sedation was used during the scanning and the brothers were in good physical condition at the time of the examinations.

The study was approved by the local ethics committee.

MRI Acquisition

The MR imaging was performed using a 3.0 T scanner (Achieva, Philips Medical Systems, Best, The Netherlands). The examination included a T2 (Turbo spin echo) TSE axial series (TR 4,000 ms, TE 80 ms, slice thickness 4 mm, flip angle 90°, matrix 512 × 512), a T1 3D Turbo field echo (TFE) series with isotropic voxel size (TR 8.3, TE 3.8, flip angle 8°, matrix 256 × 256) and a diffusion tensor series (single-shot diffusion weighted sequence, TR 10,600 ms, TE 59.5 ms, 16 diffusion gradients, 32 + 1 directions, NA 2, matrix 112 × 112, FOV 224 × 224, $b = 1{,}000$ s/mm^2, 1 $b = 0$).

Visual Analysis

Visual analysis of the T1 and T2 weighted images was performed by two radiologists. The first examination of the affected twin had been included in a previous study (Tokola et al. 2015).

MR Image Segmentation

MR image segmentation was carried out by two different and complementary processing pipelines. In the first, we segmented the brain into tissue classes (GM, WM and CSF). In the second pipeline, we assigned neuroanatomical labels to subcortical GM structures (segmentation of anatomical classes).

The segmentation of tissue classes was performed by FMRIB Software Library v5.0 (FSL) (Jenkinson et al. 2012). First, the Brain Extraction tool (BET) was used to delete non-brain tissue from the MR images. The result was manually corrected where necessary. Then, FMRIB's Automated Segmentation Tool (FAST) was used to segment the brain-extracted images into GM, WM and CSF using the default options. The volumes of GM, WM and CSF were estimated using the partial volume estimates (Zhang et al. 2001).

The segmentation of subcortical GM structures (left and right thalami, hippocampi, amygdala, nucleus caudatus, putamen, globus pallidus and accumbens) was carried out by using the volume-based (subcortical) stream of the FreeSurfer image analysis suite (Fischl et al. 2002). The total volumes of the structures (left + right) are presented in Table 1. This method is based on both subject-specific measured values and on the alignment with a subject-independent probabilistic atlas (MNI305).

The segmentations of subcortical structures were visually checked for errors by two radiologists and minor manual corrections were made using Slicer 4 (Fedorov et al. 2012) and the nac-hncma-atlas (Halle et al. 2015). The consensus of opinion was used for the volumetric measurements.

Tractography

DTI data was processed and analysed using tools in FMRIB Software Library v5.0 (Jenkinson et al. 2012). Eddy current distortions and minor head motions were corrected using eddy correction following brain extraction from the skull and creating brain masks using bet2. Diffusion tensors, fractional anisotropy (FA), mean diffusivity (MD) and axial diffusivity (AD = $\lambda 1$) were determined using dtifit and radial diffusivity (RD) was calculated with fslmaths as $(\lambda 2 + \lambda 3)/2$. A distribution of diffusion parameters was built for each voxel on the basis of Markov Chain Monte Carlo (MCMC) by bedpostx. Two fibers per voxel were modelled and 1,000 iterations before sampling was used. Probabilistic tractography analysis of the CC frontal projections and the thalamocortical tracts from the pulvinar nuclei were carried out with probtrackx2 (5,000 sample pathways, curvature threshold 0.4, step length 0.5 mm and subsidiary fiber volume fraction threshold 0.01) utilising seed, exclusion and inclusion masks as described in detail in Supplementary Fig. 1. The masks were delineated by two radiologists and the mean values are presented. The protocol for CC frontal projections was modified from Huang et al. (2005), and the pulvinar masks were delineated based on the nac-hncma-atlas (Halle et al. 2015). Tract volumes were thresholded at 0.5% and used as masks to assess mean FA, MD, AD and RD along the tract.

Results

MRI Findings

At the age of 10 years, typical findings associated with AGU were noticed in visual evaluation. In T2-weighted images, an SI decrease in the thalami, more intense SI decrease in the pulvinar nuclei and mild periventricular SI increase were found in the images of the affected twin. Also, poor differentiation between GM and WM, mild lateral ventricle dilatation, thin corpus callosum, pineal multilocular cyst (6 mm) and some prominent perivascular spaces were seen. The skull thickness in the occipital bone of the affected twin was 6 mm, which was twice as much as the skull of the unaffected twin. No patchy WM lesions were noted. The cerebral and cerebellar atrophy was evaluated as mild.

At the age of 15 years, there was no change in the thalamic or periventricular SI alterations, but differentiation between GM and WM was better, especially in the frontal lobe. A slight progression of cerebral and cerebellar atrophy was noted.

No pathological changes were found in the visual evaluation of the images of the unaffected twin, except for small areas of artifact in the follow-up images caused by cranial fixation implants in the left temporal region.

The main findings on T1- and T2-weighted images are shown in Fig. 1.

Volumetry

The delineation of the subcortical GM structures is presented in Fig. 2 and the change in volumes at follow-up in Fig. 3. The volumes and the percentage change are also presented in Table 1.

Table 1 Brain volumes and subcortical gray matter volumes of an adolescent boy with aspartylglucosaminuria and his healthy twin brother

	Age (years)	TBV	GM	WM	CSF	Thalami	Hippocampi	Amygdala	Caudatus	Putamen	Pallidum
Patient	9.9	1,314.21	790.28	523.93	239.61	12.82	10.11	3.93	8.07	10.76	3.50
	15.1	1,251.28	737.07	514.21	297.67	12.00	9.63	3.92	7.86	9.80	3.25
Change[a]		−4.8%	−6.7%	−1.9%	24.2%	−6.4%	−4.7%	−0.3%	−2.6%	−8.9%	−7.1%
Control	9.9	1,307.06	739.94	567.12	250.42	18.01	9.88	3.34	8.33	10.99	3.51
	15.1	1,308.15	725.81	582.34	284.38	17.95	10.18	3.74	8.95	10.86	3.48
Change[a]		0.1%	−1.9%	2.7%	13.6%	−0.3%	3.0%	11.7%	7.4%	−1.2%	−0.9%
Difference patient vs. control[b]	9.9	0.5%	6.8%	−7.6%	−3.8%	−28.8%	2.3%	17.7%	−3.1%	−2.1%	−0.3%
	15.1	−4.4%	1.6%	−11.7%	4.7%	−33.1%	−5.4%	5.1%	−12.2%	−9.8%	−6.6%

The volumes are all shown in cm^3 and the subcortical volumes are sums of the left and right volume

[a] The change during follow-up is presented as percentage change from original volume

[b] Difference between the volumes of the patient and healthy twin are presented as percentage comparing the volume of the patient with the volume of healthy twin. *TBV* total brain volume, *GM* total gray matter, *WM* total white matter

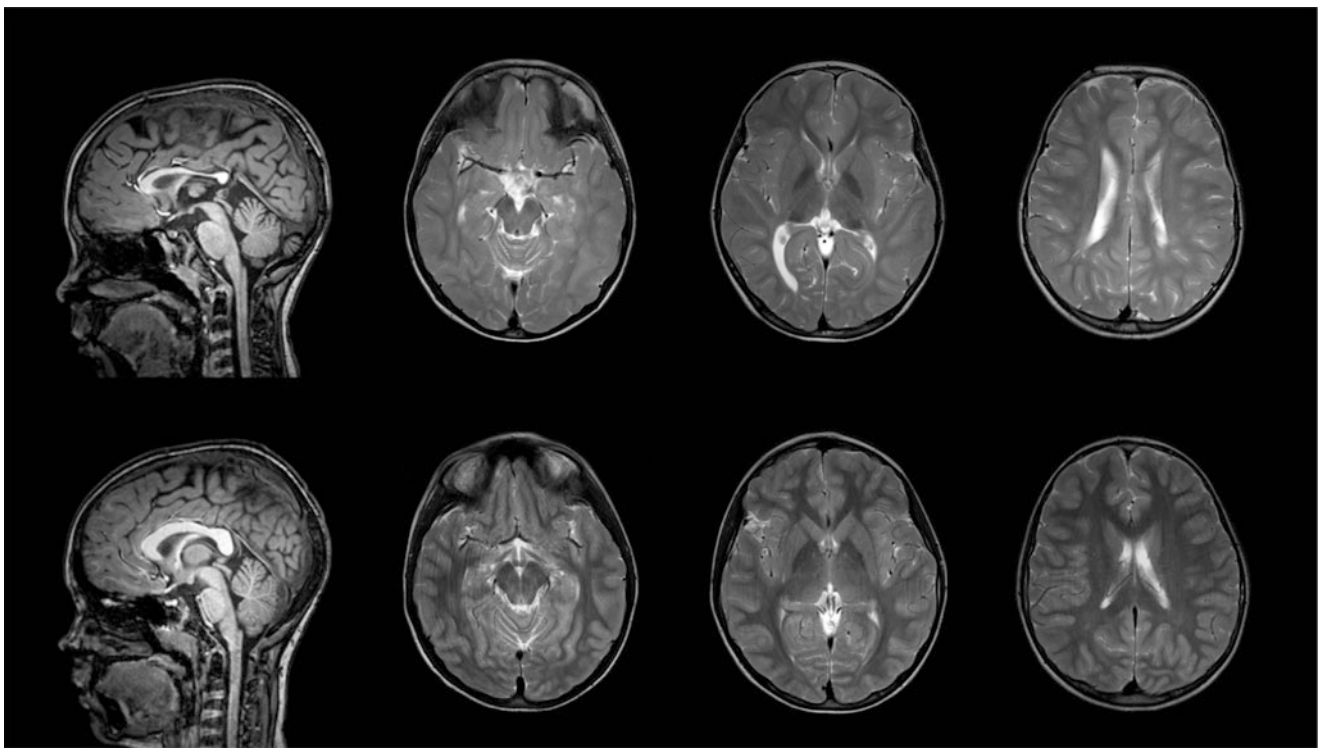

Fig. 1 Typical changes in aspartylglucosaminuria, 3.0 T T1-weighted sagittal and T2-weighted axial images. *Top row*, male patient at the age of 10 years, showing decreased signal intensity in the pulvinar nuclei of the thalami bilaterally, and signs of delayed myelination and increased signal intensity in the deep white matter in the T2-weighted images. Thin corpus callosum, mild ventricular dilatation and some slightly prominent sulci are also visible. *Second row*, healthy twin brother imaged at the same age with normal findings

At 10 years of age, the estimated total brain volume (TBV) was nearly equal between the twins, being 0.5% larger in the affected twin. At follow-up, TBV of the twin with AGU decreased by 5% and at 15 years of age, it was 4% less than the TBV of the unaffected twin. The total volume of GM was larger in the affected twin than his healthy twin brother at both time points. At onset, the total GM volume was 7% larger in the affected twin. At

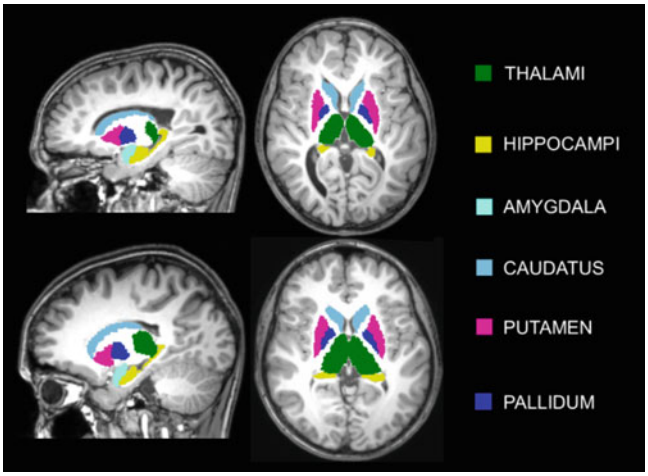

Fig. 2 Segmentation of the subcortical gray matter structures using an atlas-based method by Freesurfer. The color-coded structures are superimposed on T1-weighted images. *Top row*, patient at the age of 15 years and *second row*, healthy twin brother at the same age

follow-up, the total GM volume decreased substantially in the affected twin, by 7%, but it was still 2% larger compared with the healthy twin.

At 10 years of age, most of the subcortical GM structures were smaller in the twin with AGU than his healthy brother. The largest difference in volume was found in the thalami, which were 29% smaller at onset. The only structures that were substantially larger in the affected than the unaffected twin were amygdala, which were 18% larger. The amygdala was also the only structure to remain the size in the affected twin. Other subcortical GM structures diminished 3–9% at follow-up. The largest difference in volume at 15 years of age was found in the thalami, which were 33% smaller in the twin with AGU. Automatic segmentation for accumbens did not succeed, and in our opinion, manual correction would not have been reliable. Therefore, accumbens volumes are not included.

The total WM volume was smaller already at onset in the twin with AGU, 8% less than the healthy twin's. At follow-up, the volume reduction of the WM was milder than the reduction of GM. At the age of 15 years, the total WM volume of the affected twin was 12% less than the volume of the unaffected twin. The CSF volume increased significantly by 24% in the affected twin and 13% in the healthy twin.

DTI

Results of the quantitative DTI analysis of the CC frontal projections and thalamocortical tracts from the PU are presented in Supplementary Tables 1 and 2. The DTI color map is shown in Fig. 4 and the change in DTI parameters in Fig. 5. The masks used for the tractography are shown in Supplementary Fig. 1.

The FA values were distinctly decreased in the affected twin in all tracts evaluated already at onset, and there was no remarkable change in the FA values at the 5-year follow-up.

The MD values in the tracts under evaluation were increased in the affected twin compared with the healthy twin already at onset, and the difference between the twins grew at follow-up. Also, both AD and RD values were increased in the affected twin at onset in all tracts under evaluation, the RD values more apparently. The difference between the twins in AD and RD also grew slightly at follow-up, but overall the changes in MD, RD and AD values were modest at follow-up in both twins.

The tract volumes differed substantially between the first and second examination in both twins, but there was a tendency of volume increase in the healthy twin and volume decrease in the affected twin.

Discussion

This longitudinal study revealed volume reduction in total WM, total GM and most subcortical GM structures of an adolescent AGU patient compared with the age, sex and environment matched healthy twin brother. Also, DTI with quantitative tractography detected differences in WM microstructure, and a slight progression at follow-up was noticed.

Only a few neurohistopathologic reports describing changes in AGU patients have been published. These are based on autopsy tissues of older individuals with a progressed disease. Vacuolized neurons, glial cells and endothelial cells have been found in various brain regions including cerebral cortex, cerebellum, thalami, basal ganglia and amygdala (Haltia 1975; Autti et al. 1997; Jalanko

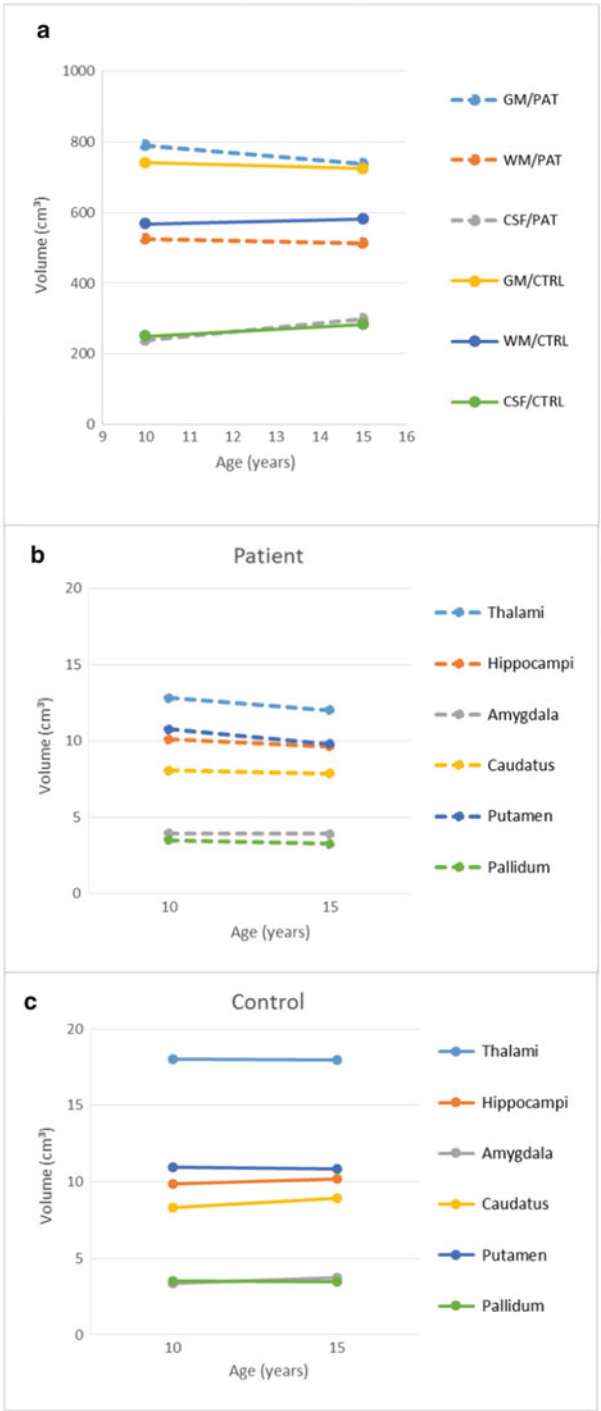

Fig. 3 (**a**) The gray matter, white matter and cerebrospinal fluid volumes of both twins at the ages of 10 and 15. The twin with AGU shows smaller white matter volume at onset but a larger gray matter volume compared with the healthy twin. The gray matter volume shows a steeper decline at follow-up. The *dotted line* represents the twin with AGU (PAT = twin with AGU, CTRL = healthy twin). (**b**, **c**) The subcortical gray matter structure volumes (*left* + *right*) of both twins at the ages of 10 and 15. The biggest difference between the brothers is seen in the thalami. In the twin with AGU, the amygdala is the only structure that does not show volume decline

et al. 1998). The basic cortical cytoarchitecture seems to be generally preserved but most neurons contain vacuoles, and the WM shows diffuse pallor of myelin staining and in some cases gliosis (Autti et al. 1997). MRI studies with volumetric evaluations and DTI based methods can provide valuable information in vivo about the changes in the brains of younger individuals with AGU.

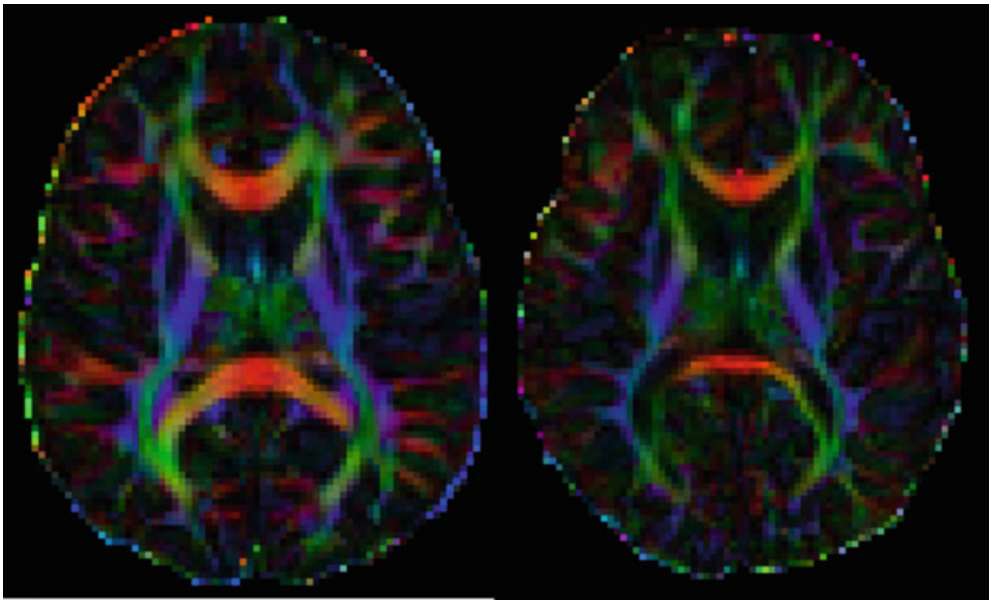

Fig. 4 DTI color map, axial images at the level of the genu of the corpus callosum overlaid on T1-weighted images. On the *left*, healthy twin at the age of 10 years and on the *right*, the twin with AGU at the same age. The figure shows color-coded white matter tracts in the transverse (*red*), longitudinal (*green*) and horizontal (*blue*) directions. There is a visible difference between the twins, with several white matter tracts being thinner in the images of the twin with AGU. Remarkable differences are noted e.g. in the genu, splenium, forceps minor and forceps major of corpus callosum

Knock-out mouse models for AGU have shown similar histopathologic findings in the CNS, including vacuolation of neurons and glial cells and signs of delayed or deficient myelination (Tenhunen et al. 1998; Jalanko et al. 1998; Gonzalez-Gomez et al. 1998). No major differences in the distribution of myelin have been detected. Vacuolation is seen also in the oligodendroglia, which may have an impact on the myelination process. Also, pathologic, hypertrophic axons have been detected in the brains of AGA−/− mice (Tenhunen et al. 1998).

Volumetry

Human brain MRI studies on healthy individuals have shown that total brain volume, GM and WM volume are highly hereditable (Thompson et al. 2002; Giedd et al. 2007). Smaller structures, perhaps because of greater proportion of measurement error, tend to have lower hereditability values and WM volumes tend to be more hereditable than GM volumes. Lower GM hereditability is consistent with the finding that plastic synapses change in response to environment and activity (Giedd et al. 2007). Some small differences in volumes in our study might be explained by normal variation between twins. Still, the most significant finding is that the difference increases between the affected twin and his healthy brother in adolescence in most volumes measured (Fig. 3).

Data from previous studies among healthy individuals indicate that the change in GM volume during adolescence has an “inverted U”-shape pattern and greater regional variation than WM (Giedd 2004; Gogtay et al. 2004; Sowell et al. 2004). Therefore, at this age in normally developing males, a slight reduction in GM volume is seen. Interestingly, in our study the total GM volume was larger in the affected twin at onset. At follow-up, the total GM volume of the affected twin decreased more than the volume of the unaffected twin, but still remained larger (Table 1). This may be explained by abnormal GM organization, considered an explanation for GM volume loss in puberty in normal development.

In contrast to the GM growth pattern, the WM volume increases almost linearly throughout adolescence (Giedd et al. 1999). In normal adolescent development, the increase in WM volume possibly reflects continuing myelination and increased axonal calibre within fiber bundles (Paus 2010). Our finding is in line with previous studies, since the total WM volume of the healthy twin increased slightly at follow-up. However, in the affected twin, the total WM volume slightly diminished between examinations, possibly related to the discontinuing myelination and loss of connections.

Even if the total GM volume in the affected twin was larger compared to the healthy twin, most of the subcortical GM structures were smaller already at onset and the volume reductions continued, as measured at follow-up. The

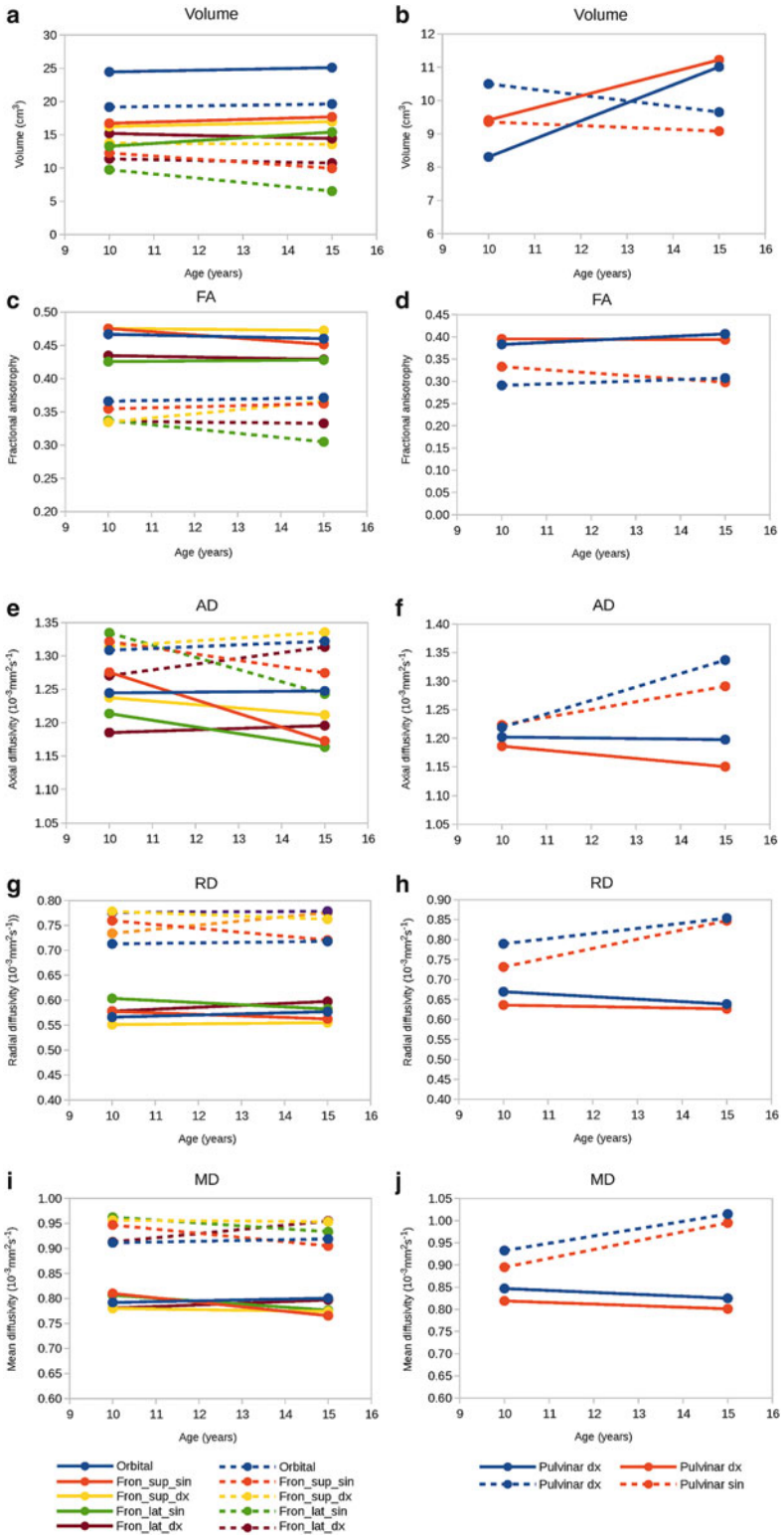

Fig. 5 Results for the quantitative diffusion tensor imaging analysis of corpus callosum frontal projections and thalamocortical pulvinar tracts. The *dotted line* represents the twin with AGU. The *left row* shows the results for the corpus callosum frontal projections and the *right row* shows the results for the thalamocortical pulvinar tracts (color coding of the tracts is explained under the diagrams). A tendency of reduction in tract volumes is seen in the affected twin (diagrams (**a**) and (**b**)). Also, decreased FA, as well as increased AD, RD and MD is noticed in the twin with AGU (diagrams (**c**)–(**j**)) in the tracts under evaluation

functions of the basal ganglia are linked to control of voluntary motor movements, but also higher cognitive function and emotions, with a major role in learning and memory. Volume reduction and dysfunction in subcortical GM structures may be involved in the progressive worsening of motor and cognitive functions that typically occurs at adolescence in AGU. The only structure to remain the same size was amygdala, which in normally developing males increases in size at this age (Wierenga et al. 2014). In the affected twin, there is probably simultaneous age-related volume increase and reduction caused by the disease.

In our study, the biggest difference in volume between the twins was found in the thalamus, in line with data suggesting that the thalamus has a central role in the pathogenesis of AGU. In previous MRI studies a decreased T2 SI in the thalami and especially pulvinar nuclei has been found even in young patients (Autti et al. 2008) and in some histopathologic studies, vacuolation has been particularly severe in the lateral nuclei of thalami and the basal nuclei (Autti et al. 1997; Gonzalez-Gomez et al. 1998). The thalamus is a paired nuclear complex serving as a relay station for sensory inputs to the cerebral cortex. It has also been suggested that the thalamus modulates information between cerebral cortical areas and is evolved in regulation of emotion, motivation and multimodal cognition. Therefore, dysfunction of the thalamus may have substantial impact on the clinical picture of AGU.

DTI

DTI allows quantification of WM integrity and organization based on the degree and directionality of tissue water diffusion. Four parameters (FA, MD, AD and RD) are used to describe WM structural properties. According to previous DTI studies on healthy individuals, the maturation of WM continues during childhood and adolescence in various areas (Barnea-Goraly et al. 2005; Lebel et al. 2008), including the areas of interest in our study. The thalamocortical pulvinar tracts and the CC frontal projections were chosen for the analysis due to previously reported MRI findings in AGU patients on conventional sequences.

We found widespread alterations to WM microstructure in the CC frontal projections and thalamocortical pulvinar tracts and the difference between the siblings was evident for all DTI parameters. As expected, the FA values were decreased in the affected twin and MD was increased, indicating microstructural disintegration and increased overall diffusion. Both the AD and RD values of the studied tracts were increased in the AGU subject. This agrees with prior findings that both the axons and the myelin are affected by the disease.

In our study, the water diffusivity was increased in the affected twin. It is possible, however, that there is simultaneous restriction (because of the vacuoles), but the increase in diffusion is emphasized. Probably the basic metabolic disturbance interferes with the growth and maturation of both neurons and glial cells, and early microstructural changes may impact the development of efficient WM fiber networks. Later, accumulation might disturb cell functions and cause cell death. Wallerian-like degeneration may also have a role in progressive general atrophy and gliosis in older individuals with AGU.

The difference in MD, AD and RD values between the siblings increased slightly at follow-up, but there was no marked age-related FA, MD, AD or RD change in our patient. This suggests that microstructural changes (including axonal membrane features and myelination level) of the CC and pulvinar tracts may occur in early childhood, and the tract volume loss in the patient is likely related to the loss of connections and GM involvement. These alterations may explain some of the motor, cognitive and emotional features of AGU.

A possible limitation of tract-based analysis is choosing the appropriate FA threshold and deflection angle (Mukherjee et al. 2008). We used a percentage threshold of 0.5% instead of a fixed threshold for the FA to reduce the effect on tract volumes. In our opinion, a fixed FA threshold could have distorted the patient results by cutting off areas of lower anisotropy.

This is a preliminary study with only one patient, which is obviously the major limitation of the study. However, FA measurements in the large Human Connectome Project are highly hereditable in major WM tracts (Kochunov et al. 2015). Also, in a prior DTI study on twins, it was noted that WM hereditability is markedly high in adolescent males (Chiang et al. 2011), which makes the twin brother in our study an especially suitable control person. Two radiologists delineated the ROIs for inclusion and exclusion masks independently to reduce subjectivity.

All examinations were performed with the same device and the same imaging protocol, minimizing variations due to technical reasons.

Future Directions

In studies of several other lysosomal storage disorders (i.e. Krabbe disease, Cystinosis, Niemann-Pick type C, Gaucher type I and II, Mucolipidosis type IV and Fabry disease), it has been suggested that GM volumetric analysis and/or quantitative DTI may be useful modalities for indexing illness stage and monitoring response to emerging treatment (Escolar et al. 2009; Bava et al. 2010; Walterfang et al. 2010; Davies et al. 2011; Schiffmann et al. 2014; Paavilainen et al. 2013). Based on our preliminary study,

automated volumetric brain analysis and quantitative DTI may be suitable biomarkers for evaluating effects of possible AGU treatments, although further studies with a larger population size, including patients from different age groups, are necessary. Moreover, complementary studies including other parts of the brain are needed to better understand the microstructural and volume changes related to AGU.

Acknowledgements The authors wish to thank the twins and their family for participating in the study and PhD Jaana Hiltunen for her assistance.

Funding This study was supported by Finnish Brain Foundation, Arvo and Lea Ylppö Foundation, Yrjö Jahnsson Foundation and Helsinki University Hospital Research Funds, Department of Radiology. No financial or other relationships that might lead to perceived conflict of interest exist.

Author Contributions

Conception and design of the study (TA, AT, NB, AH, ES), acquisition and analysis of data (AT, AH, NB, ES, LÅ), drafting the manuscript or figures (AT, NB, ES, AH, LÅ).

References

Arvio P, Arvio M (2002) Progressive nature of aspartylglucosaminuria. Acta Paediatr 91:255–257

Autti T, Raininko R, Haltia M et al (1997) Aspartylglucosaminuria: radiologic course of the disease with histopathologic correlation. J Child Neurol 12:369–375

Autti T, Lonnqvist T, Joensuu R (2008) Bilateral pulvinar signal intensity decrease on T2-weighted images in patients with aspartylglucosaminuria. Acta Radiol 49:687–692

Banning A, Gulec C, Rouvinen J et al (2016) Identification of small molecule compounds for farmacological chaperone therapy of aspartylglucosaminuria. Nat Sci Rep 6:37583

Barnea-Goraly N, Menon V, Eckert M et al (2005) White matter development during childhood and adolescence: a cross-sectional diffusion tensor imaging study. Cereb Cortex 15:1848–1854

Basser PJ, Pierpaoli C (1996) Microstructural and physiological features of tissues elucidated by quantitative-diffusion-tensor MRI. J Magn Reson B 111:209–219

Bava S, Theilmann RJ, Sach M et al (2010) Developmental changes in cerebral white matter microstructure in a disorder of lysosomal storage. Cortex 46:206–216

Chiang MC, McMahon KL, de Zubicaray GI et al (2011) Genetics of white matter development: a DTI study of 705 twins and their siblings aged 12 to 29. Neuroimage 54:2308–2317

Davies EH, Seunarine KK, Banks T, Clark CA, Vellodi A (2011) Brain white matter abnormalities in paediatric Gaucher type I and type III using diffusion tensor imaging. J Inherit Metab Dis 34:549–553

Dunder U, Kaartinen V, Valtonen P et al (2000) Enzyme replacement therapy in a mouse model of aspartylglycosaminuria. FASEB J 14:361–367

Escolar ML, Poe MD, Smith JK et al (2009) Diffusion tensor imaging detects abnormalities in the corticospinal tracts of neonates with infantile Krabbe disease. AJNR Am J Neuroradiol 30:1017–1021

Fedorov A, Beichel R, Kalpathy-Cramer J et al (2012) 3D slicer as an image computing platform for the quantitative imaging network. Magn Reson Imaging 30:1323–1341

Fischl B, Salat DH, Busa E et al (2002) Whole brain segmentation: automated labeling of neuroanatomical structures in the human brain. Neuron 33:341–355

Giedd JN (2004) Structural magnetic resonance imaging of the adolescent brain. Ann N Y Acad Sci 1021:77–85

Giedd JN, Blumenthal J, Jeffries NO et al (1999) Brain development during childhood and adolescence: a longitudinal MRI study. Nat Neurosci 2:861–863

Giedd JN, Schmitt JE, Neale MC (2007) Structural brain magnetic resonance imaging of pediatric twins. Hum Brain Mapp 28:474–481

Gogtay N, Giedd JN, Lusk L et al (2004) Dynamic mapping of human cortical development during childhood through early adulthood. Proc Natl Acad Sci U S A 101:8174–8179

Gonzalez-Gomez I, Mononen I, Heisterkamp N et al (1998) Progressive neurodegeneration in aspartylglycosaminuria mice. Am J Pathol 153:1293–1300

Halle M, Talos I, Jakab M et al (2015) Multi-modality MRI-based atlas of the brain. SPL, Boston

Haltia M, Palo J, Autio S (1975) Aspartylclucosaminuria: a generalized storage disease. Morphological and histochemical studies. Acta Neuropathol 31:243–255

Huang H, Zhang J, Jiang H et al (2005) DTI tractography based parcellation of white matter: application to the mid-sagittal morphology of corpus callosum. Neuroimage 26:195–205

Jalanko A, Tenhunen K, McKinney C et al (1998) Mice with an aspartylglucosaminuria mutation similar to humans replicate the pathophysiology in patients. Hum Mol Genet 7:265–272

Jenkinson M, Beckmann CF, Behrens TEJ, Woolrich MW, Smith SM (2012) FSL. Neuroimage 62:782–790

Kochunov P, Jahanshad N, Marcus D et al (2015) Heritability of fractional anisotropy in human white matter: a comparison of human connectome project and ENIGMA-DTI data. Neuroimage 111:300–311

Lebel C, Walker L, Leemans A, Phillips L, Beaulieu C (2008) Microstructural maturation of the human brain from childhood to adulthood. Neuroimage 40:1044–1055

Mukherjee P, Chung SW, Berman JI, Hess CP, Henry RG (2008) Diffusion tensor MR imaging and fiber tractography: technical considerations. AJNR Am J Neuroradiol 29:843–852

Paavilainen T, Lepomaki V, Saunavaara J et al (2013) Diffusion tensor imaging and brain volumetry in Fabry disease patients. Neuroradiology 55:551–558

Paus T (2010) Growth of white matter in the adolescent brain: myelin or axon? Brain Cogn 72:26–35

Saarela J, Laine M, Oinonen C et al (2001) Molecular pathogenesis of a disease: structural consequences of aspartylglucosaminuria mutations. Hum Mol Genet 10:983–995

Schiffmann R, Mayfield J, Swift C, Nestrasil I (2014) Quantitative neuroimaging in mucolipidosis type IV. Mol Genet Metab 111:147–151

Sowell ER, Thompson PM, Toga AW (2004) Mapping changes in the human cortex throughout the span of life. Neuroscientist 10:372–392

Tenhunen K, Uusitalo A, Autti T et al (1998) Monitoring the CNS pathology in aspartylglucosaminuria mice. J Neuropathol Exp Neurol 57:1154–1163

Thompson P, Cannon TD, Toga AW (2002) Mapping genetic influences on human brain structure. Ann Med 34:523–536

Tokola AM, Aberg LE, Autti TH (2015) Brain MRI findings in aspartylglucosaminuria. J Neuroradiol 42:345–357

Virta S, Rapola J, Jalanko A, Laine M (2006) Use of nonviral promoters in adenovirus-mediated gene therapy: reduction of lysosomal storage in the aspartylglucosaminuria mouse. J Gene Med 8:699–706

Walterfang M, Fahey M, Desmond P et al (2010) White and gray matter alterations in adults with Niemann-pick disease type C: a cross-sectional study. Neurology 75:49–56

Wierenga L, Langen M, Ambrosino S, van Dijk S, Oranje B, Durston S (2014) Typical development of basal ganglia, hippocampus, amygdala and cerebellum from age 7 to 24. Neuroimage 96:67–72

Zhang Y, Brady M, Smith S (2001) Segmentation of brain MR images through a hidden Markov random field model and the expectation-maximization algorithm. IEEE Trans Med Imaging 20:45–57

JIMD Reports
DOI 10.1007/8904_2017_18

RESEARCH REPORT

Erratum to: White Matter Microstructure and Subcortical Gray Matter Structure Volumes in Aspartylglucosaminuria; a 5-Year Follow-up Brain MRI Study of an Adolescent with Aspartylglucosaminuria and His Healthy Twin Brother

Anna Tokola • Nina Brandstack • Antti Hakkarainen • Eero Salli • Laura Åberg • Taina Autti

Received: 6 September 2016 / Revised: 6 December 2016 / Accepted: 9 December 2016 / Published online: 25 March 2017

Erratum to: JIMD Reports
DOI: 10.1007/8904_2016_36

Publisher regrets that Acknowledgement and Funding information were not included in the published chapter. The details are included in the updated version of the chapter.

The updated online version for this chapter can be found under DOI 10.1007/8904_2016_36

A. Tokola (✉) · N. Brandstack · A. Hakkarainen · E. Salli · L. Åberg · T. Autti
HUS Medical Imaging Center, Helsinki, Finland
e-mail: anna.tokola@hus.fi